5-2015

Measurement of Transfer and Development Lengths of 0.7 in. Strands on Pretensioned Concrete Elements

Canh Ngoc Dang
University of Arkansas, Fayetteville

Measurement of Transfer and Development Lengths of 0.7 in. Strands
on Pretensioned Concrete Elements

Measurement of Transfer and Development Lengths of 0.7 in. Strands
on Pretensioned Concrete Elements

A dissertation submitted in partial fulfillment
of the requirements for the degree of
Doctor of Philosophy in Civil Engineering

by

Canh Ngoc Dang
Ho Chi Minh City University of Technology
Bachelor of Engineering in Civil Engineering, 2009
Ho Chi Minh City University of Technology
Master of Engineering in Civil Engineering, 2011

May 2015
University of Arkansas

This dissertation is approved for recommendation to the Graduate Council.

Dr. Micah Hale
Dissertation Director

Dr. Ernie Heymsfield
Dissertation Committee

Dr. Douglas Spearot
Dissertation Committee

Dr. Daniel Luecking
Dissertation Committee

Dr. J.R. Martí-Vargas
Dissertation Committee

Abstract

The implementation of 0.7 in. (17.8 mm), Grade 270 (1860), low-relaxation prestressing strands in construction is slow regardless of its advantages over the use of 0.6 in. (15.2 mm) and 0.5 in. (12.7 mm) strands. The limited research data and unavailable design guidelines partially account for the slow utilization. This study measured transfer and development length, and evaluated applicable strand spacing of 0.7 in. (17.8 mm) prestressing strands for 24 pretensioned concrete beams. Each beam contained one prestressing strand or two prestressing strands placed at spacing of 2.0 in. (51 mm). The beams were fabricated with high strength, conventional concrete or high strength, self-consolidating concrete. The concrete compressive strengths varied from 5.9 ksi to 9.8 ksi (40.7 MPa to 67.6 MPa) at 1 day, and from 9.2 ksi to 13.4 ksi (63.4 MPa to 92.4 MPa) at 28 days. Transfer lengths were determined using concrete surface strains along with the 95% Average Maximum Strain method. Initial strand end-slips were also measured for predicting transfer length at release using an empirical formula. The development lengths were determined by conducting bending tests with different embedment lengths.

Experimental results indicated ACI 318 and AASHTO specifications are applicable to predict transfer length of 0.7 in. (17.8 mm) strands at release and at 28 days. A coefficient of 2.38 was the most appropriate value to estimate transfer length at release from initial strand end-slip. Concrete compressive strength had little effect on the measured development lengths. The ACI 318 and AASHTO equations significantly over-predicted the measured development lengths. The use of strand spacing of 2.0 in. (51 mm) has no significant effect on the measured transfer end development lengths. Two simple equations were proposed to predict transfer length and development lengths of 0.7 in. (17.8 mm) prestressing strands.

Acknowledgments

I would like to thank the staff of the Graduate School at the University of Arkansas. This dissertation would not have been possible without their help.

I am extremely grateful to Dr. Micah Hale for his support and encouragement. It is difficult to express the gratitude to what he did, he does, and he is doing for me. He has changed my life forever.

I would like to thank my committee members: Dr. Ernie Heymsfield, Dr. Douglas Spearot, Dr. Daniel Luecking, and Dr. J.R. Martí-Vargas. Their contributions made this dissertation better than it should be.

This research cannot be completed without the assistance of a number of individuals at the Department of Civil Engineering. I would like to thank: Richard Deschenes Jr., Cameron Murray, Joseph Daniels III, William Phillips, Doddridge Davis, Alberto Ramirez, and Ryan Hagedorn. They helped me cast and test all the beams during a hot summer in 2014. I also would like to thank David Peachee for his assistant in technical issues and the use of his equipment.

I would like to thank my family and friends at the University of Arkansas and the Virginia Tech for their support and encouragement. I would like to thank Ms. My Hanh for helping me get through the most difficult times. I also would like to thank Dr. Vu Nguyen for being my best friend and for sharing valuable life experience and knowledge.

Finally, I would like to thank the Vietnam Education Foundation (VEF) for supporting my study. I also would like to thank the VEF staff for their assistance.

Dedication

I dedicate this dissertation to my parents, who always encouraged me to complete my Ph.D. study.

Table of Content

List of Figures

List of Tables

Notations

d_b : strand diameter

f_{pe} : effective stress in the prestressing steel after losses

f_{pj} : stress in the prestressing steel at jacking

f_{pt} : stress in prestressing steel immediately after transfer

f_{ps} : average stress in prestressing steel at the time for which the nominal resistance of member is required

f_{pu} : ultimate strength of prestressing strand

f'_{ci} : concrete compressive strength at 1 day

f'_c : concrete compressive strength at 28 days

f'_{ct} : concrete compressive strength at the time of conducting a bending test

E_c : modulus of elasticity of concrete

E_p : modulus of elasticity of prestressing strand

L_t : transfer length

L_b : flexural bond length

L_d : development length

ACI 318 : American Concrete Institute Building Code Requirements for Structural Concrete

AASHTO : American Association of State Highway and Transportation Officials

AMS : average maximum strain

ASTM : American Society for Testing and Materials

CC : conventional concrete

N-CC : normal strength, conventional concrete

N-CC-S : the beams using normal strength, conventional concrete and one 0.7 in. (17.8 mm) prestressing strand

N-SCC : normal strength, self-consolidating concrete

N-SCC-S : the beams using normal strength, self-consolidating concrete and one 0.7 in. (17.8 mm) prestressing strand

H-CC : high strength, conventional concrete

H-CC-S : the beams using high strength, conventional concrete and one 0.7 in. (17.8 mm) prestressing strand

H-CC-D : the beams using high strength, conventional concrete and two 0.7 in. (17.8 mm) prestressing strands

H-SCC : high strength, self-consolidating concrete

H-SCC-S : the beams using high strength, self-consolidating concrete and one 0.7 in. (17.8 mm) prestressing strand

H-SCC-D : the beams using high strength, self-consolidating concrete and two 0.7 in. (17.8 mm) prestressing strands

SCC : self-consolidating concrete

A List of Published Journal Articles

Dang, C. N., Murray, C. D., Floyd, R. W., Micah Hale, W., and Martí-Vargas, J. R. (2014). "Analysis of bond stress distribution for prestressing strand by Standard Test for Strand Bond." Eng.Struct., 72 152-159.

Dang, C. N., Murray, C. D., Floyd, R. W., Micah Hale, W., and Martí-Vargas, J. R. (2014). "A Correlation of Strand Surface Quality to Transfer Length." ACI Struct.J., 111(5), 1245-1252.

CHAPTER 1 : INTRODUCTION AND RESEARCH OBJECTIVES

1.1 Introduction

This chapter aims at giving fundamental definitions regarding conventional concrete, self-consolidating concrete, and pretensioned concrete members. The calculations of transfer length and development length for pretensioned concrete members using the current specifications are addressed. In addition, the use of these specifications and possible issues relating to different strand diameters are discussed in detail. Finally, the research objectives and testing program are given at the end of this chapter.

1.1.1 Conventional Concrete

A fresh conventional concrete (CC) mixture requires external or internal vibration procedures to attain proper consolidation. This task may be noisy, time-consuming, and increase labor costs. In addition, bug holes or voids often occur on the surfaces of pretensioned concrete members. If these voids occur at the interface of prestressing strands and surrounding concrete, they may reduce the bond strength between the prestressing strands and the concrete which decreases the shear strength and moment capacity of pretensioned concrete members.

1.1.2 Self-Consolidating Concrete

Self-Consolidating Concrete (SCC), also known as Self-Compacting Concrete, was first developed in Japan in 1980s (Okamura and Ouchi 2003; Okamura et al. 2000) due to lack of skilled workers. SCC is an improvement of the CC by adjusting the mix designs and adding superplasticizers to create a highly flowable and non-segregating concrete. The fluidity is measured by *slump flow* rather than *slump* as CC and the typical *slump flow* is between 25 in. –

30 in. (650 mm – 750 mm). The flow rate is measured by T_{20} (T_{500}) parameter which is the time to achieve *slump flow* of 20 in. (500 mm). SCC can be placed and filled formwork by its own weight without vibrating, and flows through congested reinforcement regions and confined spaces without segregating or bleeding. The fresh properties of SCC are an important improvement when compared to CC while the hardened SCC properties can maintain all the mechanical properties and durability characteristics.

1.1.3 Pretensioned Concrete

Pretensioned concrete members are widely used in a variety types of structures including bridges, buildings, and parking garage structures. Pretensioned concrete is a form of reinforced concrete. However, pretensioned concrete members include an initial compressive force to mitigate internal tensile stresses due to applied loads and to reduce cracking (Gilbert and Mickleborough 1990). In order to increase the effectiveness of using pretensioned concrete members, high grade strands or tendons (Grade 250 or Grade 270) are used instead of reinforcement rebar (Grade 60). The initial compressive force is created by the following procedures. The strands are tensioned between two fixed abutments and anchored. After placing the formwork, concrete is cast around the prestressing strands. Once the concrete achieves the required compressive strength, the prestressing strands are cut or released, and the tension force is transferred to the concrete as an axial compressive force. The prestress force is transferred by the bond between the prestressing strands and the surrounding concrete.

1.1.4 Transfer Length

In pretensioned concrete members, transfer length is the required length to transfer the effective prestress from the prestressing strands to concrete as shown in **Figure 1.1**. The transfer

length estimation affects structural design which includes the allowable stress at release, and shear strength and moment capacity during service (Russell and Burns 1993; Mitchell et al. 1993; Russell and Burns 1997). A short transfer length can increase tensile and compressive stresses at release. A long transfer length can affect shear strength and moment capacity. The design codes have similar definitions of transfer length, but there are slight differences in terms of calculation. AASHTO (2012) proposes that transfer length can be taken as $60d_b$ (where d_b is strand diameter). ACI 318 (2011) proposes a transfer length of $50d_b$ (where d_b is strand diameter) for shear design specifications or can be estimated using Eq. 1.1.

$$L_t = \frac{1}{3} f_{pe} d_b \tag{1.1}$$

where L_t is transfer length (in.), d_b is strand diameter (in.), f_{pe} is the effective stress in the prestressing steel after losses (ksi).

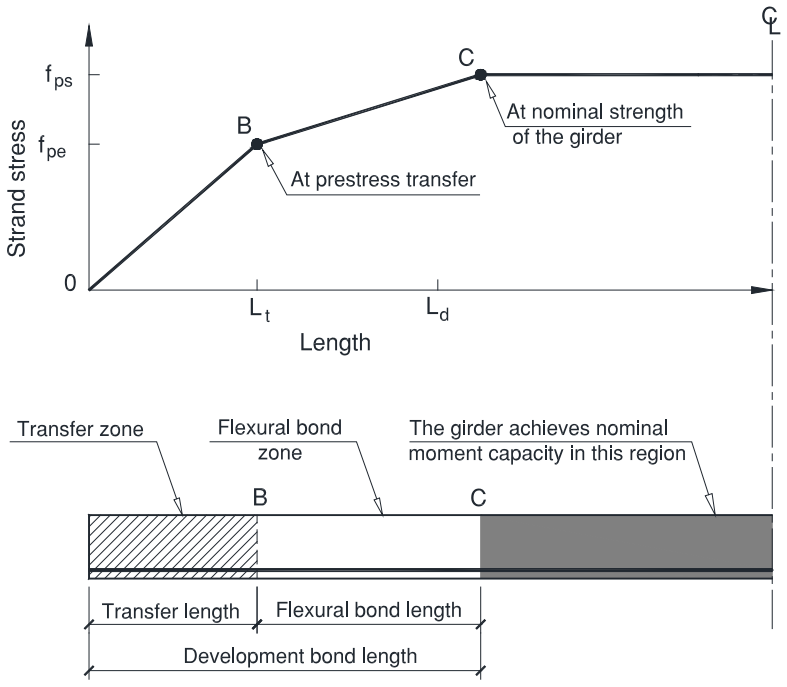

Figure 1.1 – Transfer and development length diagram.
(Note: L_t = transfer length; L_d = development length; f_{pe} = effective stress in the prestressing steel after losses; f_{ps} = average stress in prestressing steel at the time for which the nominal resistance of member is required or specific strand stress)

1.1.5 Development length

The development length is the required length for prestressing strands to develop f_{ps} (where f_{ps} is the average stress in prestressing steel at the time for which the nominal resistance of member is required or specific strand stress) under ultimate stage as illustrated in **Figure 1.1**. The member is able to achieve nominal moment capacity in the region beyond the development length. If the required development length is shorter than the predicted development length by current codes, the member exhibits flexural failure under ultimate stage which show visible warning before collapsed. Otherwise, the member tends to exhibit bond failure if the required development length is greater than the predicted development length. These assessments are based on an assumption that the member is adequately designed for shear. The bond failure is due to the prestressing strands do not have enough length to develop the bond with the adjacent concrete. This failure type is unpredictable and unacceptable in the design of pretensioned concrete members.

The codes have several equations to predict development length of 0.5 in. (12.7 mm) and 0.6 in. (15.2 mm) prestressing strands. Technically, development length is a summation transfer length (Eq. 1.1) and flexural bond length (Eq. 1.2). The ACI 318 (2011) development length equation is shown in Eq. 1.3. AASHTO (2012) proposes a similar equation to estimate development length but including a multiplier κ to account for high shear effects as shown in Eq. 1.4. A κ of 1.6 is used for members having the depth greater than 24 in. (610 mm), otherwise, κ receives a value of 1.0. In the latter case, the AASHTO equation is identical with the ACI 318 equation.

$$L_b = \left(f_{ps} - f_{pe}\right) d_b \tag{1.2}$$

$$L_d = \frac{1}{3} f_{pe} d_b + \left(f_{ps} - f_{pe} \right) d_b \tag{1.3}$$

$$L_d = \kappa \left(f_{ps} - \frac{2}{3} f_{pe} \right) d_b \tag{1.4}$$

Where L_b = flexural bond length; L_d is development length (in.); d_b is strand diameter (in.); f_{pe} is the effective stress in the prestressing steel after losses (ksi); f_{ps} is the average stress in prestressing steel at the time for which the nominal resistance of member is required or specific strand stress (ksi); κ is a multiplier.

1.1.6 Prestressing Strand

In the United States, 0.5 in. (12.7 mm) and 0.6 in. (15.2 mm) prestressing strands are dominant while 0.7 in. (17.8 mm) prestressing strands were first used in practice in 2008 (Morcous et al. 2010). A 0.7 in. (17.8 mm) strand has a cross-sectional area of 0.294 in.^{2} (189.7 mm^2). Accordingly, tensioning a 0.7 in. (17.8 mm) strand to 0.75f_{pu} (where f_{pu} is the ultimate strength of prestressing strand) results in a prestress force of 60 kip (265 kN) which is 35% and 92% greater than the corresponding force of a 0.6 in. (15.2 mm) and 0.5 in. (12.7 mm) strand, respectively. This increase of prestress force can enhance shear strength and moment capacity, decrease girder depth, or reduce the required number of strands in the girder.

ACI Committee 323 (1963) proposed minimum strand spacing of 4d_b (where d_b is strand diameter) center-to-center for the strand diameters varying from 3/8 in. (9.5 mm) to 0.5 in. (12.7 mm). For instance, minimum spacing of 0.5 in. (12.7 mm) strands was 2.0 in. (51 mm). Accordingly, transfer length and development length were predicted using Eq. 1.1 and Eq. 1.3, respectively. In 1988, the Federal Highway Administration (FHWA) issued a memorandum that forbade the use of 0.6 in. (15.2 mm) strands when this type of strand was started using in

construction. The FHWA also included a multiplier of 1.6 for the development length equation as a safety factor when researchers reported the measured development lengths were greater than the predicted development length for several pretensioned concrete members (Buckner 1995; Lane and Rekenthaler Jr 1998). The strand spacing requirement of $4d_b$ (where d_b is strand diameter) was maintained until 1996 when the FHWA made a number of changes to accommodate the use of 0.6 in. (15.2 mm) strands to the current codes (Lane and Rekenthaler Jr 1998). The changes included the reduction of the minimum SS of 0.5 in. (12.7 mm) strands to 1.75 in. (44 mm), and the establishment minimum SS of 2.0 in. (51 mm) for 0.6 in. (15.2 mm) strands. These spacing values were approximately to $3.5d_b$ (where d_b is strand diameter). Cousins et al. (1994) and Deatherage et al. (1994) determined that the use of strand spacing of 1.75 in. (44 mm) for 0.5 in. (12.7 mm) strands had no effect on transfer and development length, and resulted in no splitting cracks. The sufficiency of using 0.6 in. (15.2 mm) strands at spacing of 2.0 in. (51 mm) was confirmed by a number of studies (Russell and Burns 1996; Russell and Burns 1997; Shahawy et al. 1992; Gross and Burns 1995; Barnes et al. 1999).

The changes of strand spacing requirements were adapted and maintained to the current ACI 318 specifications (2011) without modifying the transfer and development length equations. AASHTO also adapted changes regarding the strand spacing requirements. However, AASHTO (2012) uses a transfer length of $60d_b$ (where d_b is strand diameter) instead of Eq. 1.1, and includes a multiplier κ for development length equation as mentioned in previous section.

The Pacific Street Bridge and the Oxford South Bridge in Omaha, Nebraska were the two first bridges using 0.7 in. (17.8 mm) prestressing strands fabricate pretensioned concrete bridge girders. The current ACI 318 and AASHTO specifications regarding transfer length, development length, and SS are only valid for 0.5 in. (12.7 mm) and 0.6 in. (15.2 mm) strands.

Therefore, a limited number of studies have been conducted to evaluate mechanical properties and bond strength (Morcous et al. 2012; Hatami et al. 2011; Dang et al. 2014a), and to determine these parameters for the two bridges in Nebraska and for research recommendations as presented in section 2.6 in this chapter.

1.2 Objectives

The use of 0.7 in. (17.8 mm) prestressing strands has advantages over the use of 0.5 in. (12.7 mm) and 0.6 in. (15.2 mm) strands. However, the lack of design specifications and limited research data prevent its use (Morcous et al. 2012). This project focused on investigating the bond performance of 0.7 in. (17.8 mm) strands on pretensioned members cast with CC and SCC. The project's main objective was to verify if the contemporary specifications of transfer length and development length are applicable for 0.7 in. (17.8 mm) strands. Concrete compressive strength has been recognized as a major factor affecting the bond behavior. Thus, there are two other objectives were included in this project. The first objective was to measure transfer and development lengths of 0.7 in. (17.8 mm) strands cast with a wide range of concrete compressive strengths. The second objective was to examine the effect of concrete compressive strength on transfer and development lengths.

1.3 Testing Program

The testing program included four tasks:

Task 1: Concrete mixture development

Four concrete mixtures were designed. The two conventional concrete mixtures consisted of normal strength, conventional concrete (N-CC) and high strength, conventional

concrete (H-CC) which had targeted compressive strengths of 9 ksi (62.1 MPa) and 13 ksi (89.6 MPa) at 28 days, respectively. The two self-consolidating concrete mixtures included normal, self-consolidating concrete (N-SCC) and high strength, self-consolidating (H-SCC) which had targeted compressive strengths of 8 ksi (55.2 MPa) and 10 ksi (69.0 MPa) at 28 days, respectively.

Task 2: Beam fabrication

Twenty-four pretensioned concrete beams were cast with the designed concrete mixtures and different number of prestressing strands as outlined in **Table 1.1**. The beam had a cross-section of 6.5 in. by 12.0 in. (165 mm by 305 mm) and a length of 18 ft (5.5 m).

Table 1.1 – Pretensioned concrete beams

Concrete mixture	Number of strand	Beam designation	Number of beams	Targeted concrete strength at 1 day (ksi)	Targeted concrete strength at 28 days (ksi)
N-CC	1 (S)	N-CC-S1 – N-CC-S4	4	6	9
H-CC	1 (S)	H-CC-S1 – H-CC-S4	4	9	13
H-CC	2 (D)	H-CC-D1 – H-CC-D4	4	9	13
N-SCC	1 (S)	N-SCC-S1 – N-SCC-S4	4	6	8
H-SCC	1 (S)	H-SCC-S1 – H-SCC-S4	4	8	10
H-SCC	2 (D)	H-SCC-D1 – H-SCC-D4	4	8	10

(Note: 1 ksi = 6.895 MPa)

Task 3: Measure transfer length

Transfer lengths at release, and at 7, 14, 21, 28 days were determined for all pretensioned beams using concrete strain profiles which were measured using DEMEC gauge. The transfer at release was also determined using the measured strand end-slips.

Task 4: Measure development length

Development length was determined by conducting bending tests with different embedment lengths. The tests were performed once the beams achieve 28 days of age.

CHAPTER 2 : LITERATURE REVIEW

2.1 Introduction

This chapter presents fundamental information on the bond strength between prestressing strands and concrete and pull-out tests to quantify the bond. Research on the transfer length and development length using CC and SCC are also addressed. Benefits and applications of 0.7 in. (17.8 mm) strands are shown at the end of this chapter.

2.2 Elements of Bond

Strand bond can be defined as the shearing stress at the interface between prestressing strand and the surrounding concrete which ensures the transferring of prestress force from the strands to the concrete. In other words, the bond ensures the prestressing strand and concrete work as a composite material under external loading. When tensile stress occurs in the strand, it typically moves in the same direction as the applied force. The relative movement of the strand will be prevented by the bond of the two materials. If the bond is inadequate to prevent the movement, a bond failure will occur due to excessive slippage of the prestressing strand. Janney (1954) determined that the bond between prestressing strand and concrete can be addressed by three following factors: (1) adhesion, (2) Hoyer's effect, and (3) mechanical interlock.

Adhesion is the chemical bond between a strand and concrete, and it is formed when fresh concrete hardens. The bond due to adhesion is valid if there is no relative movement of the strand and concrete as shown in **Figure 2.1**. Along the length of a prestressed concrete member, the bond is resisted by adhesion, excluding the transfer zone (see **Figure 1.1**) because the strand

immediately slips into the concrete specimen when it is released. Therefore, the adhesion has no significant contribution to the bond in the transfer zone.

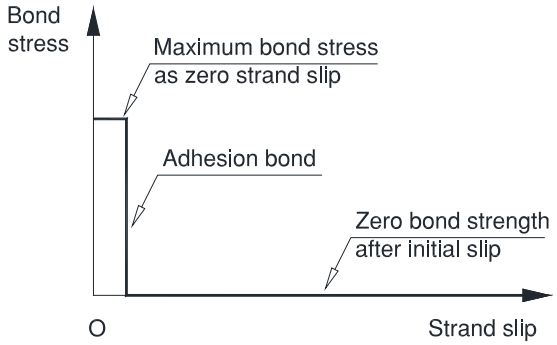

Figure 2.1 – Adhesion bond.
(Note: The figure was adapted from Russell and Burns (1993))

Hoyer's effect is the friction force produced by the outward radial pressure when the prestressed strand expands to its original diameter. When the strand is tensioned and anchored between two abutments on a prestressing bed, the strand length increases due to elongation and the strand diameter decreases due to Poisson's effect. The strand tends to expand back to its original diameter when released from the abutments as shown in **Figure 2.2**. However, the expansion is resisted by the adjacent hardened concrete. Therefore, a wedging effect develops between the strand and the concrete that produces radial pressure on the concrete and creates large frictional forces. Therefore, the Hoyer's effect significantly contributes to the bond stress in the transfer zone.

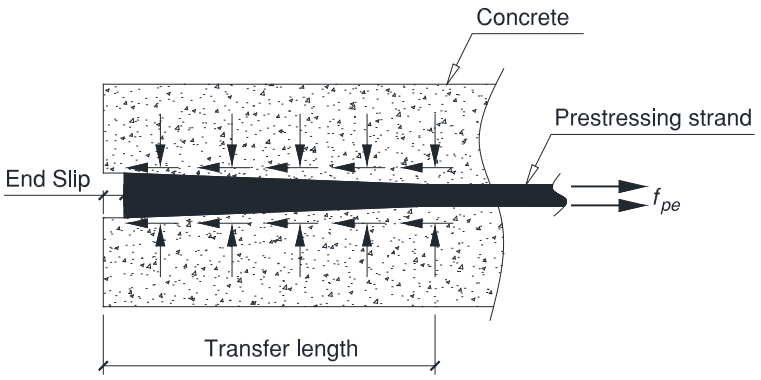

Figure 2.2 – Hoyer's effect.
(Note: The figure was adapted from Russell and Burns (1993))

Mechanical interlock is the resistance to movement generated by the helical shape of the seven-wire strands which is similar to the surface deformations on a reinforcing bar. When concrete hardens, the concrete forms around the prestressed strand and between the grooves in the wire. During release, the strand untwists and the concrete ridges formed between the strand's wires resist these movements as shown in **Figure 2.3**. Therefore, mechanical interlock is an important factor contributing to the bond stress within the transfer zone. In addition, the mechanical interlock is also a dominant factor accounting for the bond within flexural bond zone.

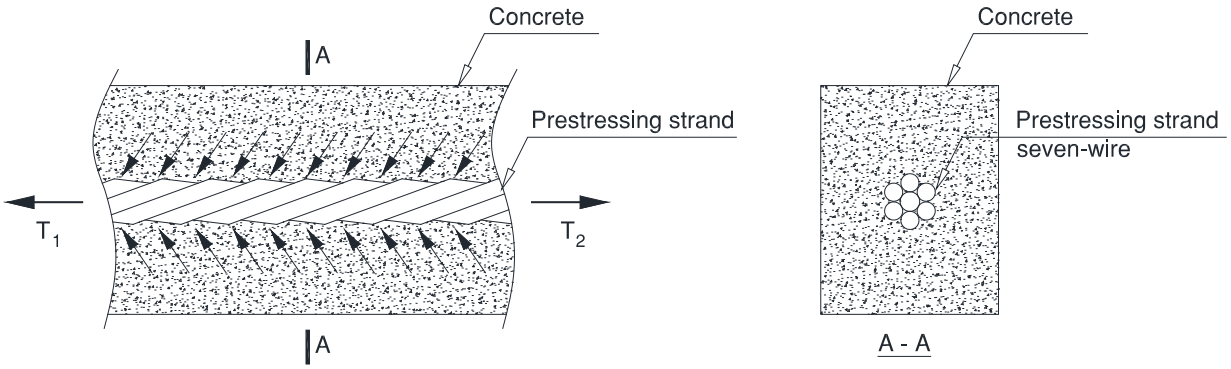

Figure 2.3 – Mechanical interlock.
(Note: The figure was adapted from Russell and Burns (1993))

2.3 Pull out Test

Many pull-out tests have been developed to assess strand bond including the Moustafa Pull-out Bond Test, the Post Tensioning Institute (PTI) Bond Test, and the North American Strand Producers Bond Test (hereafter referred as NASP) (Russell and Paulsgrove 1999a; Russell and Paulsgrove 1999b; Russell and Brown 2004). The NASP was a modification of the PTI Bond Test. This test was performed on mortar in order to increase dimensional stability and reduce shrinkage when compared to the PTI test which used only a cement and water mixture (mortar contains cement, fine aggregate, and water). The NASP test was evaluated as the most reproducible and repeatable test to assess and qualify the bond properties of prestressing strands through four rounds of testing (Ramirez and Russell 2008). During the fourth round of testing (Russell 2006), the mortar strength was limited to 4.75 ± 0.25 ksi (32.7 ± 1.7 MPa) at the time of testing (24 ± 2 hours after casting) to reduce pull-out force variation. The latest version of the NASP is known as the Standard Test for Strand Bond (STSB) which has the same testing specifications as the NASP. The STSB was adapted as the Standard Test Method for Evaluating Bond of Seven-Wire Steel Prestressing Strand by ASTM A1081 (2012). Researchers have indicated that the NASP/STSB pull-out forces not only provide a reliable assessment of bond properties but also present a good correlation with transfer length (Ramirez and Russell 2008).

Minimum thresholds for NASP Bond Test pull-out force for different strand diameters were established as shown in **Table 2.1** (Ramirez and Russell 2008; Hatami et al. 2011; Morcous et al. 2012). The table includes absolute minimum pull-out values as well as average minimum pull-out values. The bond strength is considered adequate if testing results satisfy two conditions; the pull-out force of at least six specimens is equal to or larger than the minimum recommended average pull-out force, and no specimen exhibits a pull-out value less than the

minimum pull-out force. The minimum thresholds of 0.5 in. (12.7 mm) and 0.6 in. (15.2 mm) strands were established based on the correlation of the pull-out forces and the transfer length predicted by the codes. The minimum thresholds of 0.7 in. (17.8 mm) strands were determined based on the proportional of strand diameters.

Table 2.1 – Minimum requirement for different strand diameters in NASP test

Strand diameter (in)	Average pull out force (lb)	Minimum pull out force (lb)
0.5	≥ 10500	≥ 9000
0.6	≥ 12600	≥ 10800
0.7	≥ 14700	≥ 12600

(Note: 1 in. = 25.4 mm; 1 lb = 4.448 N)

2.4 Research on Bond of Prestressing Strand in Conventional Concrete

A number of studies have been conducted to evaluate the adequacy of transfer length and development length for 0.5 in. (12.7 mm) and 0.6 in. (15.2 mm) strands. Several equations of transfer and development length were proposed as which were a function of concrete compressive strengths at 1 day and at 28 days.

2.4.1 Zia and Moustafa (1977)

Zia and Moustafa (1977) conducted an extensive literature review of transfer length and development length to verify the adequacy of the ACI 323 equations (1963) by collecting experimental data of previous studies. The ACI equations of transfer length, flexural bond length, and development length have not changed from 1963. It was determined that the earlier studies of transfer length underestimated the actual values. The authors proposed an equation to estimate transfer length as shown in Eq. 4.1. This equation was applicable to concrete compressive strengths from 2 ksi (13.8 MPa) to 8 ksi (55.2 MPa) at release, and was more

conservative than the ACI 323 equations. For the proposed development length equation (Eq. 4.2), the flexural bond length was increased by 25% in comparison to the ACI 323 equations.

$$L_t = 1.5\frac{f_{si}}{f'_{ci}}d_b - 4.6 \tag{4.1}$$

$$L_d = 1.5\frac{f_{si}}{f'_{ci}}d_b - 4.6 + 1.25\left(f_{su} - f_{se}\right)d_b \tag{4.2}$$

where L_t is transfer length (in.); L_d is development length (in.); f'_{ci} is concrete strength at 1 day (ksi); f_{se} is the effective strand stress (ksi); f_{si} is the initial strand stress (ksi); f_{su} is the specific strand stress (ksi); d_b is strand diameter (in.).

2.4.2 Mitchell et al. (1993)

Mitchell et al. (1993) measured transfer length and development length for twenty-two pretensioned beams to examine the effect of concrete compressive strength. The compressive strengths varied from 3.05 ksi (21.0 MPa) to 7.25 ksi (50.0 MPa) at release and 4.5 ksi (31.0 MPa) to 12.9 ksi (88.9 MPa) at 28 days. The study used three kinds of strand diameters: 3/8 in. (9.5 mm) stress-relieved strands having ultimate strength of 263 ksi (1813 MPa), 0.5 in. (12.7 mm) and 0.62 in. (15.7 mm) low-relaxation strands having ultimate strength of 276 ksi (1903 MPa) and 260 ksi (1793 MPa), respectively. The authors concluded that the measured transfer lengths and development lengths had a strong correlation with concrete compressive strength. Eq. 4.3 was proposed to predict transfer length at release which was shorter than the proposed transfer length for evaluating shear strength and nominal moment capacity (Eq. 4.4). The proposed development length equation is shown in Eq. 4.5.

$$L_t = 50d_b\sqrt{\frac{3}{f'_{ci}}} \tag{4.3}$$

$$L_t = \frac{1}{3} f_{si} d_b \sqrt{\frac{3}{f'_{ci}}} \tag{4.4}$$

$$L_d = \frac{1}{3} f_{si} d_b \sqrt{\frac{3}{f'_{ci}}} + \left(f_{ps} - f_{se}\right) d_b \sqrt{\frac{4.5}{f'_c}} \tag{4.5}$$

where L_t is transfer length (in.); f'_{ci} is concrete compressive strength at 1 day (ksi); f'_c is concrete compressive strength at 28 days (ksi); f_{se} is the effective stress in the prestressing steel after losses (ksi); f_{si} is the initial strand stress (ksi); f_{ps} is the average stress in prestressing steel at the time for which the nominal resistance of member is required (ksi); d_b is strand diameter (in.).

2.4.3 Cousins et al. (1990a; 1993; 1990b)

In 1980s, epoxy-coated strands were developed by *Florida Wire & Cable Co.* to improve the corrosion resistance. These strands were used for pretensioned members in adverse environments. Cousins et al. (1990a; 1993; 1990b) investigated transfer length and development length for un-coated and coated, Grade 270 (1860), low-relaxation strands. To coat the strands, a grit-impregnated epoxy was used with various densities. The coated strands included high coated strands, medium coated strands, and low coated strands. The pretensioned beams had cross-sections of 4 in. by 4 in. (100 mm by 100 mm) and 5 in. by 8 in. (125 mm by 200 mm) and contained one single prestressing strand. For the 0.5 in. (12.7 mm) strands, twenty-six transfer length tests and thirteen development length tests were performed. For the 0.6 in. (15.2 mm) strands, eleven transfer length tests and nine development length tests were conducted. The experimental results showed that the measured transfer length of coated strands was shorter than the transfer length predicted by ACI 318 (2011). However, ACI 318 was not conservative to predict transfer length for the un-coated strands. Similarly, development length of un-coated

strands was longer than that of coated strands for the same strand diameter, and greater than the development length predicted by ACI 318.

2.4.4 Logan (1997)

Logan (1997) evaluated the variation in the bond performance of prestressing strands produced by different manufacturers. The study collected 0.5 in. (12.7 mm) prestressing strands from six pretensioned concrete producers from various locations of North America. The strand quality was classified by the Moustafa Bond Test. Strands having pull-out forces greater than 36 kip (160 kN) were considered as high quality strands, and strands having pull-out forces less than 12 kip (53 kN) were considered as low quality strands. Ten pretensioned beams were cast for each kind of strand to measure transfer length and development length. The measured transfer length and development lengths were significantly different. The measured transfer and development lengths of the high quality strands were shorter those predicted by ACI 318. However, the measured transfer lengths of the poor quality strands was greater than the transfer length predicted by ACI 318. Also, for the beams containing the poor quality strands, the measured development lengths were greater than that predicted by ACI 318. These beams failed by bond without visible warning.

2.4.5 Rose and Russell (1997)

Rose and Russell (1997) examined the effect of strand surface conditions on transfer length. Their study examined 0.5 in. (12.7 mm), Grade 270 (1860), low-relaxation strands with various strand surface conditions: as-received, cleaned, silane treated, and weathered. For the as-received condition, the strands were collected from three different manufacturers. The cleaned surface was achieved by washing strands with acid, rinsing with water, and drying. The silane

treated surface was prepared in a similar way to the cleaned surface, but included an additional step of evenly spraying with silane. The weathered surface was attained by cleaning strands and placing them in an environmental chamber of 73.4°F (23°C) and 75% of relative humidity for 3 days. Transfer lengths were estimated by measuring strand end slips at release of prestressing strands. It was concluded that the weathered strands exhibited the shortest transfer length, and the silane treated strands showed the longest transfer length. Transfer length results of cleaned strands and as-received strands did not show significant differences.

2.4.6 Ramirez and Russell (2008)

Ramirez and Russell (2008) conducted an extensive study to investigate the effects concrete compressive strength on transfer and development length. The 0.5 in. (12.7 mm) and 0.6 in. (15.2 mm), Grade 270 (1860), low-relaxation strands with various surface conditions were used in the study. The concrete strengths varied from 4.0 ksi (27.6 MPa) to 10.0 ksi (68.9 MPa) at 1 day, and from 6.0 ksi (41.4 MPa) to 15.0 ksi (103.4 MPa) at 28 days. Thirty-two rectangular beams and 4 I beams were cast with 0.5 in. (12.7 mm) strands, and 11 rectangular beams and 4 I beams were cast with 0.6 in. (15.2 mm) strands. The study determined a strong correlation in which the increase of concrete compressive strength can shorten transfer length and development length. For transfer length, the proposed equation included concrete compressive strength at 1 day as shown in Eq. 4.6. When the concrete strength at release is 4 ksi (27.6 MPa), the proposed transfer length is equal to the transfer length predicted by AASHTO, $60d_b$ (where d_b is strand diameter). In addition, the equation included a minimum value of transfer length, $40d_b$ (where d_b is strand diameter), to guarantee a reasonable consideration of transfer length in design. For development length, the proposed equation included concrete compressive strength at 28 days as

shown in Eq. 4.7. This equation provided a minimum development length of $100d_b$ (where d_b is strand diameter).

$$L_t \frac{120}{\sqrt{f'_{ci}}} d_b \geq 40 d_b \tag{4.6}$$

$$L_d = \frac{120}{\sqrt{f'_{ci}}} d_b + \frac{225}{\sqrt{f'_c}} d_b \geq 100 d_b \tag{4.7}$$

where L_t is transfer length (in.); L_d is development length (in.); f'_{ci} is concrete compressive strength at 1 day (ksi); f'_c is concrete compressive strength at 28 days (ksi); d_b is strand diameter (in.).

2.5 Research on Bond of Prestressing Strand in SCC

2.5.1 Benefit of SCC

Benefits of SCC can be classified into three categories: cost-effectiveness, environmental and safety improvement, and enhancement of aesthetics. In terms of cost-effectiveness, SCC accelerates the speed of construction since it can be placed more rapid than CC. In addition, SCC can fill restricted areas and congested reinforcement sections. The placement of SCC does not require mechanical vibration which reduces the requirements of skilled workers. In terms of environmental and safety improvement, SCC eliminates the use of vibrators during concrete placement which reduces the noise exposures and increases jobsite safety. The use of SCC also decreases fall hazards by reducing the number of workers standing on the form during placement and consolidation. Regarding enhancement of aesthetics, SCC improves the surface finish with little or without remedial surface work. The SCC flows in forms by its own weight which can be placed and consolidated in complex shapes and architectural concrete components.

2.5.2 Engineering Properties

For SCC, the fresh properties are important and different from the other types of concrete. The fresh properties of SCC mixture are characterized by three primary properties: (1) filling ability, (2) stability, and (3) passing ability.

Filling ability refers to the ability to fill the formwork of concrete mixture. This ability is characterized by two parameters: *slump flow* and T_{20} (T_{500}). The *slump flow* test is used to determine the horizontal flow property of SCC without obstructions (ASTM C1611 2014). This test is similar to the slump test of CC (ASTM C143 2012). However, instead of measuring the falling height of concrete as in the slump test, the *slump flow* test measures the spreading diameter of the fresh concrete mixture. The ACI Committee 237 (2007) specifies a common range of slump flow for SCC of 18 in. - 30 in. (450 mm - 750 mm). The required *slump flow* depends on the particular application, but a range of slump flow of 24 in. - 27 in. (610 mm - 689 mm) is appropriate for the most applications (Koehler and Fowler 2007). During the slump flow test, the time for the fresh concrete mixture to spread to 20 in. (500 mm) is measured. This parameter is referred to the T_{20} (T_{500}) which measures the flow rate of SCC. A high T_{20} (T_{500}) indicates the fresh concrete mixture has high viscosity and good stability. A fresh mixture having T_{20} (T_{500}) less than 2 seconds has low viscosity and greater than 5 seconds has high viscosity (ACI Committee 237 2007). Generally, a T_{20} (T_{500}) value in a range of 2 – 7 seconds is appropriate for most applications (Koehler and Fowler 2007).

After the *slump flow* test is conducted, the slump flow paddy is observed and assigned a number from 0 to 3 which represents the stability of the concrete mixture. This number is termed as Visual Stability Index (VSI) (ASTM C1611 2014). A VSI value of 0 is assigned for a highly stable concrete, 1 is assigned for a stable concrete, 2 is assigned for an unstable concrete,

and 3 is assigned for highly unstable concrete. A VSI value from 0 – 1 is acceptable in practice (Koehler and Fowler 2007). To assist the VSI assignment, ASTM C1611 (2014) provides four figures which illustrate the stability of concrete mixture corresponding with each VSI value.

Passing ability is the ability of the concrete to flow through restricted areas without blocking. This ability ensures the fresh concrete mixture will flow through reinforcement and narrow spaces within the formwork. The passing ability is measured by the J-Ring test (ASTM C1621 2014) which operates in the same manner as the *slump flow* test. For the test, a 12 in. (300 mm) diameter ring consisting of 16 equally spaced bars is placed around the slump cone as shown in **Figure 2.4** and **Figure 2.5**. The difference between *slump flow* without the J-Ring and with the J-Ring is calculated. A difference greater than 2 in. (51 mm) indicates poor passing ability.

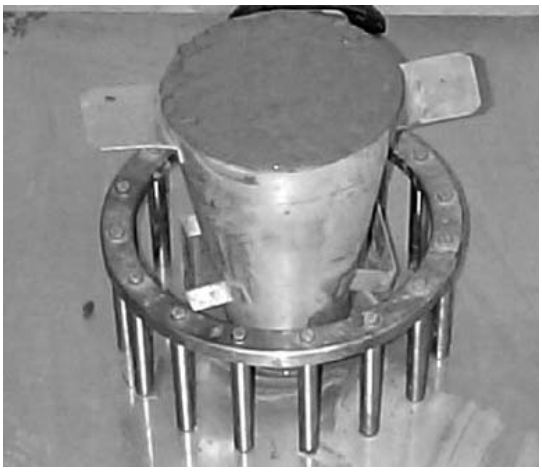

Figure 2.4 – Filling concrete in the inverted mold (ASTM C1621 2014).

Figure 2.5 – J-Ring flow after lifting the mold (ASTM C1621 2014).

2.5.3 Previous Research on Bond of Prestressing Strand in SCC

Several studies have been implemented to investigate the bond performance of prestressing strands in SCC. In particular, transfer length and development length of

pretensioned concrete members using SCC were compared with those using CC. The applicability of ACI 318 and AASHTO specifications were also addressed.

2.5.3.1 Girgis and Tuan (2005)

Girgis and Tuan (2005) investigated the bond strength of 0.6 in. (15.2 mm) prestressing strands with SCC and measured transfer length of pretensioned bridge girders including NU-1100, NU-900, and NU-1350. These girders were cast with SCC and 0.6 in. (15.2 mm) prestressing strands. In particular, the Moustafa Bond Test was used to examine the bond strength. Eighteen strand specimens were pulled out of a large block of SCC. Test data indicated the use of viscosity-modifying admixtures (VMA) in SCC significantly reduced the bond strength at early age which increased transfer lengths at release. The measured transfer length at release of the girders using SCC were up to 50% greater than those using CC due to low the bond strength of SCC. At 28 days, however, the measured transfer lengths of the girders using SCC were shorter than those using CC. In other words, SCC had higher bond strength than CC at 28 days.

2.5.3.2 Larson et al. (2007)

Larson et al. (2007) conducted an experimental program to measure transfer length and development length of fifteen full-scale pretensioned concrete beams using SCC and 0.5 in. (12.7 mm) prestressing strands placed at different locations within the beams. In particular, five bottom-strand beams were cast with SCC having compressive strengths of 5.0 ksi (34.5 MPa) at 1 day and 7.5 ksi (51.8 MPa) at 28 days. Six top-strand beams were cast with SCC having compressive strengths of 3.6 ksi (24.8 MPa) at release and 7.0 ksi (48.1 MPa) at 28 days. Four T-beams were cast with SCC having compressive strengths of 5.0 ksi (34.5 MPa) at release and 8.0 ksi (54.8 MPa) at 28 days. Transfer lengths were estimated by measuring initial strand end-

slip and Guyon's empirical formula (1953) with a bond stress distribution coefficient of 2.0. The test data indicated ACI 318 (2011) and AASHTO (2012) specifications are adequate to predict transfer length at release and 21 days. Development lengths were quantified by conducting bending texts for all beams. It was concluded that ACI 318 and AASHTO specifications are conservative to predict development length for the proposed SCC mixtures and specimen geometries.

2.5.3.3 Boehm et al. (2010)

Boehm et al. (2010) measured transfer length and development length for six full-scale AASHTO Type I pretensioned girders using 0.5 in. (12.7 mm) prestressing strands. Three types of concrete mixtures were used: (i) moderate-strength CC mixture, (ii) moderate-strength SCC mixture, and (iii) high-strength SCC mixture. The moderate-strength concrete and high-strength concrete had compressive strengths of 5.0 ksi (34.5 MPa) and 10.0 ksi (68.9 MPa) at 1 day, respectively. Two girders were cast for each type of concrete. The measured transfer lengths showed that there was no significant difference in bond strength between moderate-strength SCC and moderate-strength CC. Transfer lengths measured on high-strength SCC were shorter than those measured on moderate-strength SCC and CC due to the effect of concrete compressive strength. Development length tests were conducted for all the girders by performing bending tests with different embedment lengths. A bridge deck was placed on the top of the girder. The test data indicated ACI 318 (2011) and AASHTO (2012) specifications are conservative to predict development length pretensioned concrete members using SCC.

2.5.3.4 Staton et al. (2009)

Staton et al. (2009) measured the transfer length of 20 pretensioned concrete beams cast with SCC and high-strength CC (HSC) and 0.6 in. (15.2 mm) prestressing strands. Eight beams

were cast with SCC using Type I cement (SCC-I) and having compressive strengths of 7.76 ksi (52.5 MPa) at 1 day and 12.24 ksi (84.4 MPa) at 28 days. Six beams were cast with SCC using Type III cement (SCC-III) and having compressive strengths of 7.54 ksi (52.0 MPa) at 1 day and 11.42 ksi (78.7 MPa) at 28 days. The remaining beams were cast with HSC having compressive strengths of 9.22 ksi (63.6 MPa) at 1 day and 12.38 ksi (85.4 MPa) at 28 days. Transfer lengths were measured at release, and at 3, 5, 7, 14, and 28 days. The study showed the measured transfer lengths of SCC-I and HSC were similar at 28 days, and were slightly greater than SCC-III. In addition, the measured transfer lengths for all pretensioned beams were approximately 60% of those predicted by ACI 318 (2011) and AASHTO (2012).

2.5.3.5 Floyd et al. (2011a)

Floyd et al. (2011a) conducted an extensive experimental program to investigate development length of 20 pretensioned concrete beams cast with SCC and high-strength concrete. Transfer lengths of these beams were measured by Staton et al. (2009) as presented in Section 2.5.3.4. Development length was determined by performing bending tests with different embedment lengths. The authors indicated that SCC-III and HSC had similar development lengths and slightly shorter than those of SCC-I. ACI 318 (2011) and AASHTO (2012) equation overestimated more than 60% of the measured development lengths of all beams.

2.5.3.6 Myers et al. (2012)

Myers et al. (2012) evaluated transfer length and development length of 0.5 in. (12.7 mm) prestressing strands cast with CC and SCC. In particular, four concrete mixtures were used: (1) normal-strength CC having compressive strengths of 4.81 ksi (33.2 MPa) at 1 day and 5.73 ksi (39.5 MPa) at 28 days, (2) high-strength CC having compressive strengths of 5.67 ksi (39.1 MPa) at 1 day and 8.48 ksi (58.5 MPa) at 28 days, (3) normal-strength SCC having compressive

strengths of 5.66 ksi (39.0 MPa) at 1 day and 6.95 ksi (47.9 MPa) at 28 days, and (4) high-strength SCC having compressive strengths of 6.33 ksi (43.6 MPa) at 1 day and 9.25 ksi (63.8 MPa) at 28 days. Three pretensioned concrete beams were fabricated for each type of concrete. The measured transfer lengths of girders using SCC and CC showed no significant difference. The measured transfer lengths were shorter for the beams high-strength concrete including CC and SCC. Development length was determined by performing bending tests with different embedment lengths. The test results indicated ACI 318 (2011) and AASHTO (2012) specifications are conservative to predict development length for pretension concrete beams using CC and SCC.

2.6 Research on Bond of 0.7 in. (17.8 mm) Prestressing Strand

2.6.1 Benefit of 0.7 in. (17.8 mm) strand

The use 0.7 in. (17.8 mm), Grade 270 (1860), prestressing strands has advantages over the use of 0.5 in. (12.7 mm) and 0.6 in. (15.2 mm) strands. A 0.7 in. (17.8 mm) strand has a cross-sectional area of 0.294 in.^{2} (189.7 mm^2). Accordingly, tensioning a 0.7 in. (17.8 mm) strand to 0.75f_{pu} (where f_{pu} is the ultimate strength of prestressing strand) results in a prestress force of 60 kip (265 kN) which is 35% and 92% greater than the corresponding force of a 0.6 in. (15.2 mm) and 0.5 in. (12.7 mm) strand, respectively. This increase in prestress force can increase moment capacity, decrease girder depth, or reduce the required number of strands in the girder.

Economic benefits are also realized by using 0.7 in. (17.8 mm) strands in bridge girders. For instance, to achieve the same flexural capacity of a beam using 0.6 in (15.2 mm) strands, fewer 0.7 in. (17.8 mm) strands and chucks are required. Akhnoukh (2008) suggested that a

girder using 0.7 in (17.8 mm) strands and a concrete compressive strength of 15 ksi (103 MPa) can reduce by 14% of the material costs in comparison to a girder containing 0.6 in. (15.2 mm) strands and a concrete compressive strength of 8 ksi (55 MPa). In addition, the use of large diameter strands increases moment capacity, therefore fewer girders are required per span which directly decreases construction budget and construction time.

2.6.2 Application of 0.7 in. (17.8 mm) strand in bridge construction

2.6.2.1 Pacific Street Bridge, Omaha, NE, USA

The Pacific Street Bridge (2008) is the first bridge in the world using 0.7 in (17.8 mm) strands for pretensioned concrete girders (Schuler 2009). The bridge consists of six traffic lanes with a total width of 108-ft 8-in. (33.1 m). This bridge has two identical spans of 98 ft (29.9 m). Each span consists of ten NU-900 girders which are spaced at 10-ft 8-in. (3.3 m). The bridge supported a continuous deck that was 8 in. (200 mm) thick and composed of concrete having a compressive strength of 5.0 ksi (34.5 MPa) at 28 days. Thirty-six 0.6 in. (15.2 mm) mono strands was post-tensioned along the deck.

The bridge was constructed using twenty 98-ft 4-in. (30.0 m) long NU-900 bridge girders which were fabricated at Coreslab Structures, Omaha. These girders were cast using high performance concrete having compressive strengths of 7.0 ksi (48.3 MPa) at 1 day and 10.0 ksi (68.9 MPa) at 28 days. Each girder contained thirty 0.7 in. (17.8 mm), Grade 270 (1860) prestressing strands which were spaced at 2.0 in. (51 mm) horizontally and 2.5 in. (64 mm) vertically. These strands were tensioned up to $0.64f_{pu}$ (where f_{pu} is the ultimate strength of prestressing strand). A full-scale test was conducted at the PKI Structural Laboratory of the

University of Nebraska-Lincoln in 2007 to study the girders performance before constructing the project.

A 40 ft (12.2 m) long NU-900 girder was fabricated for the Pacific Street Bridge project (Morcous et al. 2011b). This girder used concrete having a compressive strengths of 6.7 ksi (46.2 MPa) at 1 day and 8.0 ksi (55.2 MPa) at 28 days. Twenty-four 0.7 in. (17.8 mm) strands were placed at 2.2 in. (56 mm) horizontally and 2.25 in. (57 mm) vertically, and tensioned to $0.75f_{pu}$ (where f_{pu} is the ultimate strength of prestressing strand). The measured transfer length was 35 in. (890 mm) which was equal to the predicted transfer length by ACI 318 and less than the transfer length predicted by AASHTO (2012). The development length predicted by AASHTO equation was 14 ft (4.3 m) which was included a multiplier of 1.6 for the beam having a depth greater than 24 in. (610 mm). The bending test using the predicted development length indicated that AASHTO equation is applicable and conservative to estimate development length of 0.7 in. (17.8 mm) strands.

2.6.2.2 Oxford South Bridge, Omaha, NE, USA

The Oxford South Bridge was constructed in the spring of 2012 and completed in the fall of 2013 (Morcous et al. 2013). The bridge includes five spans: 110 ft (33.5 m), 110 ft (33.5 m), 140 ft (42.7 m), 110 ft (33.5 m), 110 ft (33.5 m). This bridge has two traffic lanes with a total width of 32 ft (9.8 m). There were two design plans developed for the bridge. The preliminary design had 4 NU-1600 girders spaced at 9 ft (2.7 m). The 140 ft (42.7 m) span girder used forty-two 0.6 in. (15.2 mm) strands, and the 110 ft (33.5 m) included twenty-six 0.6 in. (15.2 mm) strands. The revised design used NU-1350 girders and 0.7 in. (17.8 mm) strands instead of NU-1600 girders and 0.6 in. (15.2 mm) strands. The use of NU-1350 girders increased the vertical

clearance by 10 in. (250 mm), and the use of 0.7 in. (17.8 mm) decreased the required number of prestressing strands.

The NU-1350 girder contained thirty-four 0.7 in. (17.8 mm), Grade 270 (1860) prestressing strands for the 140 ft (42.7 m) span, and twenty-four 0.7 in. (17.8 mm), Grade 270 (1860) prestressing strand for the 110 ft (33.5 m) span. These strands were spaced at 2.0 in. by 2.0 in. (51 mm by 51 mm), and tensioned to $0.75f_{pu}$ (where f_{pu} is the ultimate strength of prestressing strand). SCC was used for all girders. In particular, the 140 ft (42.7 m) girders used concrete which had compressive strengths of 7.0 ksi (48.3 MPa) at 1 day and 9.0 ksi (62.1 MPa) at 28 days. The 110 ft (33.5 m) used concrete which had compressive strengths of 6.0 ksi (41.4 MPa) at 1 day and 8.0 ksi (55.2 MPa) at 28 days.

Morcous et al. (2014) measured transfer length in three girder ends of the NU-1350 110 ft (33.5 m) girders. Transfer length was determined by measuring concrete surface strains along with 95% average maximum strain (AMS) method. The measured transfer lengths at release and at 14 days were 32 in. (813 mm) and 36 in. (915 mm), respectively. The transfer length at 14 days was approximately with the transfer length predicted by ACI 318 ($50d_b$ = 35 in. (890 mm)), and less than the length predicted by AASHTO ($60d_b$ = 42 in. (1070 mm)). At the end of girders, there were no visible cracks at the transfer zone and in the area between prestressing strands due to the use of 0.7 in. (17.8 mm) strands at a pacing of 2 in. by 2 in. (51 mm by 51 mm).

2.6.3 Previous Research on Bond of 0.7 in. (17.8 mm) strand

Several studies using 0.7 in. (17.8 mm), Grade 270 (1860), prestressing strands have been conducted. These studies can be categorized into three groups: (1) mechanical and bond properties (Morcous et al. 2012; Dang et al. 2014a; Hatami et al. 2011), (2) the required strand

spacing (Vadivelu 2009; Maguire et al. 2013; Morcous et al. 2014; Arab 2012), and (3) transfer length, development length, and shear capacity (Morcous et al. 2011b; Morcous et al. 2013; Patzlaff et al. 2012; Morcous et al. 2011a; Morcous et al. 2010; Song et al. 2013; Akhnoukh 2008).

2.6.3.1 Morcous et al. (2012)

Morcous et al. (2012) examined the mechanical properties and bond strength of 0.7 in. (17.8 mm), Grade 270, low-relaxation strand. The mechanical properties of 0.7 in. (17.8 mm) strands were first mentioned by the ASTM A416 in 2006 (ASTM A416 2012). According to the code, a 0.7 in. (17.8 mm) strand has a cross-sectional area of 0.294 in.^{2} (189.7 mm^2), a minimum breaking strength of 79.4 kips (353.2 kN), a minimum load at 1% extension of 71.5 kips (318.1 kN), and a minimum extension at failure of 3.5%. These properties were verified by testing 102 strand specimens obtained from two manufacturers. Experimental results indicated that all strand specimens met the ASTM A416 (2012) requirements of breaking strength and elongation. The study also proposed an equation to estimate the strain-stress relationship of 0.7 in. (17.8 mm) strands as shown in Eq. 4.8.

$$f_{ps} = \varepsilon_{ps} E_{ps} \left[Q + \frac{1-Q}{\left\{ 1 + \left(\frac{E_p \varepsilon_p}{K f_{py}} \right)^R \right\}^{1/R}} \right] \tag{4.8}$$

where $Q = 0.02$; $K = 1.03$; $R = 7.33$; f_{ps} = is the ultimate stress; f_{py} = is the yielding stress; ε_p is strain of prestressing stress; E_p = is modulus of elasticity.

The authors investigated the bond strength of 0.7 in. (17.8 mm) strands which were tested on mortar and concrete. For the mortar, the researchers performed three NASP tests to

determine the NASP pull-out forces. It was noted that only four strand specimens were tested to achieve a NASP pull-out force instead of six specimens as stated by the NASP protocol (Russell 2006). All three NASP pull-out forces were excessive the minimum thresholds of 0.7 in. (17.8 mm) strand as mentioned in **Table 2.1**. For concrete, the researchers performed six NASP tests on concrete which had compressive strengths of 4.0 ksi - 10.0 ksi (27.6 MPa - 69.0 MPa). The experimental results showed that NASP pull-out force had a high correlation with concrete compressive strength. The authors proposed an equation shown in Eq. 4.9 to estimate the NASP pull-out force of 0.7 in. (17.8 mm) strands cast in concrete. Noting that the difference in NASP pull-out forces of 0.7 in. (17.8 mm) strands cast on concrete and mortar was not addressed.

$$P_{01} = 6.96 f_{ci}'^{0.77} \tag{4.9}$$

where P_{01} is the pull-out force corresponding with a free-end slip of 0.1 in. (2.5 mm) (kip); f'_{ci} is concrete compressive strength at 1 day (ksi).

2.6.3.2 Vadivelu (2009) and Song et al. (2013)

Vadivelu (2009) investigated the applicability of using a strand spacing of 2 in. by 2.0 in. (51 mm by 51 mm) as the minimum spacing for 0.7 in. (17.8 mm), Grade 270 (1860) strands. One full-scale finite element models of AASHTO Type I was made using the ABAQUS software. This model used 0.7 in. (17.8 mm) strands with strand spacing of 2.0 in. by 2.0 in. (51 mm by 51 mm). In these models, concrete and strands were considered as linear materials. The concrete had a compressive strength of 8.0 ksi (55.2 MPa), the modulus of elasticity of 5100 ksi (35165 MPa), and a Poisson's ratio of 0.18. The strand was Grade 270 (1860), the modulus of elasticity of 28500 ksi (195500 MPa), and a Poisson's ratio of 0.27. The analytical investigation indicated the transition zone between the web and bottom flange of the girder using 0.7 in. (17.8 mm) strands was susceptible to cracking.

The experimental program was conducted by Vadivelu (2009) and Song et al. (2013) to evaluate the analytical investigation as mentioned above. One full-scale AASHTO Type I girder which had a span of 56 ft (18.5 m) was fabricated with 12 – 0.7 in. (17.8 mm) prestressing strands. The strands were placed at spacing of 2.0 in. by 2.0 in. (51 mm by 51 mm) and tensioned to $0.75f_{pu}$ (where f_{pu} is the ultimate strength of prestressing strand). This girder used high strength concrete which had a compressive strength of 10 ksi (69.0 MPa) at 1 day and 14.2 ksi (97.9 MPa) at 28 days. The average measured transfer length at release was 21.2 in. (540 mm) which was approximately $30d_b$ (where d_b is strand diameter). This measured transfer length was shorter than the predicted transfer length using ACI 318 and AASHTO equation.

2.6.3.3 Morcous et al. (2011a)

This study evaluated transfer length, development length and end-zone cracking of two full-scale NU-900 girders using 0.7 in. (17.8 mm), Grade 270 (1860) prestressing strands (Morcous et al. 2011a). Each girder had different number of strands, strand spacing, and concrete compressive strength. Transfer length was measured using concrete surface strains along with AMS method (Russell and Burns 1996). Development length was measured by performing bending tests in which the development length predicted by AASHTO equation was used as the tested embedded length.

The first girder had a length of 40 ft (12.1 m), and contained twenty-four 0.7 in. (17.8 mm), Grade 270 (1860) prestressing strands tensioned to $0.75f_{pu}$ (where f_{pu} is the ultimate strength of prestressing strand). These strands were spaced at 2.25 in. (57 mm) vertically and at 2.2 in. (56 mm) horizontally. The end-zone reinforcement included 8 No. 6 (19 M), Grade 60 (420) bars which were spaced at 2 in. (51 mm) along a length of 8 in. (200 mm) at the girder ends. The girder was cast with SCC which had compressive strengths of 6.0 ksi (41.4 MPa) at 1

day and 8.0 ksi (55.2 MPa) at 28 days. The measured transfer length was approximately 35 in. (890 mm) which was approximately with the transfer length predicted by ACI 318 (2011) and shorter than the transfer length predicted by AASHTO (2012). The first girder had visible cracks at the web and the top flange after detensioning the prestressing strands.

The second girder had the same length and cross section with the first girder. This girder contained thirty 0.7 in. (17.8 mm), Grade 270 (1860) prestressing strands tensioned to $0.66f_{pu}$ (where f_{pu} is the ultimate strength of prestressing strand). This prestress was slightly less than the prestress in the first girder because of the limited capacity of the prestressing bed. However, these strands were placed at spacing of 2.0 in. by 2.0 in. (51 mm by 51 mm). The end-zone reinforcement consisted of 4 No. 6 (No. 19), Grade 60 (420) bars which were spaced at 2 in. (51 mm) along a length of 8 in. (200 mm) at the girder ends. The second girder was cast with high strength concrete which had compressive strengths of 12.0 ksi (82.7 MPa) at 1 day and 15.0 ksi (103.4 MPa) at 28 days. The measured transfer length was 27 in. (690 mm) which was 30% shorter than that of the first girder. The reduction in the measured transfer length in the second girder can be attributed to the effect of concrete compressive strength. The second girder had no visible cracks as the first girder.

For development length, both girders were able to achieve the nominal flexural strength by using the development length predicted by AASHTO (2012) as the tested embedment length. The study indicated the AASHTO specifications are adequate to predict transfer length and development length of 0.7 in. (17.8 mm) prestressing strands.

2.6.3.4 Patzlaff et al. (2012)

This study examined the effect of confining reinforcement, and measured transfer length, development length, and shear strength of pretensioned girders using 0.7 in. (17.8 mm), Grade

270 strands (Patzlaff et al. 2012). The experimental investigation included fabrication and testing of 8 T-girders and 3 NU-1100 girders. Transfer length was measured using concrete surface strains along with the AMS method. Development was measured for all girders by performing bending tests with the predicted development length by AASHTO equation.

The T-girders had an overall depth of 24 in. (610 mm) and were 28 ft (8.53 m) in length. These girders were cast with high strength concrete which had compressive strengths of 8.7 ksi - 9.6 ksi (60.0 MPa - 66.2 MPa) at 1 day, and 9.0 ksi - 13.5 ksi (62.1 MPa - 93.1 MPa) at 28 days. Each girder contained 6 – 0.7 in. (17.8 mm), Grade 270 (1860) prestressing strands which were tensioned to $0.75f_{pu}$ (where f_{pu} is the ultimate strength of prestressing strand). These strands were place into two rows with a strand spacing of 2 in. by 2.0 in. (51 mm by 51 mm). The confinement reinforcement was varied for each beam. The measured transfer lengths at release varied from 19 in. to 25 in. ((475 mm to 625 mm), and the average transfer length was 23.3 in. (532 mm). It was concluded that the amount and distribution of confinement reinforcement had no significant influence on transfer length.

The NU-1100 girders had an overall depth of 43.3 in. (1,100 mm) and were 40-ft (12.19 m) in length. These girders were cast with SCC which had compressive strengths of 7.8 ksi (54 MPa) at 1 day and 10.0 ksi (69.0 MPa) at 28 days. Each girder contained 34 – 0.7 in. (17.8 mm), Grade 270 (1860) prestressing strands which were tensioned up to 75% of the ultimate strength. These strands were placed at spacing of 2.0 in. by 2.0 in. (51 mm by 51 mm). The confinement reinforcement was placed according to requirement of 2008 Nebraska Department of Roads and Bridge Operations and AASHTO LRFD 4th. Transfer length measurements were not conducted for the I-girders.

Bending tests were used to evaluate development length for all T-girders and NU-1100 girders. The development length predicted by AASHTO equation was used as the embedded length for the bending tests. A multiplier of 1.6 was used because the depths of these girders were greater than 24 in. (610 mm). The experimental results indicated that all girders achieved the nominal moment capacity by using the predicted development length. The authors determined the amount of confinement reinforcement had no effect on the moment capacity, but the distribution of confinement reinforcement enhanced the ductility of pretensioned girders.

2.6.3.5 Maguire et al. (2013)

The study presented the structural performance of 2 double-Tee girders using high strength concrete, welded wire reinforcement, and 0.7 in. (17.8 mm), Grade 270 (1860) prestressing strands (Maguire et al. 2013). Two full-scale 50 ft (15.24 m) in length double-Tee girders were used to measure transfer length, development length, and shear strength. These girders used SCC which had compressive strength of 12.0 ksi (83.0 MPa) at 1 day and 15.0 ksi (103.0 MPa) at 28 days. Ten 0.7 in. (17.8 mm) prestressing strands were placed at spacing of 2 in. by 2.0 in. (51 mm by 51 mm) in each single-Tee of the girders. The strands were tensioned up to $0.60f_{pu}$ (where f_{pu} is the ultimate strength of prestressing strand) of the ultimate stress instead of $0.75f_{pu}$ due to the limited capacity of prestressing bed.

Transfer length was measured using concrete surface strains along with the AMS method. However, the concrete strain profiles were measured at the top flange of the double-Tee girders instead of at the centroid of prestressing strands due to the presence of forms at the time of release. The average measured transfer length at release was 16.5 in. (419 mm) which was less than the transfer length predicted by ACI 318 (2011) and AASHTO (2012) equation, 35 in. (889 mm) and 42 in. (1067 mm), respectively. Bending tests were used to determine development

length. The development length predicted by AASHTO was used as the tested embedment lengths. Experimental results indicated that the AASHTO equation is adequate to predict development length of 0.7 in. (17.8 mm) strands.

2.6.3.6 Arab (2012)

This study used the finite element method to investigate an applicable spacing of 0.7 in. (17.8 mm), Grade 270 (1860) prestressing strands (Arab 2012). The prestressing strands were modeled as small elements which were accommodated in concrete host elements using two techniques: (1) embedment technique and (2) extrusion technique. For the embedment technique, the strand was modeled as truss elements which were only in compression or tension. The displacement of the truss elements was dependent on the transitional degree of freedom of the host elements. For the extrusion technique, the strand was modeled as solid elements which were able to slip in the host elements. The slippage of the prestressing strand was dependent on the friction between the prestressing strand and the adjacent concrete. Friction coefficients of 0.7 and 1.4 were used for the embedment technique. Based on the proposed techniques, the effects of strand spacing and the amount of confinement reinforcement on the transfer length were investigated on two finite element models: (1) a single prestressing strand embedded at the center of a rectangular prism, (2) a group of nine prestressing strands embedded at the center of a larger rectangular prism. The analytical results were compared with experimental results collected from Akhnoukh's study (2008).

The first finite element model aimed at evaluating the transfer length predicted by AASHTO equation and the effect of confinement reinforcement on transfer length of 0.7 in. (17.8 mm) prestressing strands. A single of prestressing strand was placed at the center of a prism specimen of 7 in. by 7 in. by 96 in. (178 mm by 178 mm by 2438 mm). Four prism

specimens were modeled with different amounts of confinement reinforcement. The confinement reinforcement consisted of No.3 bars which spaced at 3 in. (76 mm), 6 in. (152 mm), 9 in. (229 mm), and 12 in. (305 mm), respectively. The concrete which had compressive strengths of 3.0 ksi (20.7 MPa) at 1 day was used for all specimens. The analytical results achieved from the embedment technique and the extrusion technique were similar to the experimental results of Akhnoukh'study (2008). It was determined that the amount of confinement reinforcement had no significant effect on transfer length, and the average anticipated transfer length varied from 24 in. (610 mm) to 42 in. (1,067 mm) which is shorter than or equal to the transfer length predicted by AASHTO (2012).

The second finite element model investigated applicable strand spacing of 0.7 in. (17.8 mm) strands using the extrusion technique with different friction coefficients of 0.7 and 1.4. A group of nine prestressing strands were modeled with different strand spacing and different amounts of confinement reinforcement. The prism specimens were 11 in. by 11 in. by 240 in (280 mm by 280 mm by 6096 mm). The prestressing strands were placed at spacing of 2.8 in. by 2.8 in. (71 mm by 71 mm) which is equivalent to four times the strand diameter, and 2.0 in. by 2.0 in. (51 mm by 51 mm) which is currently using for 0.6 in. (15.2 mm) strands. The concrete had compressive strengths of 8.0 ksi (55.2 MPa) at 1 day. The analytical results indicated that the difference in amount of confinement reinforcement had no effect on transfer length. For strand spacing, it was determined that 0.7 in. (17.8 mm) prestressing strands can be placed at spacing of 2.0 in. by 2.0 in. (51 mm by 51 mm) for concrete having compressive strengths of 10.0 ksi (68.9 MPa) or greater at the time of releasing of the strands.

2.7 Conclusion

The ACI 318 and AASHTO specifications of transfer length, development length, strand spacing were established based on experimental results of pretensioned girders cast with 0.5 in. (12.7 mm), Grade 250 (1760) prestressing strands and CC. These specifications were revised when 0.6 in. (15.2 mm), Grade 270 (1860) strands were used in pretensioned members. The revised specifications are used in current practice. A number of studies have been performed to confirm the adequacy of the current specifications for 0.5 in. (12.7 mm) and 0.6 in. (15.2 mm) strands. However, limited research has been conducted to investigate the applicability of the current specifications for 0.7 in. (17.8 mm), Grade 270 (1860) prestressing strands.

In terms of concrete, SCC is a recent development in concrete industry, and has more advanced features than CC. Several studies have been conducted to investigate the bond strength of prestressing strands with SCC which may be greater, comparable, or lower than with CC. This study provides a unique investigation regarding the transfer length, development length, and applicable strand spacing of 0.7 in. (17.8 mm) prestressing strands. Both CC and SCC which have a wide range of compressive strengths are investigated. Therefore, the results of this study will further the application of SCC and 0.7 in. (17.8 mm) prestressing strands in bridge construction.

Several studies have investigated transfer length, development length, and applicable spacing of 0.7 in. (17.8 mm) strands as discussed in the introduction section. Most of these studies were conducted on the members having a depth equal to or greater than 24 in. (610 mm) which include a multiplier of 1.6 for the development equation. This study represented for the members having a depth less than 24 in. (610 mm) in which the development length equation would not include the multiplier. The measured transfer lengths for these members may be

longer than for the members having a depth equal to or greater than 24 in. (610 mm) (Russell and Burns 1993).

CHAPTER 3 : EXPERIMENTAL PROGRAM

3.1 Introduction

The experimental program consisted of five tasks. Task 1 focused on designing four concrete mixtures including two normal strength and two high strength concrete mixtures. Task 2 aimed at quantifying the strand surface conditions using STSB. Task 3 consisted of fabricating 24 pretensioned concrete beams using the designed concrete mixtures. Task 4 measured transfer lengths for all beams at release, and at 7, 14, 21, and 28 days. Strand end-slip was also measured to determine transfer length at release. The final task concentrated on determining development length by conducting bending tests after the beams had reached 28 days of age.

3.2 Mix design

3.2.1 Overview

High strength concrete is widely used in bridge construction. Russell et al. (1997) recommended the concrete compressive strength used for bridge girders should be greater than 8 ksi (55.2 MPa). The researchers also indicated that the use of 0.7 in. (17.8 mm) prestressing strands at spacing of 2.0 in. by 2.0 in. (51 mm by 51 mm) and concrete compressive strength of 10 ksi (69.0 MPa) in bulb-tee girder (BT-72) results in the longest span and the most cost-effective design compared to the use of 0.5 in. (12.7 mm) and 0.6 in. (15.2 mm) strands. Morcous et al. (2011a) determined that the use of 0.7 in. (17.8 mm) prestressing strands and high strength concrete presents significant enhancements in bridge construction. These enhancements include increasing moment capacity, lengthening girder span, or extending girder spacing.

3.2.2 Mixture proportions

Four concrete mixtures were designed to cast the pretensioned concrete beams. All concrete mixtures had compressive strength at 28 days greater than 8 ksi (55.2 MPa) as recommended (Russell et al. 1997). These mixtures included: (1) normal strength, conventional concrete (N-CC), (2) high strength, conventional concrete (H-CC), (3) normal strength, self-consolidating concrete (N-SCC), and (4) high strength, self-consolidating concrete (H-SCC). The normal strength group (N-CC and N-SCC) had targeted compressive strengths of 6 ksi (41.4 MPa) at 1 day and 9 ksi (62.1 MPa) at 28 days. For H-SCC, the targeted compressive strengths were 8 ksi (55.2 MPa) at 1 day and 10 ksi (69.0 MPa) at 28 days. For H-CC, the targeted compressive strengths were 9 ksi (62.1 MPa) at 1 day and 13 ksi (89.6 MPa) at 28 days. The mixture proportions and concrete compressive strengths are presented in **Table 3.1**.

Table 3.1 – Concrete mixtures

Material	H-CC	N-CC	H-SCC	N-SCC
Cement (lb/yd^3)	700	700	825	775
Coarse aggregate (lb/yd^3)	1678	1678	1406	1406
Fine aggregate (lb/yd^3)	1454	1363	1392	1485
Water (lb/yd^3)	245	280	330	310
Water / Cement ratio	0.35	0.40	0.4	0.4
High range water reducer (fl oz/cwt)	5 – 6	5 – 6	9 – 10	9 – 10
Targeted compressive strength at 28 days (ksi)	13	9	10	8

(Note: 1 yd^3 = 0.765 m^3; 1 lb = 0.454 kg; 1 cwt = hundred weight = 100 lb; 1 fl oz = 29.57 mL; 1 ksi = 6.895 MPa)

For CC group (N-CC and H-CC), which had slumps of 9 in. to 10 in. (230 mm to 250 mm), a mechanical vibrator was used to ensure proper consolidation. For SCC group (N-SCC and H-SCC), the mixtures were able to flow and fill the form without needing vibrator. Several tests were conducted to evaluate the filling ability, passing ability, and segregation resistance of the fresh concrete mixtures as shown in **Table 3.2**. The test results were compared with the recommended thresholds of SCC used for prestressed concrete bridge members (Khayat and

Mitchell 2009). The filling ability was determined by slump flow test (ASTM C1611 2014) and T_{20} (T_{500}) (ASTM C1611 2014). The slump flow varied from 22 in. to 26 in. (560 mm to 660 mm). The lower bound of slump flow was slightly less than the recommended range of 23.5 in. – 29.0 in. (600 mm – 740 mm). The T_{20} (T_{500}) was in a range of 2.0 – 4.0 seconds which showed a good agreement with the recommended range of 1.5 – 6.0 seconds. The passing ability was determined by the J-Ring test (ASTM C1621 2014). The J-Ring test results varied from 0 in. to 2.5 in. (0 mm to 64 mm) which was within the recommended range of 0 – 3 in. (0 – 75 mm). For the segregation resistance, the Visual Stability Index (VSI) varied from 0 to 1 which indicated that the fresh SCC mixtures showed no evidence of segregation and little to no evidence of bleeding.

Table 3.2 – Concrete properties

Beam	Fresh concrete properties				
	Slump flow (in.)	T_{20} or T_{500} (sec)	J-Ring (in.)	Slump flow – J-Ring (in.)	VSI
N-SCC-S1 and N-SCC-S2	26	2	24.5	1.5	1
N-SCC-S3 and N-SCC-S4	24	2	23	1	0
H-SCC-S1 and H-SCC-S2	22	5	20	2	1
H-SCC-S3 and H-SCC-S4	25	2	23.5	1.5	1
H-SCC-D1 and H-SCC-D2	24	2	21.5	2.5	1
H-SCC-D3 and H-SCC-D4	25	1	25	0	0
Khayat and Mitchell (2009)	23.5 – 29	1.5 – 6	21.5 – 26	0 – 3	0 – 1
ACI 237 (2007)	18 – 30	2 – 5	N/A	N/A	0 – 1

(Note: N/A = not available; T_{20} or T_{500}= time required for the slump flow to reach a diameter of 20 in. or 500 mm; VSI = visual stability index; 1 in. = 25.4 mm)

3.2.3 Concrete compressive strengths

The concrete compressive strengths at release of prestressing strands (approximately 1 day), at 28 days, and at the times of conducting bending tests are summarized in **Table 3.3**. The average compressive strengths of each concrete mixture are presented in **Figure 3.1**. The columns indicate the measured concrete compressive strengths, and the cross lines represent the targeted concrete strengths. In particular, the average concrete strengths at release varied from

approximately 5.9 ksi (40.7 MPa) to 9.8 ksi (67.6 MPa). The concrete compressive strengths at 28 days were slightly smaller or greater than the targeted strengths for all concrete mixtures. The variation ranged from -2% to 15%. The concrete compressive strengths at the times of conducting bending tests were measured to determine the nominal moment capacity for each beam. These compressive strengths were by 0% to 9% higher than the strengths at 28 days.

Table 3.3 – Concrete compressive strengths

Beam	Concrete compressive strengths		
	f'_{ci} (ksi)	f'_c (ksi)	f'_{ct} (ksi)
N-CC-S1 and N-CC-S2	5.9	9.3	9.7
N-CC-S3 and N-CC-S4	6.6	9.7	10.5
H-CC-S1 and H-CC-S2	9.5	13.7	14.2
H-CC-S3 and H-CC-S4	8.9	13.2	12.8
H-CC-D1 and H-CC-D2	9.7	12.3	13.9
H-CC-D3 and H-CC-D4	9.9	13.3	13.8
N-SCC-S1 and N-SCC-S2	5.8	8.8	9.1
N-SCC-S3 and N-SCC-S4	6.1	9.6	9.7
H-SCC-S1 and H-SCC-S2	8.1	11.0	11.4
H-SCC-S3 and H-SCC-S4	7.8	10.4	10.7
H-SCC-D1 and H-SCC-D2	7.7	10.2	10.6
H-SCC-D3 and H-SCC-D4	8.1	10.6	10.0

(Note: f'_{ci} = concrete compressive strength at release; f'_c = concrete compressive strength at 28 days; f'_{ct} = concrete compressive strength at time of testing; 1 ksi = 6.895 MPa)

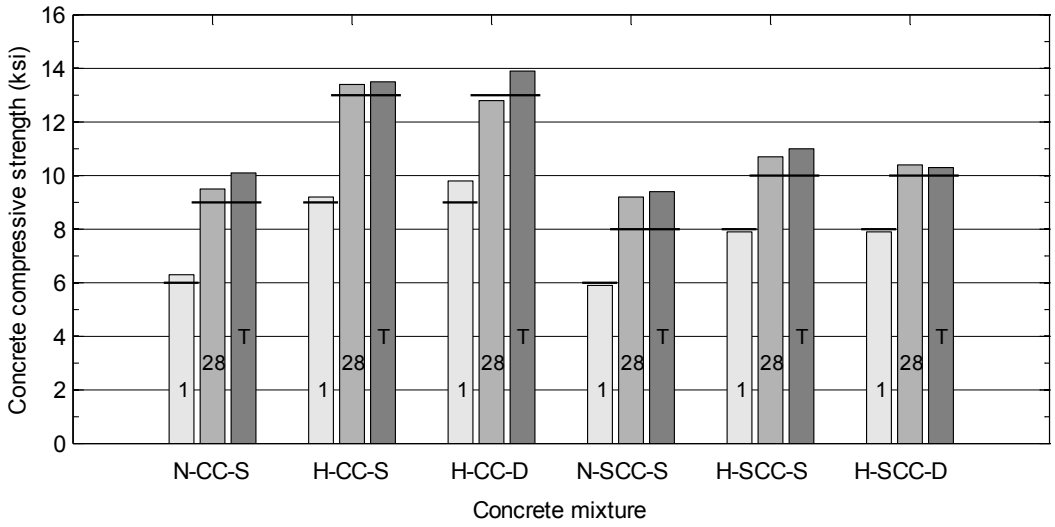

Figure 3.1 – Average concrete compressive strengths.
(Note: The number in each column represents the time at which concrete compressive strength was measured; *T* = at the time of conducting bending tests; 1 ksi = 6.895 MPa)

3.3 Beam specimen testing

3.3.1 Beam fabrication

Twenty-four pretensioned concrete beams were cast at the Engineering Research Center (ENRC). Each beam had a cross-section of 6.5 in. by 12 in. (165 mm by 305 mm) and a length of 18 ft (5.5 m). The beams were cast with one or two 0.7 in. (17.8 mm), Grade 270 (1860) prestressing strands. For the beams using one prestressing strand (**Figure 3.2**), the strand was placed at a distance of 10 in. (254 mm) and two No. 5 (No. 16) reinforcing bars were placed at a distance of 2 in. (51 mm) from the top fiber of the beam. For the beams using two prestressing strands (**Figure 3.3**), the strands were placed at a distance of 10 in. (254 mm) from the top fiber of the beam and at spacing of 2 in. (51 mm) from center-to-center. Two No. 6 (No. 19) reinforcing bars were placed at a distance of 2 in. (51 mm) from the top fiber of the beam. The placement of reinforcing bars aimed at controlling the anticipated tensile stresses which may induce cracks on the top fiber of the beams at release.

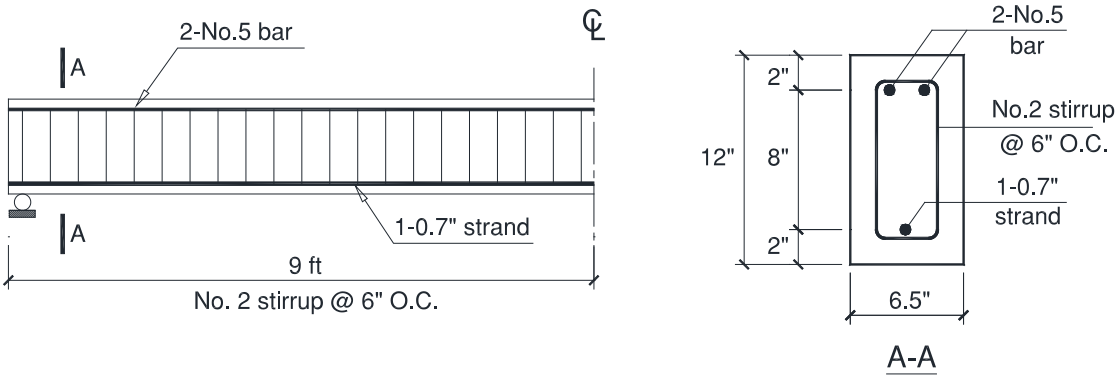

Figure 3.2 – Section properties of the beams using one prestressing strand
(Note: 1 in. = 25.4 mm; 1 ft = 305 mm; No. 5 = No. 16; 0.7 in. strand = 17.8 mm strand)

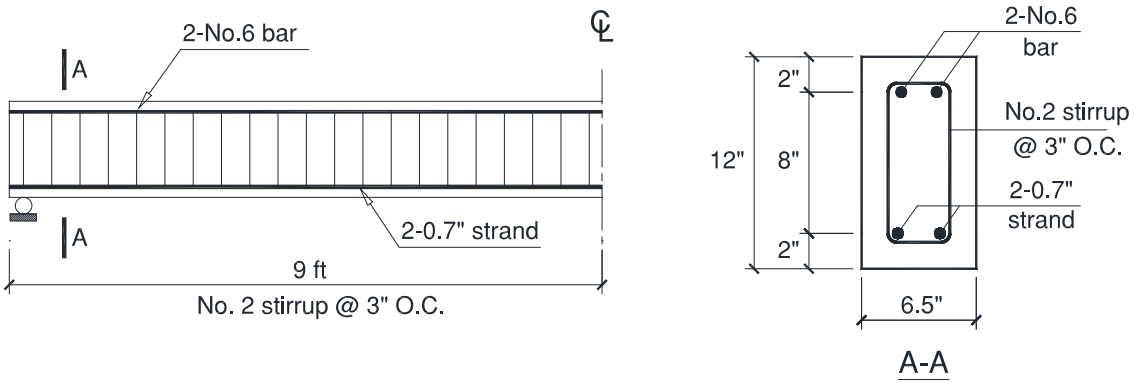

Figure 3.3 – Section properties of the beams using two prestressing strands
(Note: 1 in. = 25.4 mm; 1 ft = 305 mm; No. 6 = No. 19; 0.7 in. strand = 17.8 mm strand)

The shear reinforcement was designed according to ACI 318 specifications (2011). Each beam had different amount of required shear reinforcement due to the variation of concrete compressive strengths. In this study, however, the shear reinforcement was selected identically for all beams to decrease fabrication time as shown in **Figure 3.2** and **Figure 3.3**. Shear reinforcement consisted 0.25 in. (6.4 mm) smooth bars spaced at 6.0 in. (152 mm) and 3 in. (76 mm) along the entire beam length for the beams using one and two prestressing strands, respectively.

Prior to casting, the prestressing strand was tensioned to $0.75f_{pu}$ (where f_{pu} is the ultimate strength of prestressing strand), 202.5 ksi or 1396 MPa. At the dead end, the prestressing strands were anchored by chucks as shown in **Figure 3.4**. At the live end, the prestressing strands were tensioned using hydraulic actuator as shown in **Figure 3.5**. Thin plastic sheets were placed inside the forms to facilitate the removal of the forms and to hold the moisture as the concrete cured in the forms as shown in **Figure 3.6**. A pair of beams was simultaneously cast on a 50 ft (15.24 m) prestressing bed using one concrete batch of 0.9 yd^3 (0.7 m^3) as shown in **Figure 3.7**. Therefore, the concrete compressive strength was identical for each pair of beams (**Table 3.3**).

Figure 3.4 – Anchor prestressing strand using chucks (dead end).

Figure 3.5 – Tension prestressing strands using hydraulic actuator (live end).

Figure 3.6 – Beam preparation.

Figure 3.7 – Casting concrete.

3.3.2 Transfer length measurements

After removing forms, approximately 20 hours after casting the concrete, target points were glued onto the surface of the beams at the level of prestressing strand as shown in **Figure 3.8** and **Figure 3.9**. The first point was placed at 1 in. (25 mm) from the beam end and the subsequent points were spaced at 4 in. (102 mm) for the first 60 in. (1524 mm). The concrete strains were obtained using the Demountable Mechanical Strain Gauge (DEMEC). The initial reading was taken two hours after the target points were affixed to the concrete. Three 4 in. by 8

in. cylinders (102 mm by 204 mm) were tested to evaluate the concrete compressive strength before release of the prestressing strand. The prestressing strand was gradually detensioned 24 to 26 hours after casting and moved to a storage area at ENRC. The sequential readings were conducted immediately after release, and at 7, 14, 21 and 28 days.

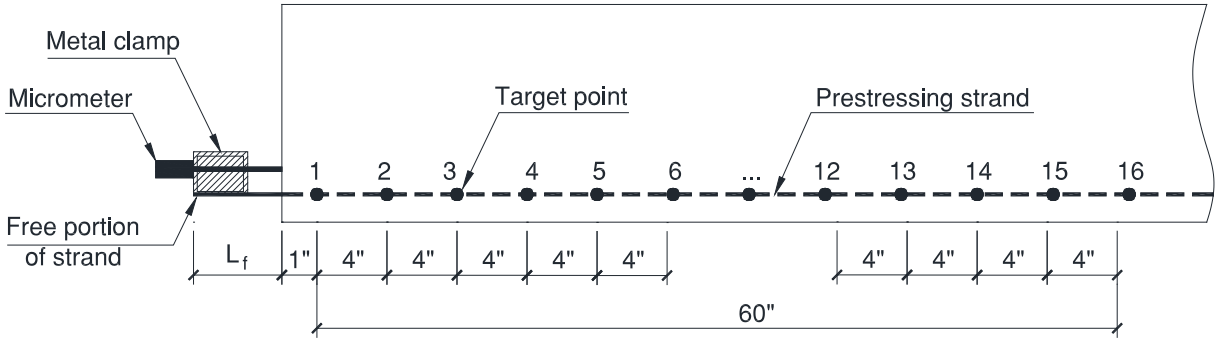

Figure 3.8 – Attachment of target points.
(Note: L_f is the end of the free portion of strand; 1 in. = 25.4 mm)

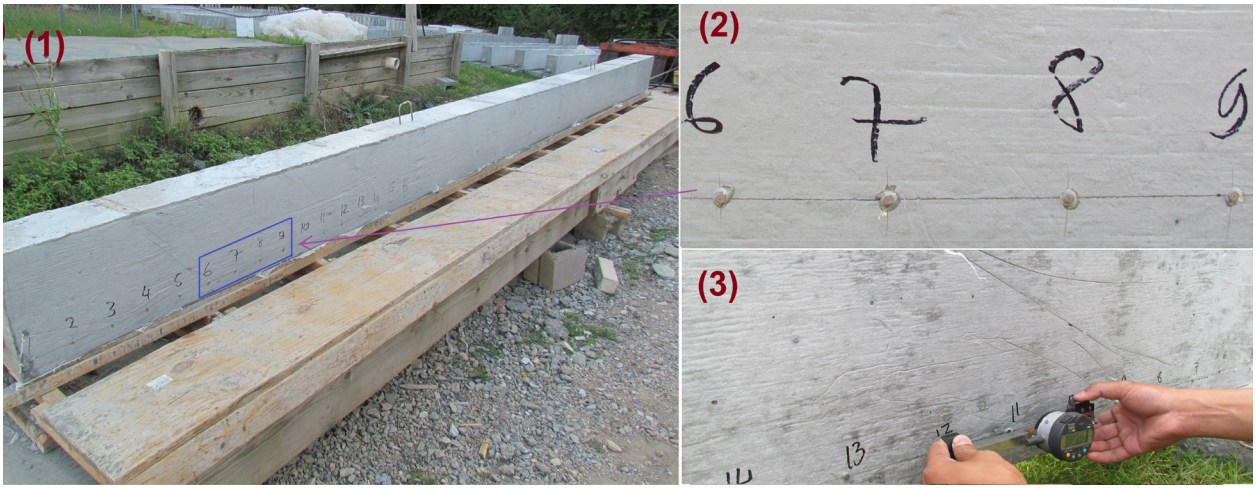

Figure 3.9 – Transfer length measurement. (1) The attachment of target points on the surface of a pre-tensioned concrete beam after removing the form; (2) A set of target points at spacing of 4 in. (100 mm); (3) The use of mechanical strain gauge to measure concrete strains.

The gradual detensioning technique was used instead of the flame cut (or sudden transfer) because of two reasons. Firstly, transfer lengths of 0.7 in. (17.8 mm) prestressing strands were measured on the pretensioned concrete beams which had a relatively small cross-section in

comparison to full-scale bridge girders. The use of gradual detensioning technique reduces the shock of transferring energy in the prestressing strand to the beam. Secondly, the gradual detensioning technique does not yield the worst case for release of the prestressing strand (Russell and Burns 1993), but it reduces the damage to the bond between the prestressing strand and the adjacent concrete at the live end of the beam. After detensioning the prestressing strand to an age of 28 days, there were no cracks on the top fiber of the beams. The concrete adjacent the prestressing strand had no sign of splitting cracks.

Concrete strains were measured two times independently for each side of the beam ends. The DEMEC readings were recorded at a precision of 10 microstrains. In total, four sets of concrete strains were attained for each beam end. The measured concrete strains were averaged after using a three point moving average (see Eq. 3.1) to smooth the data. The attained concrete strain profiles were used along with the 95% Average Maximum Strain (AMS) method to determine transfer length for each specimen (Russell and Burns 1997; Oh and Kim 2000). A detail explanation regarding the utilization of the three point moving technique and the AMS method was given by Gross and Burns (1995) and Russell and Burns (1993). It should be noted that two smoothed data points were missing due to the application of smoothing technique. These points were at the beginning and ending of a set of target points which were located at 1 in. (25 mm) and 61 in. (1,550 mm) from the beam end.

$$\varepsilon_i^{smoothed} = \frac{\varepsilon_{i-1} + \varepsilon_i + \varepsilon_{i+1}}{3} \tag{3.1}$$

where ε_{i-1}, ε_i, ε_{i+1} are the raw data at $i-1$, i, $i+1$ measurement, respectively; $\varepsilon_i^{smoothed}$ is the smoothed data point at i measurement.

The use of AMS method relies on the determination of constant strain plateau. As shown in **Figure 3.10**, G1 is the initial point of the constant strain plateau, and G2 and G3 are two

consecutive points of G1. Point G1 was manually determined which based on the change in slopes of the concrete strain profile. In general, there is a significant change in slope between the G1G2 and G1G3 line. Therefore, the concrete strain profile can be divided into two plateaus: (1) the constant strain plateau, and (2) the linear strain plateau.

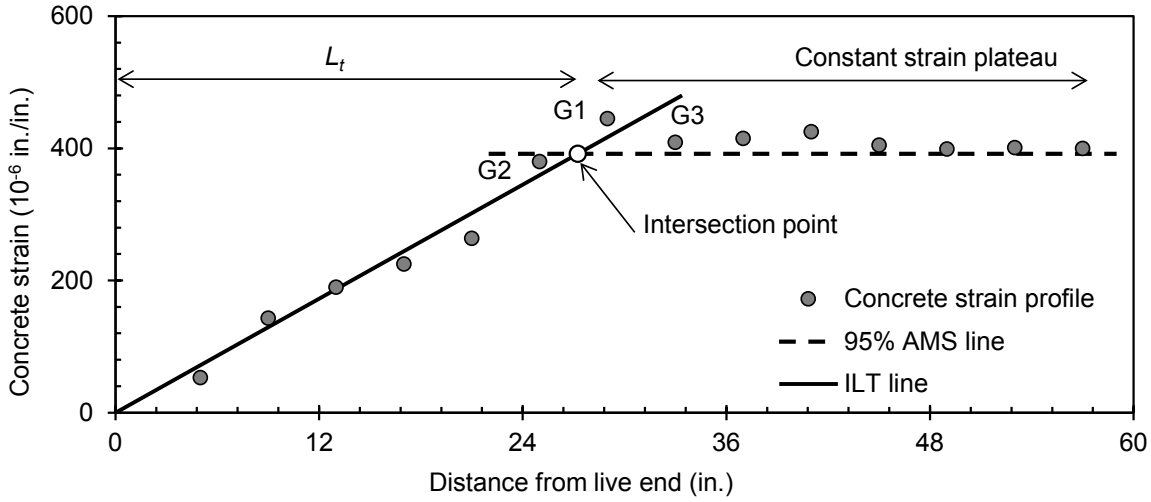

Figure 3.10 – Determination of transfer length.
(Note: L_t = transfer length; AMS = average maximum strain; ILT = initial linear trend; 1 in. = 25.4 mm)

Figure 3.10 illustrates the transfer length determination. The following steps were used to determine transfer length:

Step 1: Plot the concrete strain profile along the beam length.

Step 2: Determine the constant strain plateau to calculate the AMS value.

Step 3: Draw the 95% AMS line. This is the horizontal line passing through the 95% AMS value.

Step 4: Draw the initial linear trend (ILT) line. The ILT line passes through the origin and is the best-fit trend line of target points within the transfer zone.

Step 5: Determine the intersection of the 95% AMS line and the ILT line. Transfer length is the distance from the beam end to the intersection point.

Previous studies used the distance from the beam end to intersection of the concrete strain profile with the 95% AMS line as the defined transfer length (Gross and Burns 1995; Staton et al. 2009; Floyd et al. 2011b; Dang et al. 2014b). The advantage of using the ILT in determining transfer length is to reduce the effect of strain fluctuation near the end of transfer zone (Meyer et al. 2002) and to give more precise and consistent results (Carroll 2009). Each target point within the transfer zone has the same contribution in defining the ILT line. The use of the intersection of the 95% AMS line and the ILT line has been implemented to estimate transfer length in several studies (Morcous et al. 2011b; Maguire 2009; Patzlaff 2010; Morcous et al. 2013; Morcous et al. 2014) and has been applied in this study.

3.3.3 Strand end-slip measurement

In order to measure strand end-slip, a metal clamp was attached to the prestressing strand as shown in **Figure 3.11**. The initial and subsequent readings were conducted at the same time concrete surface strains were measured. The nominal end-slip (δ_n) was computed as the difference between the initial reading and the subsequent reading. Initial strand end-slip (δ) was determined by subtracting the elastic shortening (ES) of the free strand portion from the nominal end slip using Eq. 3.2 and 3.3.

$$ES = \frac{f_{pj} L_f}{E_p} \tag{3.2}$$

$$\delta = \delta_n - ES \tag{3.3}$$

where ES is the elastic shortening of the free portion of strand; L_f the length of the free portion of strand as shown in **Figure 3.8**; f_{pj} is the jacking stress; E_p is the modulus of elasticity of prestressing strand; δ_n is the nominal strand end-slip; δ is the initial strand end-slip.

Figure 3.11 – End-slip measurement.

3.3.4 Development length measurements

Bending test was used to evaluate development length of prestressing strands. A concentrated load was applied to the beam at a given distance from the beam end and increased until the beam failed. This distance is defined as the embedment length as shown in **Figure 3.12**. The determination of development length is an iterative procedure in which the beams are tested with different embedment lengths. The selection of initial embedment length may base on the development length predicted by the codes or by prior studies. In this study, the initial embedment length was approximately 50% to 60% of the predicted development length using ACI 318 equation. This was based on recommendations of study conducted by Floyd et al. (2011a) which used 0.6 in. (15.2 mm) prestressing strands and SCC.

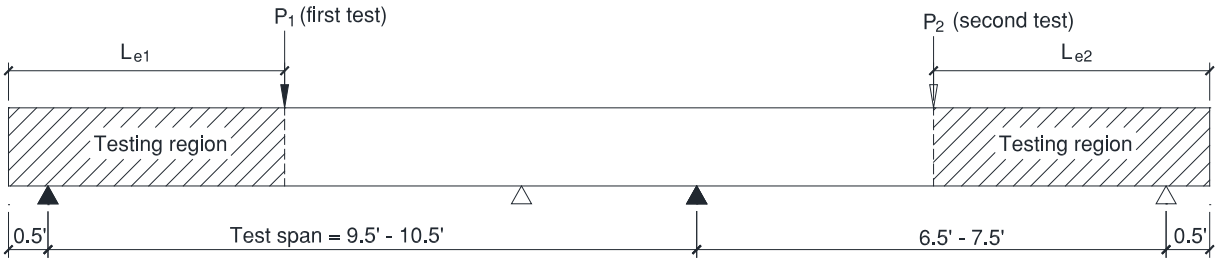

Figure 3.12 – Bending test setup.
(Note: P = concentric force; L_e = embedment length; 1 ft = 305 mm)

Three cylinders were tested to evaluate the concrete compressive strength before conducting the bending tests (**Table 3.3**). The strain compatibility method was used to calculate f_{ps} (where f_{ps} is average stress in prestressing steel at the time for which the nominal resistance of member is required). This value varied from $0.970f_{pu}$ to $0.989f_{pu}$ as shown in **Table A.7**. The AASHTO (2012) Refined method was used to predict prestress losses and calculate the effective strand stress (f_{pe}) at 28 days as summarized in **Table A.4**, **Table A.5**, and **Table A.6**. The effective strand stress ranged from $0.639f_{pu}$ to $0.688f_{pu}$. These stress values were used to calculate the nominal moment capacity shown in **Table A.7** and the predicted transfer and development lengths using ACI 318 or AASHTO equations as summarized in **Table A.8**.

The failure mode of a bending test was used to determine whether the tested embedment length is longer than the required development length. The required development length is the shortest embedment length at which the tested specimens exhibited flexural failure. The flexural failure is characterized by three requirements: (1) the measured moment capacity is equal or greater than the nominal moment capacity, (2) the prestressing strand experiences no slippage before the beam achieves the nominal moment capacity, and (3) the specimen exhibits large deformation before collapse. The third requirement is based on the ductile requirement of designing flexural members which need to show visible warning before collapse. The bond

failure was defined as the prestressing strand was slipped before the specimen achieved nominal moment capacity regardless of the measured moment and the specimen deflection. This was since the strand slippage is a sign of losing bond between the prestressing strand and concrete. The failure of PCMs due to losing bond strength is unpredictable and sudden.

Two bending tests were conducted for each beam as illustrated in **Figure 3.12**. Therefore, a total of 48 bending tests were performed for 24 pretensioned concrete beams. Initial tests were started with N-SCC-S beams and following tests were conducted for H-SCC-S, H-SCC-D, N-CC-S, H-CC-S, and H-CC-D beams. During a bending test, the strand slippage, beam deflection at the loading position, and hydraulic pressure were continuously monitored. In particular, the strand slippage was quantified using a linear variable differential transformer (LVDT) and the beam deflection was measured using a linear cable encoder (LCE) as shown in **Figure 3.13**. Hydraulic pressure was monitored using a pressure transducer connected to the hydraulic system. These devices were connected to a data acquisition system which transferred the received data to a computer.

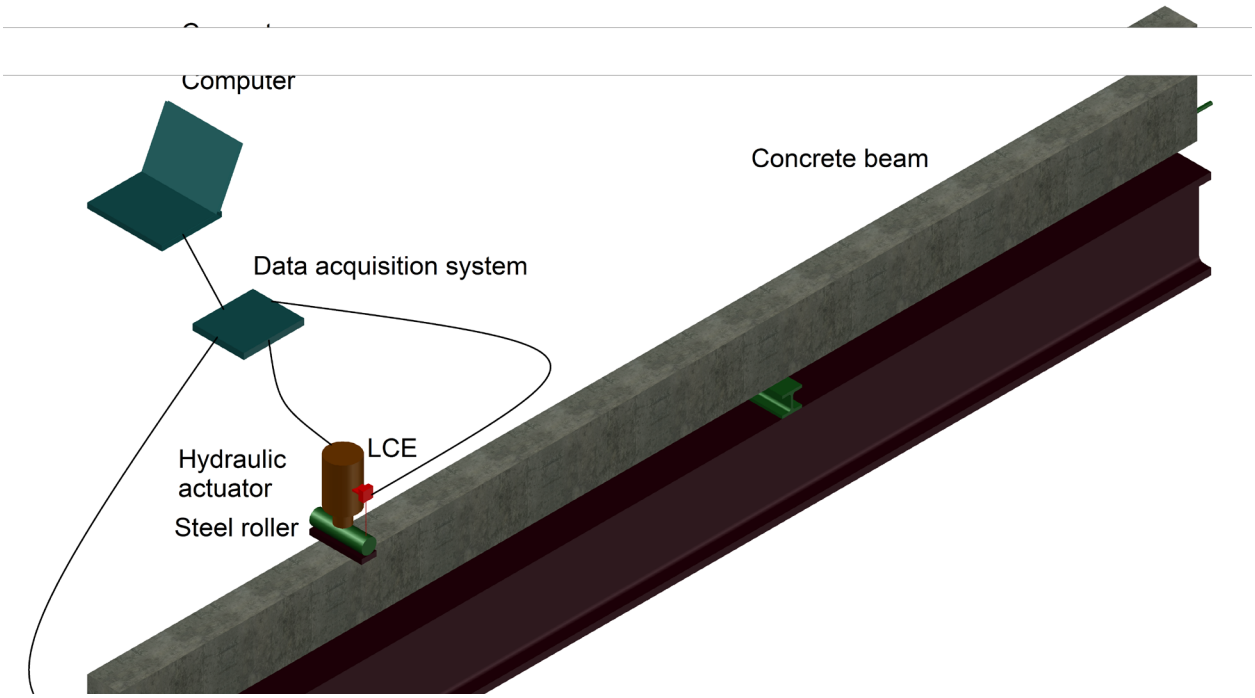

Figure 3.13 – Bending test frame.
(Note: LVDT = linear variable differential transformer; LCE = linear cable encoder)

CHAPTER 4 : TRANSFER LENGTH RESULTS

This chapter presents the measured transfer lengths and strand end-slips of 24 pretensioned concrete beams. The beams were fabricated with conventional concrete and self-consolidating concrete. The concrete strengths at 1 day ranged from 5.9 ksi to 9.8 ksi (40.7 MPa to 67.6 MPa). Transfer lengths were determined using concrete surface strains along with the Average Maximum Strain method. Initial strand end-slips were also measured for predicting transfer length at release using an empirical formula. Experimental results indicated ACI 318 and AASHTO specifications are applicable for estimating transfer length of 0.7 in. (17.8 mm) strands at release and at 28 days. A coefficient of 2.38 was the most appropriate value for estimating transfer lengths at release from initial strand end-slips.

4.1 Measured transfer lengths

Figure 4.1 shows the determination of transfer lengths at the live end of beam N-CC-2 at release and at 28 days. As shown in the figure, the concrete strain profiles fluctuated near the end of transfer zone, so it was not suitable to use this region for determining transfer length. The ILT line, however, best represents that strain measured by the target points within the transfer zone. The measured transfer length using this technique may be more or less than that using the first technique which used the distance from the beam end to intersection of the concrete strain profile with the 95% AMS line as the defined transfer length. The differences are dependent upon the fluctuation of the concrete strain profiles. The determination of transfer lengths for remaining beams is shown in Appendix B.1.

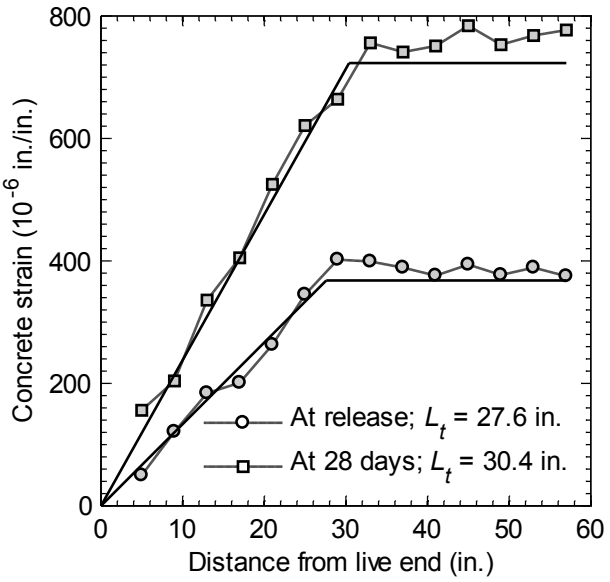

Figure 4.1 – Determination of transfer length at release at the live end of beam N-SCC-2. (Note: L_t = transfer length; 1 in. = 25.4 mm)

The measured transfer lengths at release at the live ends and the dead ends of 24 pretensioned concrete beams are shown in **Figure 4.2**. In general, there was no significant difference in the transfer lengths measured at the live ends and the dead ends. The measured transfer lengths were shorter than the transfer length predicted by ACI 318 (2011) and AASHTO (2012), $50d_b$ = 35 in. (890 mm) and $60d_b$ = 42 in. (1067 mm), respectively. As shown in the figure, the transfer length predicted by Eq. 1.1 and AASHTO were approximately 42 in. (1067 mm). Therefore, the ACI 318 and AASHTO equations of transfer length are applicable for 0.7 in. (17.8 mm) prestressing strands cast with CC and SCC which had compressive strengths at release varied from 5.9 ksi to 9.2 ksi (40.7 MPa to 63.4 ksi). The measured transfer length at 7, 14, 21, and 28 days for all beams are summarized in **Table B.1**and **Table B.2**.

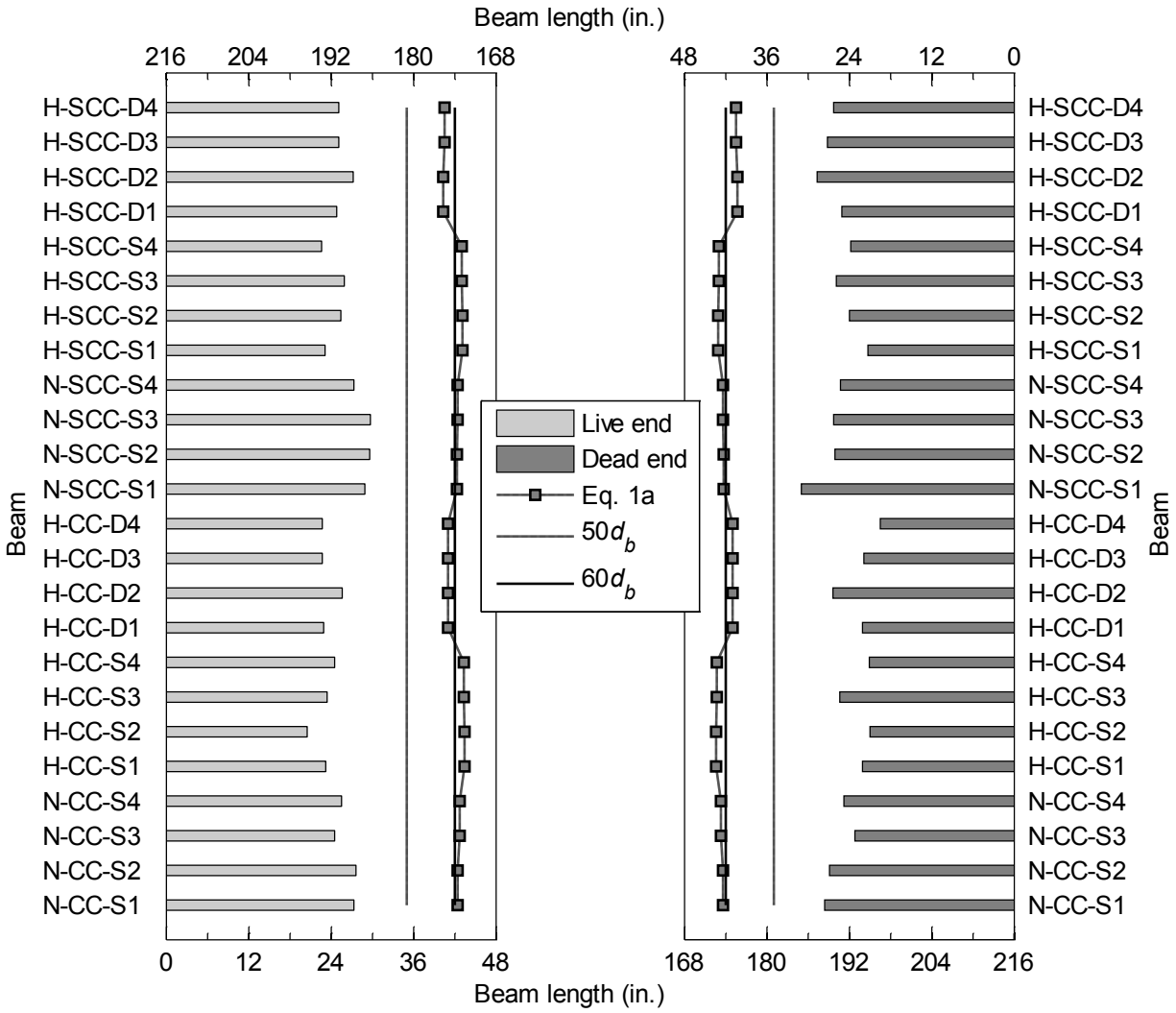

Figure 4.2 – Transfer length at release at the live ends and dead ends of 24 pretensioned concrete beams.
(Note: d_b = strand diameter; 1 in. = 25.4 mm)

4.2 Statistical transfer lengths

For a given beam group, the measured transfer lengths were assumed to be normally distributed. This assumption was applicable for the beams using the same type of prestressing strands and casting procedures. **Figure 4.3** shows the normal distribution of transfer lengths obtained from N-CC-S beams which had an average concrete compressive strength of 6.3 ksi

(43.2 MPa) at 1 day. A least squares estimation was used to calculate the lower bound and upper bound of the measured transfer lengths with a confidence interval of 95%. The 95% region is represented by the shaded area in the figure. This area was limited by the lower and upper bound of transfer lengths of 22.7 in. and 29.2 in. (575 mm and 741 mm), respectively. The figure indicates that 95% of the measured transfer lengths varied from 22.7 in. to 29.2 in. (575 mm and 741 mm). The upper bounds, lower bounds, and average transfer lengths of different beam groups at release, and 7, 14, 21, and 28 days are shown in **Figure 4.4**, and the detail calculation of these parameters are summarized in **Table B.3**.

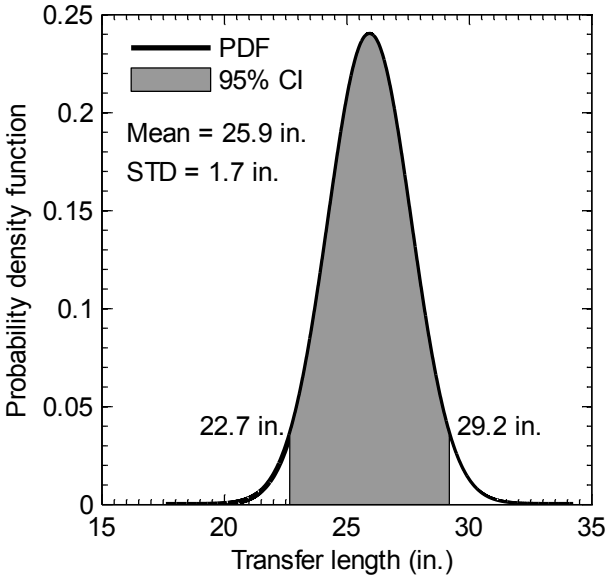

Figure 4.3 – Normal distribution model of the measured transfer lengths at release of N-CC-S beams.
(Note: PDF = probability density function; CI = confidence interval; STD = standard deviation; 1 in. = 25.4 mm)

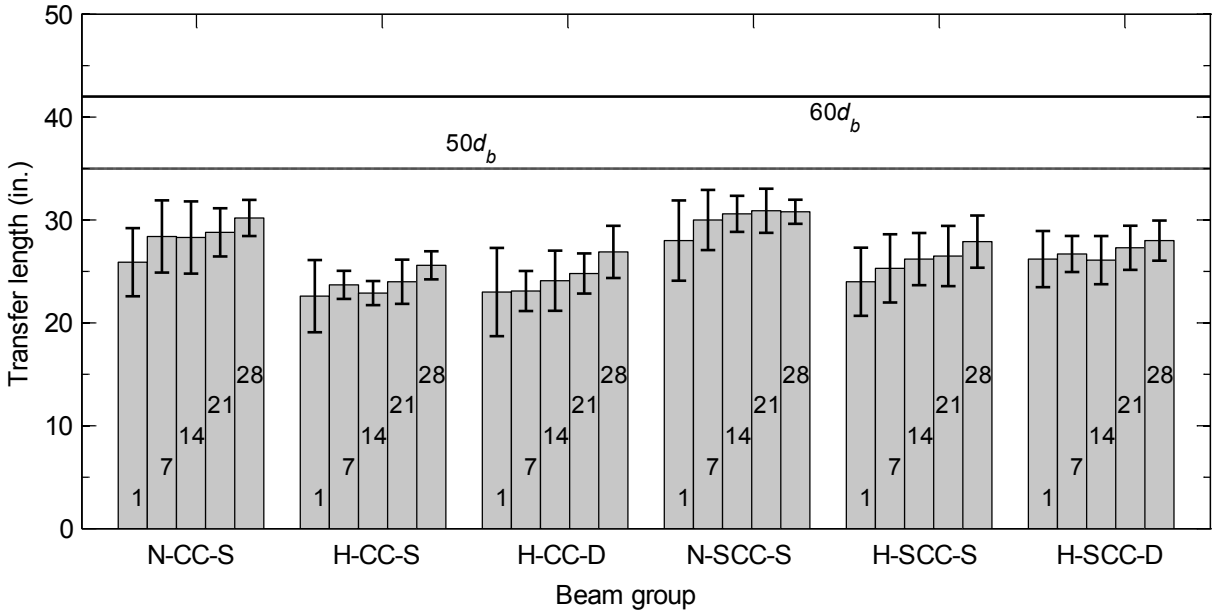

Figure 4.4 – Increase of transfer length over time
(Note: d_b = strand diameter; the number in each column indicates the time at which transfer lengths were measured; 1 in. = 25.4 mm)

4.3 Increase of transfer lengths by time

The increase of transfer lengths was observed for all beams. Barnes et al. (2003) determined the increase varied from 10% to 20% on average and was significant for the first four weeks after release. In this study, the observed increase varied from 7% to 17% which was slightly less than the reported values as shown in **Figure 4.4**. The types of concrete and concrete compressive strengths were likely independent factors in the increase. For normal concrete strength groups, the increase of transfer length for the N-CC-S beams was greater than for the N-SCC-S beams. For high strength concrete groups, the H-SCC-S beams experienced a greater increase than H-CC-S beams. For the beams using two prestressing strand, the H-CC-D beams experienced a greater increase than H-SCC-D beams.

Figure 4.4 also shows error bars of the measured transfer lengths at a specific time for each beam group. These error bars were calculated according to the upper bound and lower

bound of a normal distribution with a confidence interval of 95%. As shown in the figure, the ACI 318 equation ($50d_b$) and AASHTO equation ($60d_b$) overestimate the upper bounds of measured transfer lengths at 28 days. The transfer length predicted by ACI 318 equation (Eq. 1.1) was approximate with the transfer length predicted by AASHTO equation. In summary, the current specifications are applicable to predict transfer lengths of 0.7 in. (17.8 mm), Grade 270 (1860) prestressing strands for the first 28 days.

4.4 Transfer length comparison of CC and SCC

In this study, the N-CC-S and N-SCC-S beams had similar compressive strengths at release of 6.3 ksi (43.4 MPa) and 5.9 ksi (40.7 MPa), respectively. The difference in these strengths was approximately 7%, therefore, it was appropriate to compare the measured transfer lengths regardless of the effect of concrete compressive strength. The measured transfer lengths of these beams at release and at 28 days are shown in **Figure 4.4**. At release, the beams using SCC exhibited greater transfer lengths than those of the beams using CC. This finding was similar to the conclusion determined by Girgis and Tuan (2005). The average and maximum difference were 8% and 21%, respectively. At 28 days, however, transfer lengths measured on the beams using SCC and CC were similar. This indicated that the bond strength of prestressing strands with SCC was lower than that with CC at early age. At 28 days, however, there was no difference in the bond strength of prestressing strands with SCC and CC.

4.5 Effect of strand spacing

The effect of strand spacing on the measured transfer lengths are shown in **Figure 4.5**. The average transfer length of H-CC-D and H-CC-S beams was similar regardless of the

concrete compressive strength of H-CC-D beams was 7% greater than the concrete strength of H-CC-S beams. The H-SCC-S and H-SCC-D beams had an identical concrete compressive strength at release, but the average transfer length of H-SCC-D beams was 9% greater than that of H-SCC-S beams. Therefore, the use of 0.7 in. (17.8 mm) prestressing strands at spacing of 2 in. (51 mm) may increase transfer lengths at release. At 28 days, there was no difference in the measured transfer lengths between the beams using one and two prestressing strands as shown in **Figure 4.4**.

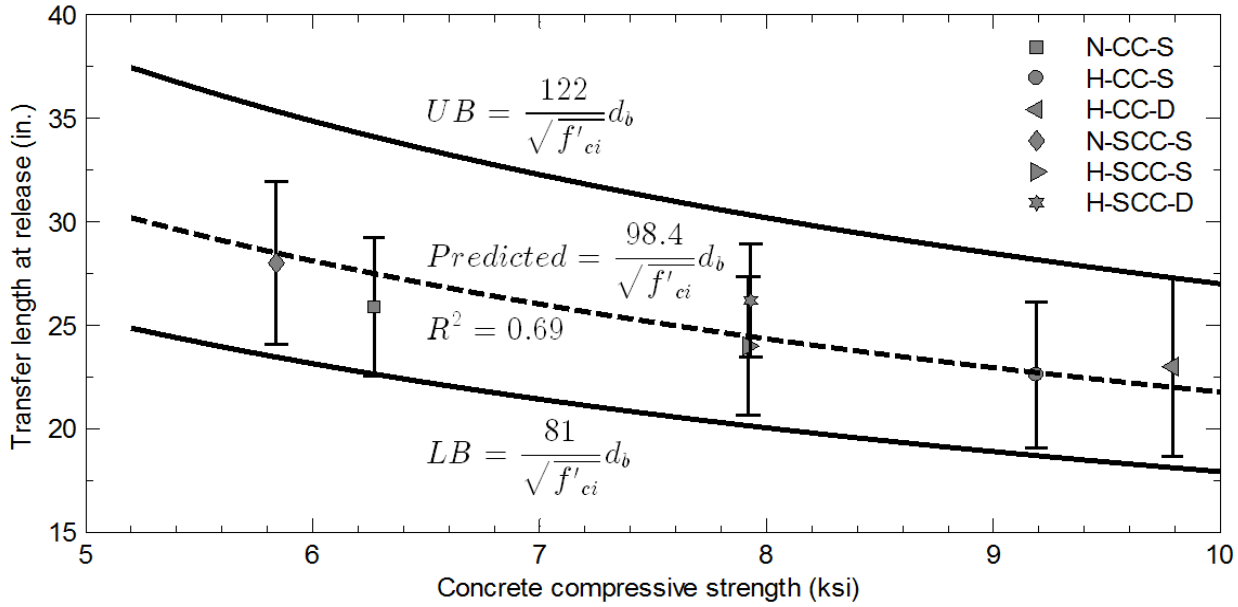

Figure 4.5 – Transfer lengths at release and concrete compressive strengths.
(Note: UB = upper bound; LB = lower bound; f'_{ci} is concrete compressive strength at 1 day and in ksi for the UB, LB, and predicted equations; 1 ksi = 6.895 MPa; 1 in. = 25.4 mm)

4.6 Effect of concrete compressive strengths

Figure 4.5 shows the upper bounds, lower bounds, and average transfer lengths of different normal distribution models. As shown in the figure, the average transfer lengths of 0.7 in. (17.8 mm) prestressing strands decreased as the concrete compressive strengths increased. This finding confirmed the effect of concrete compressive strength on the transfer length of

previous studies using 0.5 in. (12.7 mm) and 0.6 in. (15.2 mm) strands (Mitchell et al. 1993; Floyd et al. 2011b; Ramirez and Russell 2008; Martí-Vargas et al. 2012; Martí-Vargas et al. 2007b; Martí-Vargas et al. 2006). Mitchell et al. (1993) determined that transfer length at release can be predicted using Eq. 4.1. This equations indicated the transfer length of $50d_b$ predicted by ACI 318 is conservative for concrete having compressive strengths at release of 3 ksi (20.7 MPa) or greater.

$$L_t = \frac{86.6}{\sqrt{f'_{ci}}} d_b \tag{4.1}$$

where L_t is transfer length (in.); f'_{ci} is concrete compressive strength at 1 day (ksi); d_b is strand diameter (in.).

Ramirez and Russell (2008) proposed another equations for predicting the initial transfer length as shown in Eq. 4.2. These equations showed that the transfer length of $60d_b$ predicted by AASHTO is adequate for concrete having compressive strengths at release of 4 ksi (27.6 MPa) or greater.

$$L_t = \frac{120}{\sqrt{f'_{ci}}} d_b \geq 40d_b \tag{4.2}$$

where L_t is transfer length (in.); f'_{ci} is concrete compressive strength at 1 day (ksi); d_b is strand diameter (in.).

Using the experimental data from this study, an equations were proposed to predict transfer length at release for 0.7 in. (17.8 mm), Grade 270 (1860), prestressing strands as shown in Eq. 4.3. This equations considered the effect of concrete compressive strength on transfer length as discussed previously. The average transfer lengths of six beam groups shown in **Table 4.1** were used to determine the κ coefficient using a least squares estimation. A κ coefficient of 98.4 indicated the most appropriate value representing the relationship of transfer length at

release and concrete compressive strength with a coefficient of determination (R^2) of 0.69. This coefficient was 14% greater than the value proposed by Mitchell et al. (1993) , 86.6, and 18% smaller than the value proposed by Ramirez and Russell (2008), 120. The predicted equations were plotted as the dashed line in **Figure 4.5**.

$$L_t = \frac{\kappa}{\sqrt{f'_{ci}}} d_b \tag{4.3}$$

where L_t is transfer length (in.); f'_{ci} is concrete compressive strength at 1 day (ksi); d_b is strand diameter (in.); κ is a coefficient of the proposed transfer length equation.

Table 4.1 – Transfer length analysis

Beam group	f'_{ci} (ksi)	Transfer length		95% confidence interval		κ	
		Mean (in.)	STD (in.)	LB (in.)	UB (in.)	LB	UB
N-CC-S	6.3	25.9	1.7	22.7	29.2	81	104
H-CC-S	9.2	22.6	1.8	19.2	26.1	83	113
H-CC-D	9.8	23.0	2.2	18.7	27.3	84	122
N-SCC-S	5.9	28.0	2.0	24.0	32.0	84	112
H-SCC-S	7.9	24.0	1.7	20.7	27.3	83	110
H-SCC-D	7.9	26.2	1.4	23.4	28.9	94	116

(Note: f'_{ci} = concrete compressive strength 1 day; STD = standard deviation; UB = upper bound, LB = lower bound; κ = a coefficient of the proposed transfer length equation; 1 ksi = 6.895 MPa; 1 in. = 25.4 mm)

4.7 Proposed equation of transfer length

The upper bounds and lower bounds of the measured transfer lengths with a confidence interval of 95% are shown in **Figure 4.5**. These values were used to determine the corresponding bounds of the κ coefficient. The determined bounds of the κ coefficient required to satisfy all the bounds of the measured transfer lengths. The detailed calculations of the κ coefficient for each beam group are presented in **Table 4.1**. For the upper bound, the κ coefficient varied from 104 to 122. The maximum coefficient of 122, which was determined from transfer lengths of H-CC-D beam group, controlled the upper bound of the predicted

transfer length. This value was slightly smaller than a κ coefficient of 120 proposed by Ramirez and Russell (2008) for 0.5 in. (12.7 mm) and 0.6 in. (15.2 mm) strands. For the lower bound, the κ coefficient ranged from 81 to 94. The minimum coefficient of 81, which was determined from transfer lengths of N-CC-S beam group, controlled the lower bound of the predicted transfer length. The curves represented the upper bound and lower bound of the predicted transfer length are shown as solid lines in **Figure 4.5** and summarized in Eq. 4.4.

$$\frac{81}{\sqrt{f'_{ci}}} d_b \le L_t \le \frac{122}{\sqrt{f'_{ci}}} d_b \tag{4.4}$$

where L_t is transfer length (in.); f'_{ci} is concrete compressive strength 1 day (ksi); d_b is strand diameter (in.).

4.8 Initial strand end-slips

4.8.1 Measured initial strand end-slips

The measured strand end-slips are shown in **Figure 4.6**. The figure indicates that there were no apparent differences in the end-slips at the live ends and the dead ends. This was most likely due to the gradual release of the prestressing strands. **Figure 4.6** also presents the allowable strand end-slips (AESs) with different bond stress distribution (BSD) coefficient α. Researchers indicated that transfer lengths at release can be predicted from initial strand end-slips using Eq. 4.5 (Martí-Vargas et al. 2006; Russell and Burns 1996; Rose and Russell 1997). Therefore, the AESs were established based on a correlation of the empirical formula of transfer length and the transfer length of $50d_b$ predicted by ACI 318 as shown in Eq. 4.6. A prestressing strand experiencing an initial strand end-slip of δ_{all} is expected to exhibit a transfer length of

$50d_b$ as predicted by ACI 318. In the AES equations, the α coefficient is an empirical parameter and varies from 2.0 to 3.0 depending on the distribution of bond stress within the transfer zone. A coefficient of 2.0 represents a constant BSD, and a coefficient of 3.0 represents a linear BSD. As shown in **Figure 4.6**, most of the strand end-slips exceeded the AES using an α coefficient of 3.0, and none of them exceeded the AES using an α coefficient of 2.0. In particular, the measured end-slips were approximately 68% - 113% of the AES using an α coefficient of 3.0, and 45% - 75% of the AES using an α coefficient of 2.0.

$$L_t = \alpha\delta\frac{E_p}{f_{pt}} \tag{4.5}$$

$$\delta_{all} = \frac{50}{\alpha}\frac{f_{pt}}{E_p}d_b \tag{4.6}$$

where L_t is transfer length (in.); α is bond stress distribution coefficient; δ is initial strand end-slip (in.) as summarized in **Table B.4**; δ_{all} is allowable initial strand end-slip (in.) as summarized in **Table B.4**; f_{pt} is stress in prestressing steel immediately after transfer (ksi) as summarized **Table A.4**; d_b is strand diameter (in.); E_p is the modulus of elasticity of prestressing strand (ksi), 28800 ksi (198720 MPa).

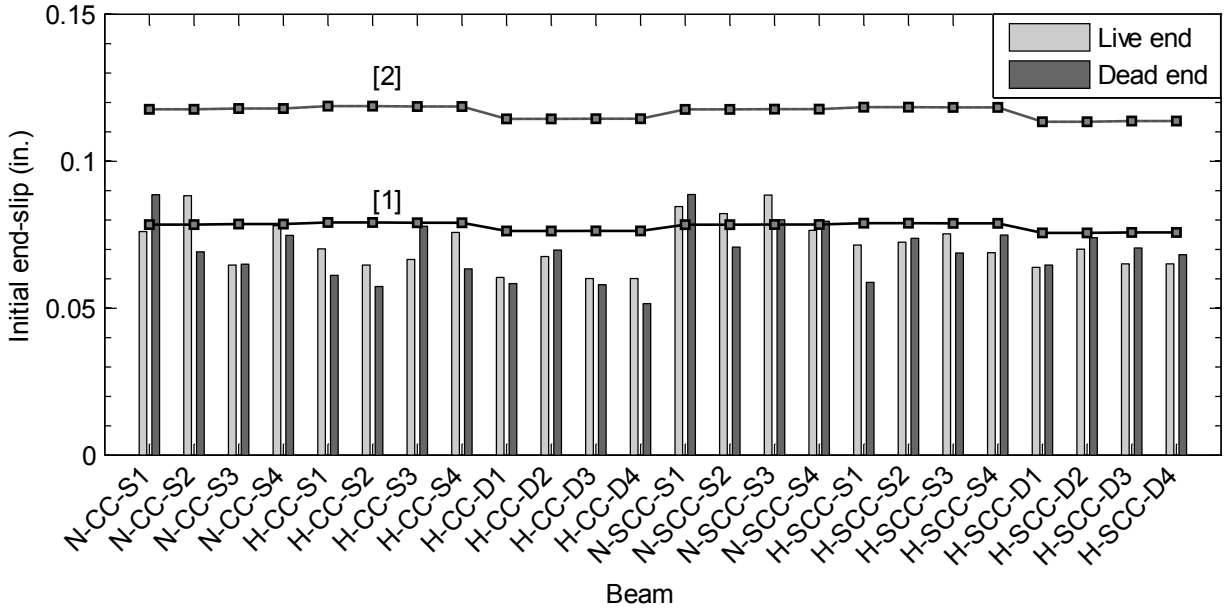

Figure 4.6 – Comparison of measured strand end-slips with the allowable strand end-slips calculated by different bond stress distribution coefficients.
(Note: [1] = allowable initial strand end-slip calculated with bond stress distribution coefficient of 3.0 as summarized in **Table B.4**; [2] = allowable initial strand end-slip calculated with bond stress distribution coefficient of 2.0 as summarized in **Table B.4**; 1 in. = 25.4 mm)

4.8.2 Predicted transfer length from initial strand end-slip

The first method used to determine transfer length was to measure concrete surface strains and use the AMS technique as discussed previously. Researchers indicated that this method provides a reliable measurement of transfer length (Russell and Burns 1993; Russell and Burns 1996; Russell and Burns 1997; Unay et al. 1991). An alternative method to estimate transfer length is derived from initial strand end-slips as discussed previously (see Eq. 4.5). This method is more simple and practical to quantify the transfer length because it is easier to measure strand end-slips than concrete surface strains (Park and Cho 2014). However, the accuracy of second method depends on an empirical coefficient of BSD, α. Previous studies showed that the α coefficient may vary from 2.0 to 3.0 (Martí-Vargas et al. 2007a).

Figure 4.7 shows the transfer lengths measured by the first method and the transfer lengths estimated by the second method. The estimated transfer lengths were represented by the shaded region with α coefficients ranging from 2.0 to 3.0. The lower and upper bound represented transfer lengths estimated with a coefficient of 2.0 and 3.0, respectively. A least squares method was used to determine the most appropriate α coefficient. The coefficient of determination, R^2, indicated the fit of the two sets of data, the measured and estimated transfer lengths. The relationship of R^2 and α coefficient is shown in **Figure 4.8**. For an α coefficient in a range of 2.0 to 2.2 and 2.55 to 3.0, the R^2 was negative which shows that the two sets of data were independent. For an α coefficient in a range of 2.2 to 2.55, the relationship of R^2 and α coefficient was represented by a nonlinear curve. The peak of the curve represented the most appropriate α coefficient for estimating transfer lengths from strand end-slips. As shown in **Figure 4.8**, the most appropriate α coefficient was 2.38 with a R^2 of 0.63. This coefficient was 3% smaller than the coefficient proposed by Martí-Vargas et al. (2007a) for 0.5 in. (12.7 mm), Grade 270 (1860) prestressing strands. The estimated transfer lengths at the dead ends and live ends of 16 pretensioned concrete beams using a coefficient of 2.38 were also plotted in **Figure 4.7**.

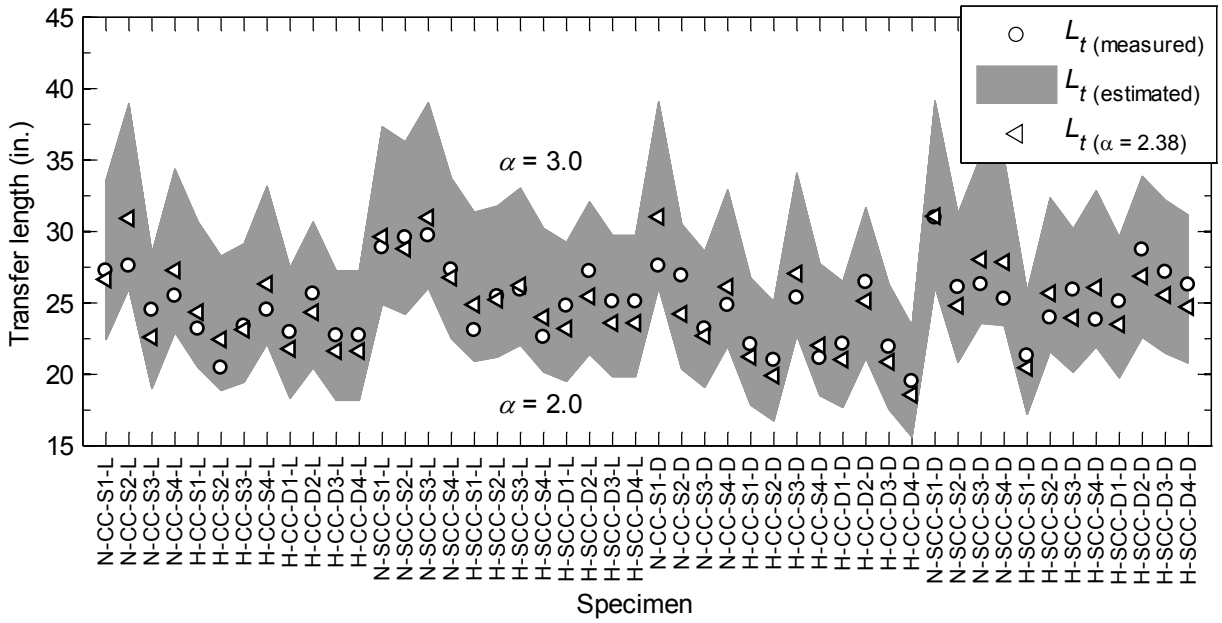

Figure 4.7 – The measured transfer lengths and the predicted transfer lengths from strand end-slips using BSD coefficients varying from 2.0 to 3.0.
(Note: L_t = transfer length; α = bond stress distribution coefficient)

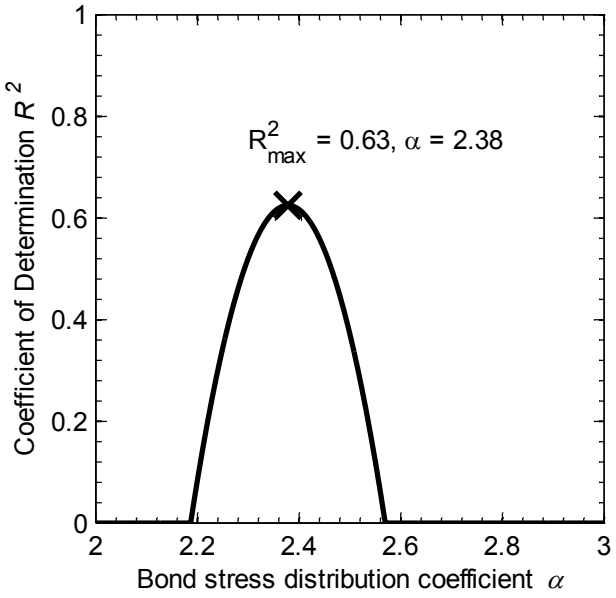

Figure 4.8 – Relationship of coefficient of determination R^2 and α coefficient.
(Note: α = bond stress distribution coefficient)

Figure 4.9 compares the measured transfer lengths with the estimated transfer lengths using an α coefficient of 2.38. Ideally, the measured and estimated transfer lengths should align with the diagonal line. The distance from a data point to the diagonal indicated the deviation of determining the α coefficient. In this study, a coefficient of 2.38 was the most appropriate coefficient for estimating transfer lengths from initial strand end-slips.

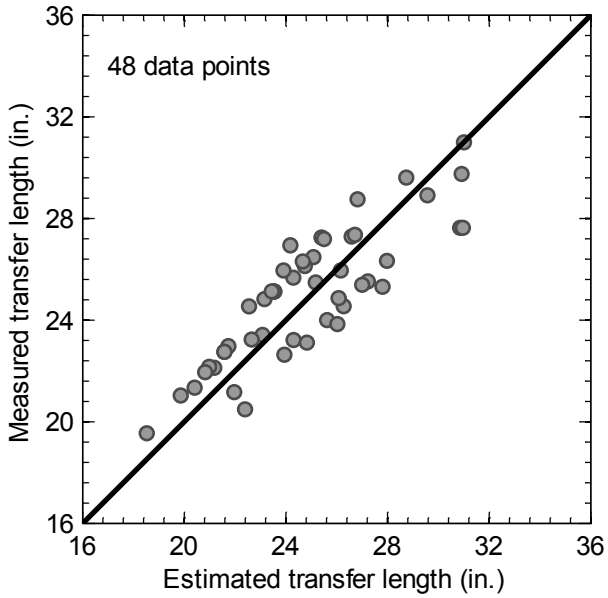

Figure 4.9 – Comparison of the measured transfer lengths and the predicted transfer lengths using an α coefficient of 2.38.
(Note: 1 in. = 25.4 mm)

4.9 Summary and conclusions

The measured transfer lengths and strand end-slips for 24 pretensioned concrete beams were presented. The beams were fabricated with 0.7 in. (17.8 mm), Grade 270 (1860), prestressing strands and different types of concrete. These types included CC and SCC which had compressive strengths at release varied from 5.9 ksi to 9.8 ksi (40.7 MPa to 67.6 MPa). Based on the investigations, the following conclusions were made:

1. The average measured transfer lengths at release varied from 23 in. to 28 in. (584 mm to 710 mm). The experimental results confirmed the effect of concrete compressive strength on transfer length of prestressing strands. The increase of concrete compressive strength can shorten the transfer length.
2. At early ages, the bond strength between the prestressing strands with SCC was lower with CC. At 28 days, however, the bond strength between prestressing strands with CC and SCC was similar.
3. Transfer lengths increased by 7% to 17% during the first 28 days after casting. The increase was independent of concrete compressive strengths and type of concrete. The average measured transfer lengths at 28 days varied from 26 in. to 31 in. (660 mm to 790 mm)
4. The beams using two prestressing strands at spacing of 2.0 in. (51 mm) had greater transfer lengths at release than the beams using one prestressing strand. At 28 days, the measured transfer lengths were similar for the beams using one and two prestressing strands.
5. The lower and upper bound of the measured transfer lengths were proposed (Eq. 4.4). The lower bound should be used to check allowable stresses at release. The upper bound should be used when determining shear strength and moment capacity.
6. A concrete compressive strength at release of 8 ksi (55.2 MPa) was adequate for detensioning 0.7 in. (17.8 mm) strands placed at spacing of 2.0 in. (51 mm).
7. The ACI 318 and ASSHTO specifications of transfer length are applicable for 0.7 in. (17.8 mm) prestressing strands cast with the CC and SCC mixtures used in this study.

8. The measured initial strand end-slips may be less or greater than the AESs calculated with different BSD coefficients. There was no apparent difference in the strand end-slips measured at the live ends and the dead ends.
9. Transfer lengths at release can be estimated from initial strand end-slips using an empirical formula. A coefficient of 2.38 was the most appropriate value for estimating the transfer length with a coefficient of determination of 0.69.

CHAPTER 5 : DEVELOPMENT LENGTH RESULTS

This chapter presents the measured development length of 0.7 in. (17.8 mm) prestressing strands for 24 pretensioned concrete beams. The beams were fabricated with conventional concrete or self-consolidating concrete. The concrete compressive strengths at 28 days varied from 9.2 ksi to 13.4 ksi (63.4 MPa to 92.4 MPa). The development length was determined by conducting bending test with different embedment lengths. The experimental results indicated the measured development length did not show a good correlation with concrete compressive strengths. The ACI 318 equations significantly over-predicted the measured flexural bond length and development length. A simple equation was proposed for predicting development length of 0.7 in. (17.8 mm) prestressing strands.

5.1 Measured development lengths

5.1.1 N-SCC-S beams

The bending test results of N-SCC-S beams are presented in **Figure 5.1** and Appendix C.1.1. In the figure, three parameters are presented for a bending test. The first column was the ratio of the maximum measured moment capacity (M_{max}) and nominal moment capacity (M_n). The second column was the ratio of the measured moment (M_{slip}) and nominal moment capacity when the prestressing strand exhibited the initial slippage recorded by LVDT. If the prestressing strand exhibited no slippage, a text of "No Slip" is shown instead of the second column. The tested embedment length is shown as a solid circle. In the figure, the specimens were arranged according to the order of conducted bending tests.

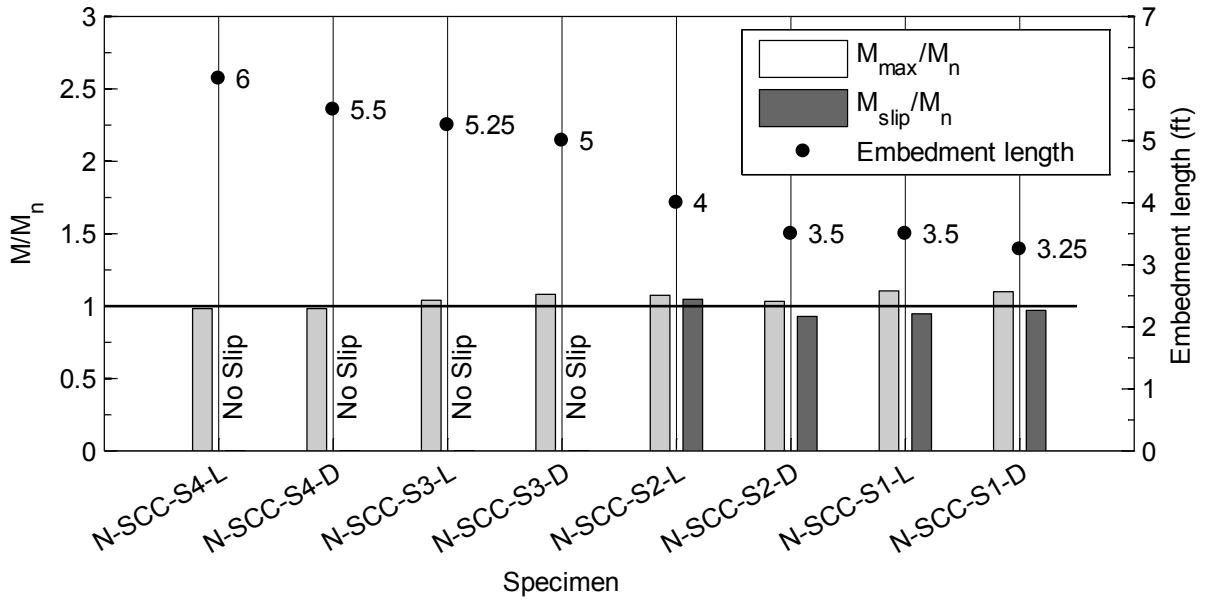

Figure 5.1 – Bending test results of N-SCC-S beams.
(Note: M_{max}/M_n = ratio of the maximum measured moment and the nominal moment capacity; M_{slip}/M_n = ratio of the measured moment at which the prestressing strand started slipping and the nominal moment capacity; 1 ft = 305 mm)

The first bending test of N-SCC-S4-L specimen exhibited flexural failure without strand slippage with a trial embedment length of 6 ft (1830 mm). Therefore, the embedment lengths were reduced for the following tests. An embedment length of 4 ft (1220 mm) was used for testing the N-SCC-S2-L specimen. This specimen exhibited flexural failure with M_{max}/M_n of 1.09, and the prestressing strand started slipping when the specimen achieved 102% of M_n as shown in **Figure 5.2**. In this figure, the dashed-line represents the relationship of M/M_n and the specimen deflection measured by LCE during the bending test. The gray dot was similar to the dashed-line, but the deflection was measured using a steel ruler. The solid-line represents the relationship of M/M_n and strand slippage. The figure indicates that the prestressing strand started slipping at M/M_n of 1.02, and the strand slippage increased to approximately 0.03 in. (0.8 mm) before the specimen collapsed. The crack pattern of N-SCC-S2-L was plotted on a 2.0 in. by 2.0 in. (51 mm by 51 mm) grid as shown in **Figure 5.3**. In this figure, the bold line indicates the

major crack occurring during the bending test and leading to the collapse of specimen, and the thin lines represents minor cracks.

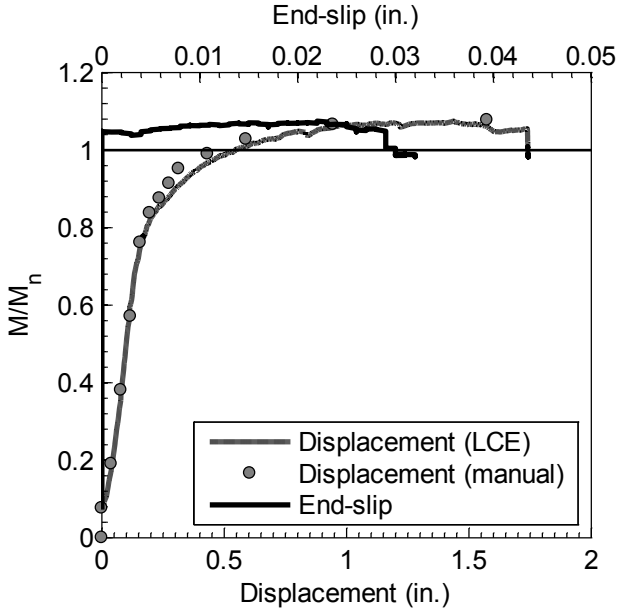

Figure 5.2 –Test results of N-SCC-S2-L with an embedment length of 4 ft (1220 mm). (Note: 1 in. = 25.4 mm; LCE = linear cable encoder; M/M_n = ratio of the measured moment and the nominal moment capacity when the prestressing strand started slipping)

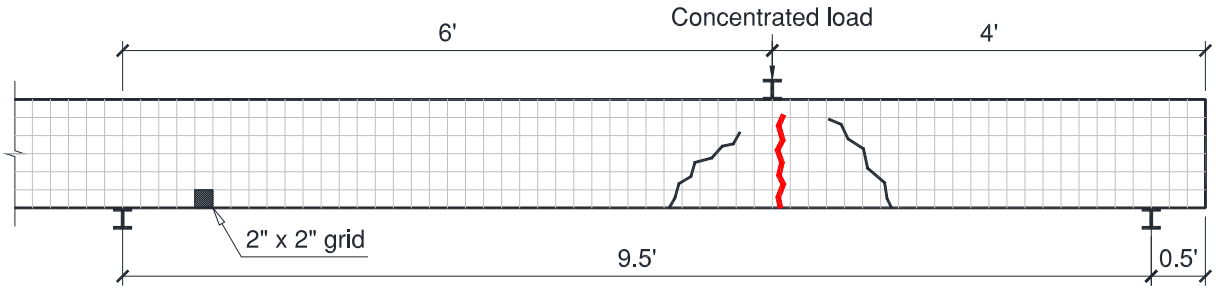

Figure 5.3 – Crack pattern of N-SCC-S2-L.
(Note: 1 ft = 305 mm; 1 in. = 25.4 mm)

The embedment length was continuously reduced to for determine the required development length for N-SCC-S beams. The N-SCC-S2-D was able to achieve M_n with an the embedment length of 3.5 ft (1067 mm), but the prestressing strand started slipping before the specimen achieved M_n as shown in **Figure 5.4**. The crack pattern of N-SCC-S2-D is shown in

Figure 5.5. The major crack occurred beneath the concentrated load and was slightly inclined to the right. The failure mode was classified as bond failure in this case. The bending test of N-SCC-S1-L with an embedment length of 3.5 ft (1067 mm) and N-SCC-S1-D with an embedment length of 3.25 ft (991 mm) presented similar results to the N-SCC-S2-D in which the prestressing strand was slipped before these specimens achieved M_n. Therefore, the required development length of prestressing strand was approximately 4 ft (1220 mm) for the N-SCC-S beams.

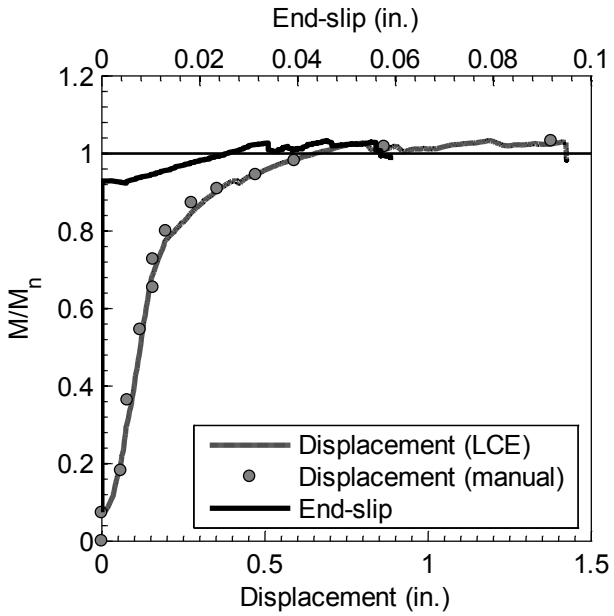

Figure 5.4 – Test results of N-SCC-S2-D with an embedment length of 3.5 ft (1067 mm). (Note: 1 in. = 25.4 mm; LCE = linear cable encoder; M/M_n = ratio of the measured moment and the nominal moment capacity when the prestressing strand started slipping)

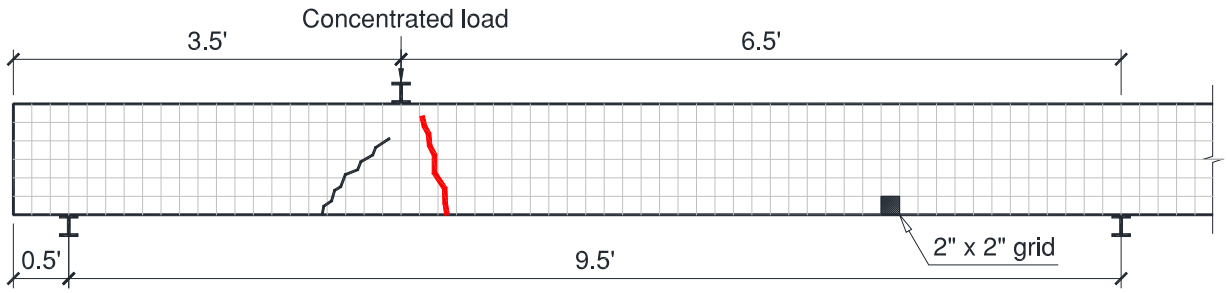

Figure 5.5 – Crack pattern of N-SCC-S2-D. (Note: 1 ft = 305 mm; 1 in. = 25.4 mm)

5.1.2 H-SCC-S beams

The H-SCC-S beams were tested with different embedment lengths varying from 4.5 ft to 3.5 ft (1372 mm to 1067 mm) as shown in **Figure 5.6** and Appendix C.1.2. Three specimens (H-SCC-S2-L, H-SCC-S2-D and H-SCC-4-L) which were tested with an embedment length equal to or greater than 4 ft (1220 mm) exhibited flexural failure without strand slippage or the prestressing strand was slipped after the specimens achieved M_n. The relationship of strand slippage and moment of H-SCC-S4-L bending test is shown in **Figure 5.7**. The figure shows the prestressing strand was slipped instantly after the specimen achieved M_n. This indicated that the required development length was very close to tested embedment length. The major crack occurred beneath the concentrated load as shown in **Figure 5.8**.

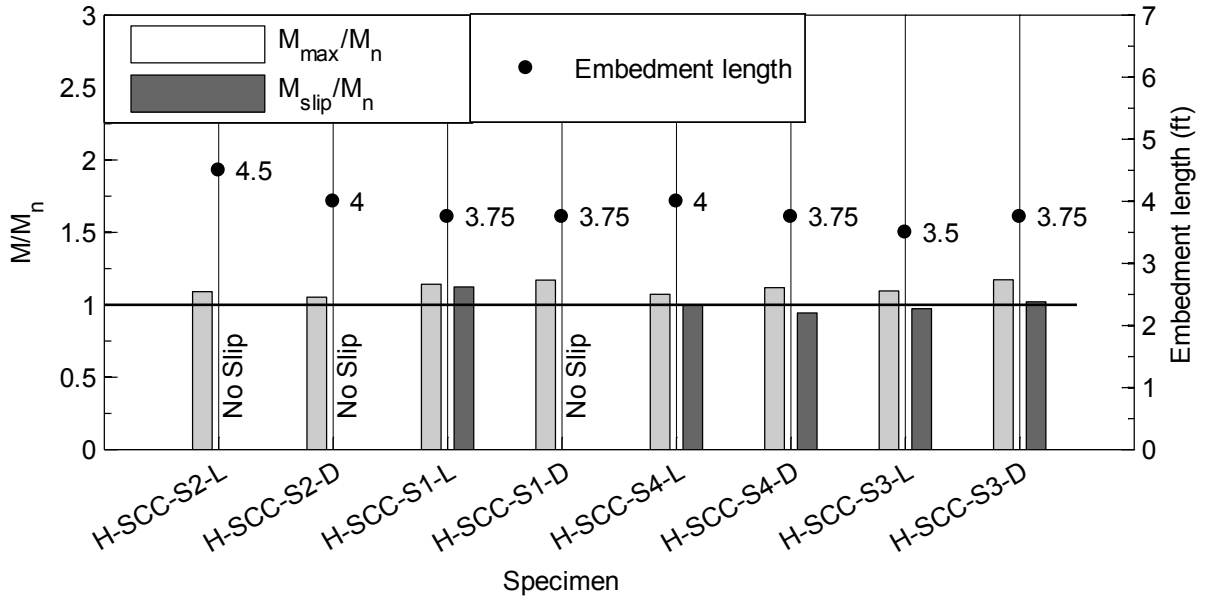

Figure 5.6 – Bending test results of H-SCC-S beams.
(Note: M_{max}/M_n = ratio of the maximum measured moment and the nominal moment capacity; M_{slip}/M_n = ratio of the measured moment at which the prestressing strand started slipping and the nominal moment capacity; 1 ft = 305 mm)

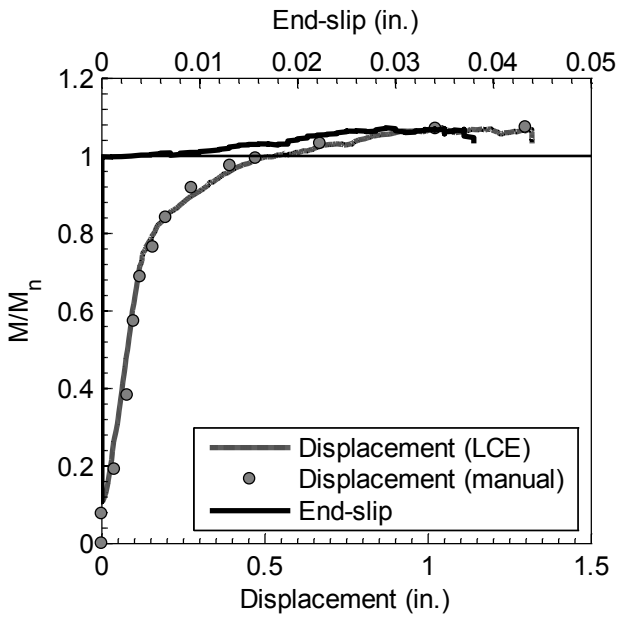

Figure 5.7 – Test results of H-SCC-S4-L with an embedment length of 4 ft (1220 mm). (Note: 1 in. = 25.4 mm; LCE = linear cable encoder; M/M_n = ratio of the measured moment and the nominal moment capacity when the prestressing strand started slipping)

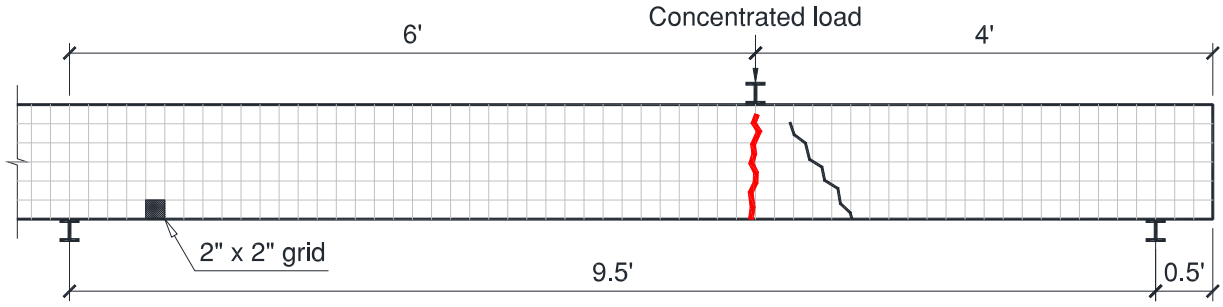

Figure 5.8 – Crack pattern of H-SCC-S4-L. (Note: 1 ft = 305 mm; 1 in. = 25.4 mm)

In addition, four specimens were tested with a shorter embedment length of 3.75 ft (1143 mm) including H-SCC-S1-L, H-SCC-S1-D, H-SCC-S4-D, and H-SCC-S3-D. Three out of four specimens presented flexural failure, and the H-SCC-S4-D specimen exhibited bond failure. The relationship of strand slippage and moment of H-SCC-S4-D bending test is shown in **Figure 5.9**. The figure shows that the moment continuously increased and exceed M_n after the prestressing

strand was slipped. However, this specimen was considered as bond failure since strand slippage is a sign of losing bond strength between the prestressing strand and the concrete. The crack pattern is shown in **Figure 5.10**. One specimen (H-SCC-S3-L) which was tested with an embedment length of 3.5 ft (1067 mm) exhibited bond failure. Therefore, the required development length was approximately 4 ft (1220 mm) for the H-SCC-S beams.

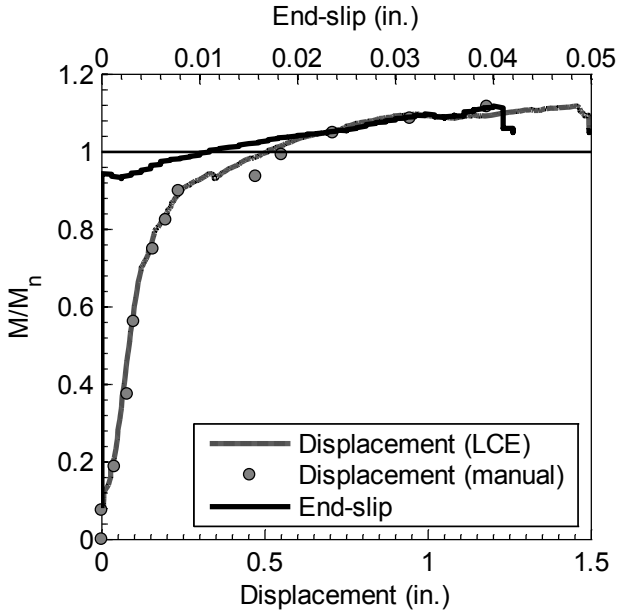

Figure 5.9 – Test results of H-SCC-S4-D with an embedment length of 3.75 ft (1143 mm). (Note: LCE = linear cable encoder; M/M_n = ratio of the measured moment and the nominal moment capacity when the prestressing strand started slipping; 1 in. = 25.4 mm)

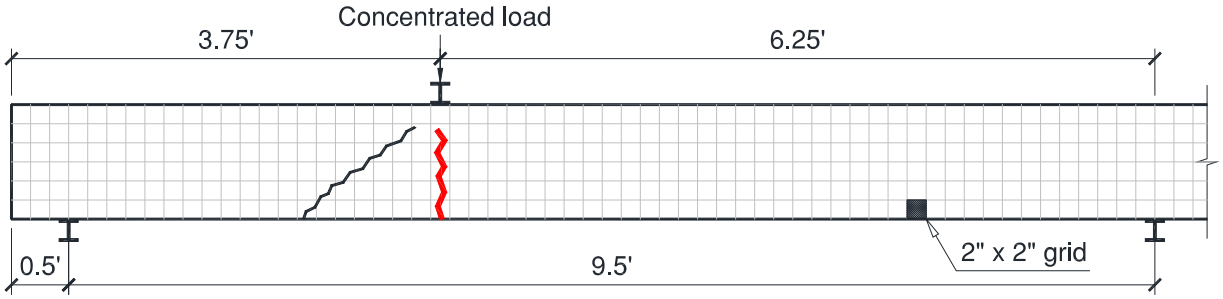

Figure 5.10 – Crack pattern of H-SCC-S4-D.
(Note: 1 ft = 305 mm; 1 in. = 25.4 mm)

5.1.3 N-CC-S beams

The bending test results of N-CC-S beams are summarized in **Figure 5.11** and Appendix C.1.3. The tested embedment lengths varied from 4 ft to 3 ft (1220 mm to 914 mm). The N-CC-S4-L was first tested with an embedment length of 4 ft (1220 mm) which was approximately 48% of the predicted development length using ACI 318 equation. This specimen exhibited flexural failure without strand slippage.

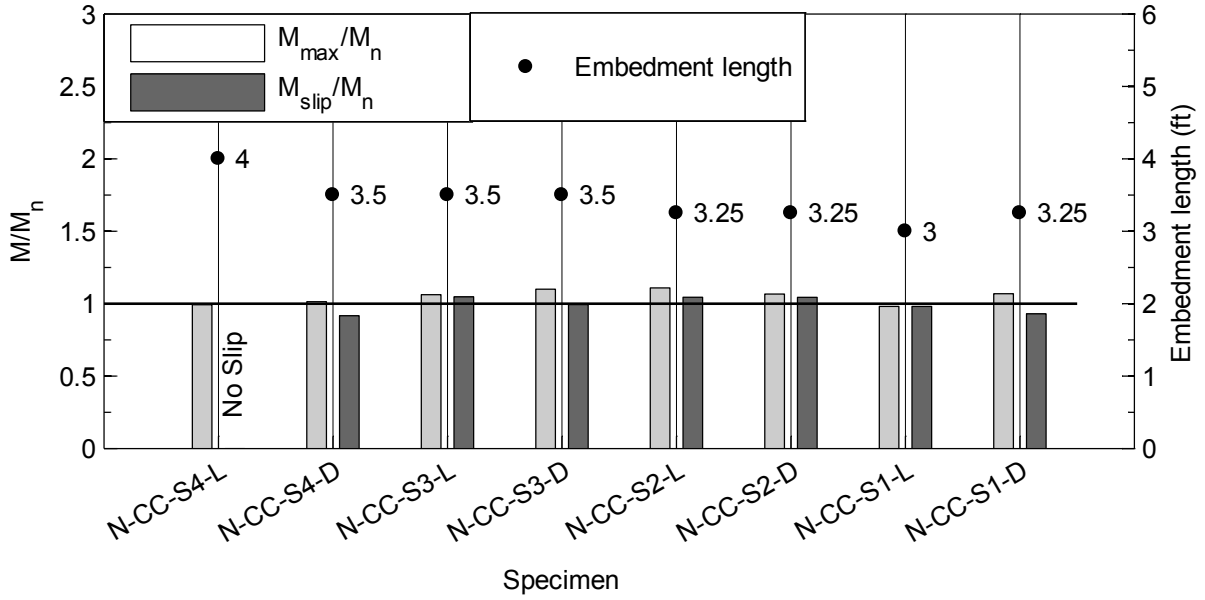

Figure 5.11 – Bending test results of N-CC-S beams.
(Note: M_{max}/M_n = ratio of the maximum measured moment and the nominal moment capacity; M_{slip}/M_n = ratio of the measured moment at which the prestressing strand started slipping and the nominal moment capacity; 1 ft = 305 mm)

Three specimens (N-CC-S4-D, N-CC-S3-L, and N-CC-S3-D) were tested with a shorter embedment length of 3.5 ft (1067 mm). The first specimen exhibited bond failure, and the latter two specimens showed flexural failure. The relation of strand slippage and moment of N-CC-S4-D bending test is shown in **Figure 5.12**. The prestressing strand was slipped as the specimen achieved 92% of M_n. The specimen was able to gain approximately 10% of M_n after initial strand slippage and collapsed when the strand slippage reached 0.05 in. (1.3 mm). The major

crack was inclined 45° to the left as shown in **Figure 5.13**. This may be due to the high shear effect when the specimen was tested with a short embedment length.

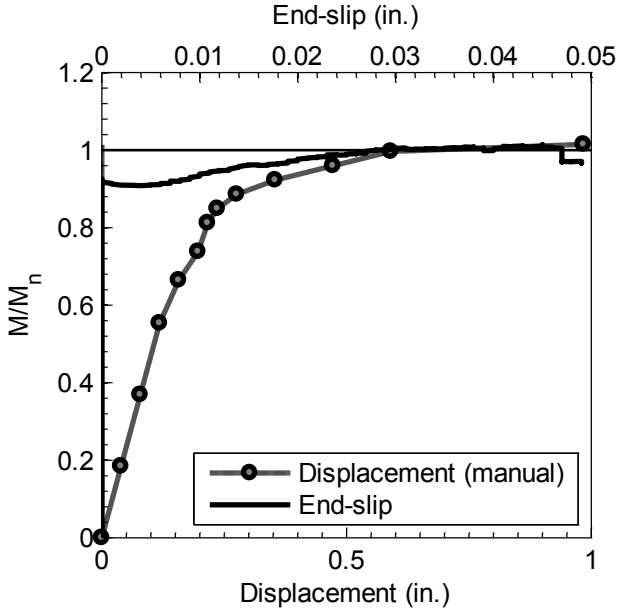

Figure 5.12 – Test results of N-CC-S4-D with an embedment length of 3.5 ft (1067 mm). (Note: 1 in. = 25.4 mm; M/M_n = ratio of the measured moment and the nominal moment capacity when the prestressing strand started slipping)

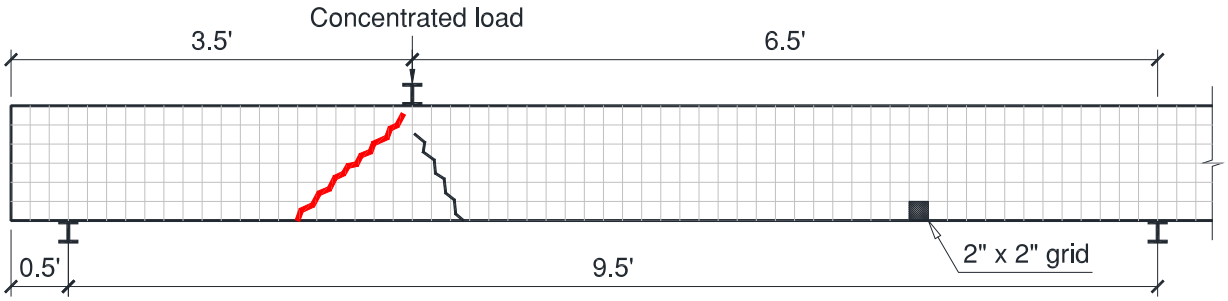

Figure 5.13 – Crack pattern of N-CC-S4-D.
(Note: 1 ft = 305 mm; 1 in. = 25.4 mm)

The other three specimens were tested with a shorter embedment length of 3.25 ft (991 mm). These specimens showed similar results to those of the specimens tested with an embedment length of 3.5 ft (1067 mm). In particular, two out of three specimens exhibited

flexural failure, and one specimen showed bond failure. In addition, one specimen (N-CC-1-L) which was tested with an embedment length of 3 ft (914 mm) reached 98% of M_n before collapsed as shown in **Figure 5.14**. The prestressing strand also experienced initial slippage at 98% of M_n. However, the moment curve rapidly dropped and this specimen collapsed without warning. This indicated that the bond strength between the prestressing strand and the concrete completely lost after the strand started slipping. Therefore, the N-CC-1-L specimen did not satisfy the requirement of ductility. The major shear crack shown in **Figure 5.15** was the reason accounting for the rapid drop of the moment curve. Based on the bending tests of 8 specimens, it was concluded that the required development length of prestressing strand was approximately 4 ft (1220 mm).

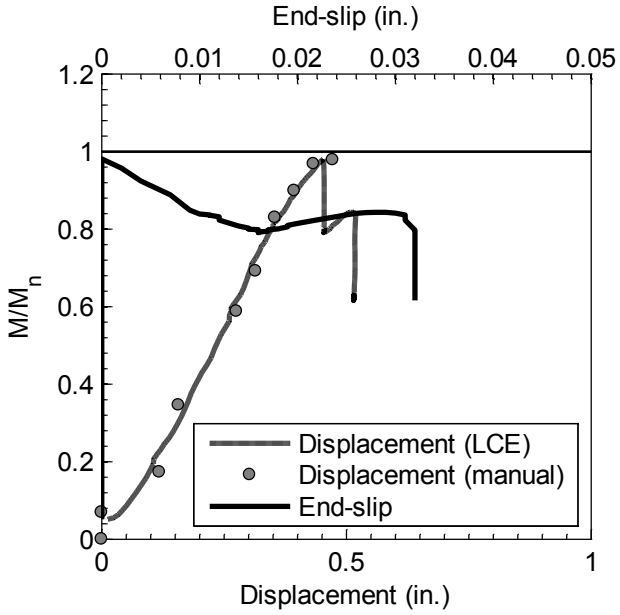

Figure 5.14 – Test results of N-CC-S1-L with an embedment length of 3 ft (914 mm). (Note: LCE = linear cable encoder; M/M_n = ratio of the measured moment and the nominal moment capacity when the prestressing strand started slipping; 1 in. = 25.4 mm)

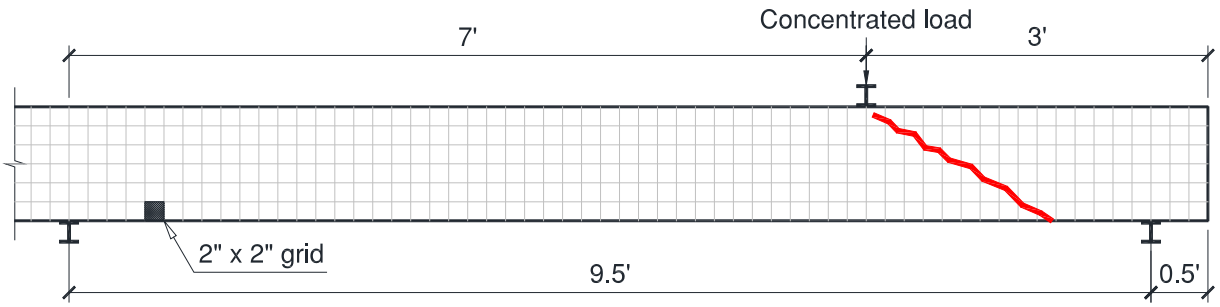

Figure 5.15 – Crack pattern of N-CC-S1-L.
(Note: 1 ft = 305 mm; 1 in. = 25.4 mm)

5.1.4 H-CC-S beams

Bending tests of H-CC-S beams showed similar results with different embedment lengths as shown in **Figure 5.16** and Appendix C.1.4. Two specimens (H-CC-S4-D and H-CC-S3-D) which were tested with an embedment length of 4.25 ft (1295 mm) showed flexural failure without strand slippage. For a shorter embedment length of 4 ft (1220 mm), three specimens (H-CC-S4-L, H-CC-S3-L, and H-CC-S2-L) exhibited flexural failure without strand slippage or the prestressing strand was slipped after the specimens achieved M_n. In particular, the H-CC-S4-L specimen achieved M_{max}/M_n of 1.03, and the prestressing strand was slipped at 102% of M_n as shown in **Figure 5.17**. This indicated that the required development length was close with the tested embedment length of 4 ft (1220 mm). The major crack occurred beneath the concentrated load as shown in **Figure 5.18**.

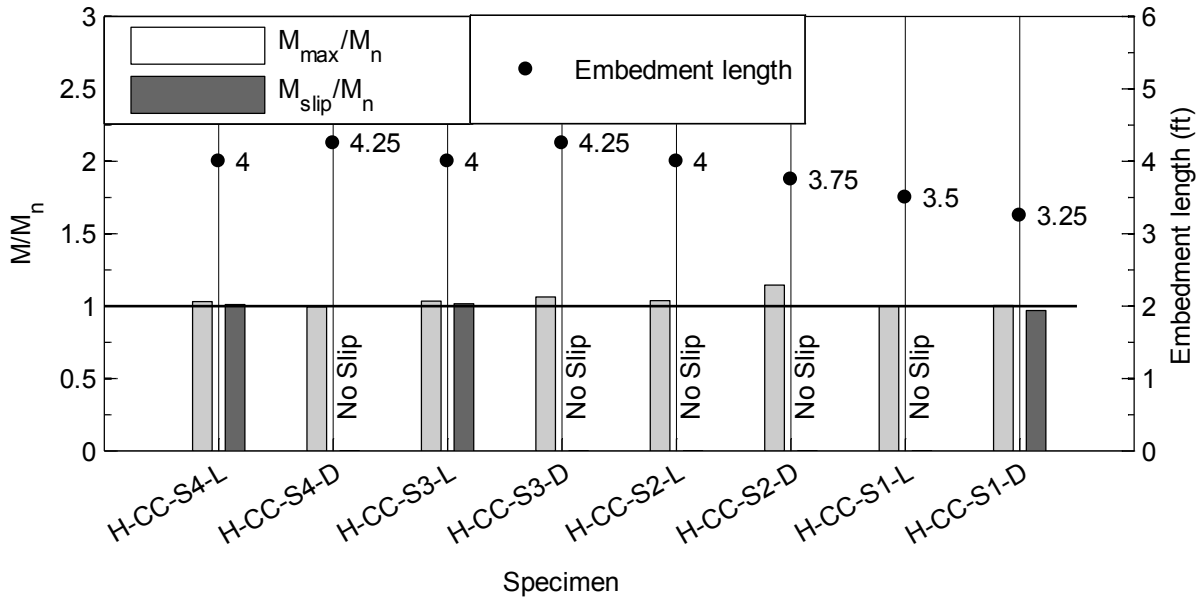

Figure 5.16 – Bending test results of H-CC-S beams.
(Note: M_{max}/M_n = ratio of the maximum measured moment and the nominal moment capacity; M_{slip}/M_n = ratio of the measured moment at which the prestressing strand started slipping and the nominal moment capacity; 1 ft = 305 mm)

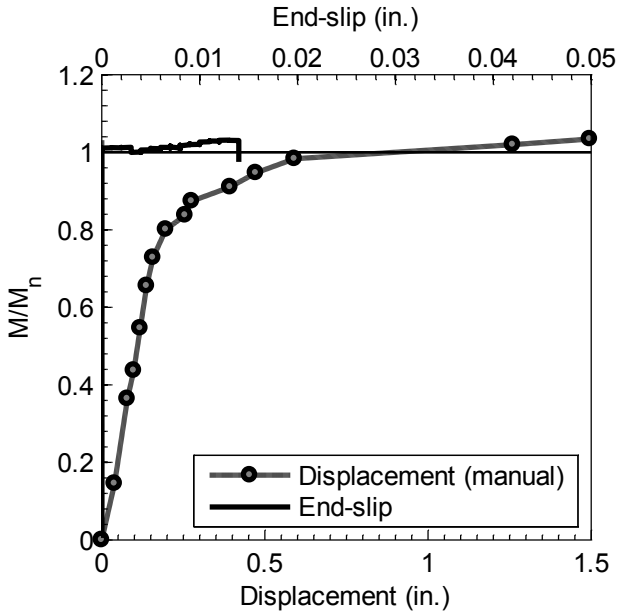

Figure 5.17 – Test results of H-CC-S4-L with an embedment length of 4 ft (1220 mm).
(Note: M/M_n = ratio of the measured moment and the nominal moment capacity when the prestressing strand started slipping; 1 in. = 25.4 mm)

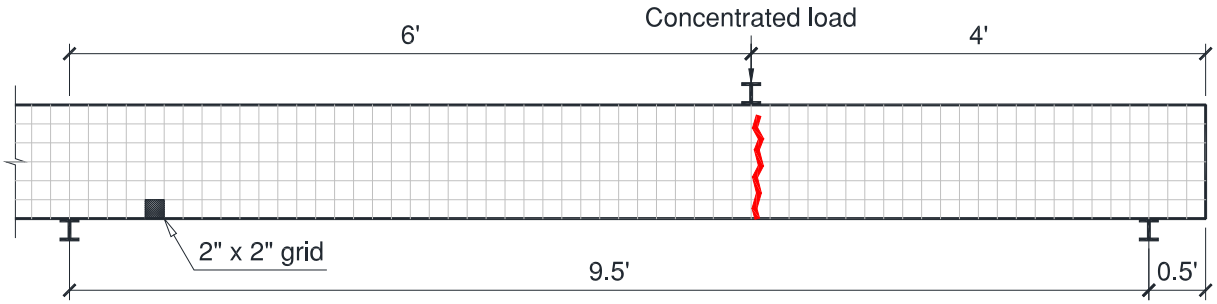

Figure 5.18 – Crack pattern of H-CC-S4-L.
(Note: 1 ft = 305 mm; 1 in. = 25.4 mm)

The embedment length was continuously reduced to determine the required development length. The bending test of H-CC-2-D specimen with an embedment length of 3.75 ft (1143 mm) and H-CC-1-L specimen with an embedment length of 3.5 ft (1067 mm) exhibited flexural failure without strand slippage. The H-CC-S1-D specimen which was tested with a shorter embedment length of 3.25 ft (991 mm) exhibited bond failure. The experimental results shown in **Figure 5.19** were similar to those of N-CC-S1-L. This specimen was able to achieve M_n before collapsed, and the prestressing strand was slipped at 97% of M_n. However, the H-CC-S1-L exhibited ductile behaviors instead of a sudden collapse as N-CC-S1-L. The major crack shown in **Figure 5.20** was due to bending effect instead of shear effect on the N-CC-S1-L specimen. Although this specimen nearly reached the three requirements of flexural failure, it was classified as bond failure in terms of determining development length. As a results, only specimens which were tested with an embedment length of 3.5 ft (1067 mm) or greater met requirements of flexural failure. Therefore, the required development length of prestressing strand was approximately 3.5 ft (1067 mm) for H-CC-S beams.

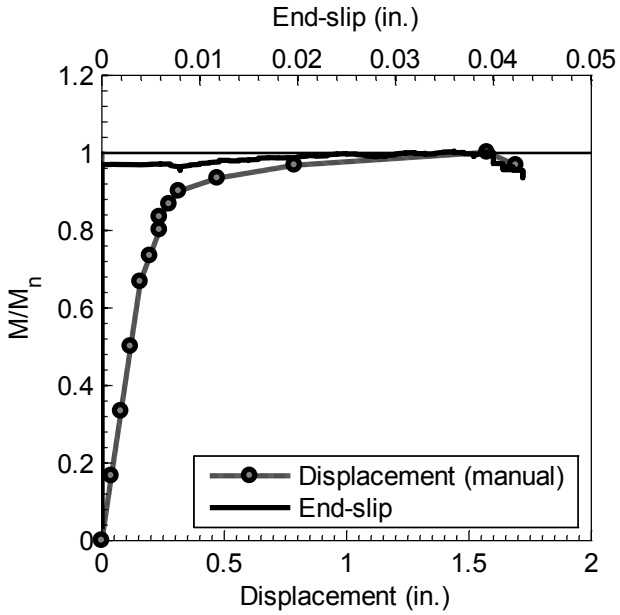

Figure 5.19 – Test results of H-CC-S1-D with an embedment length of 3.25 ft (991 mm). (Note: 1 ft = 305 mm; M/M_n = ratio of the measured moment and the nominal moment capacity when the prestressing strand started slipping)

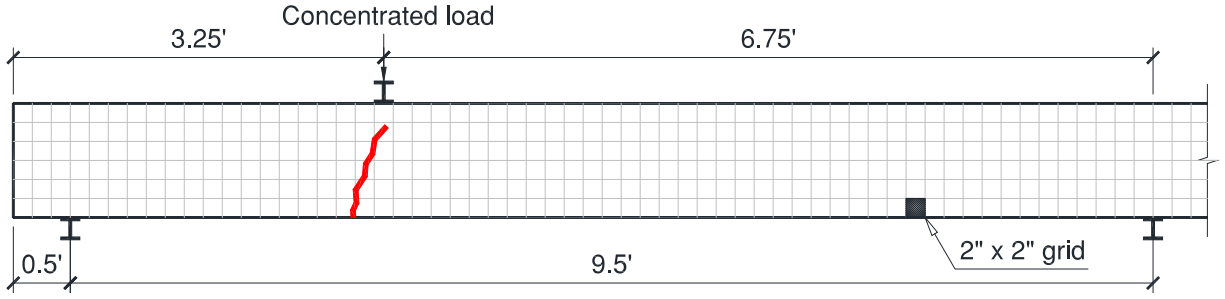

Figure 5.20 – Crack pattern of H-CC-S1-D. (Note: 1 ft = 305 mm; 1 in. = 25.4 mm)

5.1.5 H-SCC-D beams

H-SCC-D beams were tested with embedment lengths varying from 4.25 ft to 3.5 ft (1295 mm to 1067 mm). Bending test results of these beams are shown in **Figure 5.21** and Appendix C.1.5. The H-SCC-D3-L specimen which was tested with an embedment length of 4.25 ft (1295 mm) exhibited flexural failure. The specimen was able to achieve 109% of M_n before collapsed,

and the prestressing strand started slipping as this specimen reached M_n. Three other specimens (H-SCC-D2-L, H-SCC-D1-D, and H-SCC-D3-D) were tested with a shorter embedment length of 4 ft (1220 mm). All these specimens exhibited flexural failure. For the H-SCC-D3-D specimen, the prestressing strand started slipping as the specimen achieved M_n as shown in **Figure 5.22**. This specimen had several shear cracks as shown in **Figure 5.23** but the major flexural crack beneath the concentrated load leaded to the collapse of the specimen.

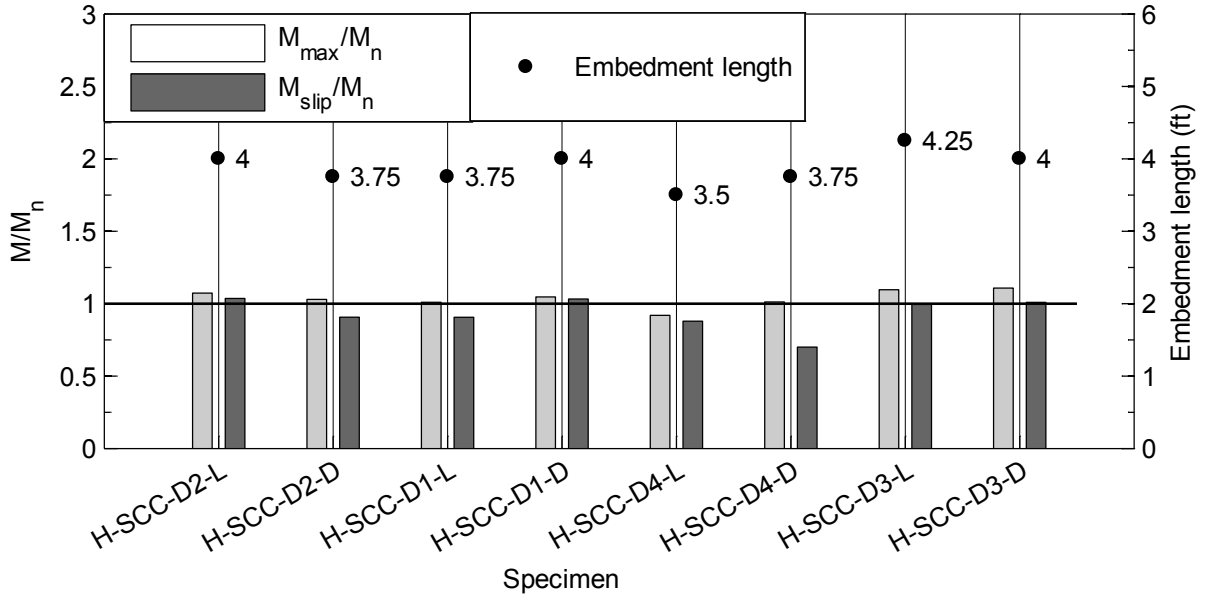

Figure 5.21 – Bending test results of H-SCC-D beams.
(Note: M_{max}/M_n = ratio of the maximum measured moment and the nominal moment capacity; M_{slip}/M_n = ratio of the measured moment at which the prestressing strand started slipping and the nominal moment capacity; 1 ft = 305 mm)

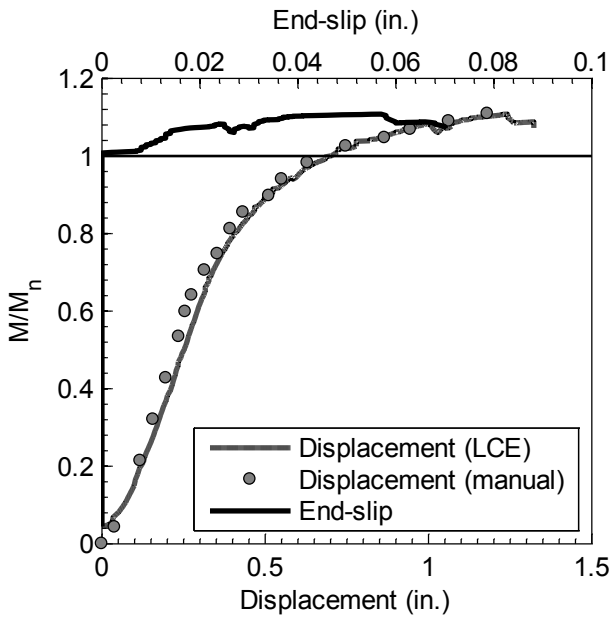

Figure 5.22 – Test results of H-SCC-D3-D with an embedment length of 4.0 ft (1220 mm). (Note: 1 in. = 25.4 mm; LCE = linear cable encoder; M/M_n = ratio of the measured moment and the nominal moment capacity when the prestressing strand started slipping)

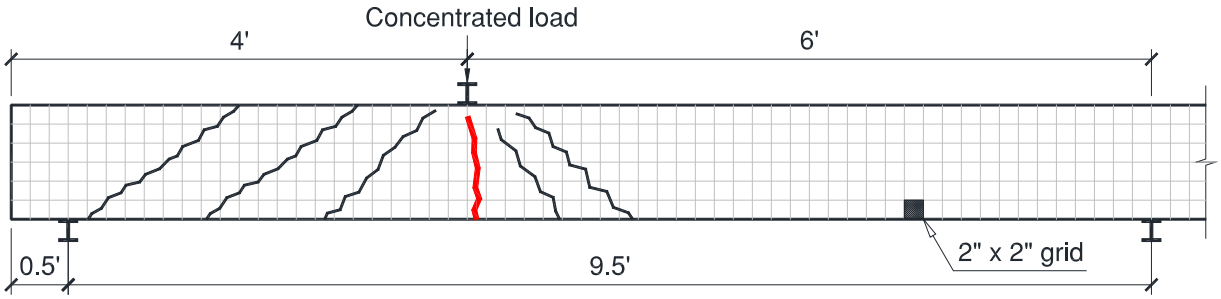

Figure 5.23 – Crack pattern of H-SCC-D3-D.
(Note: 1 ft = 305 mm; 1 in. = 25.4 mm)

Three specimens (H-SCC-D2-D, H-SCC-D1-L, and H-SCC-D4-D) were tested with an embedment length of 3.75 ft (1143 mm). All these specimens exhibited bond failure. The specimens were able to achieve M_n before collapsed, but the prestressing strands were slipped at approximately 90% of M_n for the first two specimens and 70% of M_n for the last specimen. Bending test results of H-SCC-D4-D specimen is shown in **Figure 5.24**. This specimen collapsed due to two major shear cracks as shown in **Figure 5.25**. One specimen (H-SCC-D4-L)

which was tested with an embedment length of 3.5 ft (1067 mm) was unable to achieve the M_n before collapsed. Based on experimental results of 8 bending tests, it was concluded that the required development length of H-SCC-D beams was 4 ft (1220 mm).

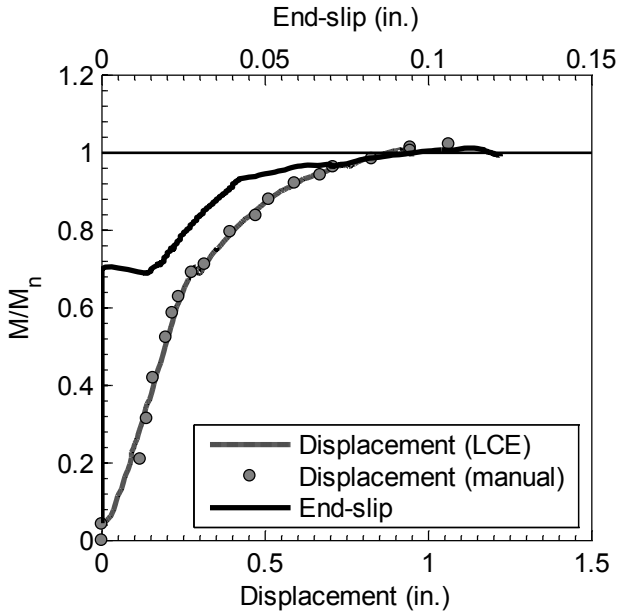

Figure 5.24 – Test results of H-SCC-D4-D with an embedment length of 3.75 ft (1143 mm). (Note: 1 in. = 25.4 mm; LCE = linear cable encoder; M/M_n = ratio of the measured moment and the nominal moment capacity when the prestressing strand started slipping)

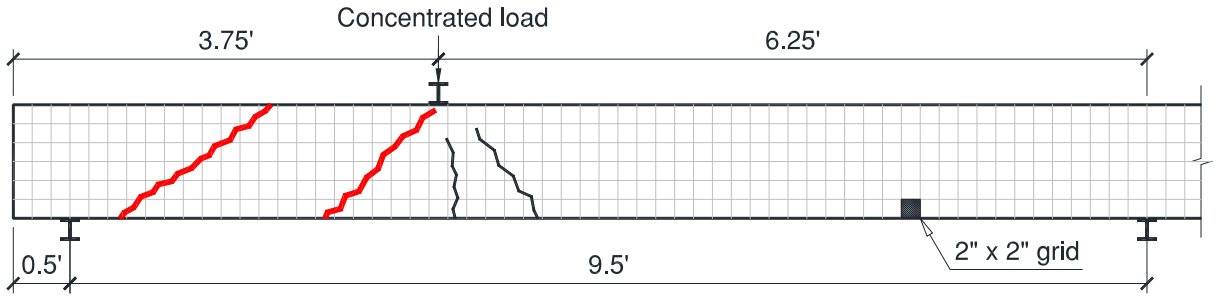

Figure 5.25 – Crack pattern of H-SCC-D4-D.
(Note: 1 ft = 305 mm; 1 in. = 25.4 mm)

5.1.6 H-CC-D beams

Bending tests of H-CC-D beams were conducted with embedment lengths varying from 4.5 ft to 3.5 ft (1372 mm to 1067 mm). The test results are presented in **Figure 5.26** and Appendix C.1.6. The specimens which were tested with embedment lengths equal to or greater than 4 ft (1220 mm) showed flexural failure without strand slippage. Two specimens (H-CC-D3-L and H-CC-D2-D) were tested with a shorter embedment length of 3.75 (1143 mm). These specimens showed flexural failure, and the prestressing strands started slipping after the specimens achieved M_n. Bending test results of H-CC-D2-D are shown in **Figure 5.27**. This specimen stopped gaining external load as the prestressing strand slipped, and was collapsed due to a major flexural crack as shown in **Figure 5.28**.

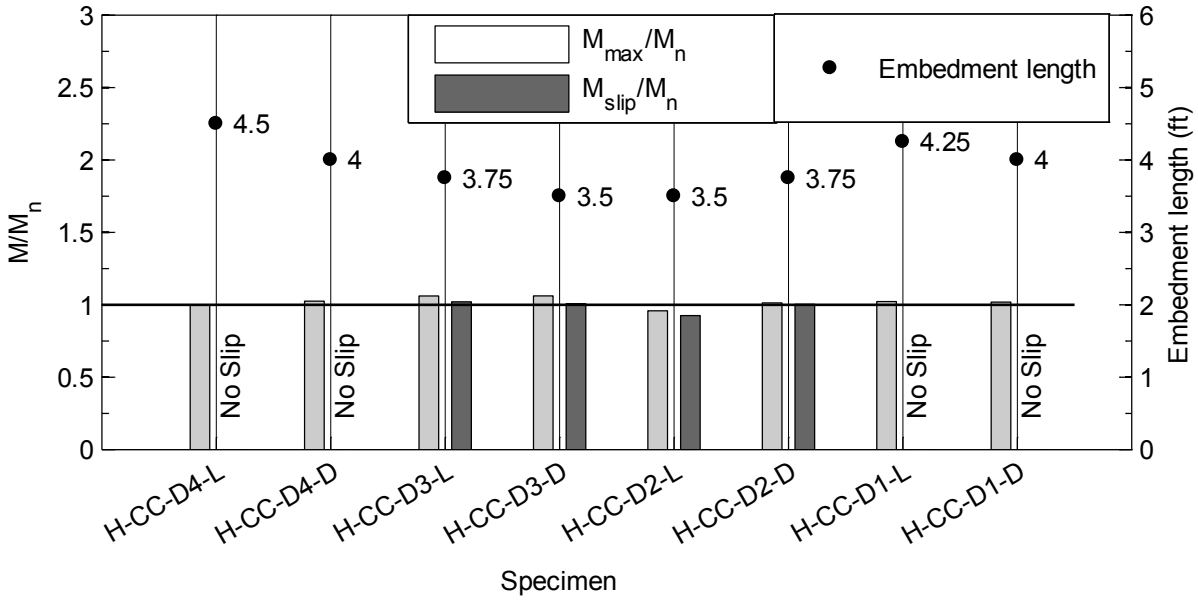

Figure 5.26 – Bending test results of H-CC-D beams.
(Note: M_{max}/M_n = ratio of the maximum measured moment and the nominal moment capacity; M_{slip}/M_n = ratio of the measured moment at which the prestressing strand started slipping and the nominal moment capacity; 1 ft = 305 mm)

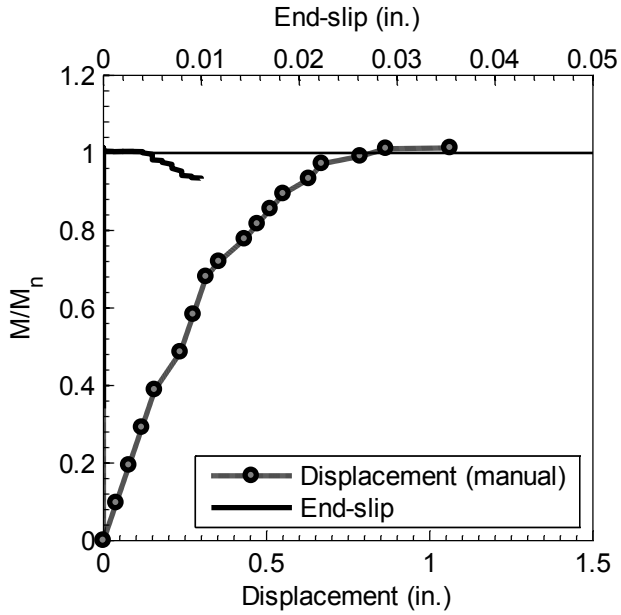

Figure 5.27 – Test results of H-CC-D2-D with an embedment length of 3.75 ft (1143 mm). (Note: 1 in. = 25.4 mm; M/M_n = ratio of the measured moment and the nominal moment capacity when the prestressing strand started slipping)

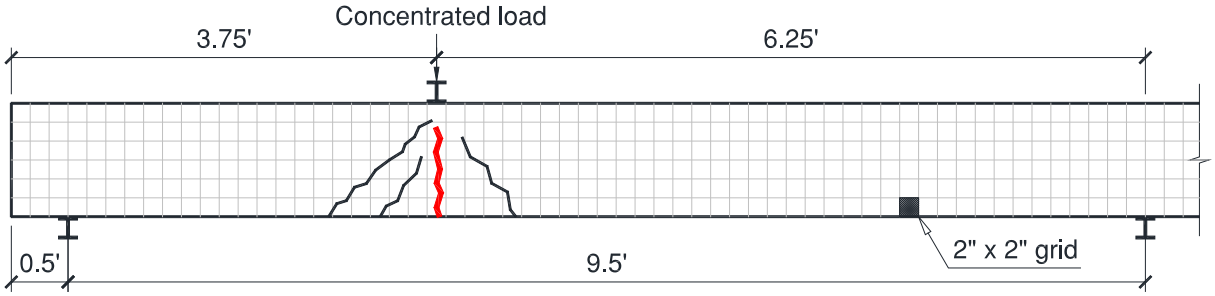

Figure 5.28 – Crack pattern of H-CC-D2-D.
(Note: 1 ft = 305 mm; 1 in. = 25.4 mm)

Two specimens (H-CC-D3-D and H-CC-D2-L) were tested with an embedment length of 3.5 ft (1067 mm). The first specimen showed flexural failure, and the prestressing strands started slipping as the specimen achieved M_n. The second specimen, however, exhibited bond failure without achieving M_n before collapsed. The prestressing strands were slipped as the specimen achieved 93% of M_n as shown in **Figure 5.29**. This specimen was collapsed due to a major

flexural crack beneath the concentrated load. Therefore, it was concluded that the required development length of H-CC-D beams was 3.75 ft (1143 mm).

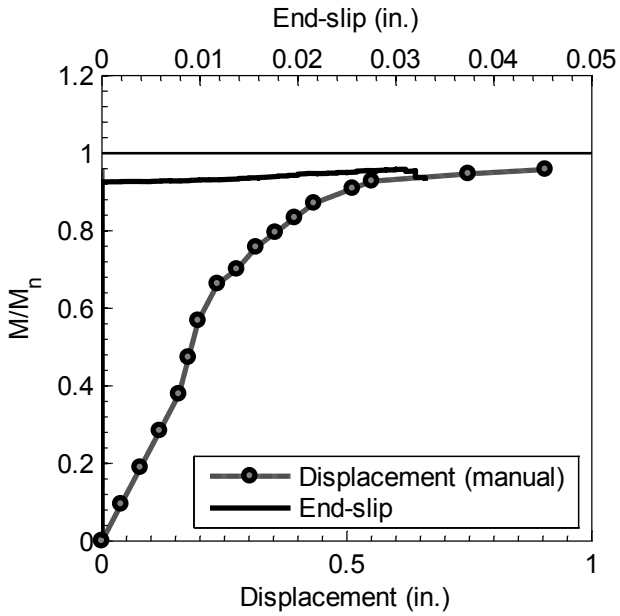

Figure 5.29 – Test results of H-CC-D2-L with an embedment length of 3.5 ft (1067 mm). (Note: 1 in. = 25.4 mm; M/M_n = ratio of the measured moment and the nominal moment capacity when the prestressing strand started slipping)

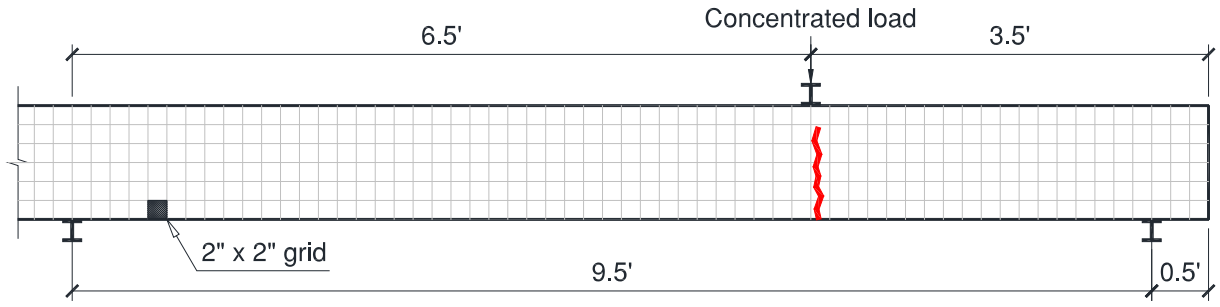

Figure 5.30 – Crack pattern of H-CC-D2-L.
(Note: 1 ft = 305 mm; 1 in. = 25.4 mm)

5.2 Effect of strand spacing

The measured and predicted development lengths are summarized in **Table 5.1**. The measured development lengths for the beams using conventional concrete (H-CC-S and H-CC-

D) were not significantly different. The difference in the measured development lengths for the beams using one strand and two strands was 0.25 ft (75 mm) which indicated that the use of 0.7 in. (17.8 mm) strands at spacing of 2.0 in. (51 mm) had little effect on the measured development lengths. For the beams using self-consolidating concrete (H-SCC-S and H-SCC-D), the measured development lengths were identical which indicated that the use of strand spacing of 2.0 in. (51 mm) had no effect on the measured development lengths.

Table 5.1 – Measured and predicted development lengths

Beam group	f'_{ct} (ksi)	Development length		
		Measured (ft)	*Predicted* (ft)*	*Measured / Predicted*
N-CC-S	10.1	4.0	8.4	0.475
H-CC-S	13.5	3.5	8.3	0.420
H-CC-D	13.9	3.75	8.6	0.438
N-SCC-S	9.4	4.0	8.4	0.475
H-SCC-S	11.0	4.0	8.3	0.480
H-SCC-D	10.3	4.0	8.5	0.468

(Note: f'_{ct} = concrete compressive strength at the time of conducting bending tests; * = using Eq. 1.3; 1 ksi = 6.895 MPa, 1 ft = 305 mm)

5.3 Effect of concrete compressive strength

The measured development lengths in this study did not show a good correlation with the concrete compressive strengths as shown in **Table 5.1**. Regardless of the difference in concrete compressive strengths of N-CC-S, N-SCC-S, and H-SCC-S the beams using these concrete mixtures presented an identical development length of 4.0 ft (1220 mm). The effect of concrete compressive strength was more apparent on the measured development length for H-CC-S beams which had a shorter development length of 3.5 ft (1060 mm). The H-CC-D beams had similar concrete compressive strength with H-CC-S beams, but the measured development length was 0.25 ft (75 mm) greater than that of H-CC-S due to the little effect of strand spacing as mentioned previously.

5.4 Proposed equation of development length

A new equation for predicting development length was proposed based on experimental results of 48 bending tests. The proposed equation was more accurate in predicting the flexural bond length and development length. Currently, ACI 318 uses Eq. 1.2 to predict the flexural bond length. This equation was three times overestimation the measured values. The proposed equation of flexural bond length is shown in Eq. 5.1. As shown in **Table 5.2**, the proposed flexural bond lengths are approximately to or greater than the measured values.

As shown in **Table 5.1**, the measured development lengths are approximately to 42% - 48% of the predicted development length using ACI 318 equation. The proposed development length equation was a combination of the existing transfer length equation of ACI 318 (Eq. 1.1) and the proposed flexural bond length equation (Eq. 5.1) which is shown in Eq. 5.2 and **Figure 5.31**. This equation was simplified as shown in Eq. 5.3. The measured development lengths were 63% - 78% of the predicted length using the proposed equation.

$$L_b = \frac{1}{3}\left(f_{ps} - f_{pe}\right)d_b \tag{5.1}$$

$$L_d = \frac{1}{3}f_{pe}d_b + \frac{1}{3}\left(f_{ps} - f_{pe}\right)d_b \tag{5.2}$$

$$L_d = \frac{1}{3}f_{ps}d_b \tag{5.3}$$

where L_d is development length (in.); L_b is flexural bond length (in.); f_{ps} is the average stress in prestressing steel at the time for which the nominal resistance of member is required (ksi); f_{pe} is the effective stress in the prestressing steel after losses (ksi); d_b is strand diameter (in.).

Table 5.2 – Development lengths

Beam group	Measured results			ACI 318 equations			Proposed equations*		
	L_t (in.)	L_b (in.)	L_d (in.)	L_t (in.) (Eq. 1.1)	L_b (in.) (Eq. 1.2)	L_d (in.) (Eq. 1.3)	L_t (in.) (Eq. 1.1)	L_b (in.) (Eq. 5.1)	L_d (in.) (Eq. 5.3)
N-CC-S	30.2	17.8	48.0	42.7	58.3	101.0	42.7	19.4	62.1
H-CC-S	25.6	16.4	42.0	43.4	56.5	100.0	43.4	18.8	62.3
H-CC-D	26.9	18.1	45.0	41.1	61.8	102.9	41.1	20.6	61.7
N-SCC-S	30.8	17.2	48.0	42.5	58.6	101.1	42.5	19.5	62.0
H-SCC-S	27.9	20.1	48.0	43.2	56.9	100.1	43.2	19.0	62.2
H-SCC-D	28.0	20.0	48.0	40.5	62.1	102.6	40.5	20.7	61.2

(Note: L_t = transfer length; L_b = flexural bond length; L_d = development length; 1 in. = 25.4 mm)

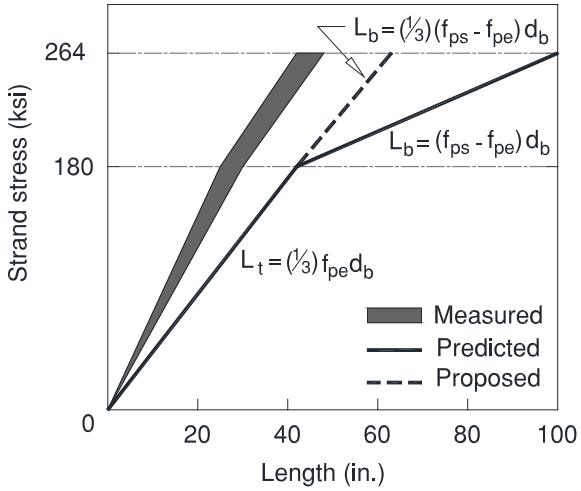

Figure 5.31 – Proposed equation of development length.
(Note: The equations are presented in customary units; L_t = transfer length; L_b = flexural bond length; L_d = development length; f_{pe} = effective stress in the prestressing steel after losses; f_{ps} = average stress in prestressing steel at the time for which the nominal resistance of member is required; d_b = strand diameter)

5.5 Summary

Forty-eight bending tests were conducted to evaluate development length of 0.7 in. (17.8 mm) prestressing strands for 24 pretensioned concrete beams. The beams were cast with different types of concrete including CC and SCC. The concrete compressive strengths at 28 days varied from approximately 9.2 ksi to 13.4 ksi (63.4 MPa to 92.4 MPa). The development

length was determined by conducting bending tests with different embedment lengths. Based on the experimental investigation, the following conclusions were made:

1. The measured development lengths of 0.7 in. (17.8 mm) prestressing strands varied from 3.5 ft to 4 ft (1067 mm to 1220 mm). These lengths were approximately 42% to 48% of the predicted development lengths using ACI 318 equation.
2. Concrete compressive strength had little effect on the measured development lengths. The N-CC-S, N-SCC-S, and H-SCC-S beams had an identical development length of 4 ft (1220 mm) regardless of the difference in concrete compressive strengths. The H-CC-S beams which used higher concrete compressive strength had a shorter development length of 3.5 ft (1070 mm).
3. The use of strand spacing of 2.0 in. (51 mm) had little to no effect on the measured development length of 0.7 in. (17.8 mm) prestressing strands. ACI 318 equation is applicable to predicted development length of 0.7 in. (17.8 mm) prestressing strands placed at spacing of 2.0 in. (51 mm).
4. The ACI 318 equation significantly over-predicted the measured flexural bond lengths. A new equation of flexural bond length was proposed based on the experimental results (Eq. 5.1). This equation was more appropriate for predicting the flexural bond lengths of 0.7 in. (17.8 mm) prestressing strands.
5. A new equation of development length of 0.7 in. (17.8 mm) prestressing strand was proposed (Eq. 5.3). The measured development lengths were approximately from 67% to 78% the predicted development length using the proposed equation. The over-prediction accounted for the limited experimental data in this study.

CHAPTER 6 : SUMMARY AND CONCLUSIONS

6.1 Summary

This study measured transfer and development lengths and evaluated applicable strand spacing of 0.7 in. (17.8 mm), Grade 270 (1860) prestressing strands for 24 pretensioned concrete beams. Twelve beams were cast with normal strength and high strength conventional concrete. The other beams were cast with normal strength and high strength self-consolidating concrete. The concrete mixtures had a wide range of compressive strengths which varied from 5.9 ksi to 9.8 ksi (40.7 MPa to 67.6 MPa) at 1 day, and 9.2 ksi to 13.4 ksi (62.4 MPa to 92.5 MPa) at 28 days. In terms of number of prestressing strands, 16 beams were cast with one prestressing strand, and 8 beams were cast with two prestressing strands. The beams using one strand provided comparable data to evaluate the effect of strand spacing on transfer end development lengths.

Transfer lengths were measured at release (approximately 1 day), and at 7, 14, 21, 28 days. Transfer lengths were determined using concrete strain profiles along with 95% AMS method. The measured transfer lengths were analyzed and compared with the current specifications. The effects of concrete compressive strength, types of concrete, and strand spacing on the measured transfer lengths were evaluated. A new equation was proposed to estimate transfer length at release based on a least square estimation method. Initial strand end-slips were measured at release of prestressing strands. The measured end-slips were compared with the allowable initial end-slips and analyzed to propose a coefficient for an existing empirical formula to predict transfer lengths at release.

Development lengths were measured by conducting 48 bending tests with different embedment lengths. The development length determination based on failure modes of the tested specimens. For the specimen exhibited flexural failure, the tested embedment length is equal to or greater than the development length. The effects of concrete compressive strength and strand spacing on the measured development lengths were evaluated. The experimental data were analyzed to propose a new equation for predicting development length of 0.7 in. (17.8 mm) prestressing strands.

6.2 Conclusion

6.2.1 Transfer length

1. The average measured transfer lengths at release varied from 23 in. to 28 in. (584 mm to 710 mm). The experimental results confirmed the effect of concrete compressive strength on transfer length of prestressing strands. The increase of concrete compressive strength can shorten the transfer length.
2. At early ages, the bond strength between the prestressing strands with SCC was lower with CC. At 28 days, however, the bond strength between prestressing strands with CC and SCC was similar.
3. Transfer lengths increased by 7% to 17% during the first 28 days after casting. The increase was independent of concrete compressive strengths and types of concrete. The measured transfer lengths at 28 days varied from 26 in. to 31 in. (660 mm to 790 mm).
4. The lower and upper bound of the measured transfer lengths were proposed (Eq. 4.4). The lower bound should be used to check allowable stresses at release. The upper bound should be used when determining shear strength and moment capacity.

5. A concrete compressive strength at release of 8 ksi (55.2 MPa) was adequate for detensioning 0.7 in. (17.8 mm) strands placed at spacing of 2.0 in. (51 mm).
6. The ACI 318 and ASSHTO specifications of transfer length are applicable for 0.7 in. (17.8 mm) prestressing strands cast with the CC and SCC mixtures used in this study.
7. The measured initial strand end-slips may be less or greater than the AESs calculated with different BSD coefficients. There were no apparent differences between the strand end-slips at the live ends and the dead ends.
8. Transfer lengths at release can be estimated from initial strand end-slips using an empirical formula. A coefficient of 2.38 was the most appropriate value for estimating the transfer length with a coefficient of determination of 0.63.

6.2.2 Development length

1. The measured development lengths of 0.7 in. (17.8 mm) prestressing strands varied from 3.5 ft to 4 ft (1067 mm to 1220 mm). These lengths were approximately to 42% - 48% of the predicted development lengths using ACI 318 equation.
2. Concrete compressive strength had little effect on the measured development lengths. The N-CC-S, N-SCC-S, and H-SCC-S beams had an identical development length of 4 ft (1220 mm) regardless of the difference in concrete compressive strengths. The H-CC-S beams which used higher concrete compressive strength had a shorter development length of 3.5 ft (1070 mm).
3. The ACI 318 equation significantly over-predicted the measured flexural bond lengths. A new equation of flexural bond length was proposed based on the experimental results (Eq. 5.1). This equation was more appropriate for predicting the flexural bond lengths of 0.7 in. (17.8 mm) prestressing strands.

4. A new equation of development length of 0.7 in. (17.8 mm) prestressing strand was proposed (Eq. 5.3). The measured development lengths were approximately from 67% to 78% the predicted development length using the proposed equation. The over-prediction accounted for the limited experimental data in this study.

6.2.3 Strand spacing

1. The use of strand spacing of 2.0 in. (51 mm) had little effect on the measured transfer lengths at release, and no effect on the measured transfer length at 28 days. This conclusion was applicable for concrete which had compressive strengths of 8 ksi (55.2 MPa) or greater at 1 day.
2. The use of strand spacing of 2.0 in. (51 mm) had little to no effect on the measured development lengths of 0.7 in. (17.8 mm) prestressing strands. This conclusion was applicable for high strength concrete which had compressive strengths of 10 ksi (69.0 MPa) or greater at 28 days.

REFERENCES

AASHTO. (2012). "LRFD Specifications for Highway Bridges." *American Association of State Highway and Transportation Officials,* Washington D.C.

ACI Committee 237. (2007). "Self-Consolidating Concrete." *American Concrete Institute,* Farmington Hills, MI.

ACI Committee 318. (2011). "Building Code Requirements for Structural Concrete (ACI 318-11) and Commentary (ACI 318R-11)." *ACI 318,* Farmington Hills, MI.

ACI Committee 323. (1963). "Building Code Requirements for Structural Concrete (ACI 318-63) and Commentary (ACI 318R-63)." *ACI 318-63,* Detroit, MI.

Akhnoukh, A. K. (2008). "Development of high performance precast/prestressed bridge girders". Ph.D. The University of Nebraska - Lincoln, United States -- Nebraska.

Arab, A. A. (2012). "Finite Element Modeling of Pretensioned Concrete Girders: A Methodological Approach with Applications in Large Strands and End Zone Cracking". Ph.D. The George Washington University, United States -- District of Columbia.

ASTM A1081. (2012). "Standard Test Method for Evaluating Bond of Seven-Wire Steel Prestressing Strand." West Conshohocken, PA.

ASTM A416. (2012). "Standard Specification for Steel Strand, Uncoated Seven-Wire for Prestressed Concrete." West Conshohocken, PA.

ASTM C143. (2012). "Standard Test Method for Slump of Hydraulic-Cement Concrete." West Conshohocken, PA.

ASTM C1611. (2014). "Standard Test Method for Slump Flow of Self-Consolidating Concrete." West Conshohocken, PA.

ASTM C1621. (2014). "Standard Test Method for Passing Ability of Self-Consolidating Concrete by J-Ring." West Conshohocken, PA.

Barnes, R. W., Burns, N. H., and Kreger, M. E. (1999). "Development Length of 0.6-Inch Prestressing Strand in Standard I-Shaped Pretensioned Concrete Beams." *Rep. No. 1388-1,* Center for Transportation Research, The University of Texas at Austin, Texas Department of Transportation.

Barnes, R. W., Grove, J. W., and Burns, N. H. (2003). "Experimental assessment of factors affecting transfer length." *ACI Struct.J.,* 100(6), 740-748.

Boehm, K. M., Barnes, R. W., and Schindler, A. K. (2010). "Performance of Self-consolidating Concrete in Prestressed Girders." *Rep. No. FHWA/ALDOT 930-602,* Alabama Department of Transportation, Alabama.

Buckner, C. D. (1995). "A review of strand development length for pretensioned concrete members." *PCI J.,* 40(2), 84-99.

Carroll, J. C. (2009). "Grade 300 Prestressing Strand and the Effect of Vertical Casting Position". Ph.D. Virginia Polytechnic Institute and State University, United States -- Virginia.

Cousins, T. E., Johnston, D. W., and Zia, P. (1990a). "Transfer and Development Length of Epoxy-Coated and Uncoated Prestressing Strands." *PCI Journal,* 35(3), 92-106.

Cousins, T. E., Stallings, J. M., and Simmons, M. B. (1993). "Effect of Strand Spacing on Development of Prestressing Strand." *Rep. No. Research Report,* Alaska Department of Transportation and Public Facilities, Alaska.

Cousins, T. E., Johnsone, D. W., and Zia, P. (1990b). "Transfer length of epoxy-coated prestressing strand." *ACI Mater.J.,* 87(3), 193-203.

Cousins, T. E., Stallings, J. M., and Simmons, M. B. (1994). "Reduced strand spacing in pretensioned, prestressed members." *ACI Struct.J.,* 91(3), 277-286.

Dang, C. N., Murray, C. D., Floyd, R. W., Micah Hale, W., and Martí-Vargas, J. R. (2014a). "Analysis of bond stress distribution for prestressing strand by Standard Test for Strand Bond." *Eng.Struct.,* 72 152-159.

Dang, C. N., Murray, C. D., Floyd, R. W., Micah Hale, W., and Martí-Vargas, J. R. (2014b). "A Correlation of Strand Surface Quality to Transfer Length." *ACI Struct.J.,* 111(5), 1245-1252.

Deatherage, J. H., Burdette, E. G., and Chew, C. K. (1994). "Development length and lateral spacing requirements of prestressing strand for prestressed concrete bridge girders." *PCI J.,* 39(1), 70-83.

Floyd, R. W., Ruiz, E. D., Do, N. H., Staton, B. W., and Hale, W. M. (2011a). "Development lengths of high-strength self-consolidating concrete beams." *PCI J.,* 56(1), 36-53.

Floyd, R. W., Howland, M. B., and Micah Hale, W. (2011b). "Evaluation of strand bond equations for prestressed members cast with self-consolidating concrete." *Eng.Struct.,* 33(10), 2879-2887.

Gilbert, R. I., and Mickleborough, N. C. (1990). *Design of prestressed concrete.*

Girgis, A. F. M., and Tuan, C. Y. (2005). "Bond Strength and Transfer Length of Pre-tensioned Bridge Girders Cast with Self-Consolidating Concrete." *PCI J.,* 72-87.

Gross, S. P., and Burns, N. H. (1995). "Transfer and development length of 15.2 mm (0.6 in.) diameter prestressing strand in high performance concrete: results of the Hoblitzell-Buckner beam tests." *Rep. No. FHWA/TX-97/580-2,* Center for Transportation Research, Texas.

Guyon, Y. (1953). "Pretensioned Concrete: Theoretical and Experimental Study." Paris, France.

Hatami, A., Morcous, G., Hanna, K. E., and Tadros, M. K. (2011). "Evaluating the Bond of 0.7-in. Diameter Prestressing Strands for Concrete Bridge Girders." *TRB,* (11-2104), 1-13.

Janney, J. R. (1954). "Nature of bond in pre-tensioned prestressed concrete." *ACI Journal,* .

Khayat, K., and Mitchell, D. (2009). "Self-consolidating concrete for precast, prestressed concrete bridge elements." *Rep. No. NCHRP-628,* Transportation Research Board, Washington, D.C.

Koehler, E. P., and Fowler, D. W. (2007). "Inspection Manual for Self-consolidating Concrete in Precast Members." *Rep. No. TxDOT Project 0-5134,* Center for Transportation Research, Texas.

Lane, S., and Rekenthaler Jr, D. (1998). "The Ties That Bind: The 10-Year Fight for 0.6-Inch Diameter Strands." *Public Roads,* 61(5), 27-29.

Larson, K. H., Peterman, R. J., and Esmaeily, A. (2007). "Bond characteristics of self-consolidating concrete for prestressed bridge girders." *PCI J.,* 52(4), 44-57.

Logan, D. R. (1997). "Acceptance criteria for bond quality of strand for pretensioned prestressed concrete applications." *PCI J.,* 42(2), 52-90.

Maguire, M. (2009). "Impact of 0.7 inch diameter prestressing strands in bridge girders". Master. University of Nebraska--Lincoln, .

Maguire, M., Morcous, G., and Tadros, M. (2013). "Structural Performance of Precast/Prestressed Bridge Double-Tee Girders Made of High-Strength Concrete, Welded Wire Reinforcement, and 18-mm-Diameter Strands." *J.Bridge Eng.,* 18(10), 1053-1061.

Martí-Vargas, J. R., Arbelaez, C. A., Serna-Ros, P., and Castro-Bugallo, C. (2007a). "Reliability of transfer length estimation from strand end slip." *ACI Struct.J.,* 104(4), 487-494.

Martí-Vargas, J. R., Arbelaez, C. A., Serna-Ros, P., Fernandez-Prada, M. A., and Miguel-Sosa, P. F. (2006). "Transfer and development lengths of concentrically prestressed concrete." *PCI Journal,* 51(5), 74-85.

Martí-Vargas, J. R., Arbelaez, C. A., Serna-Ros, P., Navarro-Gregori, J., and Pallares-Rubio, L. (2007b). "Analytical model for transfer length prediction of 13 mm prestressing strand." *Structural Engineering & Mechanics,* 26(2), 211-229.

Martí-Vargas, J. R., Serna, P., Navarro-Gregori, J., and Bonet, J. L. (2012). "Effects of concrete composition on transmission length of prestressing strands." *Construction and Building Materials,* 27(1), 350-356.

Meyer, K. F., Kahn, L. F., La, J. S., and Kurtis, K. E. (2002). "Transfer and Development Length of High Strength Lightweight Concrete Precast Prestressed Bridge Girders." *Rep. No. 02-5,* Georgia Department of Transportation, Georgia.

Mitchell, D., Cook, W. D., Khan, A. A., and Tham, T. (1993). "Influence of High Strength Concrete on Transfer and Development Length of Pretensioning Strand." *PCI J.,* 38(3), 52-66.

Morcous, G., Hanna, K., and Tadros, M. K. (2011a). "Use of 0.7-in.-diameter strands in pretensioned bridge girders." *PCI J.,* 56(4), 65-82.

Morcous, G., Hanna, K., and Tadros, M. K. (2011b). "Impact of 0.7 Inch Diameter Strands on NU I-Girders." *Rep. No. P311,* Nebraska Department of Roads (NDOR), Nebraska.

Morcous, G., Hatami, A., Maguire, M., Hanna, K., and Tadros, M. (2012). "Mechanical and Bond Properties of 18-mm- (0.7-in.-) Diameter Prestressing Strands." *Journal of Materials in Civil Engineering,* 24(6), 735-744.

Morcous, G., Asaad, S., and Hatami, A. (2013). "Implementation of 0.7 in. Diameter Strands in Prestressed Concrete Girders." *Rep. No. SPR-P1(13) M333,* Nebraska Department of Roads, Nebraska.

Morcous, G., Assad, S., Hatami, A., and Tadros, M. K. (2014). "Implementation of 0.7 in. diameter strands at 2.0× 2.0 in. spacing in pretensioned bridge girders." *PCI J.,* 59(3), 145-158.

Morcous, G., Hanna, K., and Tadros, M. K. (2010). "Transfer and Development Length of 0.7-in.(17.8-mm) Diameter Strands in Pretensioned Concrete Bridge Girders." *HPC Bridge Views,* (64), 7-9.

Myers, J. J., Volz, J. S., Sells, E., Porterfield, K., Looney, T., Tucker, B., and Holman, K. (2012). "Report B: Self-Consolidating Concrete (SCC) for Infrastructure Elements: Bond, Transfer Length, and Development Length of Prestressing Strand in SCC." *Rep. No. CMR 13-003,* Missouri Department of Transportation, Missouri University of Science and Technology.

Oh, B. H., and Kim, E. S. (2000). "Realistic evaluation of transfer lengths in pretensioned, prestressed concrete members." *ACI Struct.J.,* 97(6), 821-830.

Okamura, H., and Ouchi, M. (2003). "Self-compacting concrete." *Journal of Advanced Concrete Technology,* 1(1), 5-15.

Okamura, H., Ozawa, K., and Ouchi, M. (2000). "Self-compacting concrete." *Structural Concrete,* 1(1), 3-17.

Park, H., and Cho, J. (2014). "Bond-Slip-Strain Relationship in Transfer Zone of Pretensioned Concrete Elements." *ACI Struct.J.,* 111(3), 503-514.

Patzlaff, Q., Morcous, G., Hanna, K., and Tadros, M. (2012). "Bottom Flange Confinement Reinforcement in Precast Prestressed Concrete Bridge Girders." *J.Bridge Eng.,* 17(4), 607-616.

Patzlaff, Q. (2010). "Impact of bottom flange confinement reinforcement on performance of prestressed concrete bridge girders". Master. University of Nebraska -- Lincoln, .

Precast-Prestressed Concrete Institute. (2010). *PCI Design Handbook: Precast and Prestressed Concrete.* PCI, Chicago.

Ramirez, J. A., and Russell, B. W. (2008). "Transfer, development, and splice length for strand/reinforcement in high strength concrete." *Rep. No. NCHRP 603,* Transportation Research Board, Washington, D.C.

Rose, D., and Russell, B. (1997). "Investigation of standardized tests to measure the bond performance of prestressing strand." *PCI J.,* 42(4), 56-80.

Russell, B. W. (2006). "NASP Round IV Strand Bond Testing." *Rep. No. Final Report,* OK.

Russell, B. W., and Brown, M. D. (2004). "Evaluation of Test Methods in Assessing Bond Quality of Prestressing Strands." *Rep. No. Final Report,* Oklahoma State University, Stillwater, OK.

Russell, B. W., and Burns, N. (1997). "Measurement of Transfer Lengths on Pretensioned Concrete Elements." *J.Struct.Eng.,* 123(5), 541-549.

Russell, B. W., and Paulsgrove, G. A. (1999a). "Assessing Repeatability and Reproducibility of the Moustafa Test, the PTI Bond Test and the NASP Bond Test." *Rep. No. Final Report 99-04,* The University of Oklahoma, Fears Structural Engineering Laboratory, Norman, OK.

Russell, B. W., and Paulsgrove, G. A. (1999b). "NASP Strand Bond Testing Round One Pull-Out Tests and Friction Bond Tests of Untensioned Strand." *Rep. No. Final Report 99-03,* The University of Oklahoma, Fears Structural Engineering Laboratory, Norman, OK.

Russell, B. W., and Burns, N. H. (1996). "Measured transfer lengths of 0.5 and 0.6 in. strands in pretensioned concrete." *PCI J.,* 41(5), 44-65.

Russell, B. W., and Burns, N. H. (1993). "Design Guidelines For Transfer, Development And Debonding Of Large Diameter Seven Wire Strands In Pretensioned Concrete Girders." *Rep. No. FHWA/TX-93+1210-5F,* Texas Department of Transportation, Austin.

Russell, H., Volz, J., and Bruce, R. N. (1997). "Optimized Sections for High-Strength Concrete Bridge Girders." *Rep. No. FHWA-RD-95-180,* Transportation Research Board, Washington, D.C.

Schuler, G. (2009). "Producer's Experience with 10,000 psi Concrete and 0.7-in. Diameter Strands." *HPC Bridge Views,* (54), 9-11.

Shahawy, M. A., Issa, M., and Batchelor, B. (1992). "Strand transfer lengths in full scale AASHTO prestressed concrete girders." *PCI J.,* 37(3), 84-96.

Song, W., Ma, Z. J., Vadivelu, J., and Burdette, E. G. (2013). "Transfer Length and Splitting Force Calculation for Pretensioned Concrete Girders with High-Capacity Strands." *J.Bridge Eng.,* 19(7), 1-8.

Staton, B. W., Do, N. H., Ruiz, E. D., and Hale, W. M. (2009). "Transfer lengths of prestressed beams cast with self-consolidating concrete." *PCI J.,* 54(2), 64-83.

Unay, I. O., Russell, B., Burns, N., and Kreger, M. (1991). "Measurement of transfer length on prestressing strands in prestressed concrete specimens." *Rep. No. 1210-1,* Federal Highway Administration, Austin.

Vadivelu, J. (2009). "Impact of Larger Diameter Strands on AASHTO/PCI Bulb-Tees". Master. University of Tennessee, TN.

Zia, P., and Mostafa, T. (1977). "Development length of prestressing strands." *PCI Journal,* 22(5), 54-65.

APPENDIX A : BEAM ANALYSIS

A.1 Cross-section properties

This section presents the calculation of gross and transformed cross-section parameters (**Figure A.1**). The gross cross-section parameters do not consider effects of reinforcement and prestressing strand as shown in **Table A.1**. The transformed cross-section, however, considers the contribution of reinforcement and prestressing strand (**Table A.2**) to its parameters. The calculation results are presented in **Table A.3**.

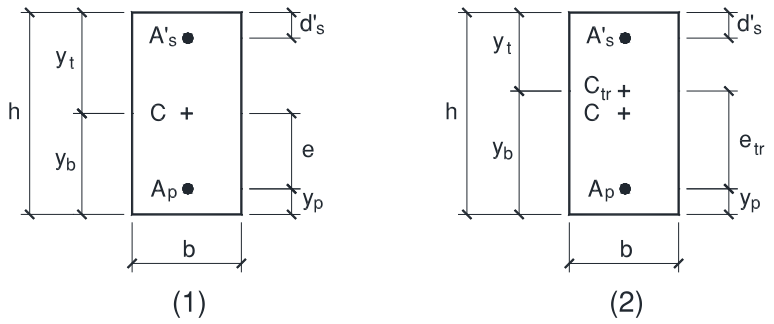

Figure A.1 – Cross-section parameters of: (1) gross cross-section and (2) transformed cross-section.
(Note: b = width of the cross-section; h = depth of the cross-section; C = center of the gross cross-section; A_p = prestressing strand area; A'_s = steel area; y_b = distance from the center of the gross cross-section to the bottom fiber of the beam; y_t = distance from the center of the gross cross-section to the top fiber of the beam; d'_s = distance from the center of reinforcement to the top fiber of the beam; y_p = distance from the center of prestressing strand to the bottom fiber of the beam; e = eccentricity of prestressing strand(s); $_{tr}$ = transformed cross-section)

Table A.1 – Gross cross-section properties

Beam	b (in.)	h (in.)	V/S (in.)	A_g (in.^{2})	I_g (in.^{4})	y_t (in.)	y_b (in.)	e (in.)
All beams	6.5	12	2.11	78	936	6	6	3.5

(Note: b = width of the cross-section; h = depth of the cross-section; V/S = volume-to-surface ratio; A_g = gross cross-sectional area; I_g = moment of inertia of the gross cross-section; y_b = distance from the center of the gross cross-section to the bottom fiber of the beam; y_t = distance from the center of the gross cross-section to the top fiber of the beam; e = eccentricity of prestressing strand; 1 in. = 25.4 mm)

Table A.2 – Concrete strengths and the placement of top steel and prestressing strand

Beam	Concrete				Reinforcement				Strand			
	f'_{ci} (psi)	f'_c (psi)	E_{ci} (ksi)	E_c (ksi)	N_s	*no.*	A'_s (in.^{2})	d'_s (in.)	N_p	d_b (in.)	A_p (in.^{2})	y_p (in.)
N-CC-S1&2	5930	9250	4389	5482	2	5	0.62	2	1	0.7	0.294	2.5
N-CC-S3&4	6610	9660	4634	5602	2	5	0.62	2	1	0.7	0.294	2.5
H-CC-S1&2	9490	13700	5553	6672	2	5	0.62	2	1	0.7	0.294	2.5
H-CC-S3&4	8890	13190	5374	6546	2	5	0.62	2	1	0.7	0.294	2.5
H-CC-D1&2	9690	12250	5611	6309	2	6	0.88	2	2	0.7	0.588	2.5
H-CC-D3&4	9880	13260	5666	6564	2	6	0.88	2	2	0.7	0.588	2.5
N-SCC-S1&2	5830	10330	4352	5793	2	5	0.62	2	1	0.7	0.294	2.5
N-SCC-S3&4	6050	9610	4434	5588	2	5	0.62	2	1	0.7	0.294	2.5
H-SCC-S1&2	8060	11030	5117	5986	2	5	0.62	2	1	0.7	0.294	2.5
H-SCC-S3&4	7770	10390	5024	5810	2	5	0.62	2	1	0.7	0.294	2.5
H-SCC-D1&2	7720	10180	5008	5751	2	6	0.88	2	2	0.7	0.588	2.5
H-SCC-D3&4	8130	10580	5139	5863	2	6	0.88	2	2	0.7	0.588	2.5

(Note: f'_{ci} = concrete compressive strength at 1 day; f'_c = concrete compressive strength at 28 days; E_{ci} = modulus of elasticity of concrete at 1 day; E_c = modulus of elasticity of concrete at 28 days; N_s = number of reinforcing bar; no. = bar size; A'_s = area of reinforcement; d'_s = distance from the center of reinforcement to the top fiber of the beam; N_p = number of prestressing strand; d_b = nominal strand diameter; A_p = area of prestressing strand; y_p = distance from the center of prestressing strand to the bottom fiber of the beam; 1 in. = 25.4 mm; 1 psi = 6.895 kPa; 1 ksi = 6.895 MPa)

Table A.3 – Transformed cross-section properties

Beam	b (in.)	h (in.)	V/S (in.)	A_{tr} (in.^{2})	I_{tr} (in.^{4})	y_t (in.)	y_b (in.)	e_{tr} (in.)
N-CC-S1&2	6.5	12	2.11	83.1	1011	5.902	6.098	3.598
N-CC-S3&4	6.5	12	2.11	82.8	1006	5.907	6.093	3.593
H-CC-S1&2	6.5	12	2.11	81.8	993	5.925	6.075	3.575
H-CC-S3&4	6.5	12	2.11	82.0	995	5.922	6.078	3.578
H-CC-D1&2	6.5	12	2.11	84.1	1024	5.927	6.073	3.573
H-CC-D3&4	6.5	12	2.11	84.0	1023	5.927	6.073	3.573
N-SCC-S1&2	6.5	12	2.11	83.2	1012	5.901	6.099	3.599
N-SCC-S3&4	6.5	12	2.11	83.1	1010	5.903	6.097	3.597
H-SCC-S1&2	6.5	12	2.11	82.3	998	5.917	6.083	3.583
H-SCC-S3&4	6.5	12	2.11	82.3	1000	5.915	6.085	3.585
H-SCC-D1&2	6.5	12	2.11	85.0	1037	5.917	6.083	3.583
H-SCC-D3&4	6.5	12	2.11	84.8	1034	5.919	6.081	3.581

(Note: b = width of the cross-section; h = depth of the cross-section; V/S = volume-to-surface ratio; A_{tr} = transformed cross-sectional area; I_{tr} = moment of inertia of the transformed cross-section; y_b = distance from the center of the transformed cross-section to the bottom fiber of the beam; y_t = distance from the center of the transformed cross-section to the top fiber of the beam; e_{tr} = eccentricity of prestressing strand; 1 in. = 25.4 mm)

A.2 Prestress losses

Prestress losses are determined using Refined Method as mentioned in Section 5.9.5 of AASHTO (2012). Parameters shown in **Table A.1**, **Table A.2**, and **Table A.3** were used to calculate the losses. **Table A.4** shows the prestress losses immediately after release the prestressing strands. Parameters used for calculating long-term losses are summarized in **Table A.5**. In the table, the age of concrete when load is initially applied (t_i) is 1 day, and the final age (t_f) is 28 days. The total losses at 28 days are shown in **Table A.6**.

Table A.4 – Prestress loss and strand stress immediately after transfer

Beam	f_{cgp} (ksi)	Δf_{pES} (ksi)	f_{pt} (ksi)
N-CC-S1&2	1.343	8.8	193.7
N-CC-S3&4	1.346	8.4	194.1
H-CC-S1&2	1.357	7.0	195.5
H-CC-S3&4	1.355	7.3	195.2
H-CC-D1&2	2.767	14.2	188.3
H-CC-D3&4	2.769	14.1	188.4
N-SCC-S1&2	1.343	8.9	193.6
N-SCC-S3&4	1.344	8.7	193.8
H-SCC-S1&2	1.352	7.6	194.9
H-SCC-S3&4	1.351	7.7	194.8
H-SCC-D1&2	2.743	15.8	186.7
H-SCC-D3&4	2.749	15.4	187.1

(Note: f_{cgp} = concrete stress at the center of gravity of prestressing tendons, that results from the prestressing force at either transfer or jacking and the self-weight of the member at sections of maximum moment; Δf_{pES} = loss in prestressing steel stress due to elastic shortening; f_{pt} = stress in prestressing steel immediately after transfer; 1 ksi = 6.895 MPa)

Table A.5 – Parameters for calculating long-time prestress loss

Beam	ε_{bid} (in./in.)	k_s	k_{hs}	k_f	k_{td}	K_{id}	$\Psi_b(t_f,t_i)$	k_{hc}
N-CC-S1&2	1.78E-04	1.176	1.020	0.722	0.429	0.931	0.691	1.000
N-CC-S3&4	1.69E-04	1.176	1.020	0.657	0.448	0.935	0.657	1.000
H-CC-S1&2	1.51E-04	1.176	1.020	0.477	0.549	0.947	0.584	1.000
H-CC-S3&4	1.53E-04	1.176	1.020	0.506	0.524	0.945	0.592	1.000
H-CC-D1&2	1.50E-04	1.176	1.020	0.468	0.557	0.901	0.582	1.000
H-CC-D3&4	1.50E-04	1.176	1.020	0.460	0.566	0.902	0.581	1.000
N-SCC-S1&2	1.80E-04	1.176	1.020	0.732	0.426	0.930	0.697	1.000
N-SCC-S3&4	1.76E-04	1.176	1.020	0.709	0.432	0.932	0.685	1.000
H-SCC-S1&2	1.57E-04	1.176	1.020	0.552	0.493	0.942	0.608	1.000
H-SCC-S3&4	1.59E-04	1.176	1.020	0.570	0.483	0.941	0.616	1.000
H-SCC-D1&2	1.59E-04	1.176	1.020	0.573	0.482	0.889	0.617	1.000
H-SCC-D3&4	1.56E-04	1.176	1.020	0.548	0.496	0.892	0.607	1.000

(Note: ε_{bid} = concrete shrinkage strain of girder between transfer and deck placement; k_s = factor for the effect of the volume-to-surface ratio; k_{hs} = humidity factor for shrinkage; k_f = factor for the effect of concrete strength; k_{td} = time development factor; K_{id} = transformed section coefficient that accounts for time-dependent interaction between concrete and bonded steel in the section being considered for time period between transfer and deck placement; $\Psi_b(t_f,t_i)$ = girder creep coefficient at final time due to loading introduced at transfer; k_{hc} = humidity factor for creep; 1 in. = 25.4 mm)

Table A.6 – Prestress losses at 28 days and effective strand stress

Beam	Δf_{pES} (ksi)	Δf_{pSR} (ksi)	Δf_{pCR} (ksi)	Δf_{pR1} (ksi)	Δf_{pT} (ksi)	f_{pe} (ksi)
N-CC-S1&2	8.8	4.8	5.7	1.6	20.9	181.6
N-CC-S3&4	8.4	4.6	5.1	1.6	19.7	182.8
H-CC-S1&2	7.0	4.1	3.9	1.7	16.7	185.8
H-CC-S3&4	7.3	4.2	4.1	1.6	17.1	185.4
H-CC-D1&2	14.2	3.9	7.5	1.4	27.0	175.5
H-CC-D3&4	14.1	3.9	7.4	1.4	26.8	175.7
N-SCC-S1&2	8.9	4.8	5.8	1.6	21.1	181.4
N-SCC-S3&4	8.7	4.7	5.6	1.6	20.6	181.9
H-SCC-S1&2	7.6	4.3	4.4	1.6	17.9	184.6
H-SCC-S3&4	7.7	4.3	4.5	1.6	18.2	184.3
H-SCC-D1&2	15.8	4.1	8.7	1.4	29.9	172.6
H-SCC-D3&4	15.4	4.0	8.3	1.4	29.1	173.4

(Note: Δf_{pES} = loss in prestressing steel stress due to elastic shortening; Δf_{pSH} = prestress loss due to shrinkage of girder concrete between transfer and deck placement; Δf_{pCR} = prestress loss due to creep of girder concrete between transfer and deck placement; Δf_{pR1} = prestress loss due to relaxation of prestressing strands between transfer and deck placemen; Δf_{pT} = total loss in prestressing steel stress; f_{pe} = effective stress in the prestressing steel after losses; 1 ksi = 6.895 MPa)

A.3 Nominal moment capacity

The nominal moment capacity is determined using Strain Compatibility as stated in Section 5.2 of PCI Design Handbook (2010). **Table A.7** summarizes the calculation results of 24 pretensioned concrete beams.

Table A.7 – Nominal moment capacity

Beam	a (in.)	c (in.)	$\varepsilon_1 \times 10^3$ (in./in.)	$\varepsilon_2 \times 10^3$ (in./in.)	$\varepsilon_3 \times 10^3$ (in./in.)	$\varepsilon_{ps} \times 10^3$ (in./in.)	$\varepsilon'_s{}^* \times 10^3$ (in./in.)	f_{ps} *(ksi)*	f'_s *(ksi)*	M_n *(k*.in.)
N-CC-S1&2	1.39	2.14	6.33	0.24	10.33	16.90	0.19	266	6	684
N-CC-S3&4	1.32	2.03	6.37	0.24	11.03	17.64	0.05	266	1	690
H-CC-S1&2	1.11	1.71	6.47	0.21	13.69	20.37	-0.51	267	15	714
H-CC-S3&4	1.18	1.82	6.45	0.22	12.70	19.37	-0.31	267	9	706
H-CC-D1&2	1.75	2.69	6.11	0.39	7.59	14.09	0.77	264	22	1317
H-CC-D3&4	1.76	2.71	6.12	0.40	7.53	14.04	0.78	264	23	1315
N-SCC-S1&2	1.44	2.22	6.32	0.25	9.86	16.43	0.29	266	8	679
N-SCC-S3&4	1.39	2.14	6.33	0.24	10.33	16.90	0.19	266	6	684
H-SCC-S1&2	1.27	1.95	6.43	0.23	11.59	18.25	-0.07	266	2	696
H-SCC-S3&4	1.31	2.02	6.42	0.24	11.14	17.80	0.02	266	1	691
H-SCC-D1&2	2.12	3.26	6.01	0.44	5.74	12.19	1.16	262	34	1272
H-SCC-D3&4	2.19	3.37	6.03	0.46	5.46	11.95	1.22	262	35	1262

(Note: * = a negative value indicates the reinforcement in tension; a = depth of equivalent rectangular stress block; c = distance from extreme compression fiber to neutral axis; ε_1 = strain caused by the effective prestress after all losses; ε_2 = strain in the concrete required to reach zero compressive stress; ε_3 = strain in the strand at failure; ε_{ps} = total strain in prestressing strand; f_{sp} = specific strand stress; f'_s = steel stress; M_n = nominal moment capacity)

A.4 Predicted transfer and development lengths

Transfer and development lengths were predicted using ACI 318 equations (Eq 1.1 and Eq. 1.3).

Table A.8 summarizes the calculation results.

Table A.8 – Predicted transfer and development lengths

Beam	L_t (in.)	L_d (in. (ft))
N-CC-S1&2	43	101 (8.4)
N-CC-S3&4	43	101 (8.4)
H-CC-S1&2	43	100 (8.3)
H-CC-S3&4	43	100 (8.3)
H-CC-D1&2	41	103 (8.6)
H-CC-D3&4	41	103 (8.6)
N-SCC-S1&2	42	101 (8.4)
N-SCC-S3&4	43	101 (8.4)
H-SCC-S1&2	43	100 (8.3)
H-SCC-S3&4	43	100 (8.3)
H-SCC-D1&2	40	103 (8.6)
H-SCC-D3&4	41	102 (8.5)

(Note: L_t = transfer length; L_d = development length; 1 in. = 25.4 mm; 1 ft = 305 mm)

APPENDIX B : TRANSFER LENGTH DATA

B.1 Transfer length measurement

This section presents the measured transfer lengths at release, and at 7, 14, 21, and 28 days. In the following figures, the first and second value represent the measured transfer lengths at the live and the dead end. For instance, the measured transfer length at release of beam N-CC-S1 (**Figure B.1**) at the live end is 27.3 in. (695 mm) and at the dead end is 27.6 in. (700 mm).

B.1.1 N-CC-S beams

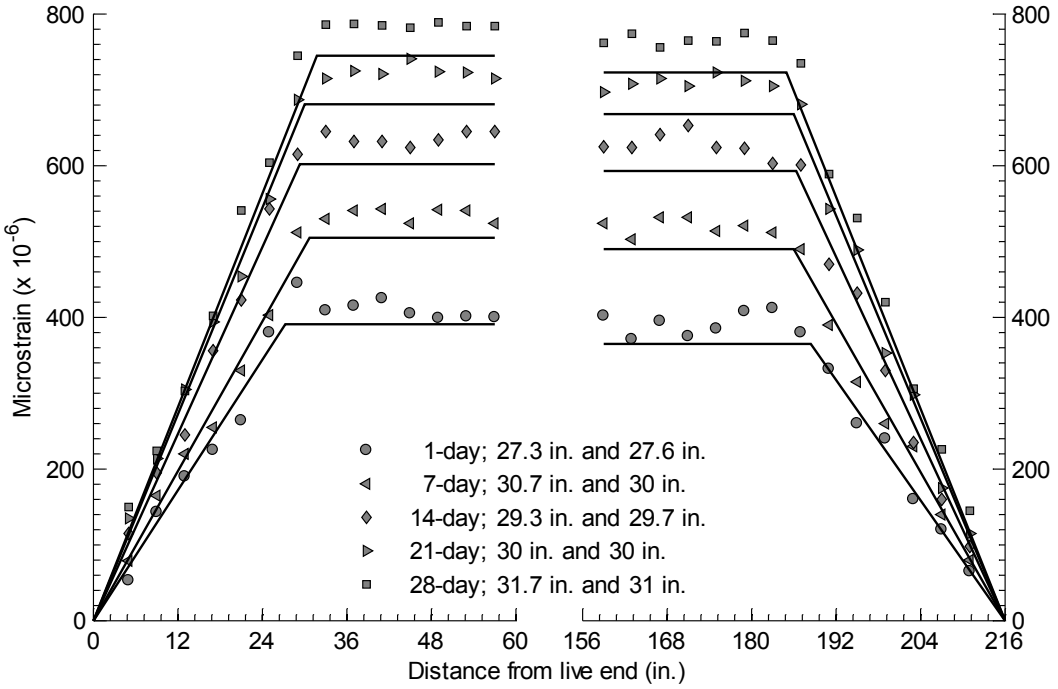

Figure B.1 – Measured transfer lengths of beam N-CC-S1
(Note: 1 in. = 25.4 mm)

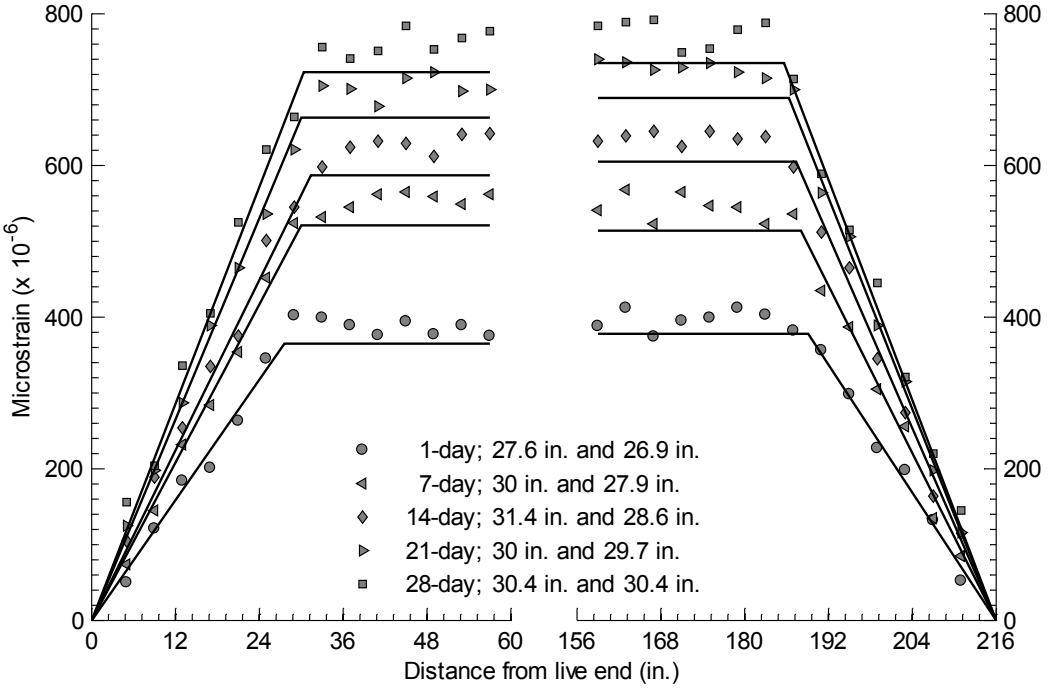

Figure B.2 – Measured transfer lengths of beam N-CC-S2
(Note: 1 in. = 25.4 mm)

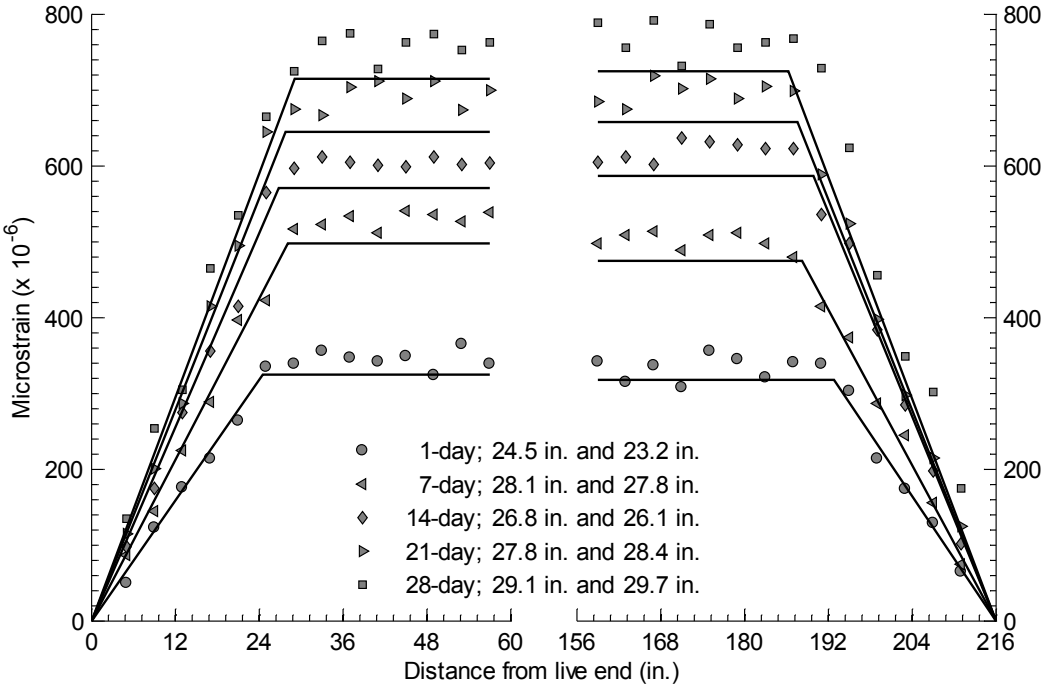

Figure B.3 – Measured transfer lengths of beam N-CC-S3
(Note: 1 in. = 25.4 mm)

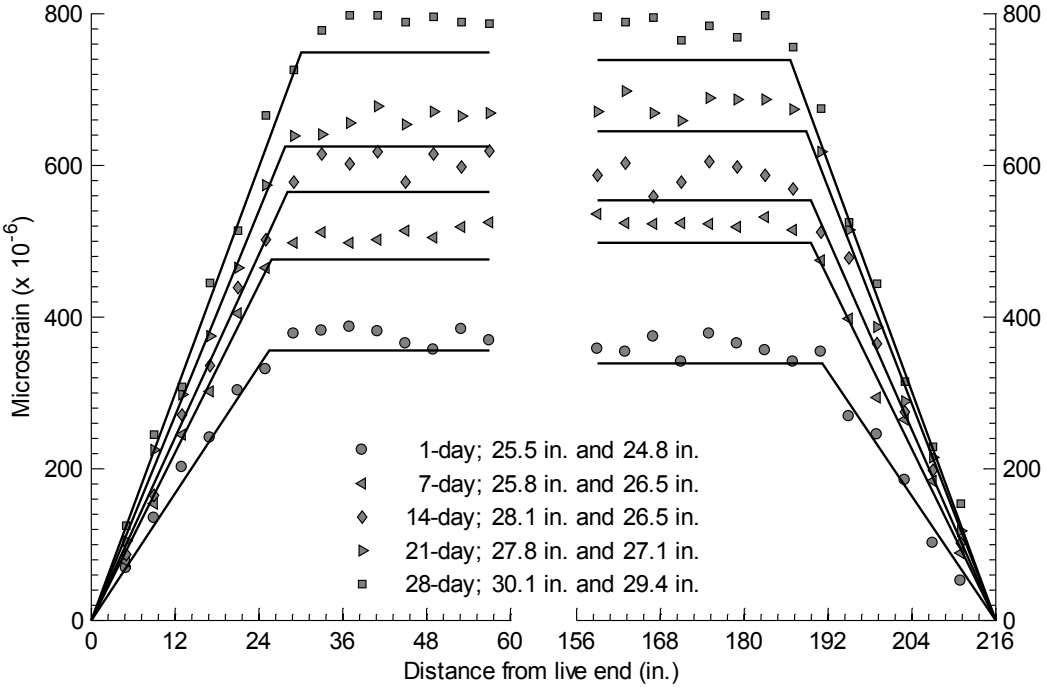

Figure B.4 – Measured transfer lengths of beam N-CC-S4
(Note: 1 in. = 25.4 mm)

B.1.2 H-CC-S beams

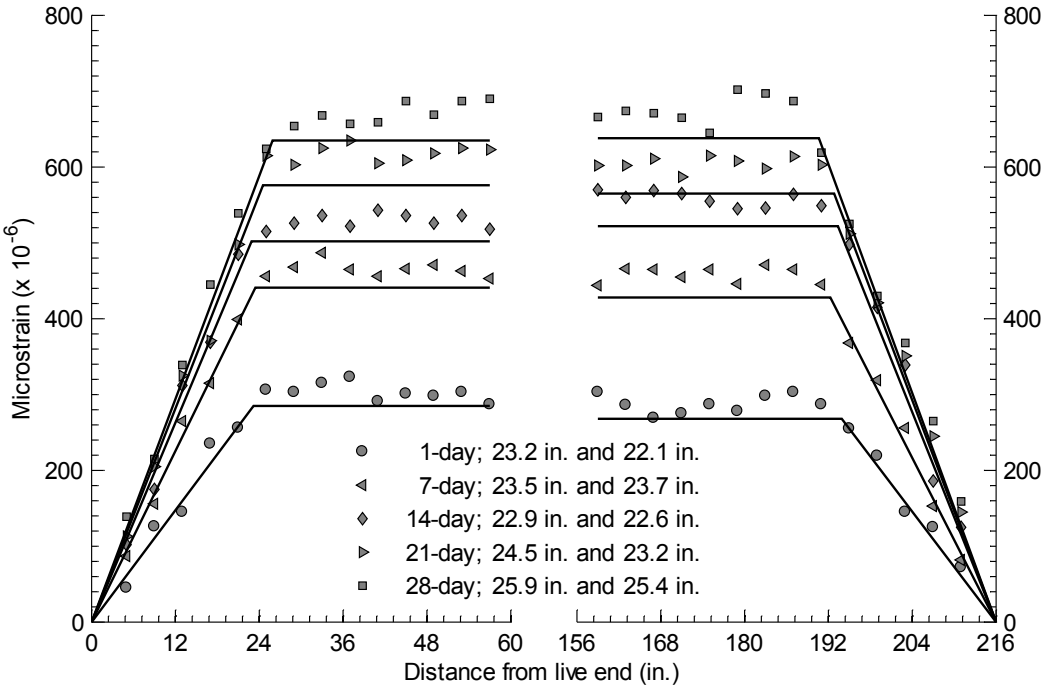

Figure B.5 – Measured transfer lengths of beam H-CC-S1
(Note: 1 in. = 25.4 mm)

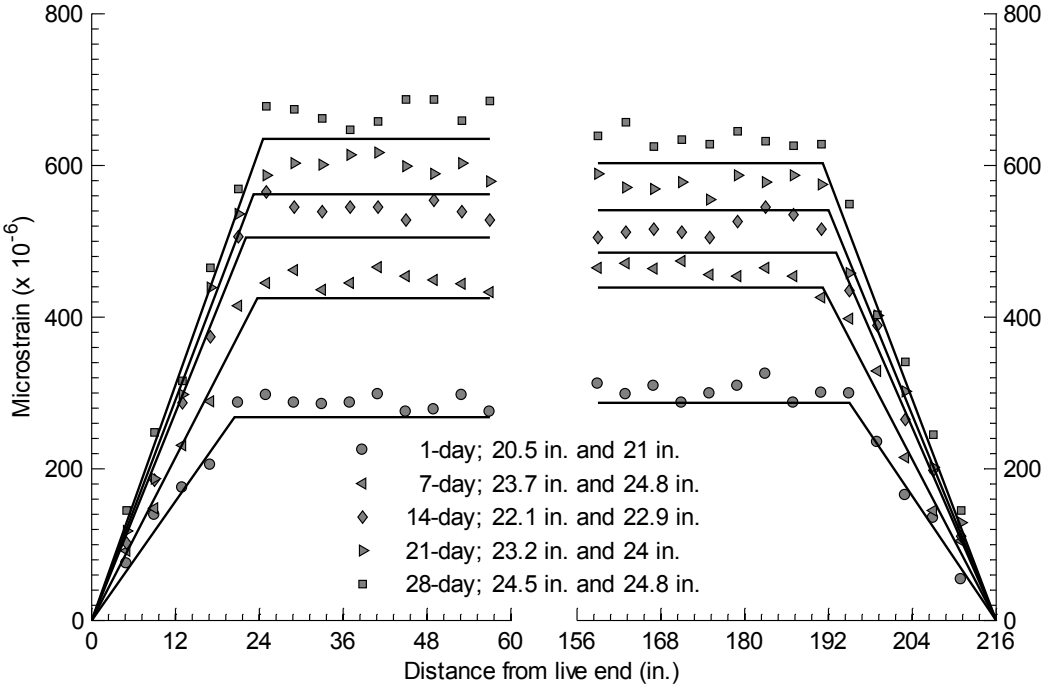

Figure B.6 – Measured transfer lengths of beam H-CC-S2
(Note: 1 in. = 25.4 mm)

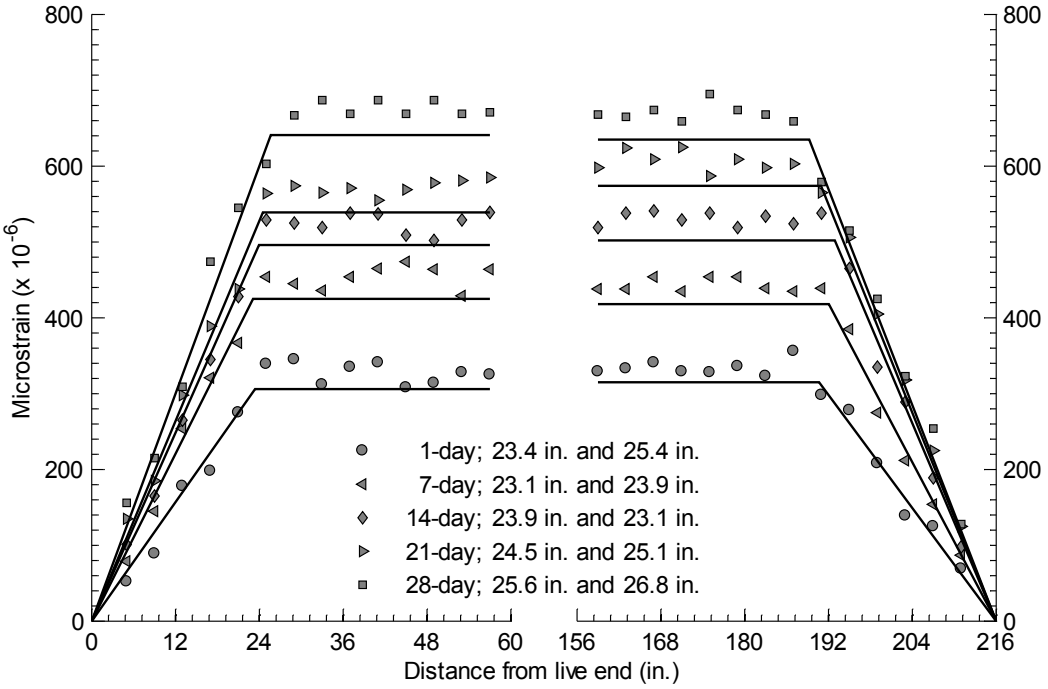

Figure B.7 – Measured transfer lengths of beam H-CC-S3
(Note: 1 in. = 25.4 mm)

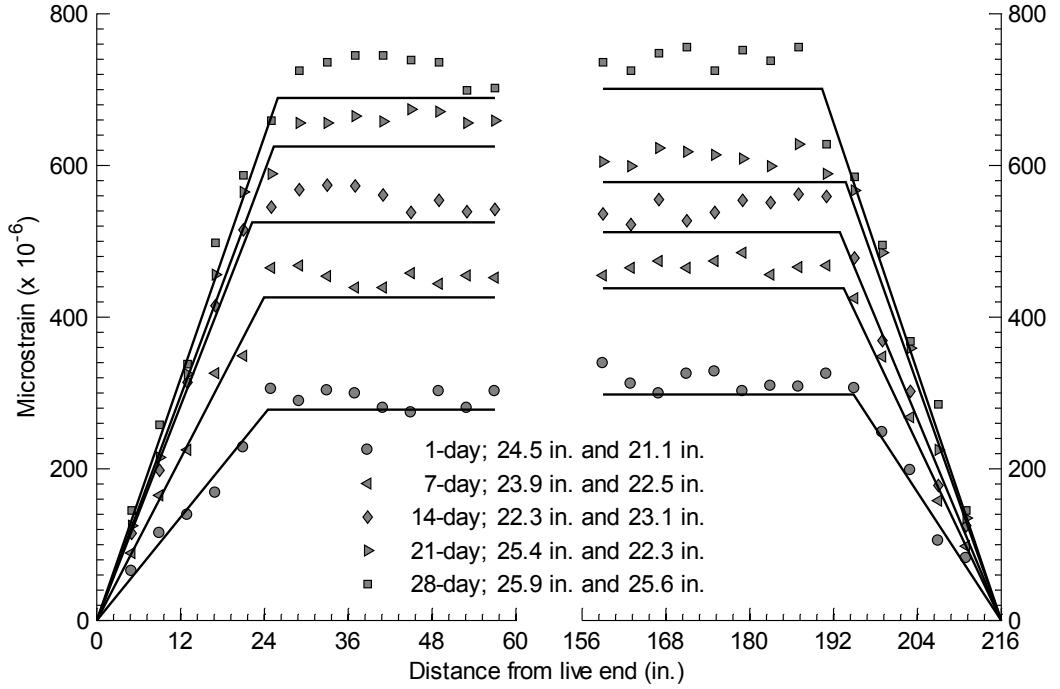

Figure B.8 – Measured transfer lengths of beam H-CC-S4
(Note: 1 in. = 25.4 mm)

B.1.3 H-CC-D beams

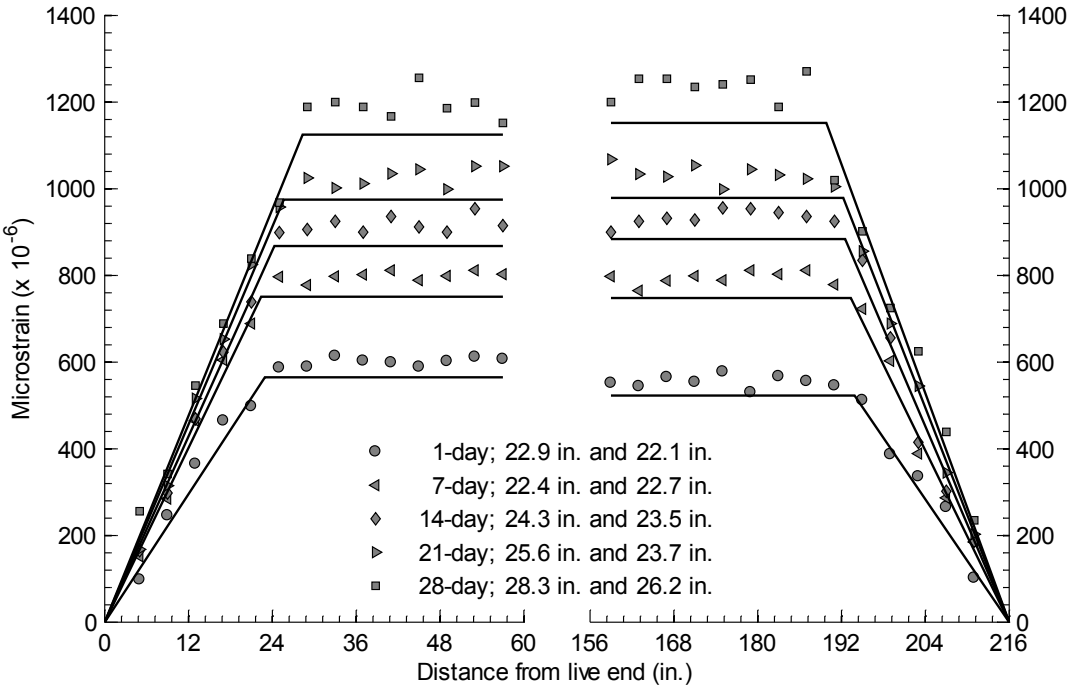

Figure B.9 – Measured transfer lengths of beam H-CC-D1
(Note: 1 in. = 25.4 mm)

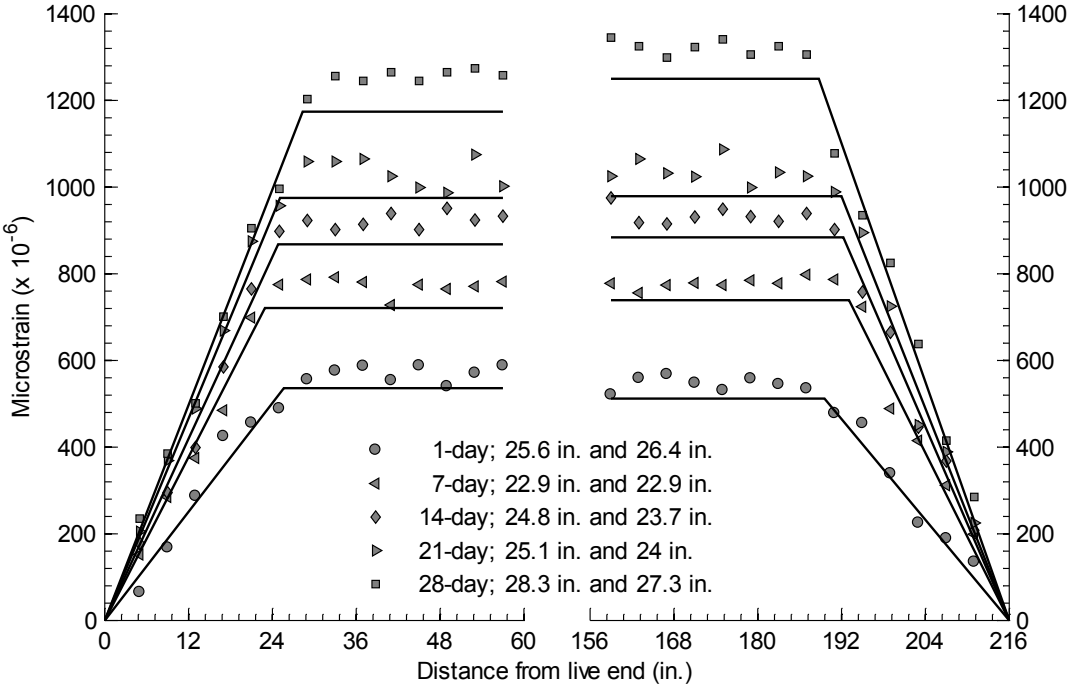

Figure B.10 – Measured transfer lengths of beam H-CC-D2
(Note: 1 in. = 25.4 mm)

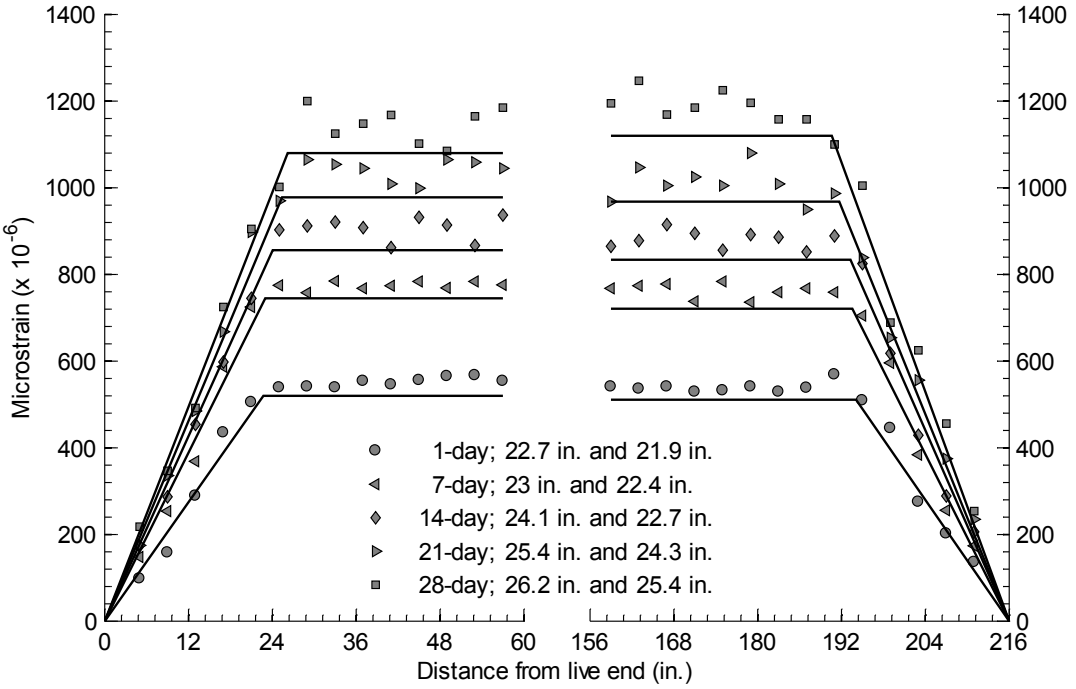

Figure B.11 – Measured transfer lengths of beam H-CC-D3
(Note: 1 in. = 25.4 mm)

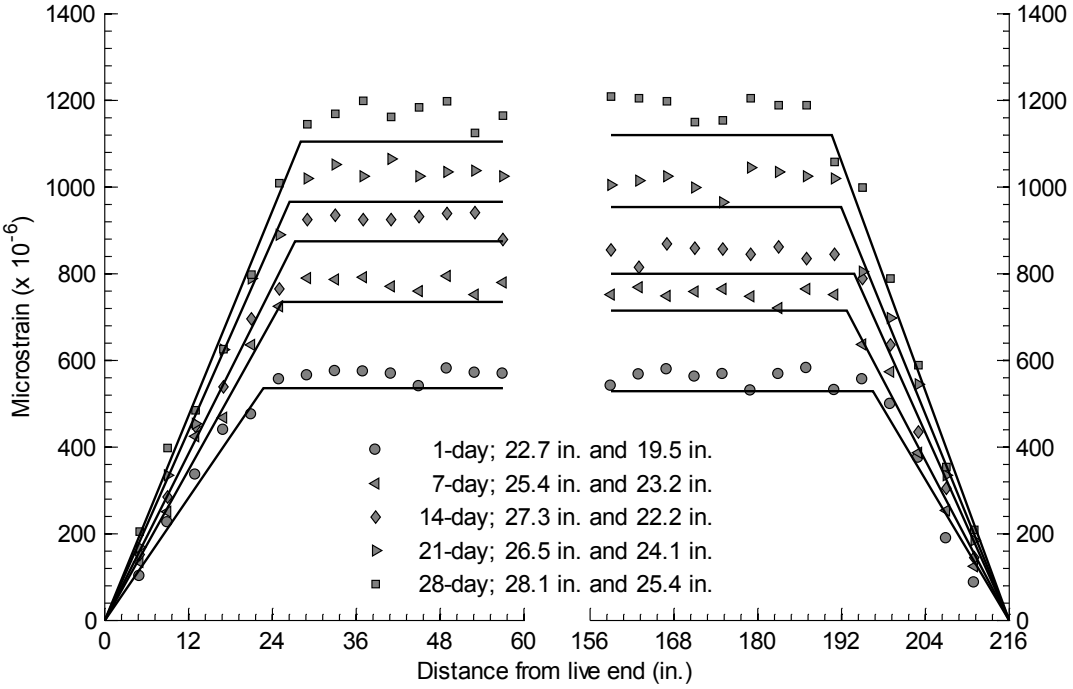

Figure B.12 – Measured transfer lengths of beam H-CC-D4
(Note: 1 in. = 25.4 mm)

B.1.4 N-SCC-S beams

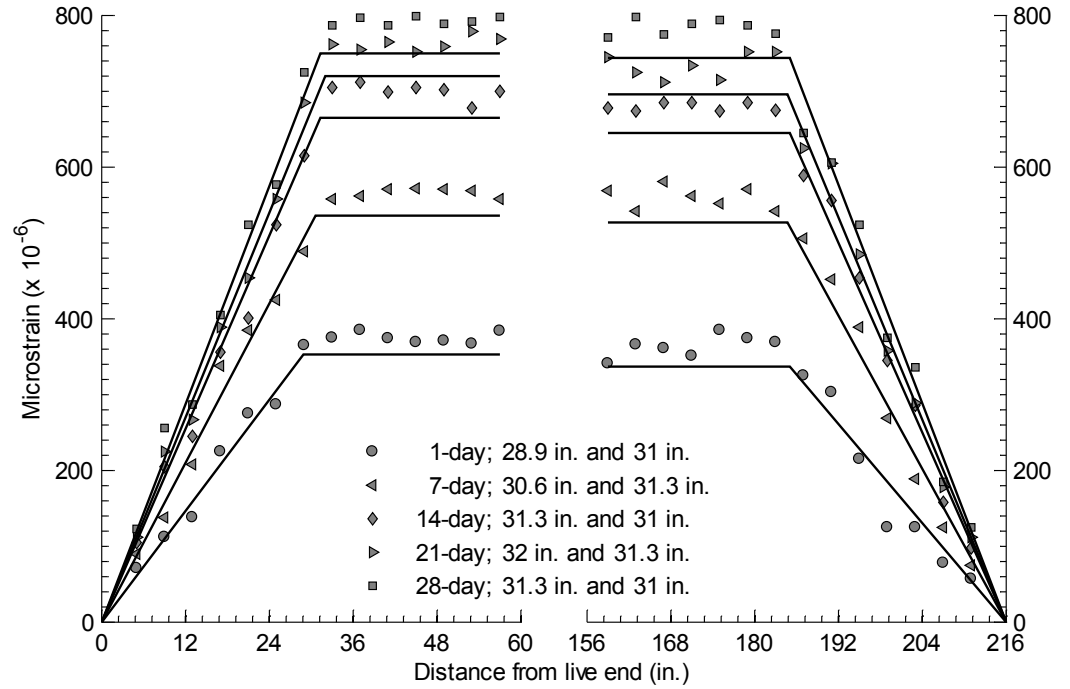

Figure B.13 – Measured transfer lengths of beam N-SCC-S1
(Note: 1 in. = 25.4 mm)

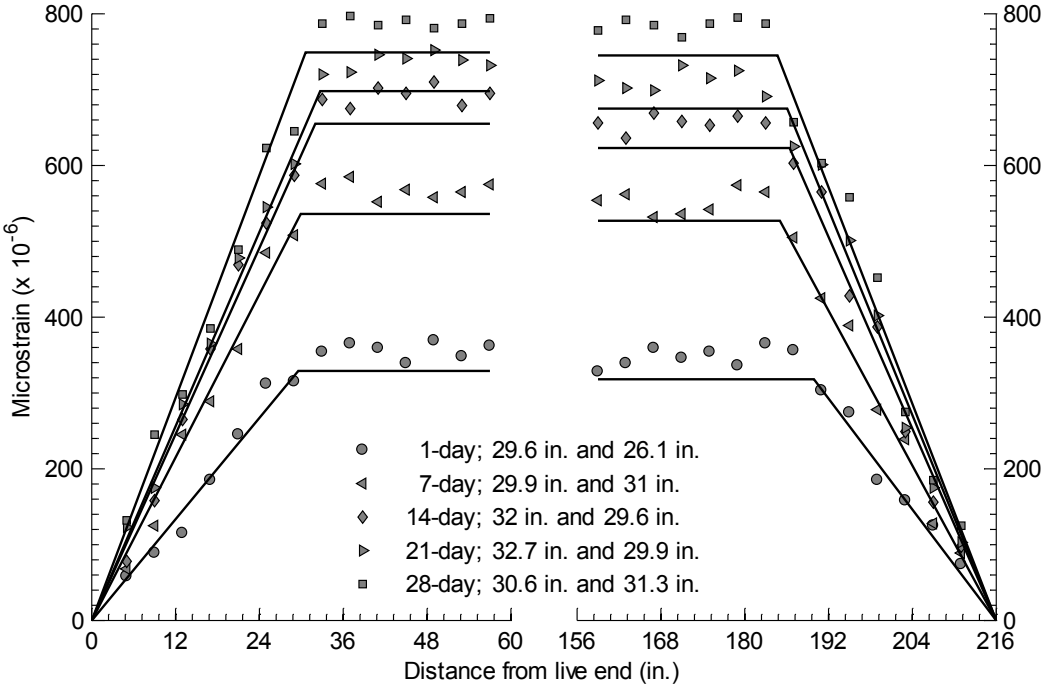

Figure B.14 – Measured transfer lengths of beam N-SCC-S2
(Note: 1 in. = 25.4 mm)

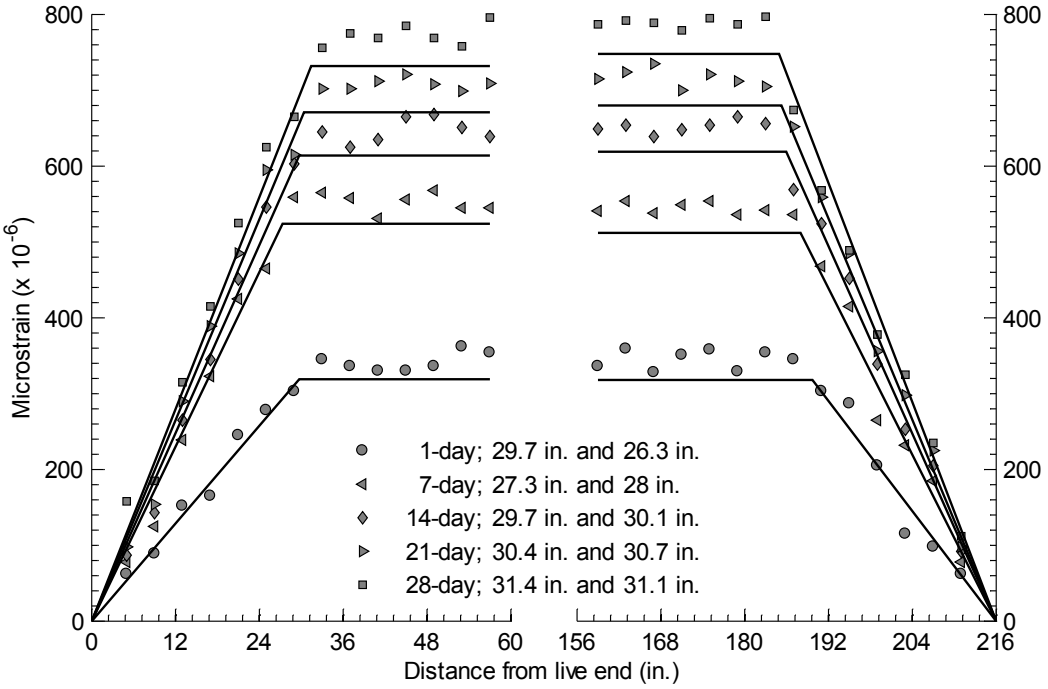

Figure B.15 – Measured transfer lengths of beam N-SCC-S3
(Note: 1 in. = 25.4 mm)

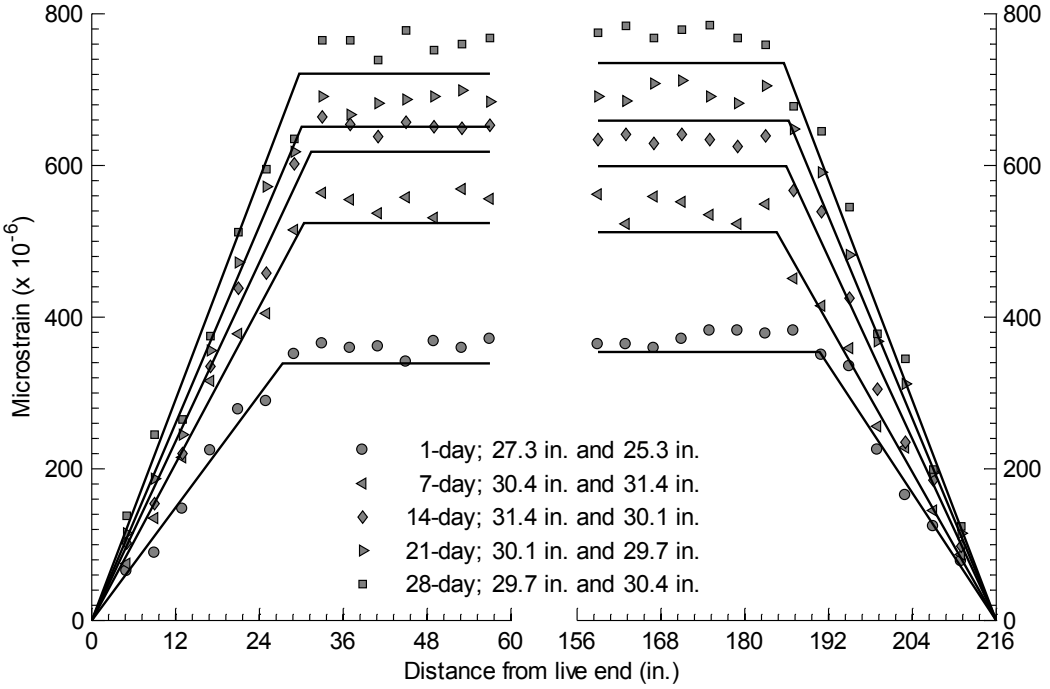

Figure B.16 – Measured transfer lengths of beam N-SCC-S4
(Note: 1 in. = 25.4 mm)

B.1.5 H-SCC-S beams

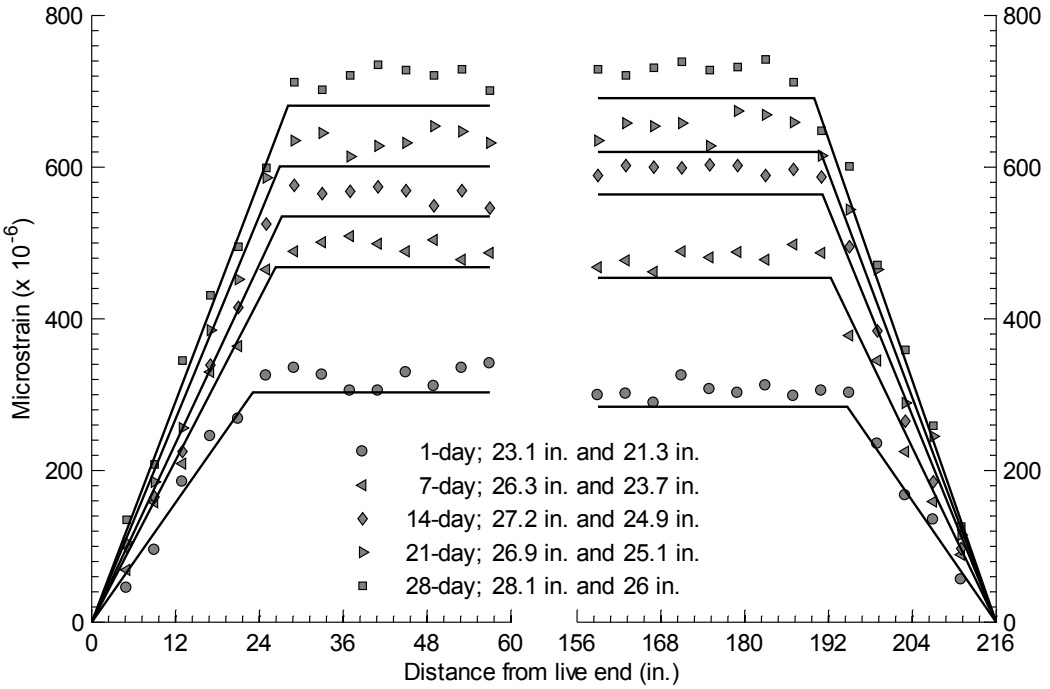

Figure B.17 - Measured transfer lengths of beam H-SCC-S1
(Note: 1 in. = 25.4 mm)

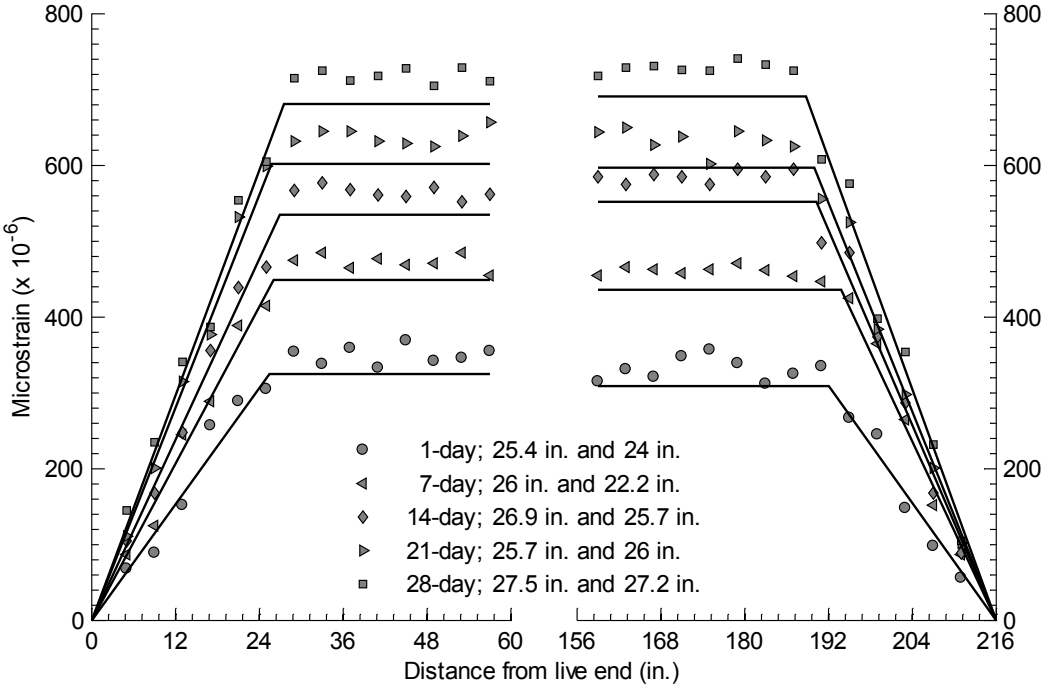

Figure B.18 – Measured transfer lengths of beam H-SCC-S2
(Note: 1 in. = 25.4 mm)

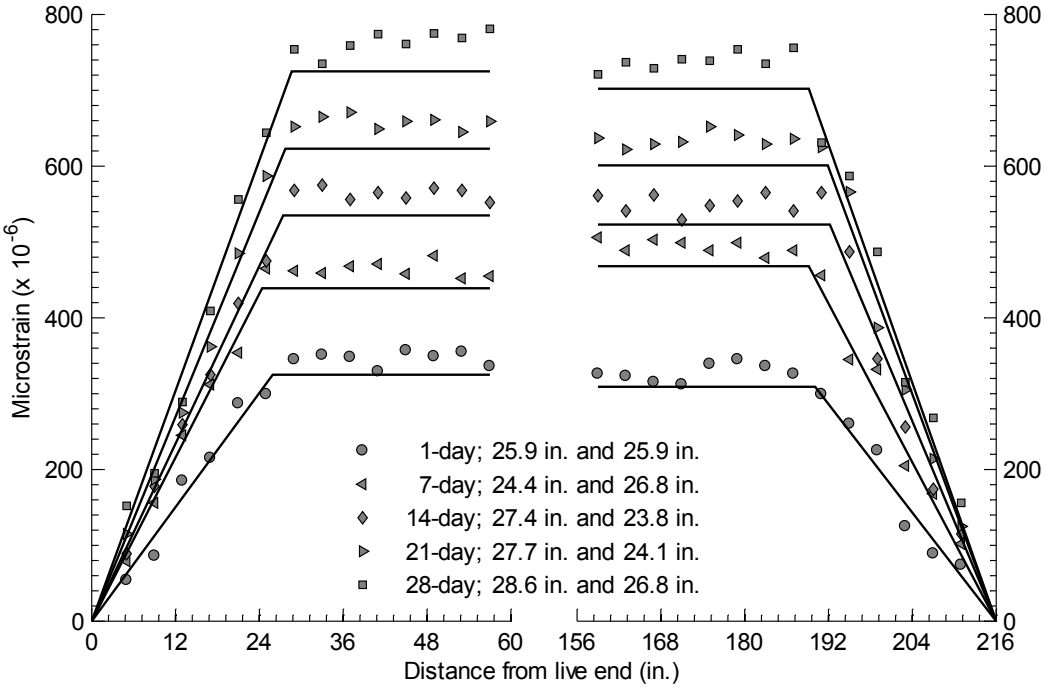

Figure B.19 – Measured transfer lengths of beam H-SCC-S3
(Note: 1 in. = 25.4 mm)

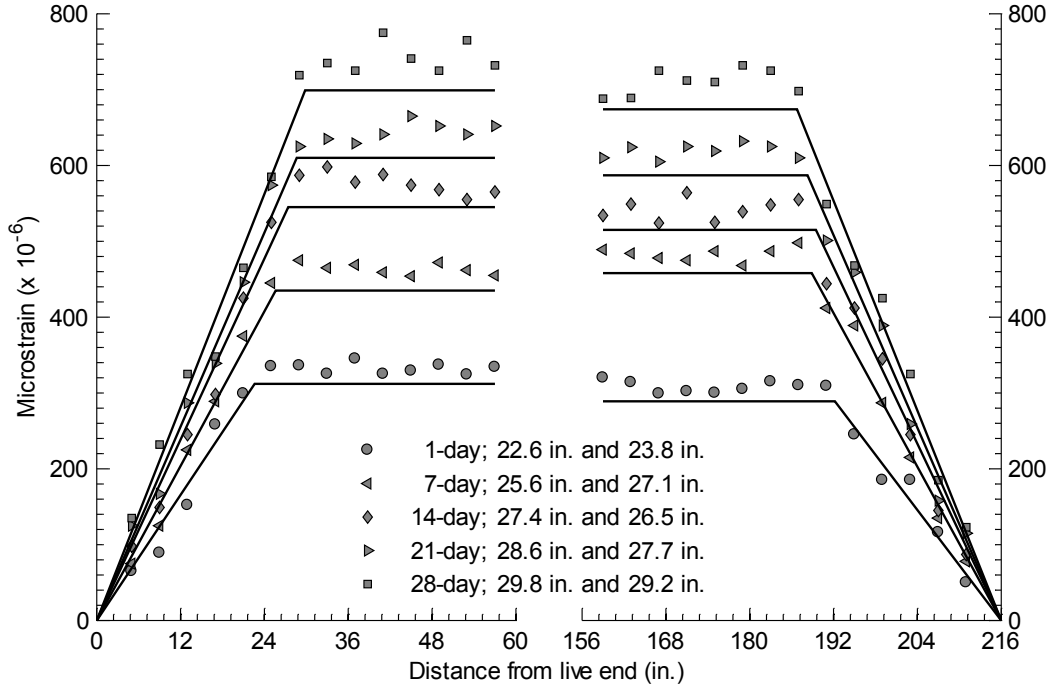

Figure B.20 - Measured transfer lengths of beam H-SCC-S4
(Note: 1 in. = 25.4 mm)

B.1.6 H-SCC-D beams

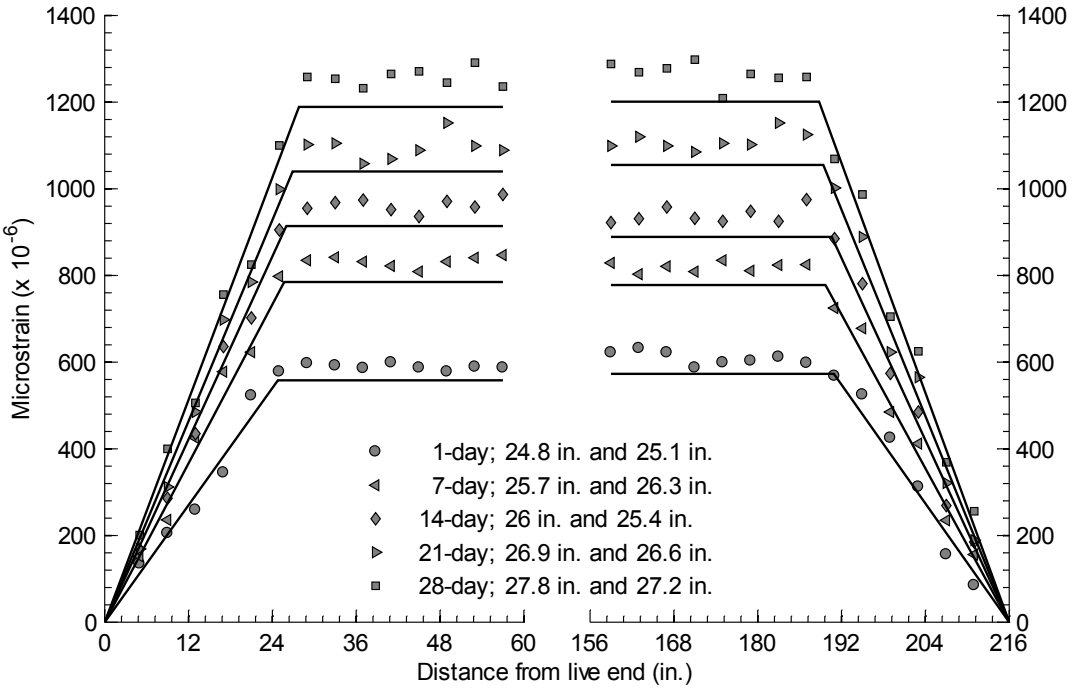

Figure B.21 – Measured transfer lengths of beam H-SCC-D1
(Note: 1 in. = 25.4 mm)

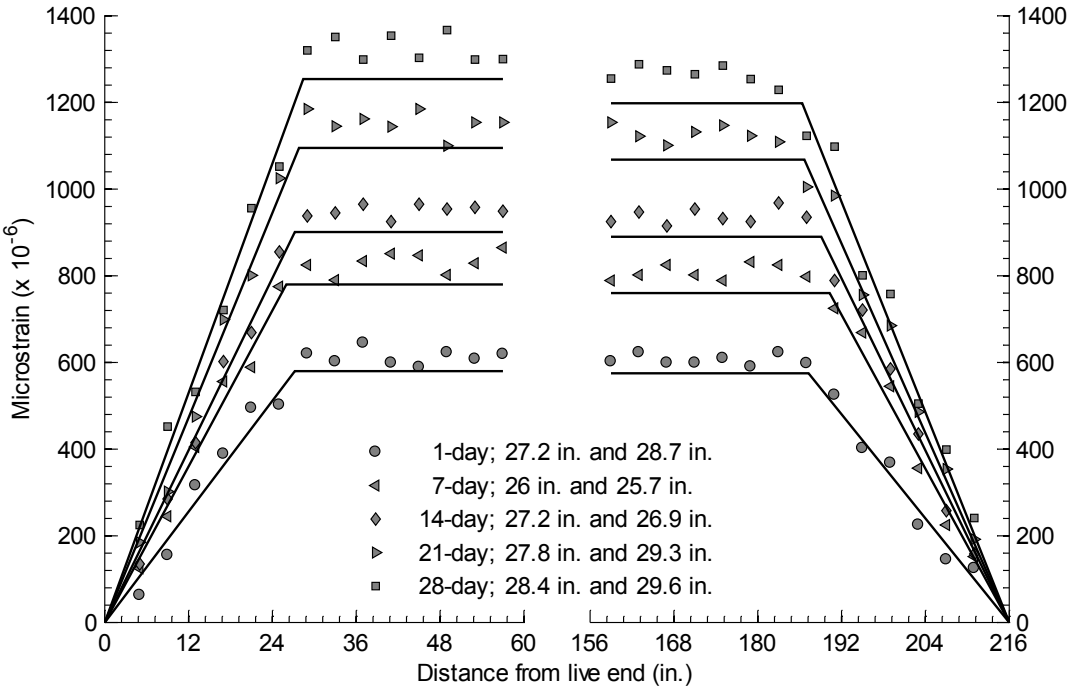

Figure B.22 – Measured transfer lengths of beam H-SCC-D2
(Note: 1 in. = 25.4 mm)

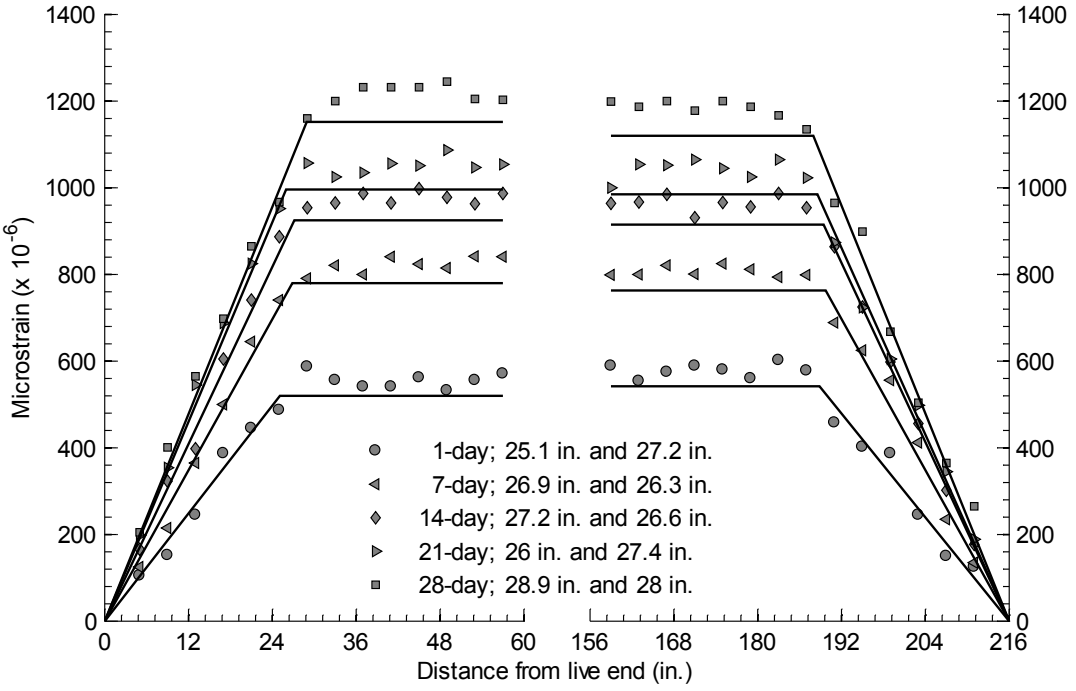

Figure B.23 – Measured transfer lengths of beam H-SCC-D3
(Note: 1 in. = 25.4 mm)

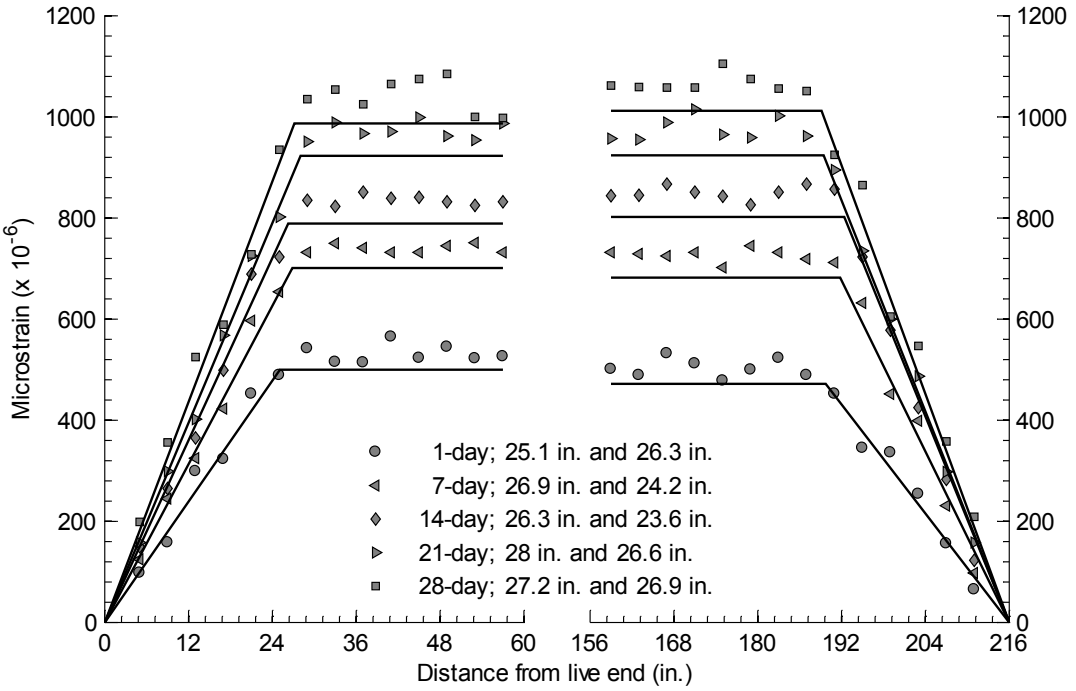

Figure B.24 – Measured transfer lengths of beam H-SCC-D4
(Note: 1 in. = 25.4 mm)

B.2 Transfer length statistics

Table B.1 and **Table B.2** summarize the measured transfer lengths of 24 pretensioned concrete beams at the live end and the dead end, respectively. **Table B.3** shows the mean value, and the upper and lower bound of 95% confidence interval. The bounds are determined using Eqs. B1-B2.

$$UB = Mean + 1.96*STD \quad (B1)$$

$$LB = Mean - 1.96*STD \quad (B2)$$

where UB is upper bound; LB is lower bound; STD is standard deviation.

Table B.1 – Measured transfer lengths at the live end

No.	Beam	End	Transfer length (in.)				
			1-day	7-day	14-day	21-day	28-day
1	N-CC-S1	Live	27.3	30.7	29.3	30.0	31.7
2	N-CC-S2	Live	27.6	30.0	31.4	30.0	30.4
3	N-CC-S3	Live	24.5	28.1	26.8	27.8	29.1
4	N-CC-S4	Live	25.5	25.8	28.1	27.8	30.1
5	H-CC-S1	Live	23.2	23.5	22.9	24.5	25.9
6	H-CC-S2	Live	20.5	23.7	22.1	23.2	24.5
7	H-CC-S3	Live	23.4	23.1	23.9	24.5	25.6
8	H-CC-S4	Live	24.5	23.9	22.3	25.4	25.9
9	H-CC-D1	Live	22.9	22.4	24.3	25.6	28.3
10	H-CC-D2	Live	25.6	22.9	24.8	25.1	28.3
11	H-CC-D3	Live	22.7	23.0	24.1	25.4	26.2
12	H-CC-D4	Live	22.7	25.4	27.3	26.5	28.1
13	N-SCC-S1	Live	28.9	30.6	31.3	32.0	31.3
14	N-SCC-S2	Live	29.6	29.9	32.0	32.7	30.6
15	N-SCC-S3	Live	29.7	27.3	29.7	30.4	31.4
16	N-SCC-S4	Live	27.3	30.4	31.4	30.1	29.7
17	H-SCC-S1	Live	23.1	26.3	27.2	26.9	28.1
18	H-SCC-S2	Live	25.4	26.0	26.9	25.7	27.5
19	H-SCC-S3	Live	25.9	24.4	27.4	27.7	28.6
20	H-SCC-S4	Live	22.6	25.6	27.4	28.6	29.8
21	H-SCC-D1	Live	24.8	25.7	26.0	26.9	27.8
22	H-SCC-D2	Live	27.2	26.0	27.2	27.8	28.4
23	H-SCC-D3	Live	25.1	26.9	27.2	26.0	28.9
24	H-SCC-D4	Live	25.1	26.9	26.3	28.0	27.2

(Note: 1 in. = 25.4 mm)

Table B.2 – Measured transfer lengths at the dead end

No.	Beam	End	Transfer length (in.)				
			1-day	7-day	14-day	21-day	28-day
1	N-CC-S1	Dead	27.6	30.0	29.7	30.0	31.0
2	N-CC-S2	Dead	26.9	27.9	28.6	29.7	30.4
3	N-CC-S3	Dead	23.2	27.8	26.1	28.4	29.7
4	N-CC-S4	Dead	24.8	26.5	26.5	27.1	29.4
5	H-CC-S1	Dead	22.1	23.7	22.6	23.2	25.4
6	H-CC-S2	Dead	21.0	24.8	22.9	24.0	24.8
7	H-CC-S3	Dead	25.4	23.9	23.1	25.1	26.8
8	H-CC-S4	Dead	21.1	22.5	23.1	22.3	25.6
9	H-CC-D1	Dead	22.1	22.7	23.5	23.7	26.2
10	H-CC-D2	Dead	26.4	22.9	23.7	24.0	27.3
11	H-CC-D3	Dead	21.9	22.4	22.7	24.3	25.4
12	H-CC-D4	Dead	19.5	23.2	22.2	24.1	25.4
13	N-SCC-S1	Dead	31.0	31.3	31.0	31.3	31.0
14	N-SCC-S2	Dead	26.1	31.0	29.6	29.9	31.3
15	N-SCC-S3	Dead	26.3	28.0	30.1	30.7	31.1
16	N-SCC-S4	Dead	25.3	31.4	30.1	29.7	30.4
17	H-SCC-S1	Dead	21.3	23.7	24.9	25.1	26.0
18	H-SCC-S2	Dead	24.0	22.2	25.7	26.0	27.2
19	H-SCC-S3	Dead	25.9	26.8	23.8	24.1	26.8
20	H-SCC-S4	Dead	23.8	27.1	26.5	27.7	29.2
21	H-SCC-D1	Dead	25.1	26.3	25.4	26.6	27.2
22	H-SCC-D2	Dead	28.7	28.7	26.9	29.3	29.6
23	H-SCC-D3	Dead	27.2	27.2	26.6	27.4	28.0
24	H-SCC-D4	Dead	26.3	26.3	23.6	26.6	26.9

(Note: 1 in. = 25.4 mm)

Table B.3 – Statistical analysis

No.	Beam group	Parameter	Parameter (in.)				
			1-day	7-day	14-day	21-day	28-day
1	N-CC-S	Mean	25.9	28.4	28.3	28.8	30.2
		STD	1.7	1.8	1.8	1.2	0.9
		95% UB	29.2	31.8	31.9	31.2	31.9
		95% LB	22.7	24.9	24.8	26.5	28.5
2	H-CC-S	Mean	22.6	23.7	22.9	24.0	25.6
		STD	1.8	0.7	0.6	1.1	0.7
		95% UB	26.1	25.0	24.0	26.1	26.9
		95% LB	19.2	22.3	21.7	21.9	24.2
3	H-CC-D	Mean	23.0	23.1	24.1	24.8	26.9
		STD	2.2	1.0	1.5	1.0	1.3
		95% UB	27.3	25.0	27.1	26.7	29.4
		95% LB	18.7	21.2	21.0	23.0	24.4
4	N-SCC-S	Mean	28.0	30.0	30.6	30.9	30.8
		STD	2.0	1.5	0.9	1.1	0.6
		95% UB	32.0	33.0	32.4	32.9	32.0
		95% LB	24.0	27.0	28.9	28.8	29.7
5	H-SCC-S	Mean	24.0	25.3	26.2	26.5	27.9
		STD	1.7	1.7	1.3	1.5	1.3
		95% UB	27.3	28.6	28.8	29.5	30.4
		95% LB	20.7	21.9	23.6	23.5	25.4
6	H-SCC-D	Mean	26.2	26.7	26.1	27.3	28.0
		STD	1.4	0.9	1.2	1.1	1.0
		95% UB	28.9	28.6	28.5	29.4	29.9
		95% LB	23.4	24.9	23.8	25.3	26.1

(Note: STD = standard deviation; UB = upper bound; LB = lower bound; 1 in. = 25.4 mm)

B.3 End-slip measurement

Table B.4 – Measured and allowable strand end-slips

No.	Beam	δ (in.)		δ_{all} (in.), ACI 318		δ_{all} (in.), AASHTO	
		Live	Dead	$\alpha = 2$	$\alpha = 3$	$\alpha = 2$	$\alpha = 3$
1	N-CC-S1	0.076	0.089	0.118	0.078	0.141	0.094
2	N-CC-S2	0.088	0.069	0.118	0.078	0.141	0.094
3	N-CC-S3	0.065	0.065	0.118	0.079	0.142	0.094
4	N-CC-S4	0.078	0.075	0.118	0.079	0.142	0.094
5	H-CC-S1	0.070	0.061	0.119	0.079	0.143	0.095
6	H-CC-S2	0.065	0.057	0.119	0.079	0.143	0.095
7	H-CC-S3	0.067	0.078	0.119	0.079	0.142	0.095
8	H-CC-S4	0.076	0.063	0.119	0.079	0.142	0.095
9	H-CC-D1	0.061	0.058	0.114	0.076	0.137	0.092
10	H-CC-D2	0.068	0.070	0.114	0.076	0.137	0.092
11	H-CC-D3	0.060	0.058	0.114	0.076	0.137	0.092
12	H-CC-D4	0.060	0.052	0.114	0.076	0.137	0.092
13	N-SCC-S1	0.085	0.089	0.118	0.078	0.141	0.094
14	N-SCC-S2	0.082	0.071	0.118	0.078	0.141	0.094
15	N-SCC-S3	0.089	0.080	0.118	0.078	0.141	0.094
16	N-SCC-S4	0.077	0.080	0.118	0.078	0.141	0.094
17	H-SCC-S1	0.072	0.059	0.118	0.079	0.142	0.095
18	H-SCC-S2	0.073	0.074	0.118	0.079	0.142	0.095
19	H-SCC-S3	0.075	0.069	0.118	0.079	0.142	0.095
20	H-SCC-S4	0.069	0.075	0.118	0.079	0.142	0.095
21	H-SCC-D1	0.064	0.065	0.113	0.076	0.136	0.091
22	H-SCC-D2	0.070	0.074	0.113	0.076	0.136	0.091
23	H-SCC-D3	0.065	0.071	0.114	0.076	0.136	0.091
24	H-SCC-D4	0.065	0.068	0.114	0.076	0.136	0.091

(Note: δ = strand end-slip at transfer; δ_{all} = allowable strand end-slip; α = bond stress distribution coefficient; 1 in. = 25.4 mm)

APPENDIX C : DEVELOPMENT LENGTH DATA

C.1 Bending test results

C.1.1 N-SCC-S beams

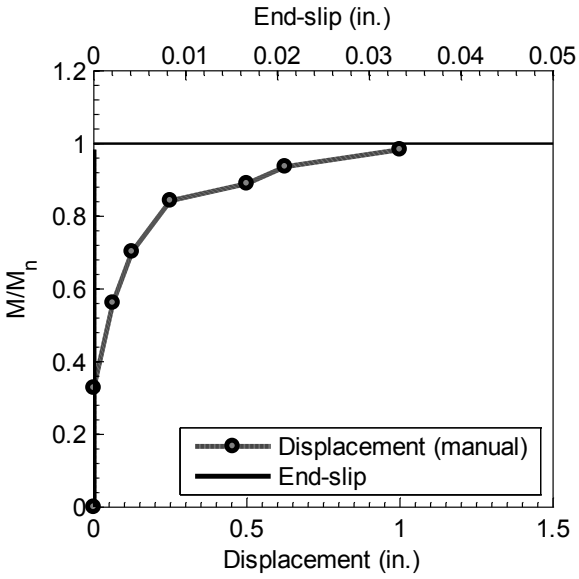

Figure C.1 – Test results of N-SCC-S4-L with an embedment length of 6.0 ft (1830 mm)
(Note: 1 in. = 25.4 mm)

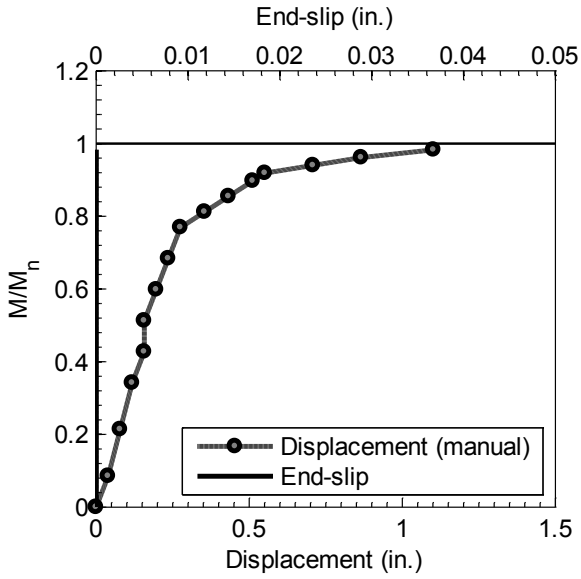

Figure C.2 – Test results of N-SCC-S4-D with an embedment length of 5.5 ft (1676 mm)
(Note: 1 in. = 25.4 mm)

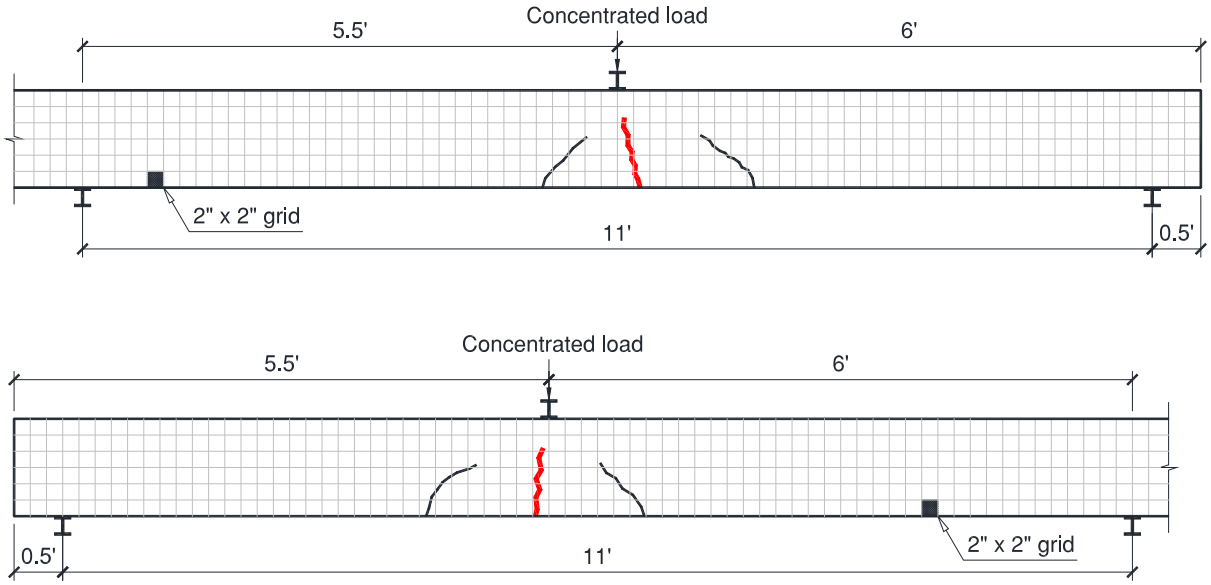

Figure C.3 – Crack pattern of N-SCC-S4-L (top) and N-SCC-S4-D (bottom).
(Note: 1 ft = 305 mm; 1 in. = 25.4 mm)

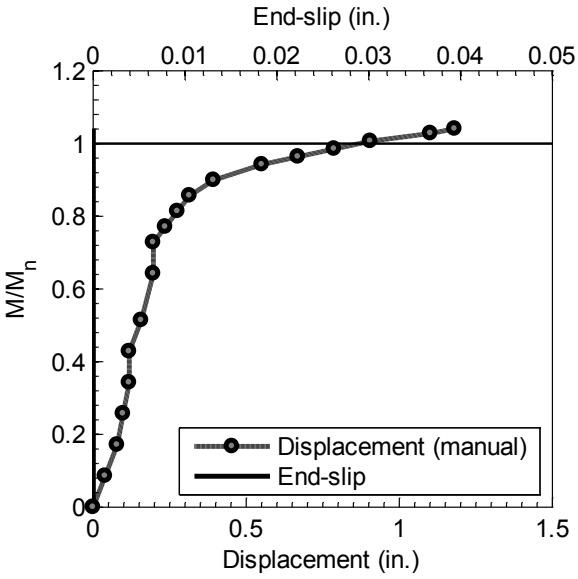

Figure C.4 – Test results of N-SCC-S3-L with an embedment length of 5.25 ft (1600 mm)
(Note: 1 in. = 25.4 mm)

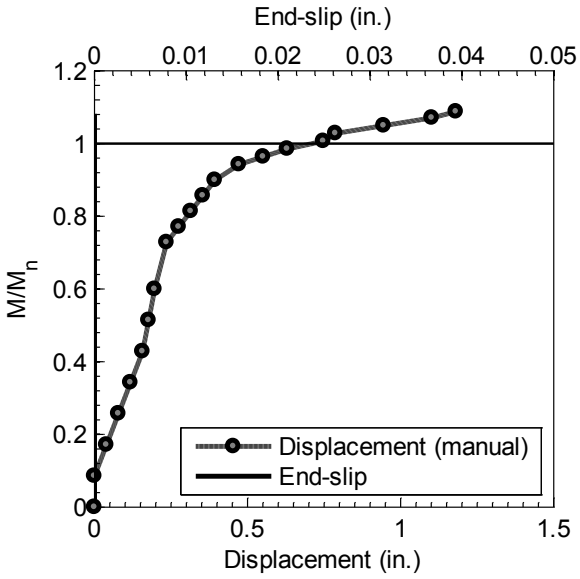

Figure C.5 – Test results of N-SCC-S3-D with an embedment length of 5.0 ft (1524 mm)
(Note: 1 in. = 25.4 mm)

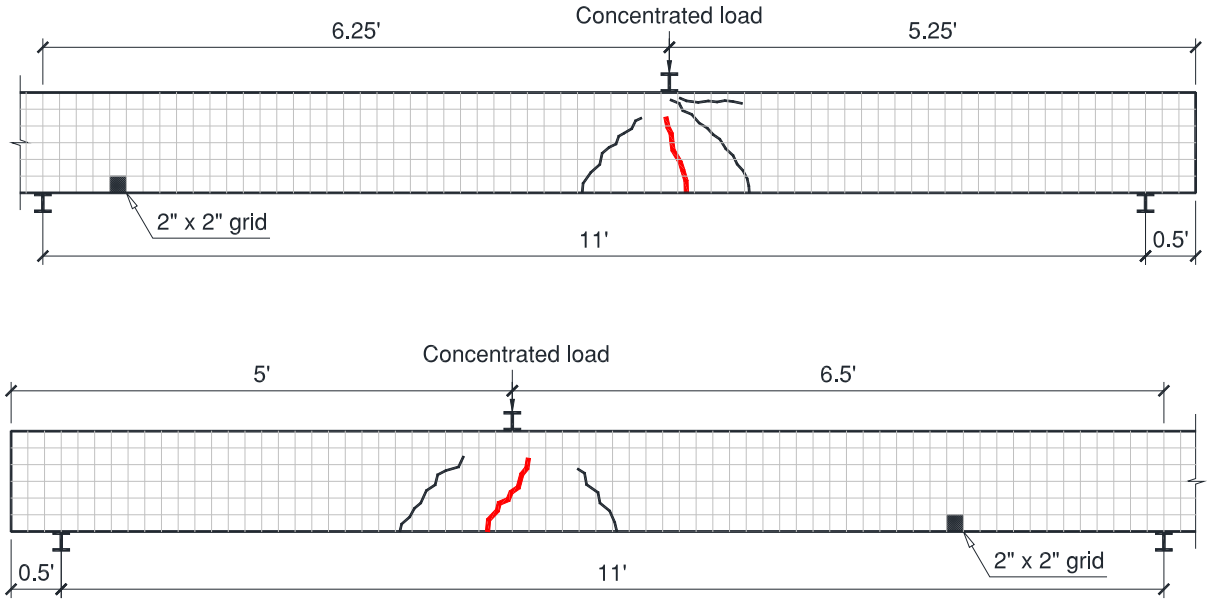

Figure C.6 – Crack pattern of N-SCC-S3-L (top) and N-SCC-S3-D (bottom).
(Note: 1 ft = 305 mm; 1 in. = 25.4 mm)

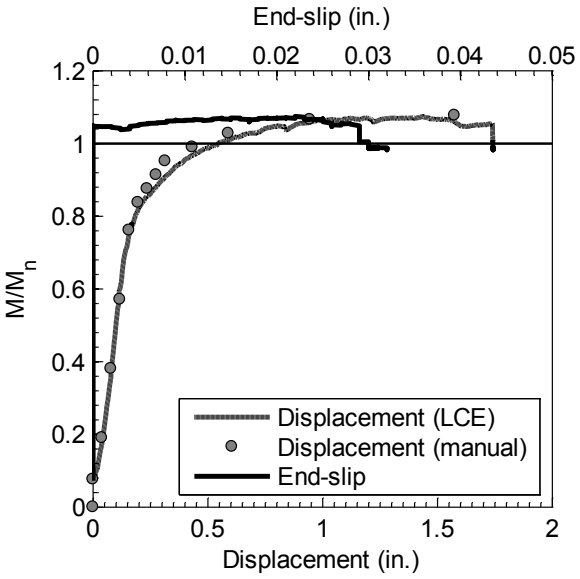

Figure C.7 – Test results of N-SCC-S2-L with an embedment length of 4.0 ft (1220 mm)
(Note: 1 in. = 25.4 mm)

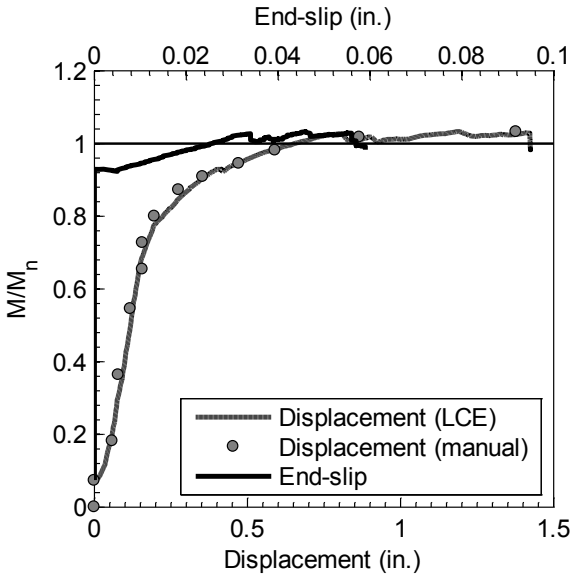

Figure C.8 – Test results of N-SCC-S2-D with an embedment length of 3.5 ft (1067 mm)
(Note: 1 in. = 25.4 mm)

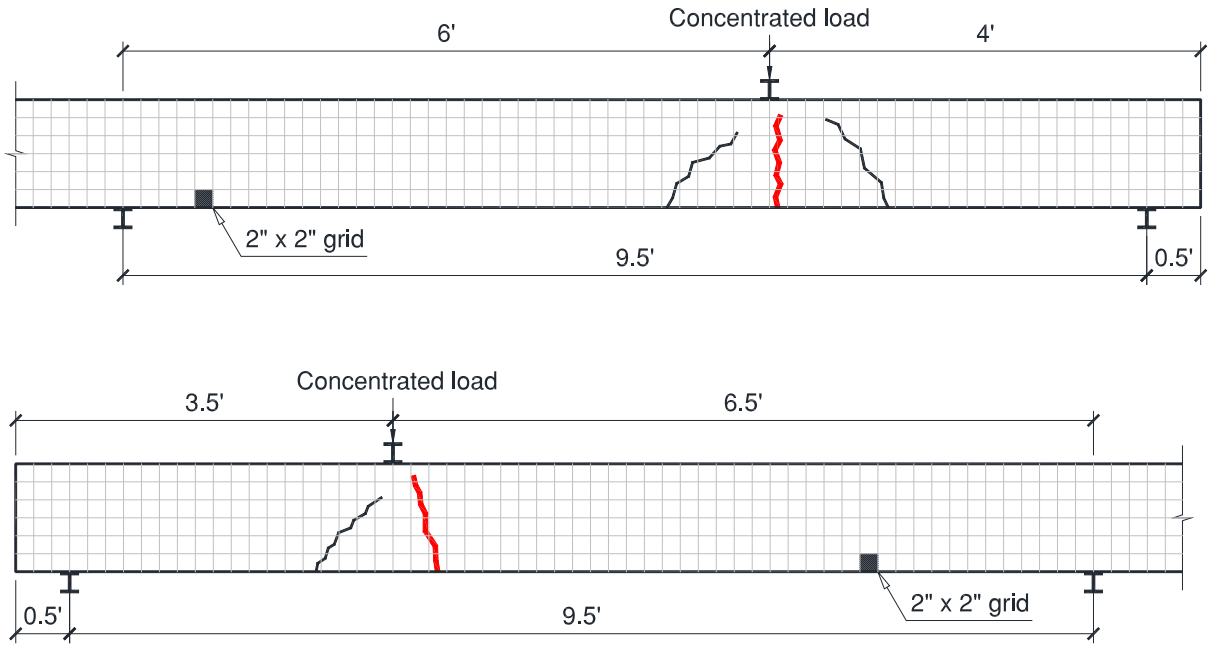

Figure C.9 – Crack pattern of N-SCC-S2-L (top) and N-SCC-S2-D (bottom).
(Note: 1 ft = 305 mm; 1 in. = 25.4 mm)

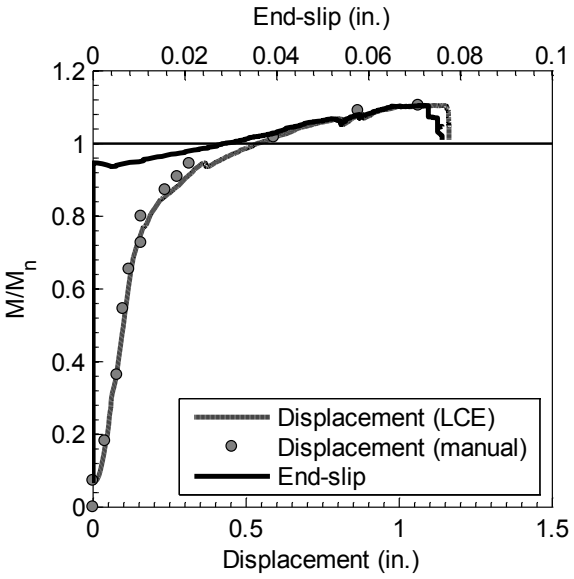

Figure C.10 – Test results of N-SCC-S1-L with an embedment length of 3.5 ft (1067 mm)
(Note: 1 in. = 25.4 mm)

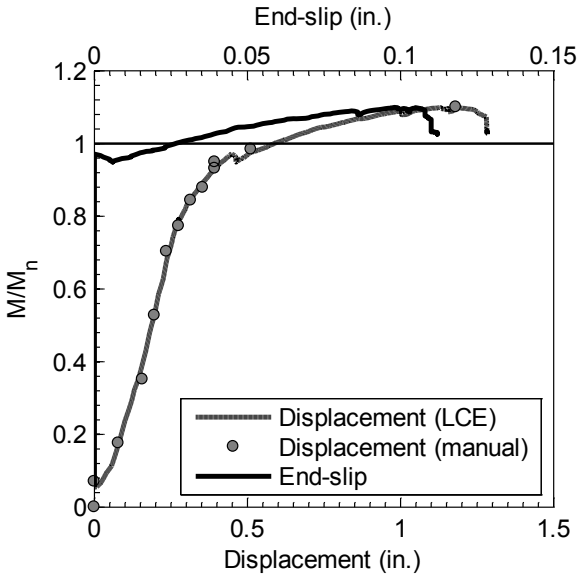

Figure C.11 – Test results of N-SCC-S1-D with an embedment length of 3.25 ft (991 mm)
(Note: 1 in. = 25.4 mm)

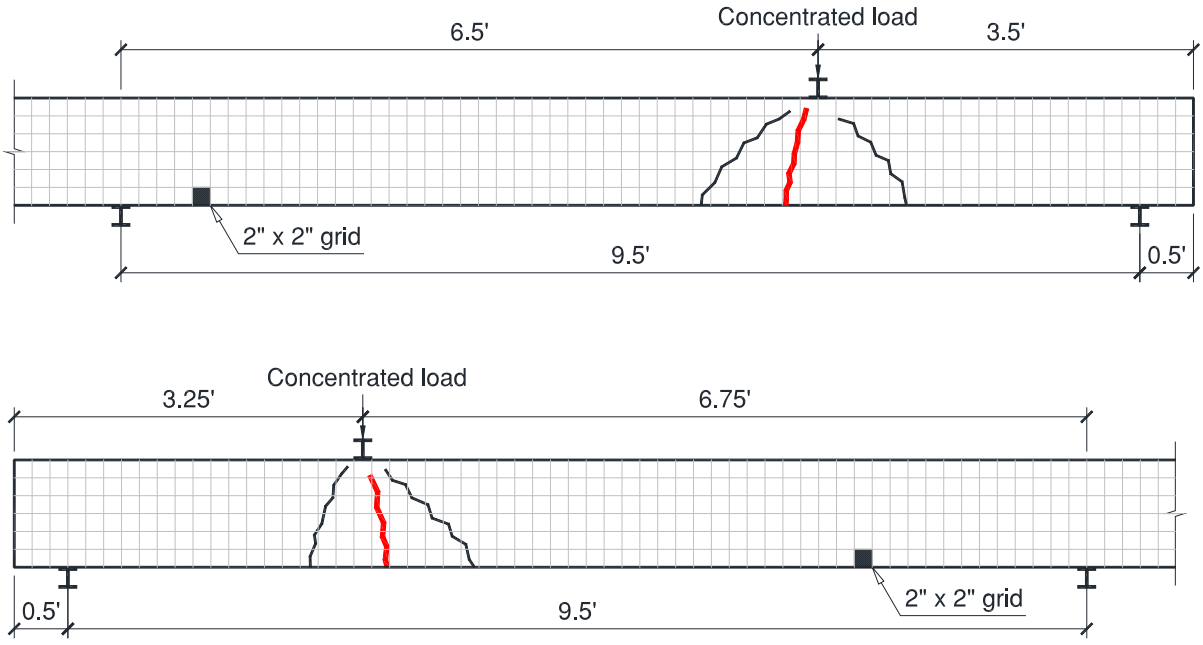

Figure C.12 – Crack pattern of N-SCC-S1-L (top) and N-SCC-S1-D (bottom).
(Note: 1 ft = 305 mm; 1 in. = 25.4 mm)

C.1.2 H-SCC-S beams

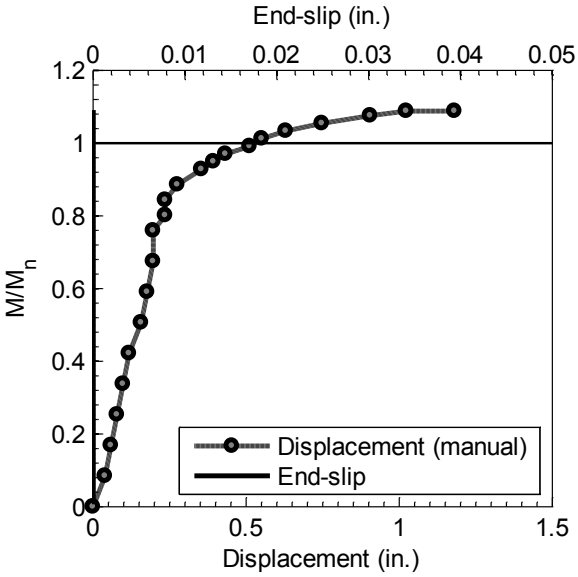

Figure C.13 – Test results of H-SCC-S2-L with an embedment length of 4.5 ft (1372 mm)
(Note: 1 in. = 25.4 mm)

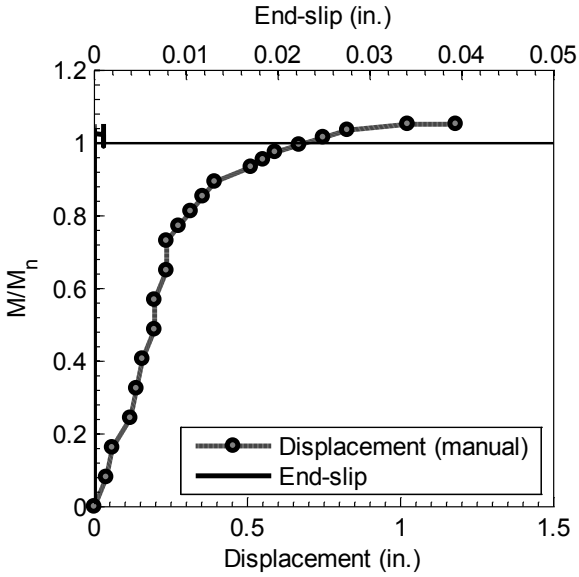

Figure C.14 – Test results of H-SCC-S2-D with an embedment length of 4.0 ft (1220 mm)
(Note: 1 in. = 25.4 mm)

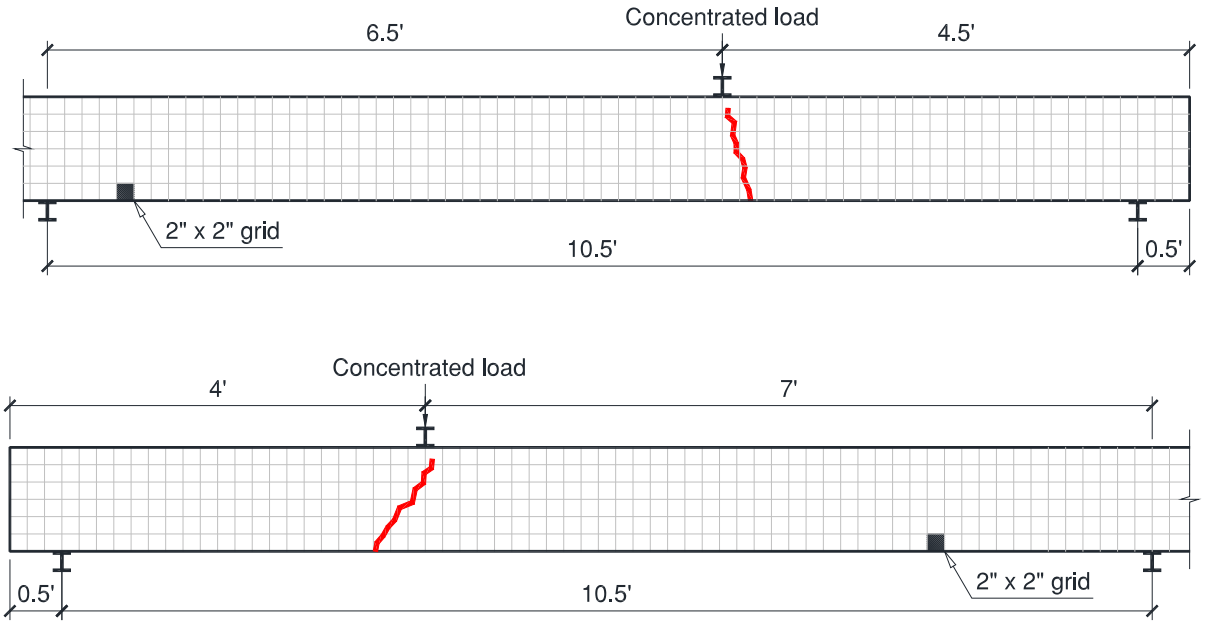

Figure C.15 – Crack pattern of H-SCC-S2-L (top) and H-SCC-S2-D (bottom).
(Note: 1 ft = 305 mm; 1 in. = 25.4 mm)

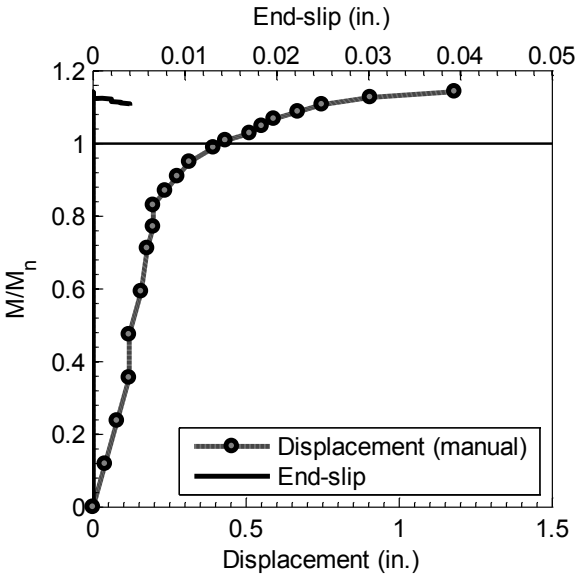

Figure C.16 – Test results of H-SCC-S1-L with an embedment length of 3.75 ft (1143 mm)
(Note: 1 in. = 25.4 mm)

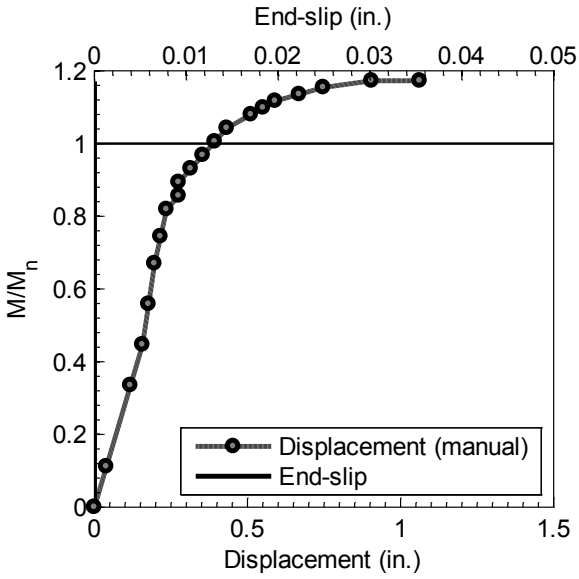

Figure C.17 – Test results of H-SCC-S1-D with an embedment length of 3.75 ft (1143 mm)
(Note: 1 in. = 25.4 mm)

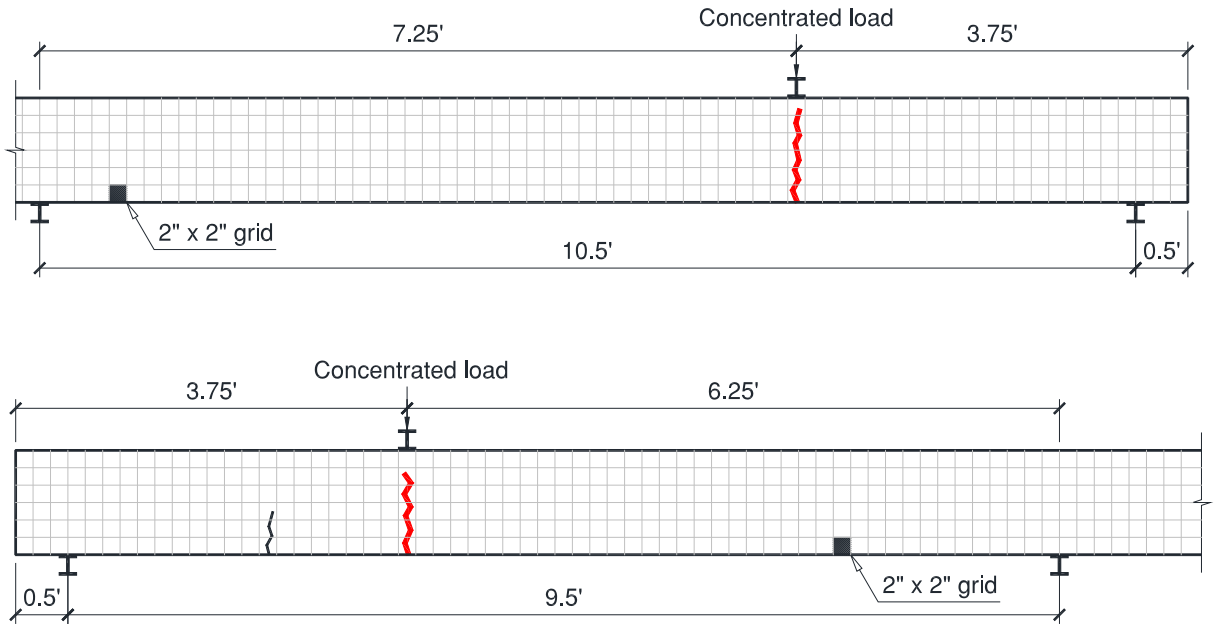

Figure C.18 – Crack pattern of H-SCC-S1-L (top) and H-SCC-S1-D (bottom).
(Note: 1 ft = 305 mm; 1 in. = 25.4 mm)

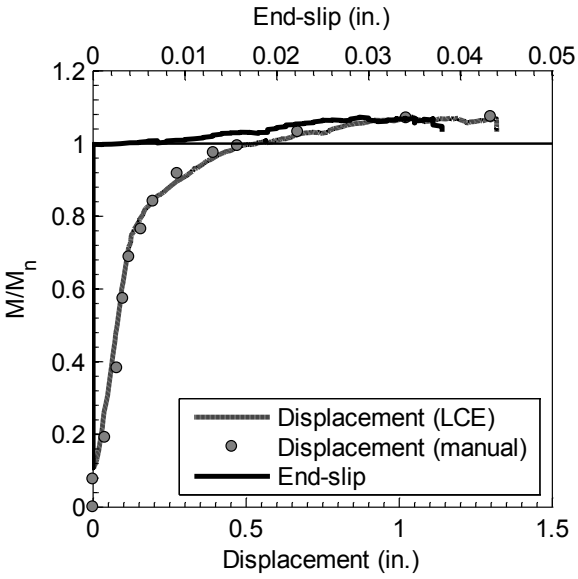

Figure C.19 – Test results of H-SCC-S4-L with an embedment length of 4.0 ft (1120 mm)
(Note: 1 in. = 25.4 mm)

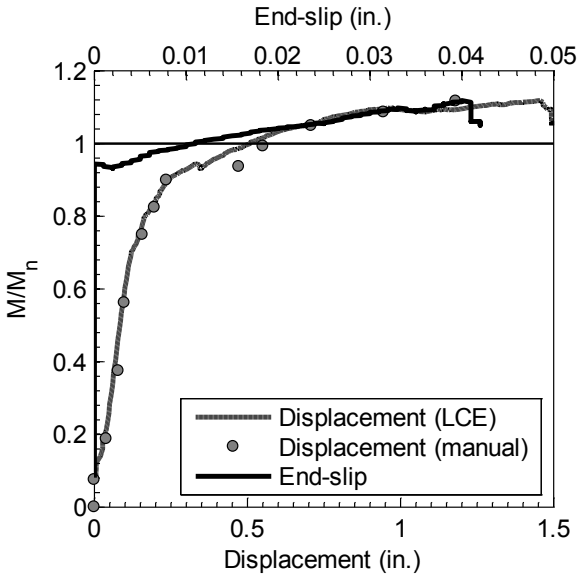

Figure C.20 – Test results of H-SCC-S4-D with an embedment length of 3.75 ft (1143 mm)
(Note: 1 in. = 25.4 mm)

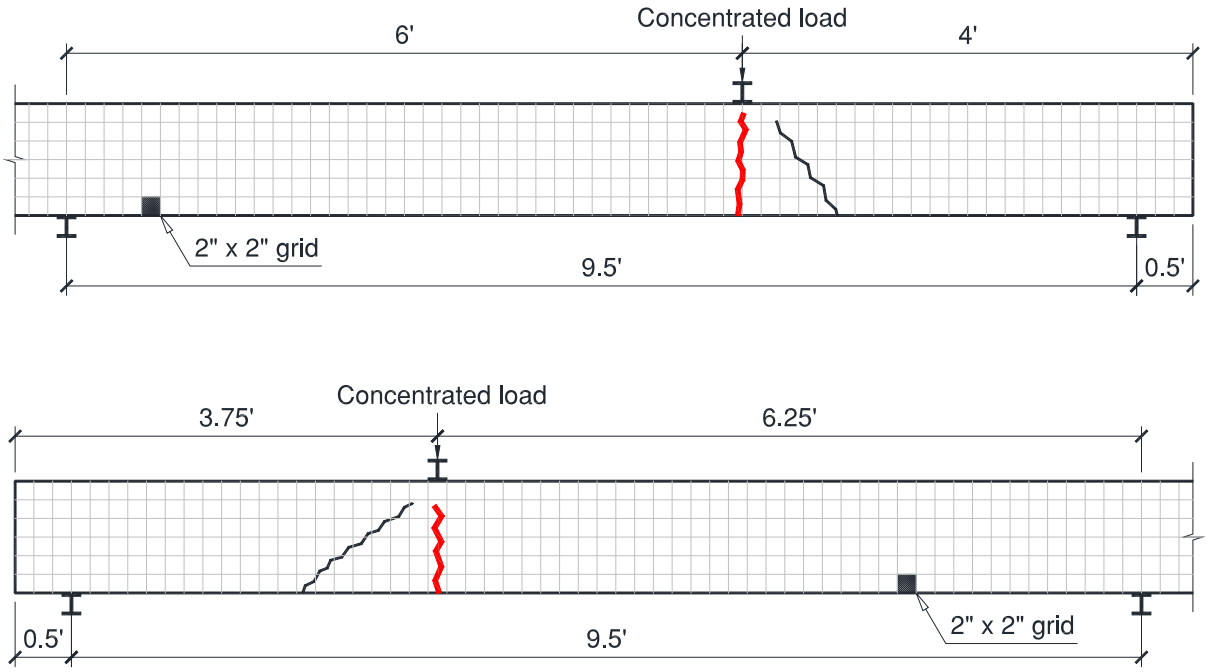

Figure C.21 – Crack pattern of H-SCC-S4-L (top) and H-SCC-S4-D (bottom).
(Note: 1 ft = 305 mm; 1 in. = 25.4 mm)

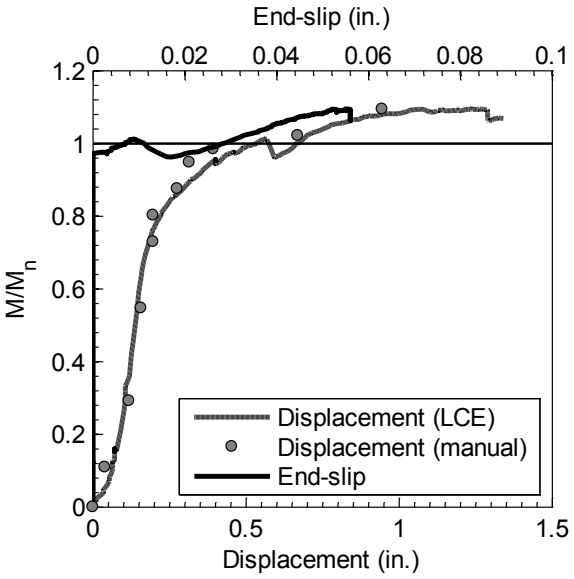

Figure C.22 – Test results of H-SCC-S3-L with an embedment length of 3.5 ft (1067 mm)
(Note: 1 in. = 25.4 mm)

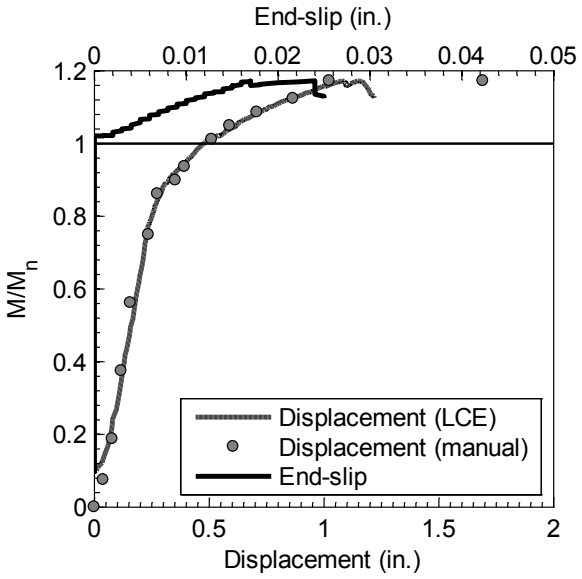

Figure C.23 – Test results of H-SCC-S3-D with an embedment length of 3.75 ft (1143 mm)
(Note: 1 in. = 25.4 mm)

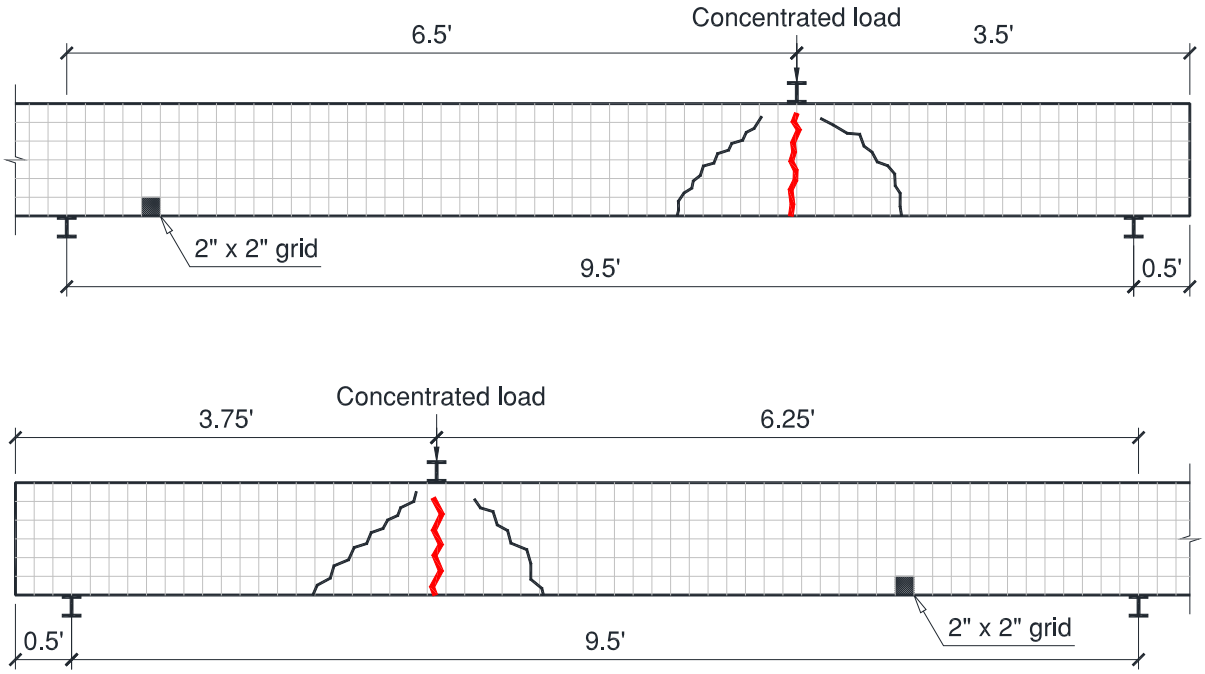

Figure C.24 – Crack pattern of H-SCC-S3-L (top) and H-SCC-S3-D (bottom).
(Note: 1 ft = 305 mm; 1 in. = 25.4 mm)

C.1.3 N-CC-S beams

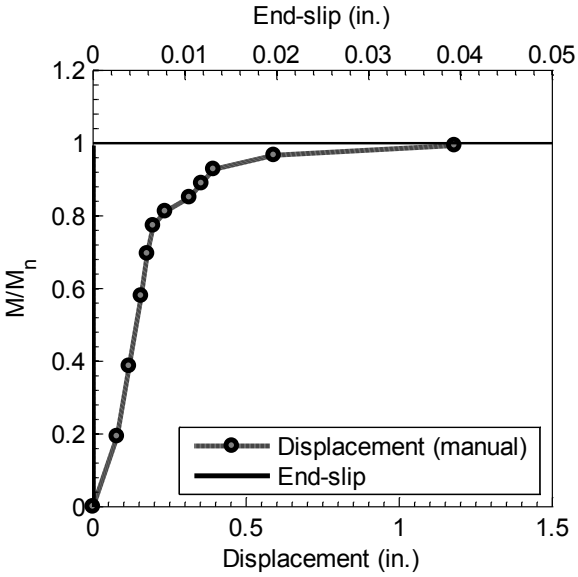

Figure C.25 – Test results of N-CC-S4-L with an embedment length of 4.0 ft (1220 mm)
(Note: 1 in. = 25.4 mm)

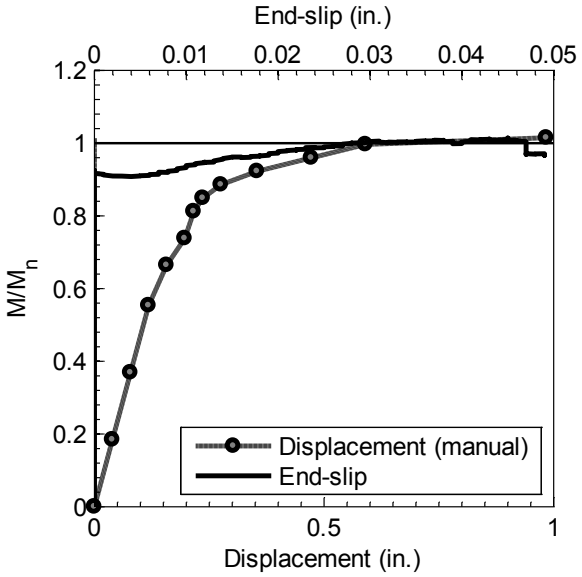

Figure C.26 – Test results of N-CC-S4-D with an embedment length of 3.5 ft (1067 mm)
(Note: 1 in. = 25.4 mm)

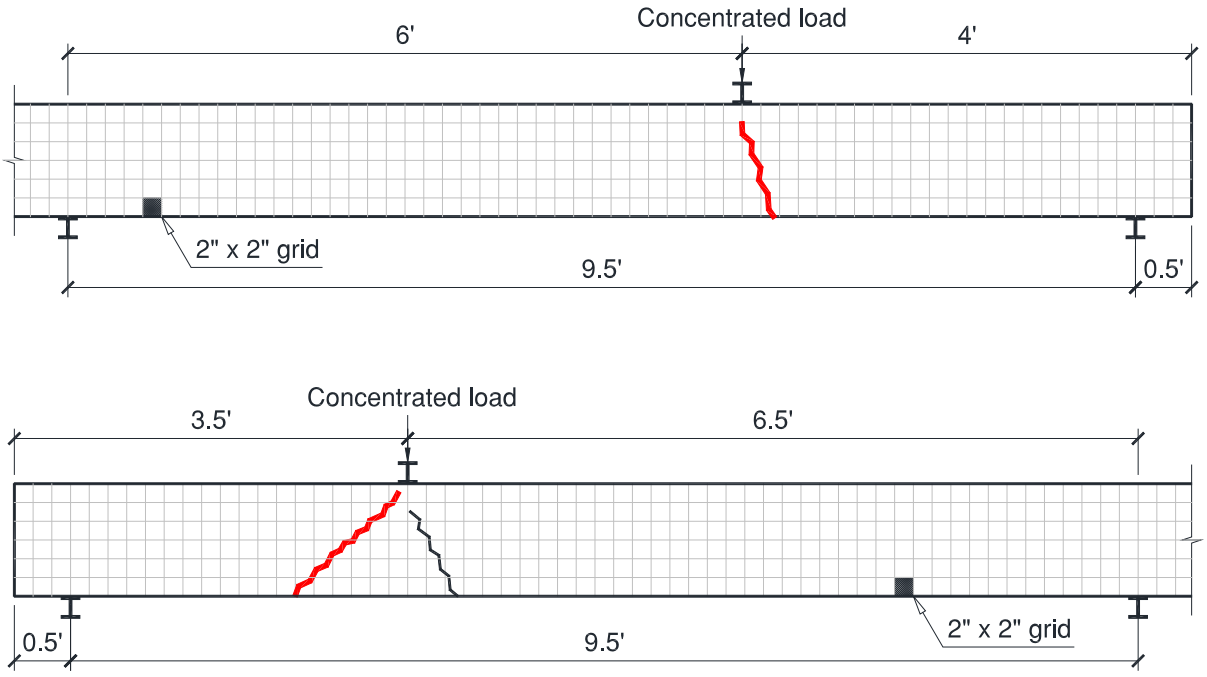

Figure C.27 – Crack pattern of N-CC-S4-L (top) and N-CC-S4-D (bottom).
(Note: 1 ft = 305 mm; 1 in. = 25.4 mm)

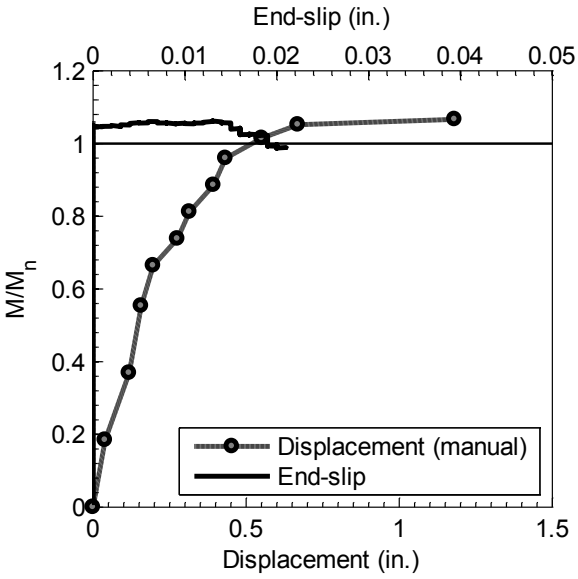

Figure C.28 – Test results of N-CC-S3-L with an embedment length of 3.5 ft (1067 mm)
(Note: 1 in. = 25.4 mm)

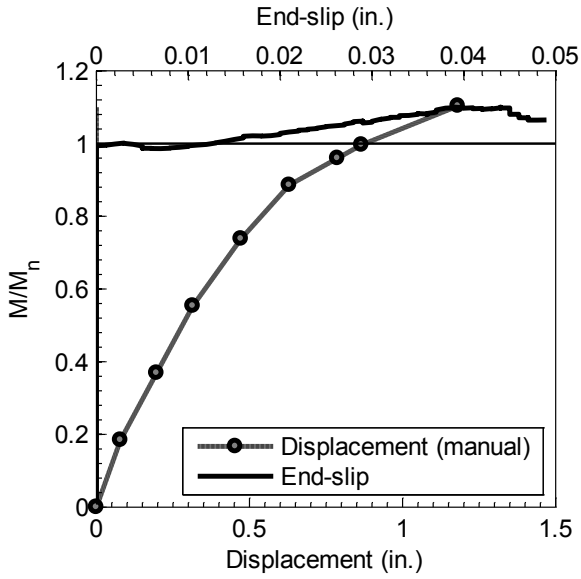

Figure C.29 – Test results of N-CC-S3-D with an embedment length of 3.5 ft (1067 mm)
(Note: 1 in. = 25.4 mm)

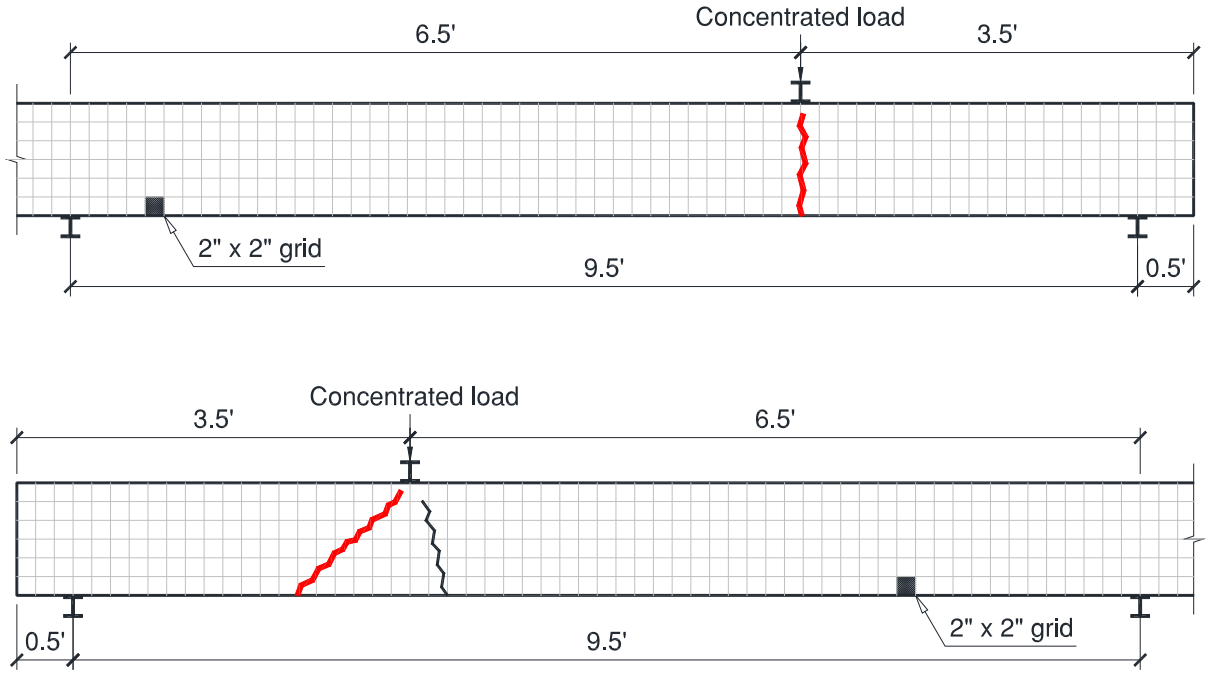

Figure C.30 – Crack pattern of N-CC-S3-L (top) and N-CC-S3-D (bottom).
(Note: 1 ft = 305 mm; 1 in. = 25.4 mm)

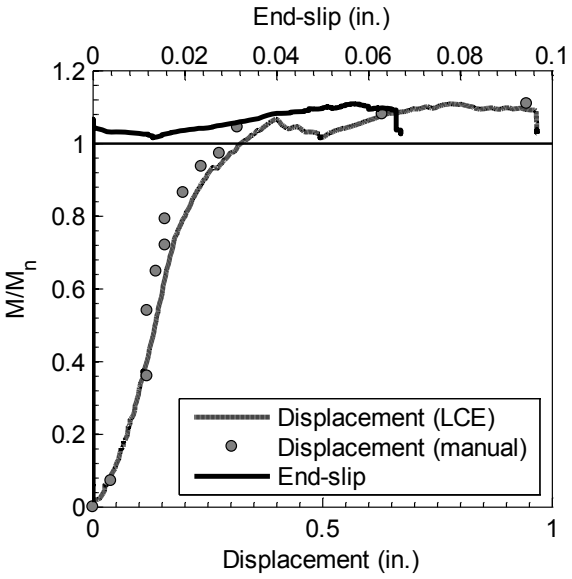

Figure C.31 – Test results of N-CC-S2-L with an embedment length of 3.25 ft (991 mm)
(Note: 1 in. = 25.4 mm)

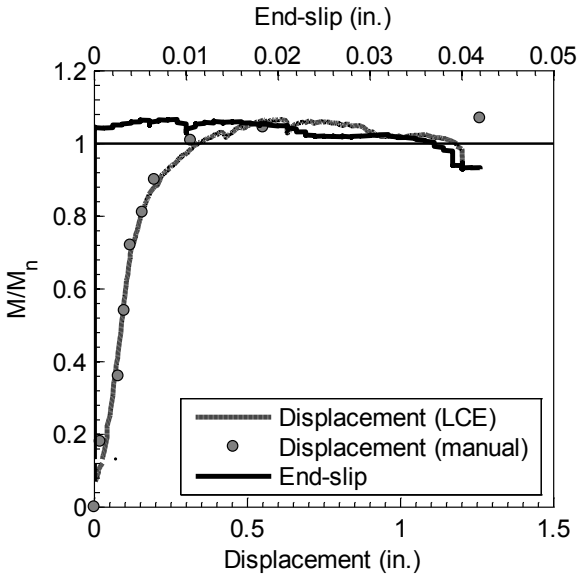

Figure C.32 – Test results of N-CC-S2-D with an embedment length of 3.25 ft (991 mm)
(Note: 1 in. = 25.4 mm)

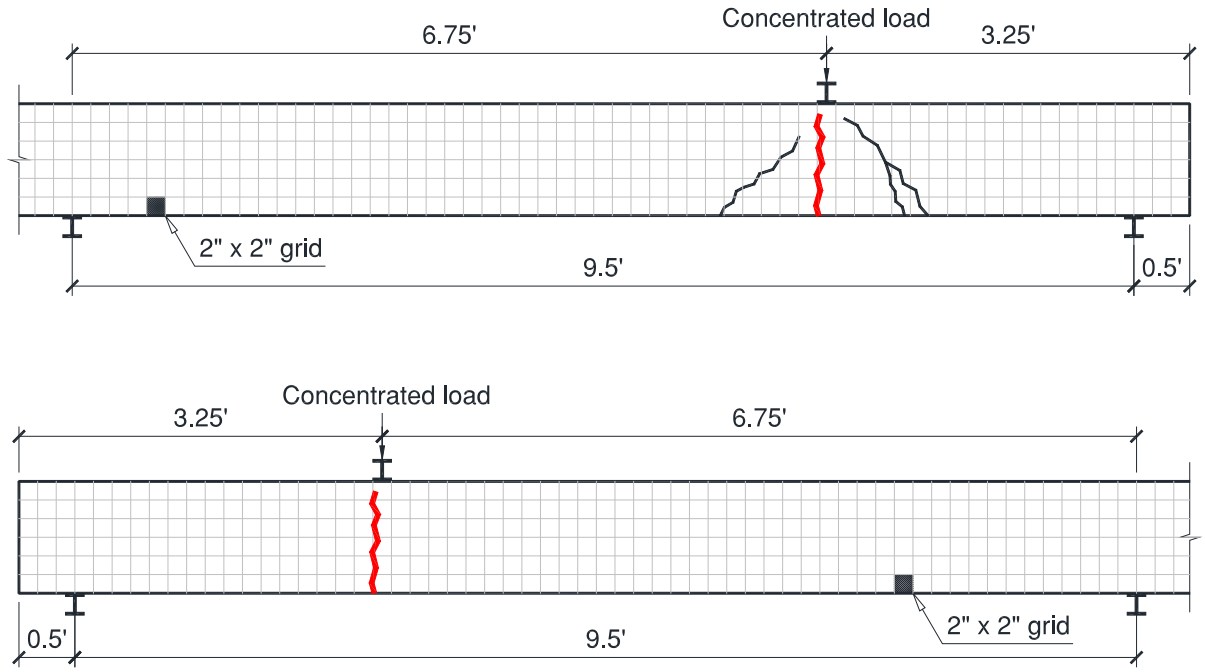

Figure C.33 – Crack pattern of N-CC-S2-L (top) and N-CC-S2-D (bottom).
(Note: 1 ft = 305 mm; 1 in. = 25.4 mm)

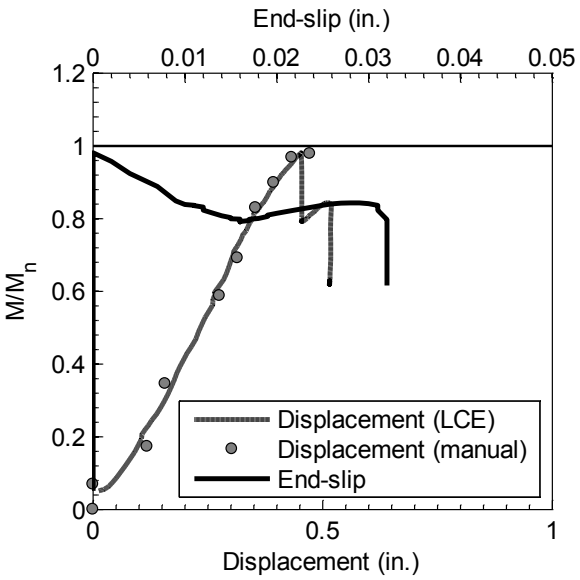

Figure C.34 – Test results of N-CC-S1-L with an embedment length of 3.0 ft (915 mm) (Note: 1 in. = 25.4 mm)

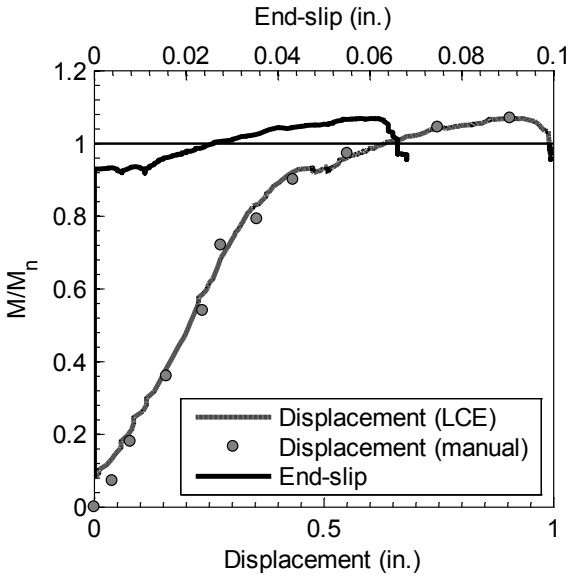

Figure C.35 – Test results of N-CC-S1-D with an embedment length of 3.25 ft (991 mm) (Note: 1 in. = 25.4 mm)

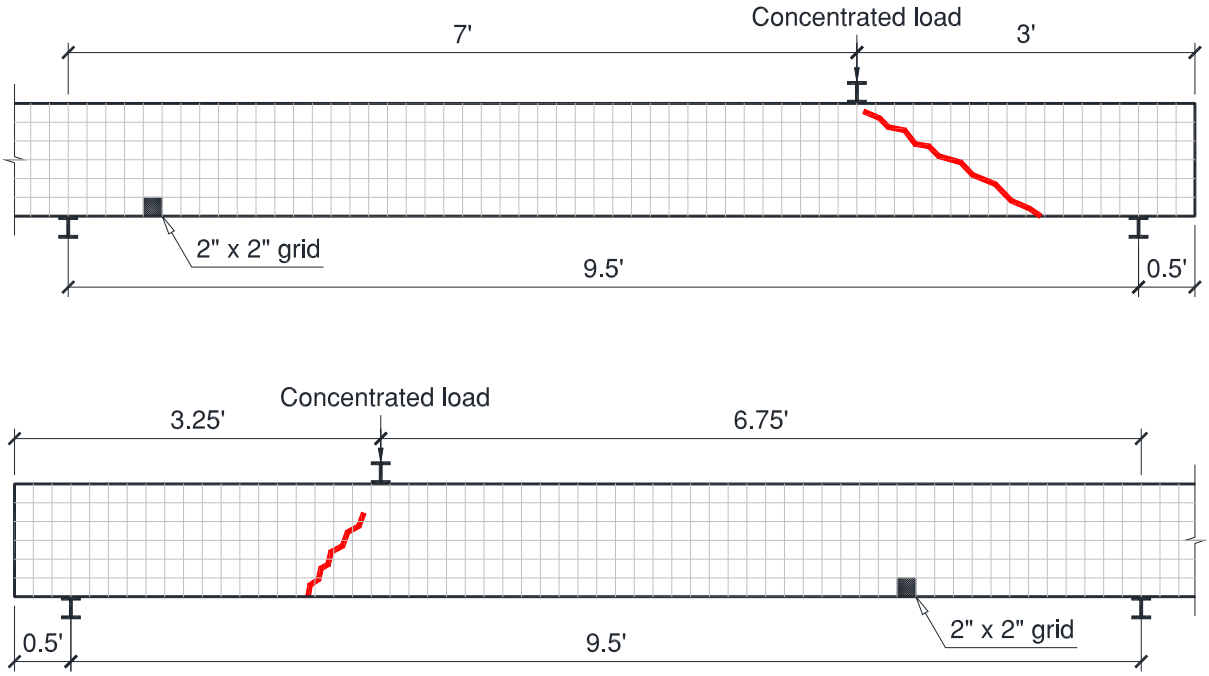

Figure C.36 – Crack pattern of N-CC-S1-L (top) and N-CC-S1-D (bottom). (Note: 1 ft = 305 mm; 1 in. = 25.4 mm)

C.1.4 H-CC-S beams

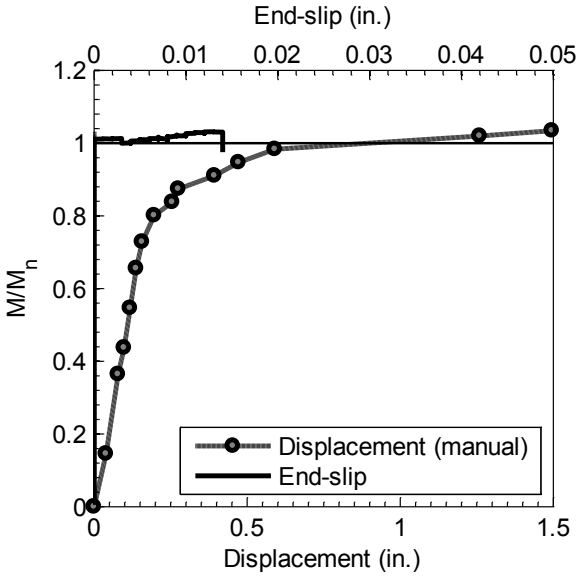

Figure C.37 – Test results of H-CC-S4-L with an embedment length of 4.0 ft (1220 mm)
(Note: 1 in. = 25.4 mm)

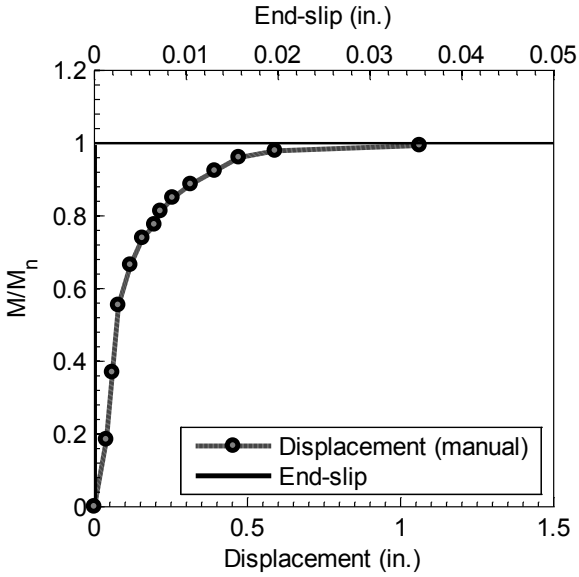

Figure C.38 – Test results of H-CC-S4-D with an embedment length of 4.25 ft (1295 mm)
(Note: 1 in. = 25.4 mm)

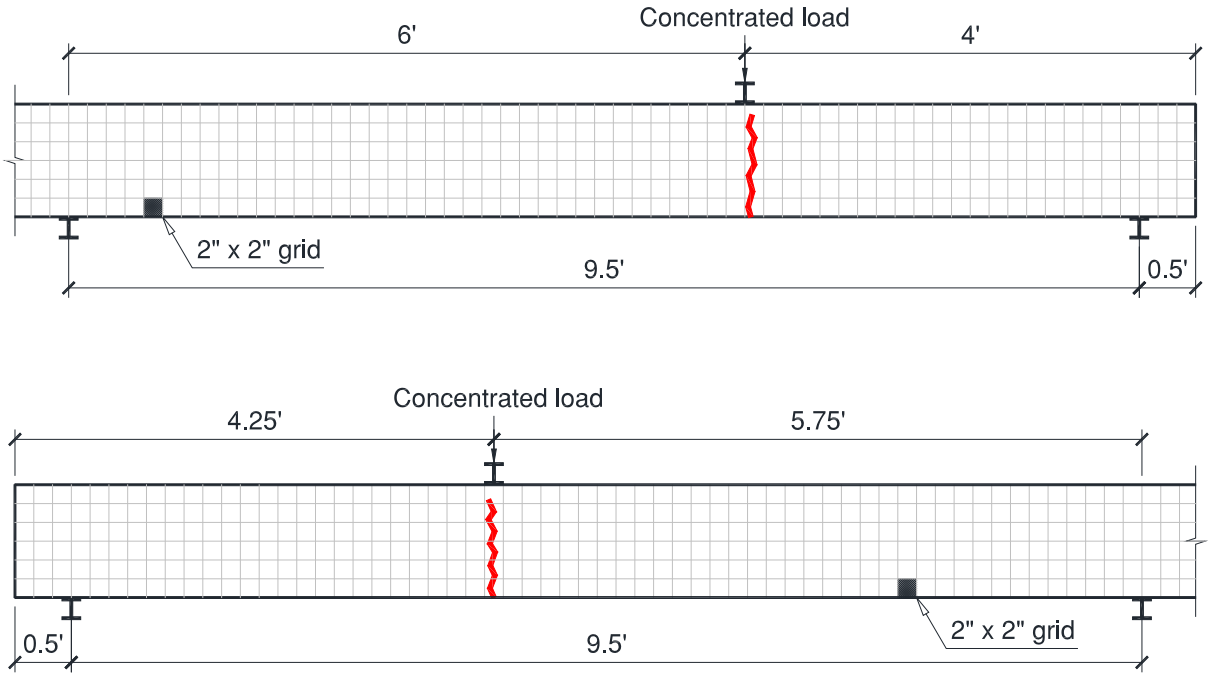

Figure C.39 – Crack pattern of H-CC-S4-L (top) and H-CC-S4-D (bottom).
(Note: 1 ft = 305 mm; 1 in. = 25.4 mm)

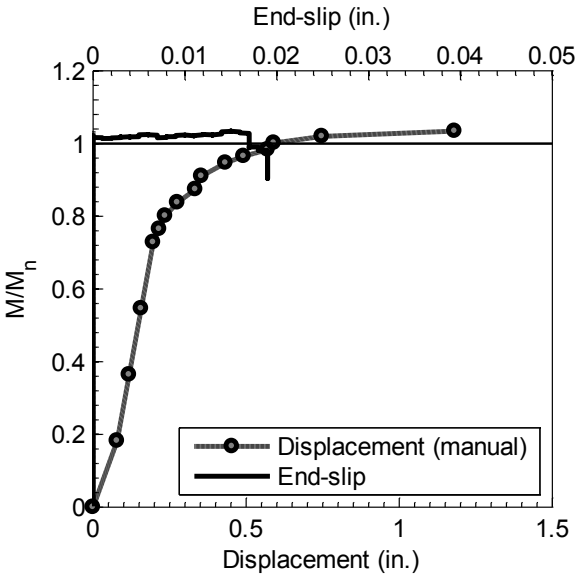

Figure C.40 – Test results of H-CC-S3-L with an embedment length of 4.0 ft (1220 mm)
(Note: 1 in. = 25.4 mm)

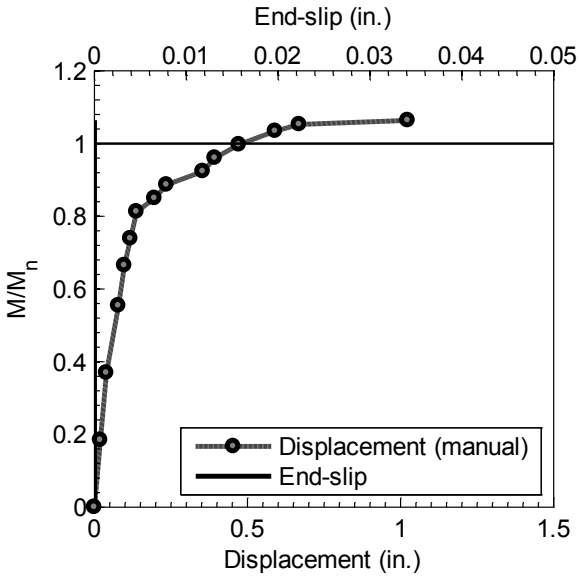

Figure C.41 – Test results of H-CC-S3-D with an embedment length of 4.25 ft (1295 mm)
(Note: 1 in. = 25.4 mm)

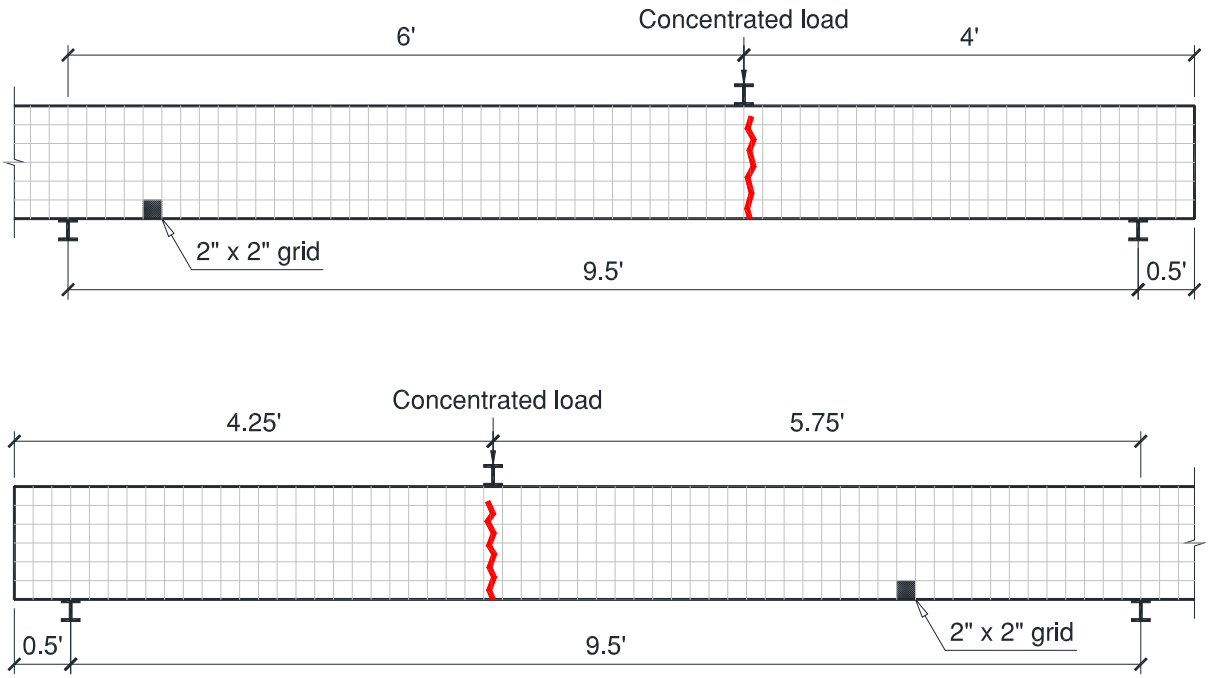

Figure C.42 – Crack pattern of H-CC-S3-L (top) and H-CC-S3-D (bottom).
(Note: 1 ft = 305 mm; 1 in. = 25.4 mm)

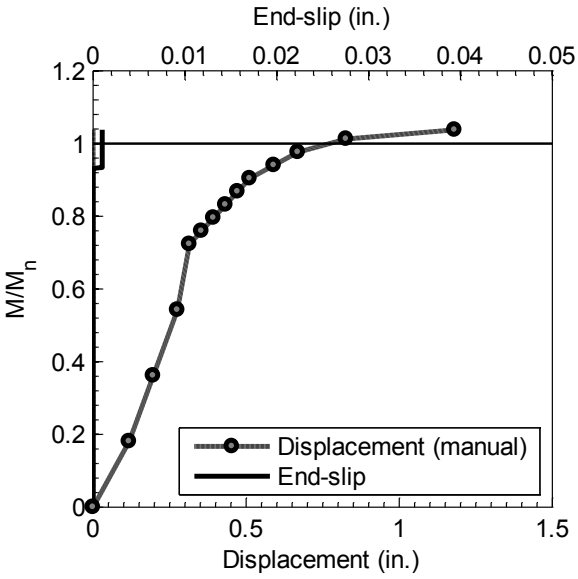

Figure C.43 – Test results of H-CC-S2-L with an embedment length of 4.0 ft (1220 mm)
(Note: 1 in. = 25.4 mm)

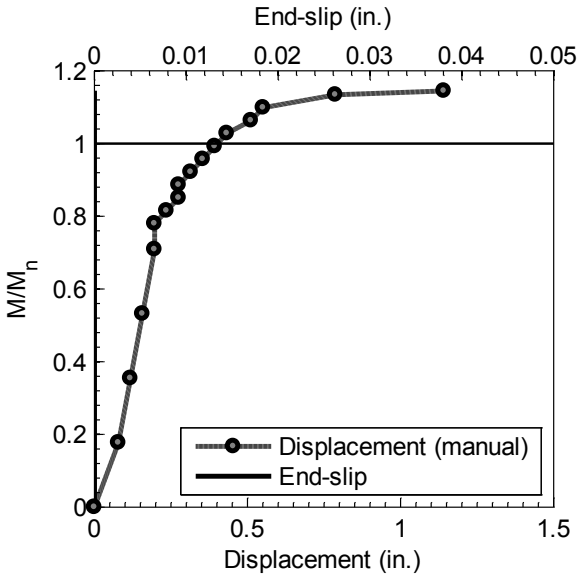

Figure C.44 – Test results of H-CC-S2-D with an embedment length of 3.75 ft (1143 mm)
(Note: 1 in. = 25.4 mm)

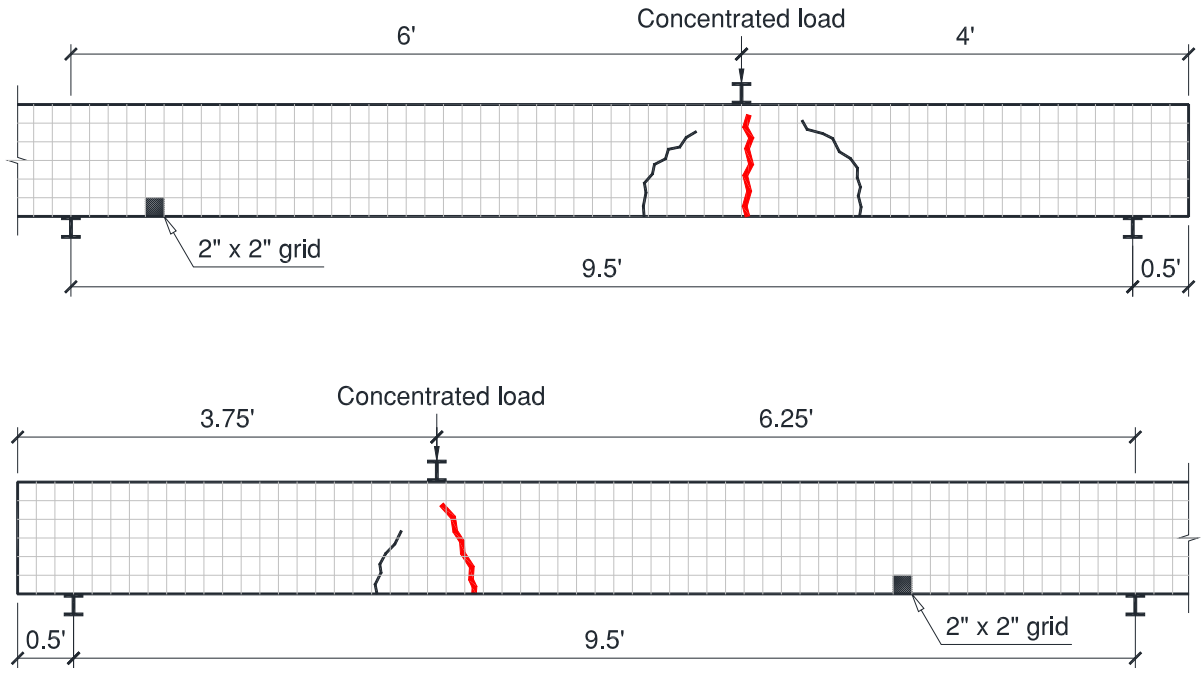

Figure C.45 – Crack pattern of H-CC-S2-L (top) and H-CC-S2-D (bottom).
(Note: 1 ft = 305 mm; 1 in. = 25.4 mm)

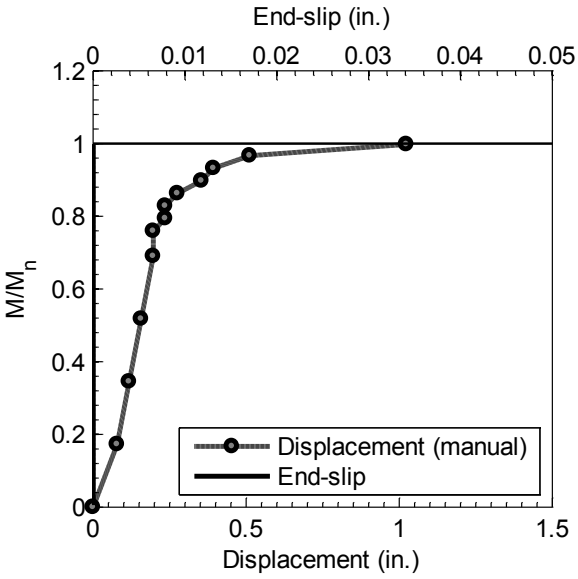

Figure C.46 – Test results of H-CC-S1-L with an embedment length of 3.5 ft (1067 mm)
(Note: 1 in. = 25.4 mm)

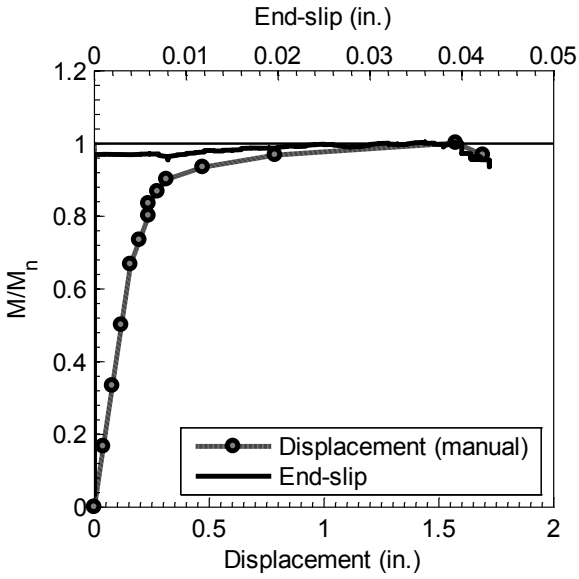

Figure C.47 – Test results of H-CC-S1-D with an embedment length of 3.25 ft (991 mm)
(Note: 1 in. = 25.4 mm)

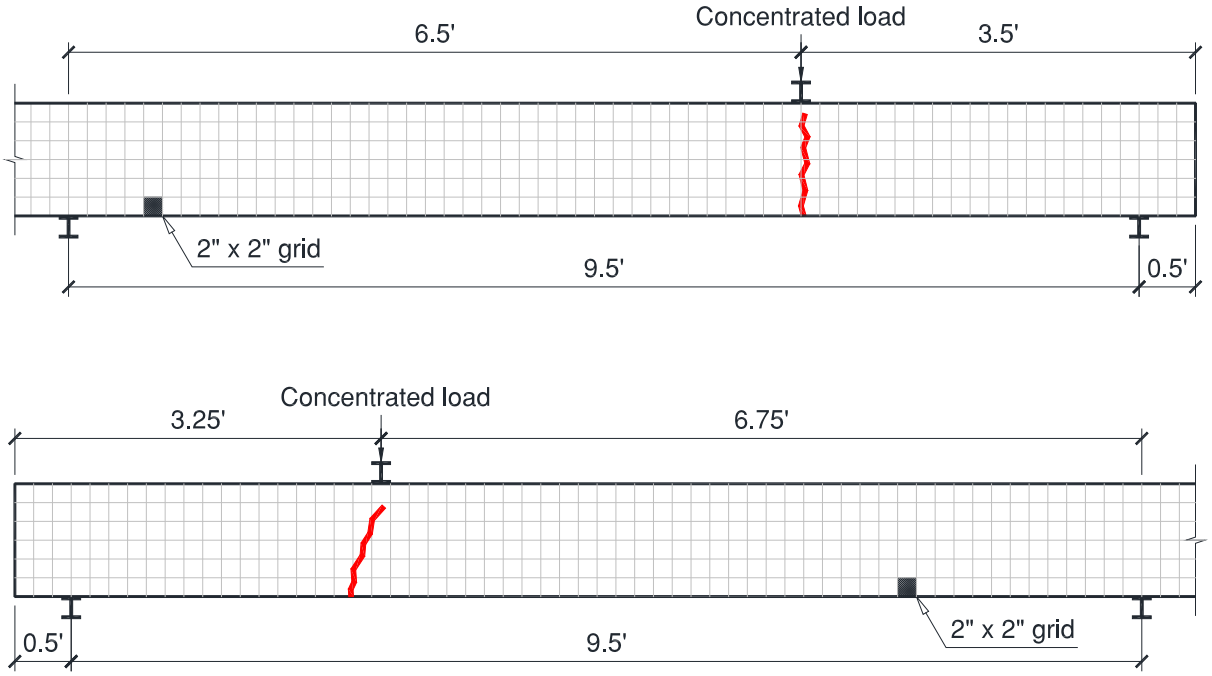

Figure C.48 – Crack pattern of H-CC-S1-L (top) and H-CC-S1-D (bottom).
(Note: 1 ft = 305 mm; 1 in. = 25.4 mm)

C.1.5 H-SCC-D beams

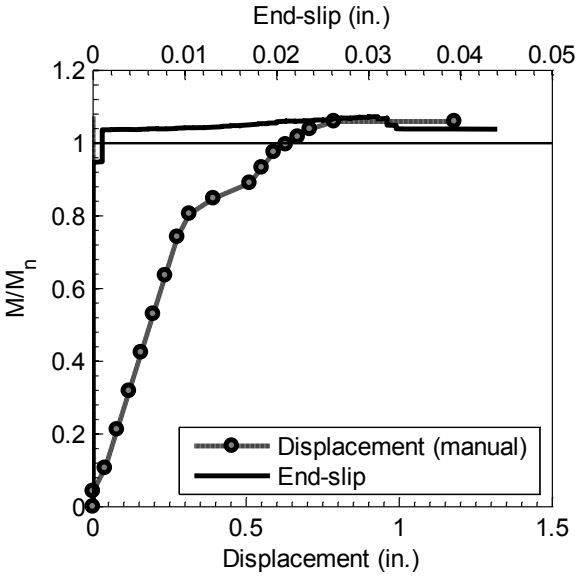

Figure C.49 – Test results of H-SCC-D2-L with an embedment length of 4.0 ft (1220 mm)
(Note: 1 in. = 25.4 mm)

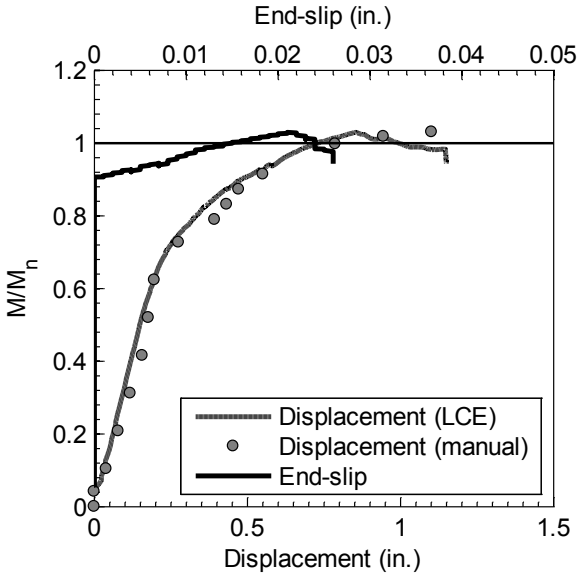

Figure C.50 – Test results of H-SCC-D2-D with an embedment length of 3.75 ft (1143 mm)
(Note: 1 in. = 25.4 mm)

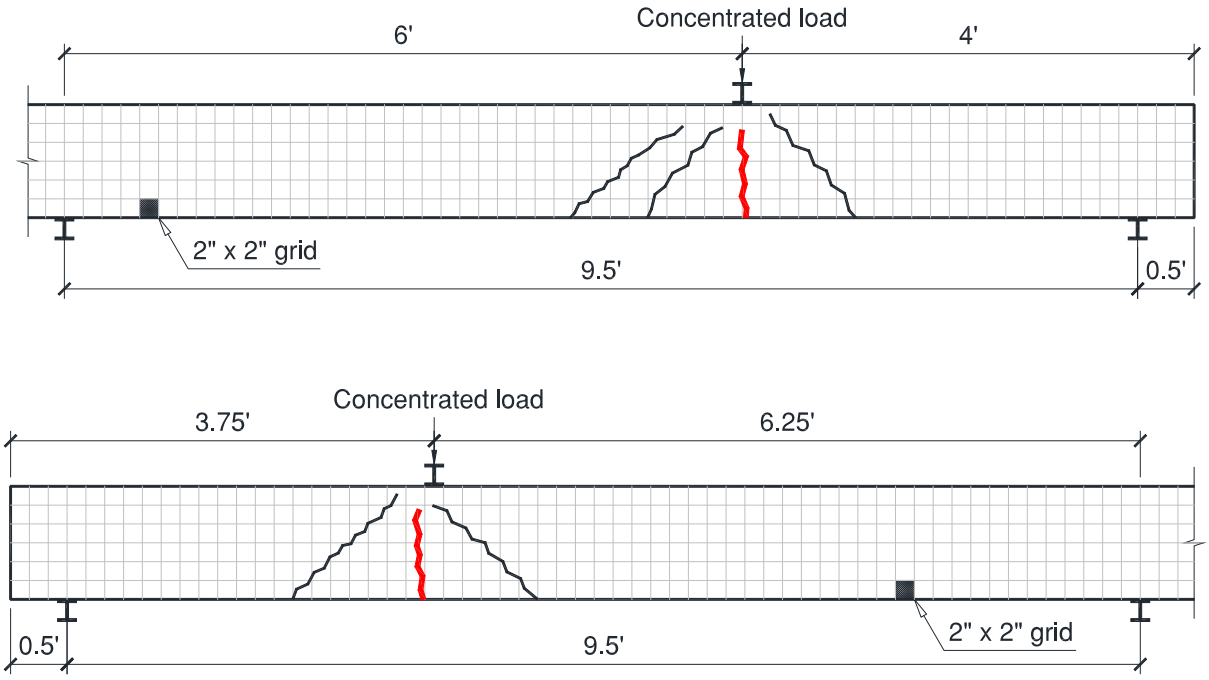

Figure C.51 – Crack pattern of H-SCC-D2-L (top) and H-SCC-D2-D (bottom).
(Note: 1 ft = 305 mm; 1 in. = 25.4 mm)

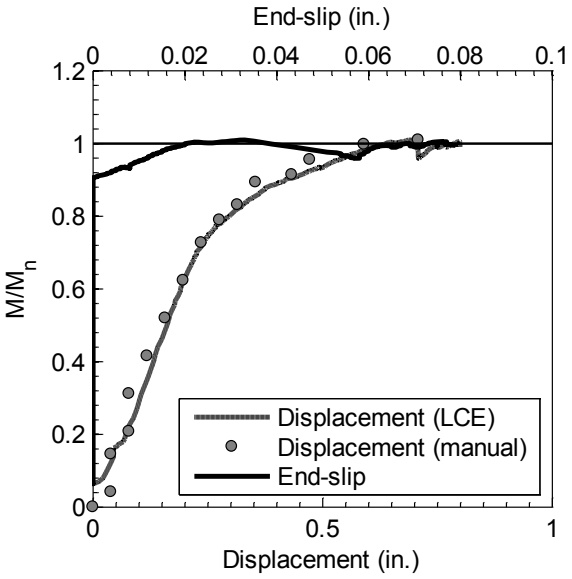

Figure C.52 – Test results of H-SCC-D1-L with an embedment length of 3.75 ft (1143 mm)
(Note: 1 in. = 25.4 mm)

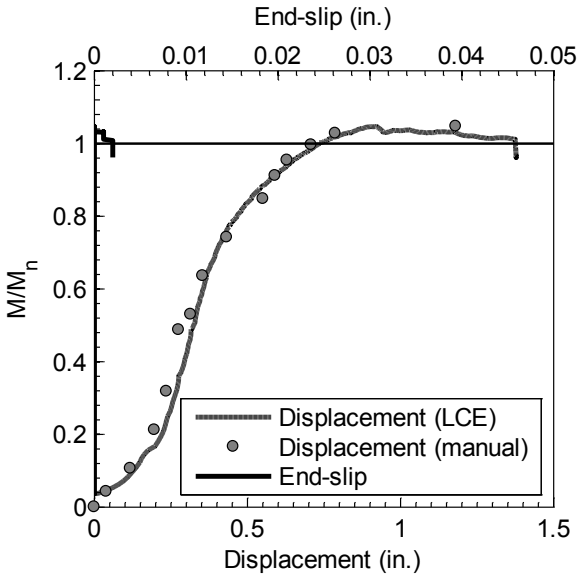

Figure C.53 – Test results of H-SCC-D1-D with an embedment length of 4.0 ft (1220 mm)
(Note: 1 in. = 25.4 mm)

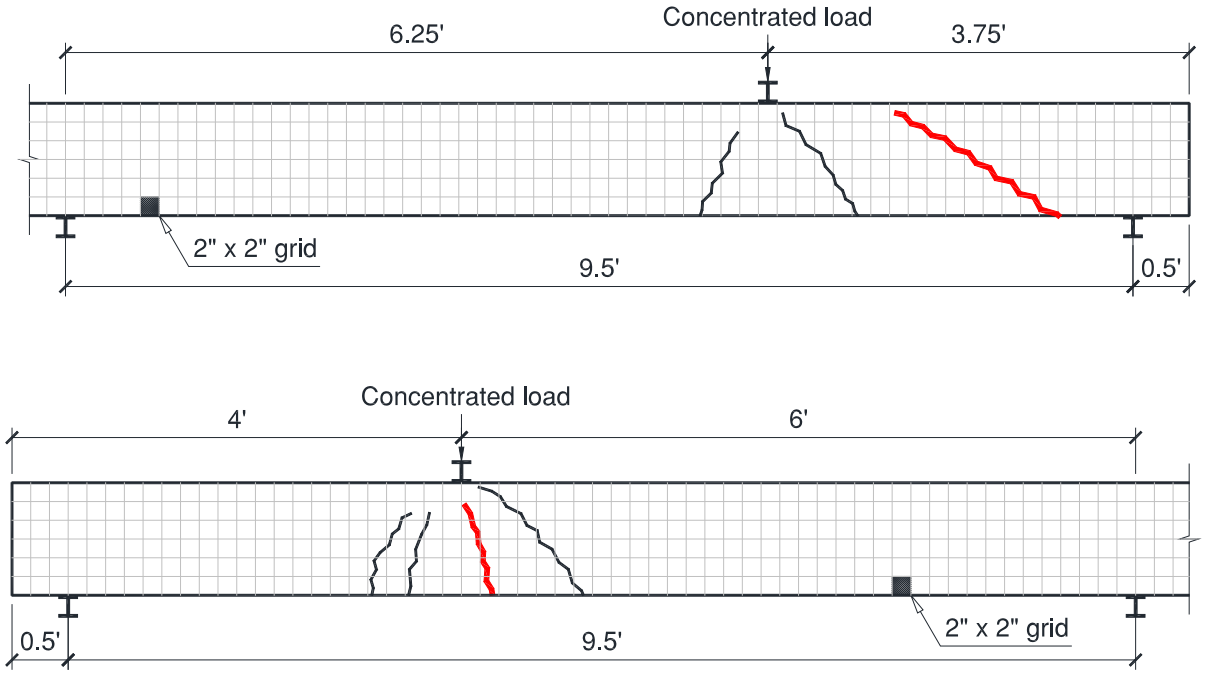

Figure C.54 – Crack pattern of H-SCC-D2-L (top) and H-SCC-D2-D (bottom).
(Note: 1 ft = 305 mm; 1 in. = 25.4 mm)

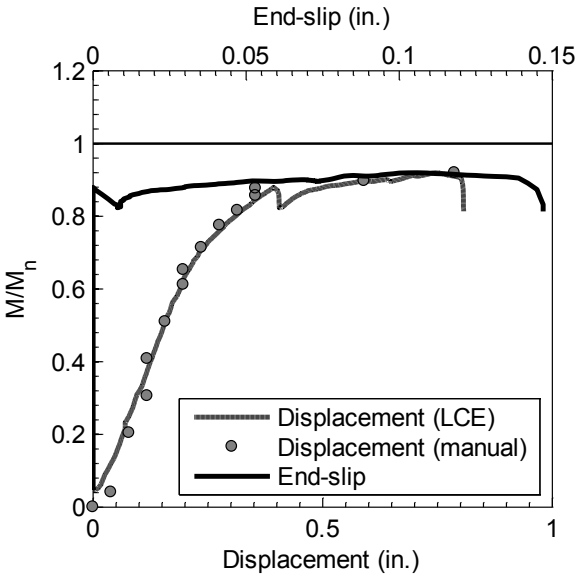

Figure C.55 – Test results of H-SCC-D4-L with an embedment length of 3.5 ft (1067 mm)
(Note: 1 in. = 25.4 mm)

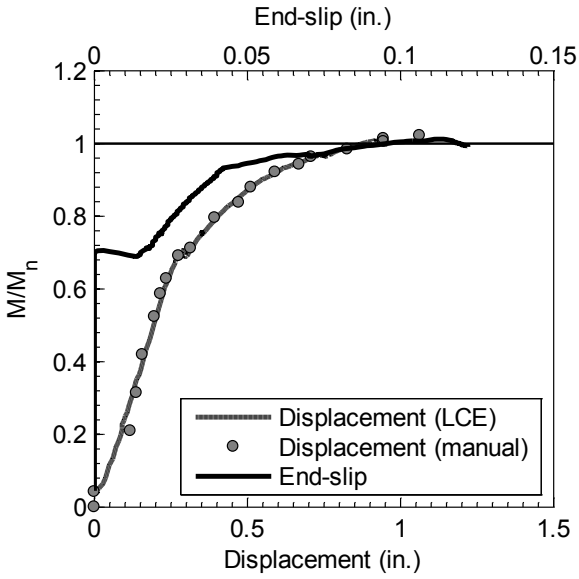

Figure C.56 – Test results of H-SCC-D4-D with an embedment length of 3.75 ft (1143 mm)
(Note: 1 in. = 25.4 mm)

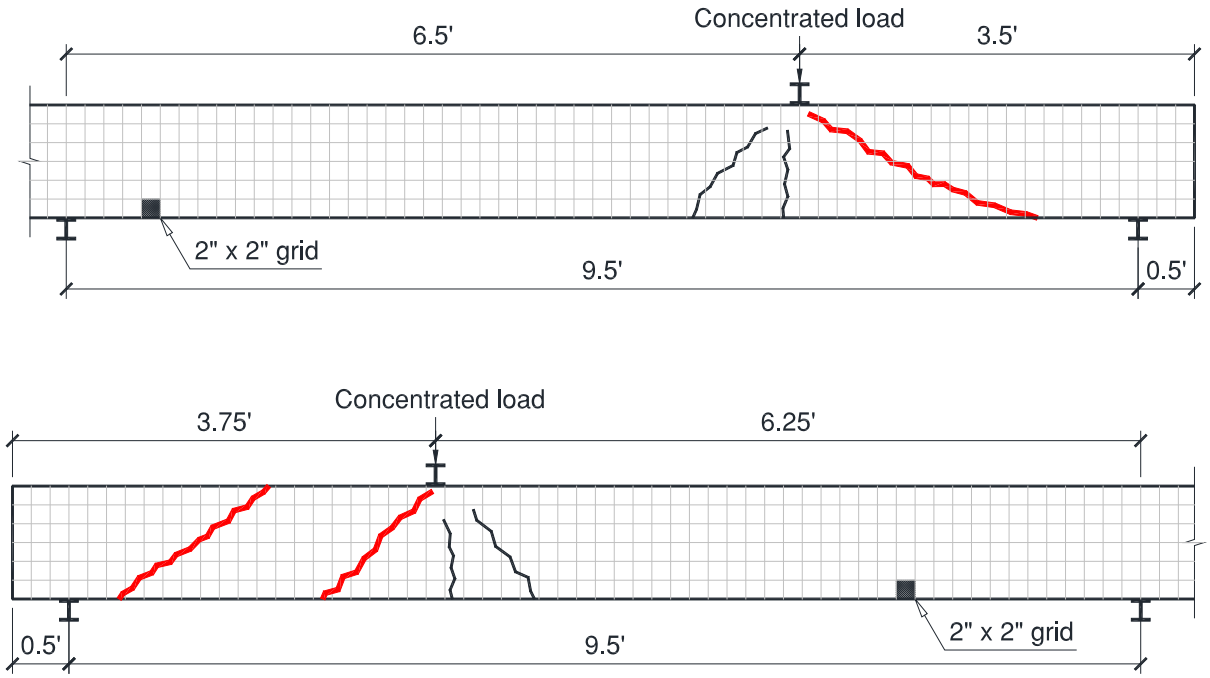

Figure C.57 – Crack pattern of H-SCC-D4-L (top) and H-SCC-D4-D (bottom).
(Note: 1 ft = 305 mm; 1 in. = 25.4 mm)

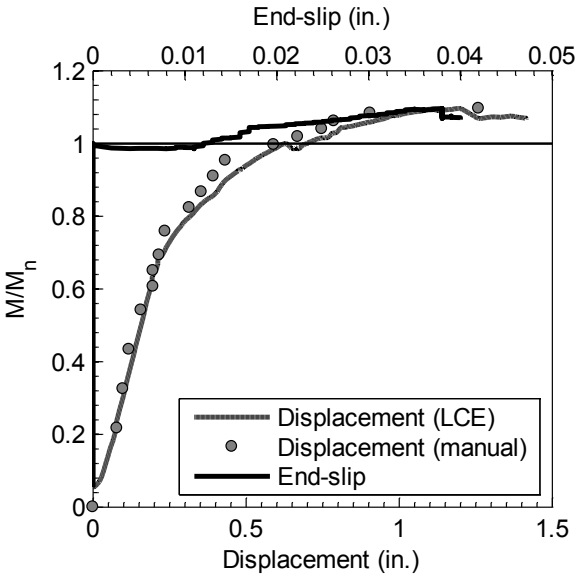

Figure C.58 – Test results of H-SCC-D3-L with an embedment length of 4.25 ft (1295 mm)
(Note: 1 in. = 25.4 mm)

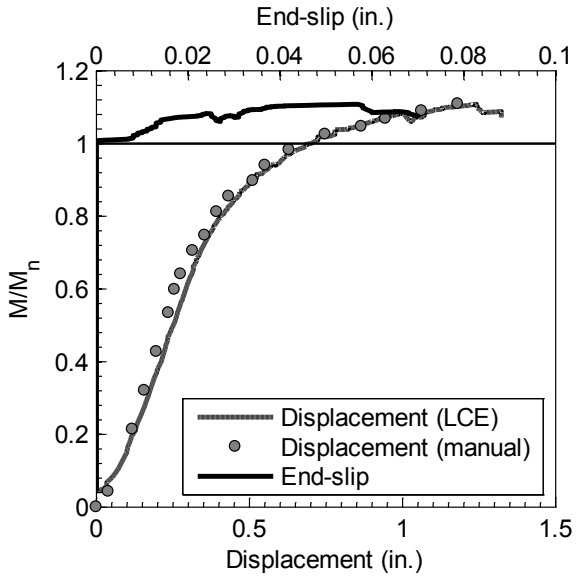

Figure C.59 – Test results of H-SCC-D3-D with an embedment length of 4.0 ft (1220 mm)
(Note: 1 in. = 25.4 mm)

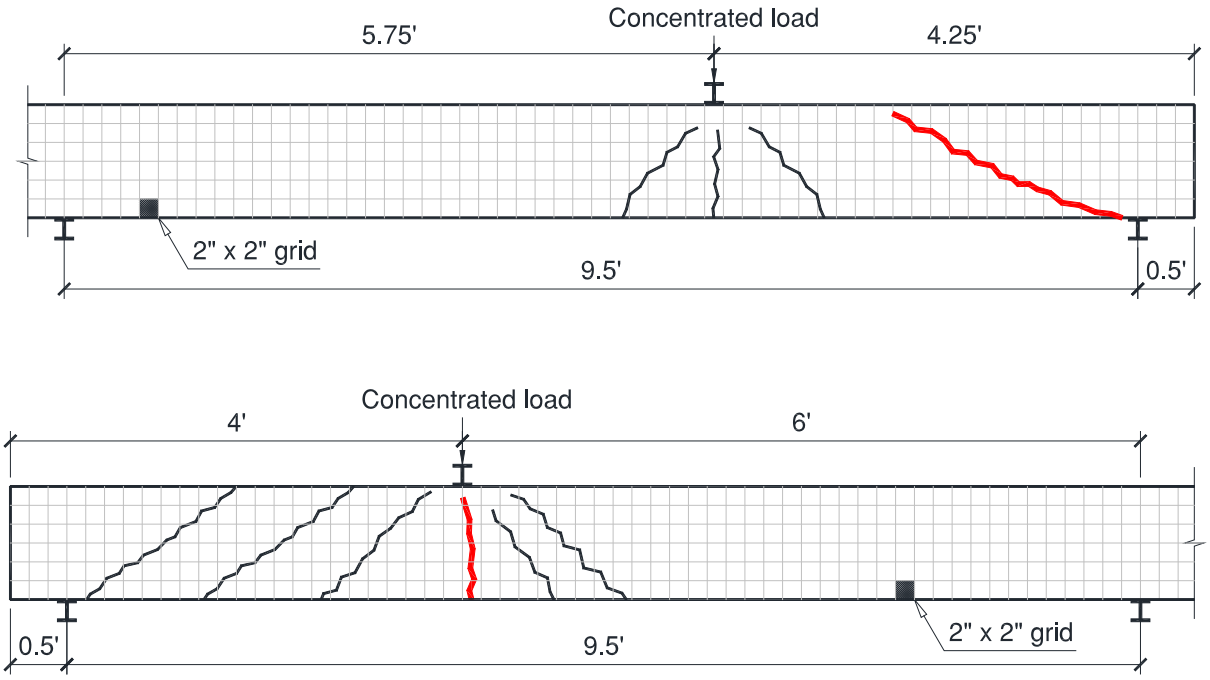

Figure C.60 – Crack pattern of H-SCC-D3-L (top) and H-SCC-D3-D (bottom).
(Note: 1 ft = 305 mm; 1 in. = 25.4 mm)

C.1.6 H-CC-D beams

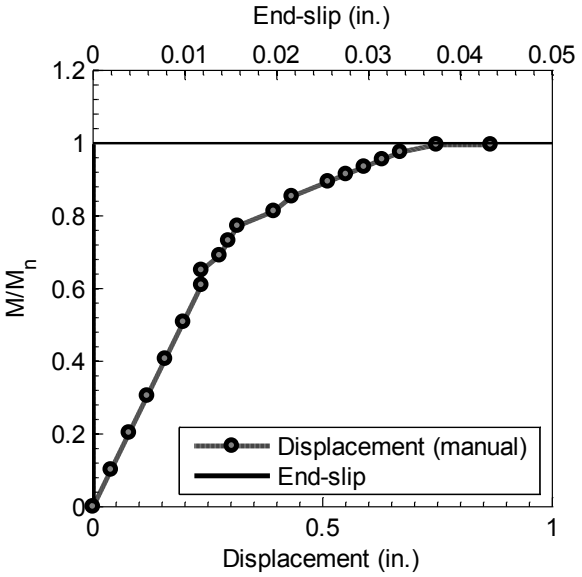

Figure C.61 – Test results of H-CC-D4-L with an embedment length of 4.5 ft (1372 mm)
(Note: 1 in. = 25.4 mm)

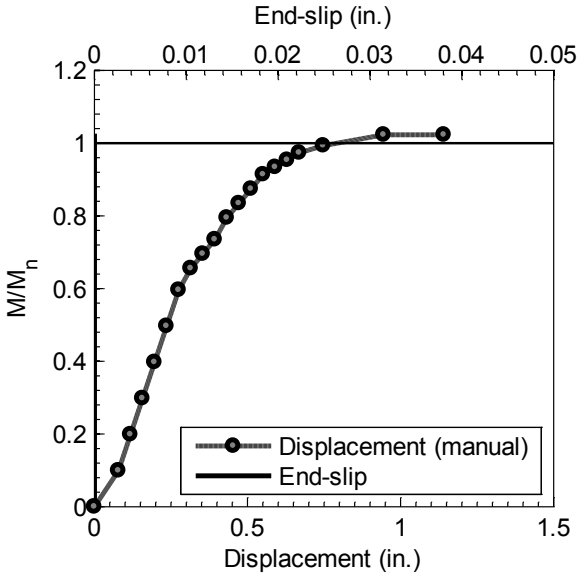

Figure C.62 – Test results of H-CC-D4-D with an embedment length of 4.0 ft (1220 mm)
(Note: 1 in. = 25.4 mm)

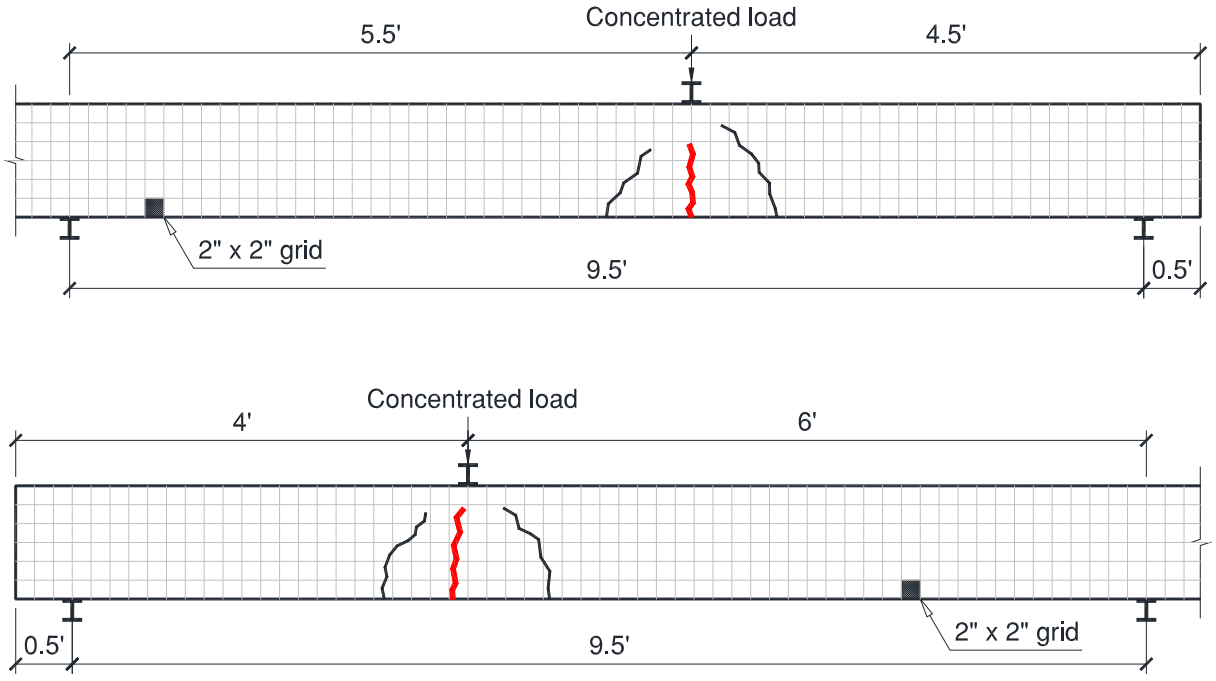

Figure C.63 – Crack pattern of H-CC-D4-L (top) and H-CC-D4-D (bottom).
(Note: 1 ft = 305 mm; 1 in. = 25.4 mm)

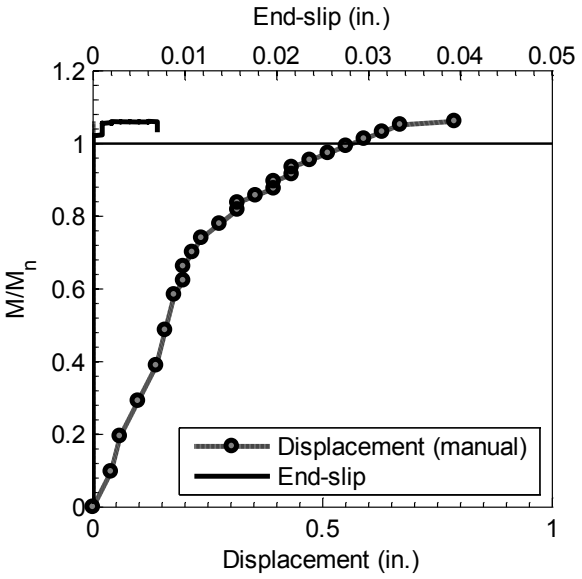

Figure C.64 – Test results of H-CC-D3-L with an embedment length of 3.75 ft (1143 mm)
(Note: 1 in. = 25.4 mm)

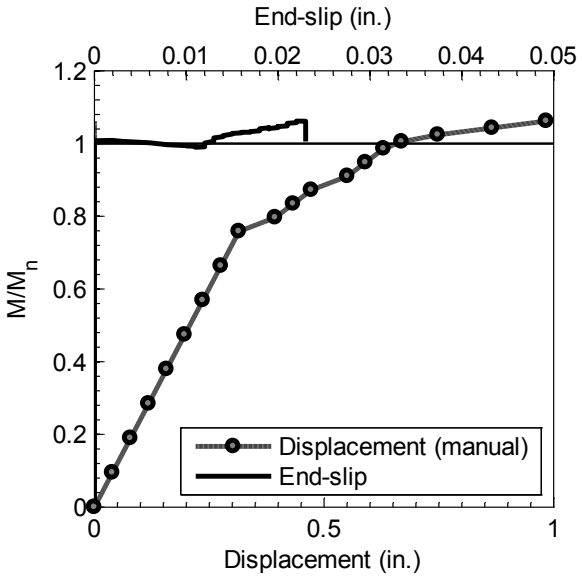

Figure C.65 – Test results of H-CC-D3-D with an embedment length of 3.5 ft (1067 mm)
(Note: 1 in. = 25.4 mm)

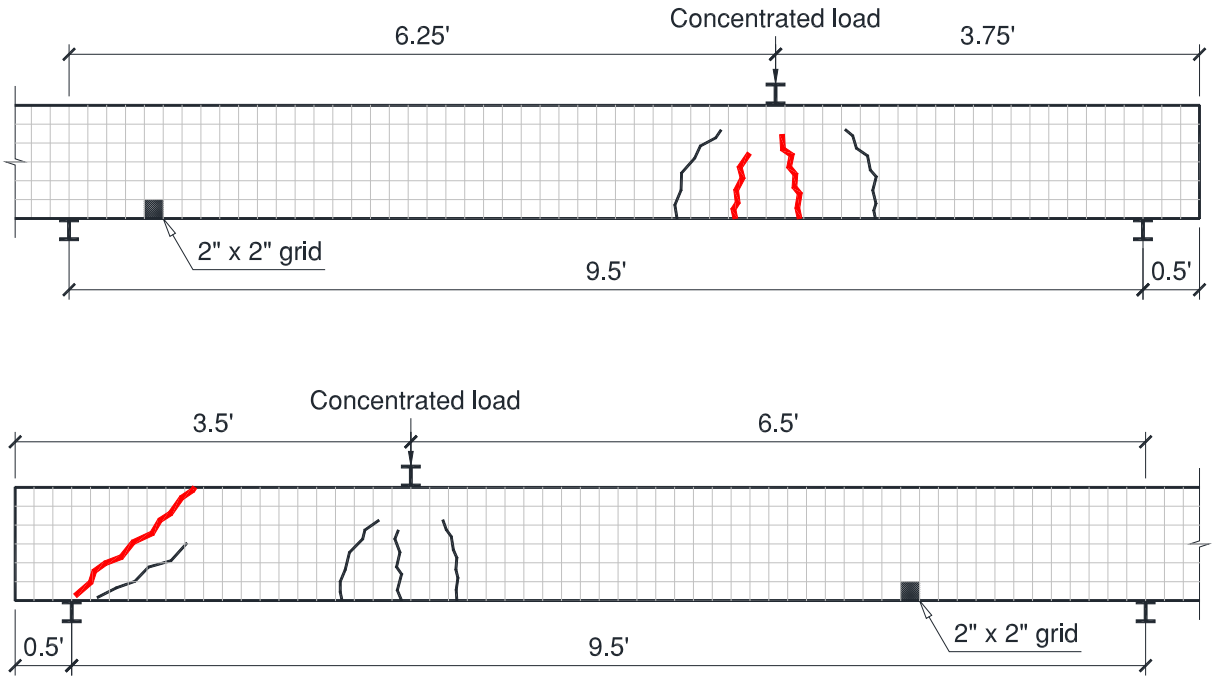

Figure C.66 – Crack pattern of H-CC-D3-L (top) and H-CC-D3-D (bottom).
(Note: 1 ft = 305 mm; 1 in. = 25.4 mm)

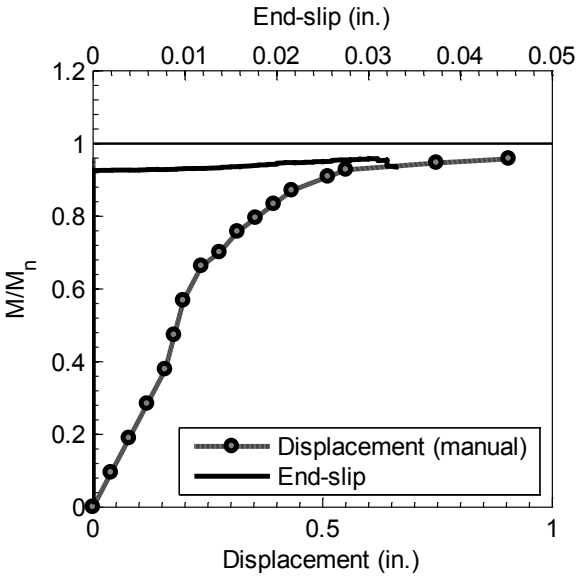

Figure C.67 – Test results of H-CC-D2-L with an embedment length of 3.5 ft (1067 mm)
(Note: 1 in. = 25.4 mm)

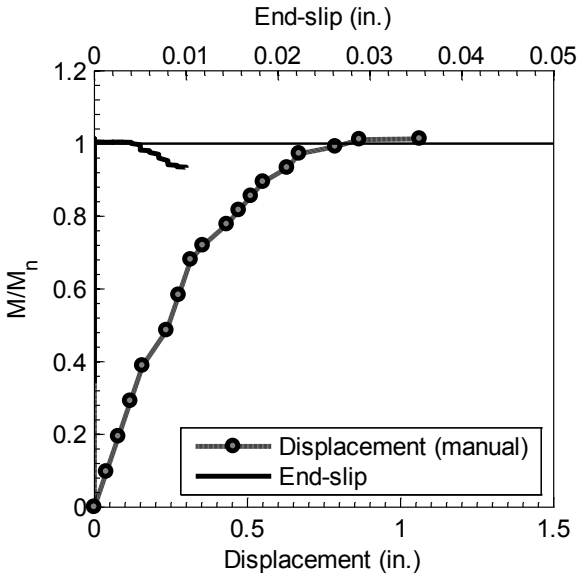

Figure C.68 – Test results of H-CC-D2-D with an embedment length of 3.75 ft (1143 mm)
(Note: 1 in. = 25.4 mm)

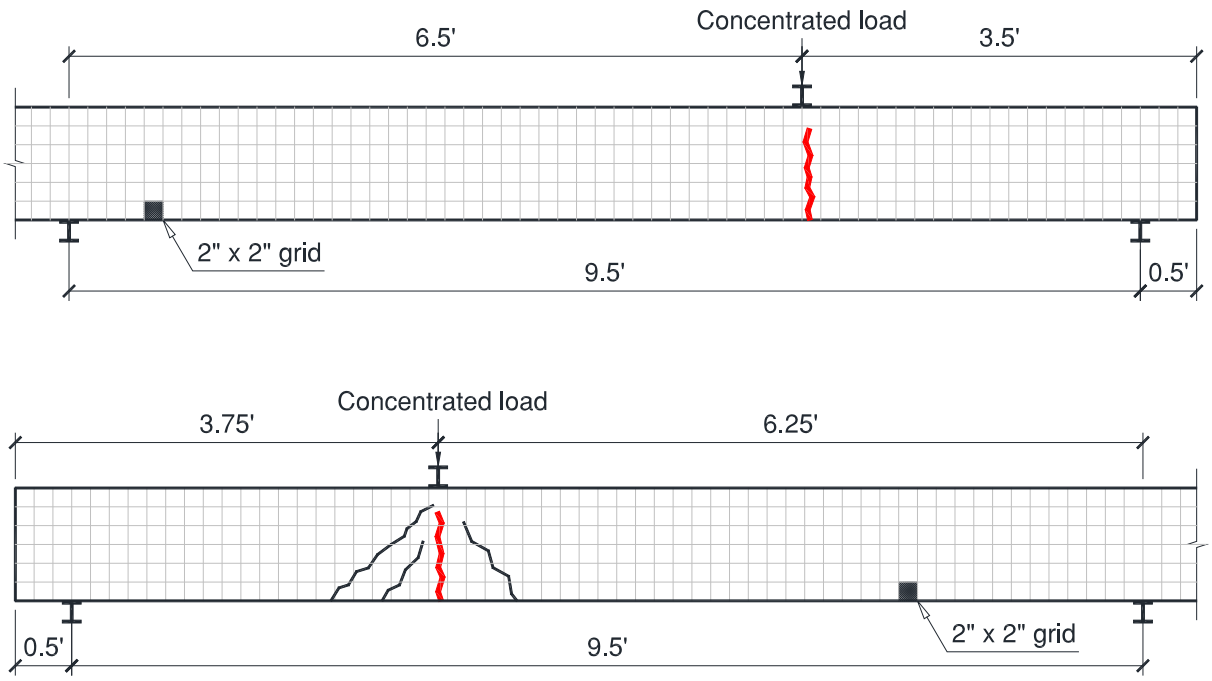

Figure C.69 – Crack pattern of H-CC-D2-L (top) and H-CC-D2-D (bottom).
(Note: 1 ft = 305 mm; 1 in. = 25.4 mm)

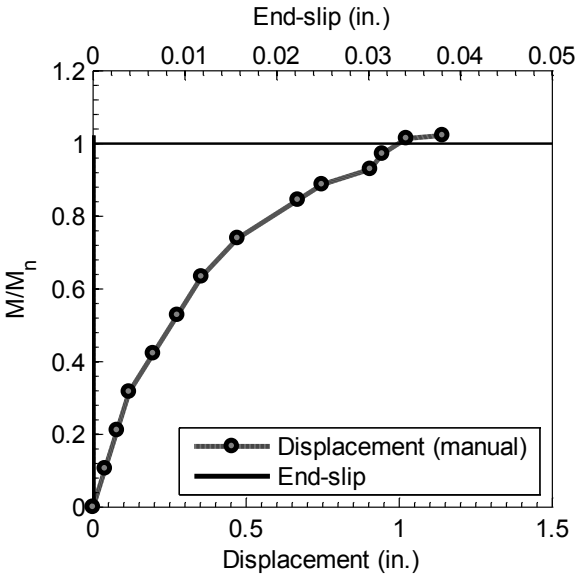

Figure C.70 – Test results of H-CC-D1-L with an embedment length of 4.25 ft (1295 mm)
(Note: 1 in. = 25.4 mm)

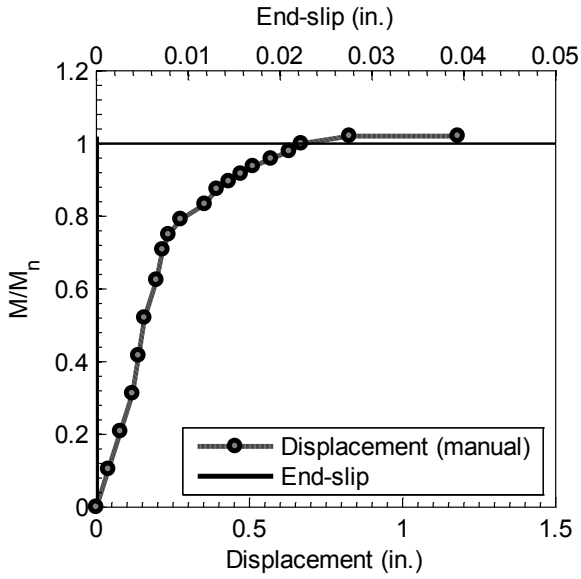

Figure C.71 – Test results of H-CC-D1-D with an embedment length of 4.0 ft (1220 mm)
(Note: 1 in. = 25.4 mm)

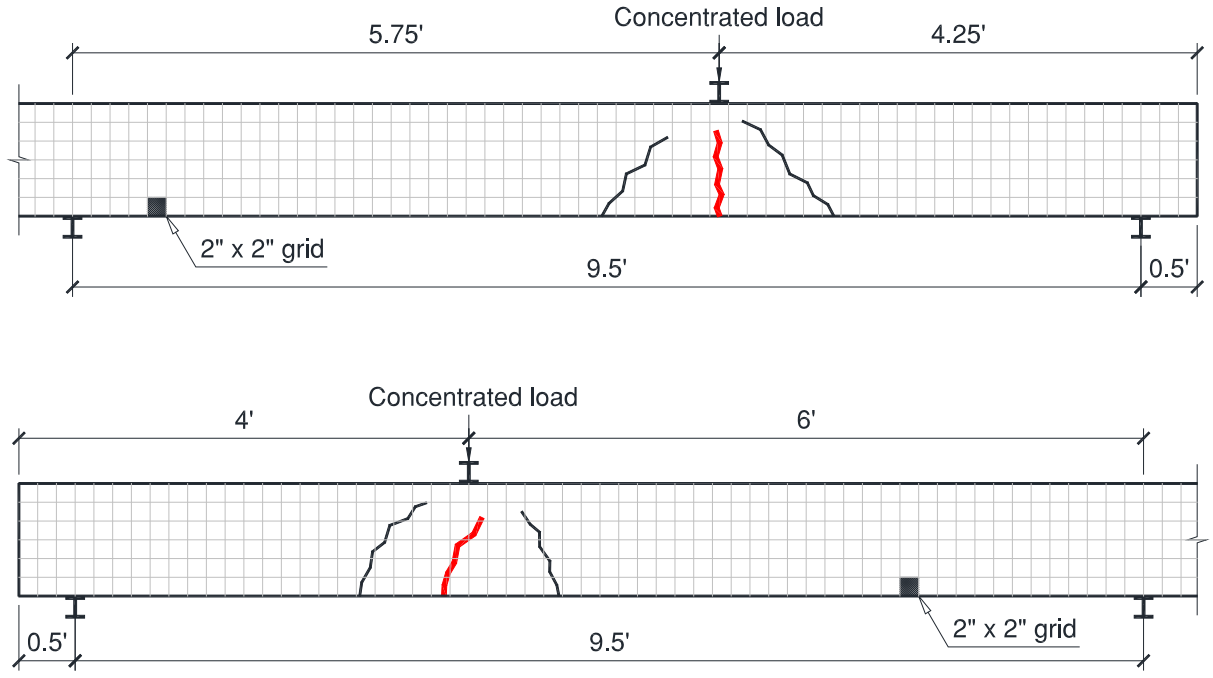

Figure C.72 – Crack pattern of H-CC-D2-L (top) and H-CC-D2-D (bottom).
(Note: 1 ft = 305 mm; 1 in. = 25.4 mm)

C.2 Development length determination

Table C.1 – Bending test results of N-SCC-S beams

No.	Specimen	Embedment length (ft)	M_{max}/M_n	M_{slip}/M_n
1	N-SCC-S4-L	6.00	0.98	No Slip
2	N-SCC-S4-D	5.50	0.98	No Slip
3	N-SCC-S3-L	5.25	1.04	No Slip
4	N-SCC-S3-D	5.00	1.08	No Slip
5	N-SCC-S2-L	4.00	1.07	1.05
6	N-SCC-S2-D	3.50	1.03	0.93
7	N-SCC-S1-L	3.50	1.11	0.95
8	N-SCC-S1-D	3.25	1.10	0.97

(Note: M_{max}/M_n = ratio of the maximum measured moment and the nominal moment capacity; M_{slip}/M_n = ratio of the measured moment at which the prestressing strand started slipping and the nominal moment capacity; 1 ft = 305 mm)

Table C.2 – Bending test results of H-SCC-S beams

No.	Specimen	Embedment length (ft)	M_{max}/M_n	M_{slip}/M_n
1	H-SCC-S2-L	4.50	1.09	No Slip
2	H-SCC-S2-D	4.00	1.05	No Slip
3	H-SCC-S1-L	3.75	1.14	1.12
4	H-SCC-S1-D	3.75	1.17	No Slip
5	H-SCC-S4-L	4.00	1.07	1.00
6	H-SCC-S4-D	3.75	1.12	0.94
7	H-SCC-S3-L	3.50	1.10	0.97
8	H-SCC-S3-D	3.75	1.17	1.02

(Note: M_{max}/M_n = ratio of the maximum measured moment and the nominal moment capacity; M_{slip}/M_n = ratio of the measured moment at which the prestressing strand started slipping and the nominal moment capacity; 1 ft = 305 mm)

Table C.3 – Bending test results of N-CC-S beams

No.	Specimen	Embedment length (ft)	M_{max}/M_n	M_{slip}/M_n
1	N-CC-S4-L	4.00	0.99	No Slip
2	N-CC-S4-D	3.50	1.01	0.92
3	N-CC-S3-L	3.50	1.06	1.05
4	N-CC-S3-D	3.50	1.10	0.99
5	N-CC-S2-L	3.25	1.11	1.04
6	N-CC-S2-D	3.25	1.07	1.04
7	N-CC-S1-L	3.00	0.98	0.98
8	N-CC-S1-D	3.25	1.07	0.93

(Note: M_{max}/M_n = ratio of the maximum measured moment and the nominal moment capacity; M_{slip}/M_n = ratio of the measured moment at which the prestressing strand started slipping and the nominal moment capacity; 1 ft = 305 mm)

Table C.4 – Bending test results of H-CC-S beams

No.	Specimen	Embedment length (ft)	M_{max}/M_n	M_{slip}/M_n
1	H-CC-S4-L	4.00	1.03	1.01
2	H-CC-S4-D	4.25	0.99	No Slip
3	H-CC-S3-L	4.00	1.03	1.02
4	H-CC-S3-D	4.25	1.06	No Slip
5	H-CC-S2-L	4.00	1.04	No Slip
6	H-CC-S2-D	3.75	1.15	No Slip
7	H-CC-S1-L	3.50	1.00	No Slip
8	H-CC-S1-D	3.25	1.00	0.97

(Note: M_{max}/M_n = ratio of the maximum measured moment and the nominal moment capacity; M_{slip}/M_n = ratio of the measured moment at which the prestressing strand started slipping and the nominal moment capacity; 1 ft = 305 mm)

Table C.5 – Bending test results of H-SCC-D beams

No.	Specimen	Embedment length (ft)	M_{max}/M_n	M_{slip}/M_n
1	H-SCC-D2-L	4.00	1.07	1.04
2	H-SCC-D2-D	3.75	1.03	0.91
3	H-SCC-D1-L	3.75	1.01	0.91
4	H-SCC-D1-D	4.00	1.05	1.03
5	H-SCC-D4-L	3.50	0.92	0.88
6	H-SCC-D4-D	3.75	1.01	0.70
7	H-SCC-D3-L	4.25	1.10	1.00
8	H-SCC-D3-D	4.00	1.11	1.01

(Note: M_{max}/M_n = ratio of the maximum measured moment and the nominal moment capacity; M_{slip}/M_n = ratio of the measured moment at which the prestressing strand started slipping and the nominal moment capacity; 1 ft = 305 mm)

Table C.6 – Bending test results of H-CC-D beams

No.	Specimen	Embedment length (ft)	M_{max}/M_n	M_{slip}/M_n
1	H-CC-D4-L	4.50	1.00	No Slip
2	H-CC-D4-D	4.00	1.03	No Slip
3	H-CC-D3-L	3.75	1.06	1.02
4	H-CC-D3-D	3.50	1.06	1.01
5	H-CC-D2-L	3.50	0.96	0.93
6	H-CC-D2-D	3.75	1.01	1.00
7	H-CC-D1-L	4.25	1.02	No Slip
8	H-CC-D1-D	4.00	1.02	No Slip

(Note: M_{max}/M_n = ratio of the maximum measured moment and the nominal moment capacity; M_{slip}/M_n = ratio of the measured moment at which the prestressing strand started slipping and the nominal moment capacity; 1 ft = 305 mm)